



UNIVERSITÀ  
DEGLI STUDI  
DI MILANO

Department of Chemistry

**Synthesis of *Haemophilus influenzae* type a oligosaccharides  
for vaccine development**

PhD Thesis submitted by

Claudia Vera Kohout

2017 - 2020

Supervisor

Prof. Luigi Lay

Dr. Laura Polito

Coordinator

Prof. Emanuela Licandro

Cycle

XXXII



*Dedicated to my beloved parents*

*Feeling my way through the darkness  
Guided by a beating heart  
I can't tell where the journey will end  
But I know where to start  
They tell me I'm too young to understand  
They say I'm caught up in a dream  
Well life will pass me by if I don't open up my eyes  
Well that's fine by me*

(Avicii, Wake me up)

This project has received funding from European Union's Horizon 2020 research and innovation programme under the Marie Curie Skłodowska-Curie grant agreement No 675671.

GLYCOVAX is a European Training Network (ETN) funded in the framework of H2020 Marie Skłodowska- Curie ITN programme: <http://glycovax.eu/>



## ***Abstract***

Glycoconjugate vaccines are a very effective way to prevent bacterial and fungal infections. By conjugation of the saccharide antigen to a carrier protein, the T-independent antigen is converted to a T-dependent antigen, resulting in the production of high affinity antibodies as well as memory B-cells. Today, most of the licensed glycoconjugate vaccines extract the required saccharide antigen from bacterial cultures. However, the isolation and purification of the polysaccharides are challenging. Synthetic polysaccharides are an effective alternative with great potential, as they are well-defined and characterized by minimal batch-to-batch variability.

The pathogen *Haemophilus influenzae* (Hi) is a major cause of severe diseases, i.e. meningitis, sepsis and otitis, especially affecting young children. Among 6 identified serotypes, type b (Hib) is the most common and most virulent strain. Additionally, Hib is the first successful example of a vaccine based on synthetic carbohydrate antigens licensed and distributed in Cuba since 2004 with the tradename QuimiHib.

In recent years, an increasing rate of infections caused by Hia raised some concern and currently, Hia causes up to 10 % of reported *Haemophilus* infections. This burden raised some concerns, as no vaccine targeting Hia is currently available or under development. The capsular polysaccharide (CPS) of Hia is a polymer of 4- $\beta$ -D-Glc-(1 $\rightarrow$ 4)-D-ribitol-5-(PO<sub>4</sub> $\rightarrow$ ) repeating units and is a potential antigen for a future protein-conjugated polysaccharide vaccine. To further explore the CPS of Hia as antigen, we synthesized well-defined oligosaccharides of different chain length of up to five repeating units using state of the art methodology.

After synthetic optimization of all required monosaccharide building blocks, they were first assembled by means of fine-tuned glycosylation reactions to obtain disaccharide repeating units and finally combined using the well-known phosphoramidite approach. In particular, a bifunctional disaccharide building block with a phosphoramidite moiety and a temporary protecting group was used for oligomerization. After n coupling(s) using 4,5-Dicyanoimidazole (DCI) as condensating agent and (1S)-(+)-(10-camphorsulfonyl)oxaziridine (CSO) for the oxidation in a one pot reaction, the temporary protecting group was removed giving the new oligomer (n+1) as new acceptor, which can be coupled again with the bifunctional building block in an iterative cycle.

As last step, a C3 linker was introduced on each oligomer followed by a deprotection sequence. Additionally, the resulting oligosaccharides were further conjugated to CRM<sub>197</sub> taking advantage of a di-N-hydroxysuccinimidyl adipate linker. Within this work, we successfully prepared five Hia oligomers containing up to five repeating units conjugated to CRM<sub>197</sub> carrier protein.

The present PhD thesis comprises 10 chapters, including the References list (Chapter 9). Chapter 1 reports a brief overview of the immune response against pathogens, with a particular focus on carbohydrate antigens, as well as the mechanism of action of glycoconjugate vaccines. Chapter 2 describes the development of a historical vaccine and additionally, novel vaccine approaches are explained. In Chapter 3 the bacterium *Haemophilus Influenzae* (Hi) with its different serotypes is defined and additionally, the successful glycoconjugate vaccine approach targeting type b is specified more precisely. The aim of the thesis is reported in Chapter 4 giving a short overview of the state-of-the-art and explaining further the idea of our approach. The experimental work is discussed in Chapter 5 with a brief summary in Chapter 6 and furthermore, detailed procedures are given in Chapter 7. Besides, all NMRs are published in Chapter 10.



## ***Abbreviations***

Ac	Acetyl
ACN	Acetonitrile
ADH	Adipic acid dihydrazide
All	Allyl
APC	Antigen presenting cell
BCA	Bicinchoninic acid
BCG	Bacille Calmette-Guerin
BCR	B-cell receptors
Bn	Benzyl
BSP	1-Benzenesulfinyl piperidine
Cbz	benzyloxycarbonyl
CMP-Neu5Ac	Cytidine-5'-monophospho-N-acetylneuraminic acid
CNS	Central nervous system
COD	Cyclooctadienet
COPD	Chronic obstructive pulmonary disease
COSY	Correlation spectroscopy
CPS	Capsular polysaccharide
CRM <sub>197</sub>	Cross-reacting material 197
CTL	Cytotoxic T lymphocytes
CSO	(1S)-(+)-(10-camphorsulfonyl)oxaziridine
CTL	Cytotoxic T lymphocytes
DBU	1,5-diazabicyclo(5.4.0)undec-7-ene
DC	Dendric cell
DCC	Dicyclohexylcarbodiimide
DCI	4,5-Dicyanoimidazole
DCM	Dichloromethane
DMAP	4-Dimethylaminopyridine
DMF	Dimethylformamide
DMSO	Dimethylsulfoxide
DMTr	4,4'-Dimethoxytrityl
DMTST	Dimethyl(methylthio) sulphonium triflate

DNA	Deoxyribonucleic acid
DT	Diphtheria toxoid
e.g.	Exempli gratia
ELISA	Enzyme-linked immunosorbent assay
EMA	European Medicines Agency
Et	Ethyl
ETN	European Training Network
EtOAc	Ethyl acetate
EtOH	Ethanol
Eq	Equivalent
FDA	Food and Drug Administration
Fmoc	Fluorenylmethyloxycarbonyl
GMMA	Generalized Modules for Membrane Antigens
GBS	Group B streptococcus
Glc	Glucose
GSK	GlaxoSmithKline
GT	Germline-targeting
HBV	Hepatitis B virus
Hex	Hexane
Hi	<i>Haemophilus influenzae</i>
HIV	Human immunodeficiency virus
HMBC	Heteronuclear Multiple-Bond Correlation
HMDS	Hexamethyldisilazane
HPLC	High-performance liquid chromatography
HPTLC	High-performance thin-layer chromatography
HPV	Human papilloma virus
HSA	Human serum albumin
HSQC	heteronuclear single quantum correlation experiment
ICS	International Circumpolar Surveillance
IDCP	Iodonium (di- $\gamma$ -collidine) perchlorate
i.e.	id est
Ig	Immunoglobuline
kDa	kiloDalton
LG	Leaving group
LPS	lipopolysaccharides

MCPBA	<i>m</i> -chloroperbenzoic acid
Me	Methyl
Men	<i>Neisseria meningitis</i>
MeOH	Methanol
MHC	Major histocompatibility complex
MPBT	S-(4-methoxyphenyl) benzenethiosulfinate
MS	Molecular sieves
NAD	Nicotinamide adenine dinucleotide
NBS	N-Bromosuccinimide
NIS	N-Iodosuccinimide
NK	Natural Killer
NMR	Nuclear Magnetic Resonance
NPhTFACl	2,2,2-Trifluoro- <i>N</i> -phenylacetimidoyl Chloride
NTHi	Non-typeable or non-encapsulated <i>H. influenzae</i>
OMV	Outer membrane vesicles
OMP	Outer membrane proteins
OMPC	Outer membrane protein complex of meningococcus
OTf	O-Triflate
PAMPs	Pathogen-Associated Molecular Patterns
PGCT	Protein Glycan Coupling technology
Ph	Phenyl
PHiD	Nontypeable <i>Haemophilus influenzae</i> protein D
Pr	Propyl
PRRs	Pathogen Recognition Receptors
PRP	Polyribosyl -ribitol phosphate
PTSA	P-toluenesulfonic Acid
PTFAI	<i>N</i> -phenyltrifluoroacetimidates
RSV	Respiratory syncytial virus
r.t.	Room temperature
SDS-PAGE	sodium dodecyl sulphate–polyacrylamide gel electrophoresis
SEC	Size Exclusion Chromatography
SCID	Severe combined immunodeficiencies
SIDEA	Adipic acid bis( <i>N</i> -hydroxysuccinimide)
TACAs	Tumor-associated carbohydrate antigens
TBAF	Tetra- <i>n</i> -butylammonium fluoride

TBHP	<i>tert</i> —butyl hydroperoxide
TBS	t-Butyldimethylsilyl
<i>t</i> -BuOK	Potassium <i>tert</i> -butoxide
TCA	Trichloroacetic acid
TCAI	Trichloroacetimidate
TCR	T-cell receptor
TD	T cell dependent
TEA	Triethylamine
TES	Triethylsilane
TFA	Trifluoroacetic Acid
TfOH	Triflic acid
Th	T helper cells
THF	Tetrahydrofuran
TI	T cell independent
TLC	Thin layer chromatography
TLRs	Toll-like receptors
TMS	Trimethyl silyl
TMSOTf	Trimethylsilyl triflate
Tol	Toluene
TPS-NT	3-Nitro-1-(2,4,6-triisopropylbenzenesulfonyl)-1,2,4-triazole
Tr	Trityl
TT	Tetanus Toxoid
TTBP	2,4,6-Tri- <i>tert</i> -butylpyrimidine
VLPs	Virus-like particles
WHO	World Health Organization

## **Table of contents**

Abstract.....	i
Abbreviations .....	iii
Table of contents.....	vii
1 Immunology and carbohydrates .....	1
1.1 General overview: Innate and adaptive immune system .....	1
1.2 Antigen depending immune response.....	3
1.3 Immunogenicity of glycoconjugate vaccines .....	5
2 Vaccines and its success .....	8
2.1 History of vaccines.....	8
2.2 Different vaccine approaches .....	11
2.2.1 Polysaccharide and Glycoconjugate vaccines .....	11
2.2.2 Recombinant DNA technology .....	15
2.2.3 A genome-based antigen approach called reverse vaccinology .....	16
3 The bacteria Haemophilus Influenzae.....	17
3.1 General overview .....	17
3.2 Diseases and their treatment.....	19
3.3 Non-encapsulated species and their fear .....	20
3.4 Encapsulated strains.....	21
3.5 Hib and the story of a successful vaccine .....	23
4 Studies towards a future vaccine targeting Hia .....	26
4.1 Increased cases of Hia and the theory of serotype replacement .....	26
4.2 State of the art synthesis of CPS of Hia fragments.....	28
4.3 Prospects within this thesis.....	29
5 Our Synthetic approaches .....	31
5.1 Retrosynthetic Analysis.....	31
5.2 Synthesis of Disaccharide 14 .....	33
5.2.1 Synthesis of the Donors .....	33
5.2.2 Acceptor .....	37
5.2.3 Glycosylation approaches .....	41
5.2.4 Summary and conclusion .....	45
5.3 Synthesis of Disaccharide 13.....	47
5.3.1 Donor .....	47
5.3.2 Glycosylation .....	49

5.3.3	Summary and conclusion .....	50
5.4	Preparation of the Oligomers.....	52
5.4.1	Phosphoramidite vs H-Phosphonate Methodology .....	53
5.4.2	Synthesis of Oligomers: Approach I.....	57
5.4.3	Coupling approach II .....	64
5.4.4	Deprotection of the oligomers.....	66
5.4.5	Summary and conclusion .....	67
5.5	Preparation of the Hia glycoconjugates.....	70
5.5.1	Carriers and their chemistry.....	70
5.5.2	Pre-activation and Conjugation to CRM <sub>197</sub> .....	71
5.5.3	Analysis of glycoconjugates.....	73
6	Resume and Outline .....	74
7	Experimental part.....	75
7.1	General experimental methods .....	75
7.2	Experimental Synthetic Procedures .....	76
7.2.1	Synthesis of Donor for Building Block I.....	76
7.2.2	Synthesis of Donor for Building Block II.....	84
7.2.3	Synthesis of Ribitol Acceptor.....	87
7.2.4	Synthesis of Disaccharides 13 and 14 .....	92
7.2.5	Preparation of the Phosphinite .....	94
7.2.6	Preparation of Building Blocks I and II .....	95
7.2.7	Different Oligomerization Approach .....	99
7.2.8	General Coupling Procedure .....	100
7.2.9	Coupling to the Linker.....	107
7.2.9.1	Preparation of the Linker-Containing Phosphoramidite.....	107
7.2.9.2	General Procedure for the Coupling with the Linker.....	108
7.2.10	General Procedure for Deprotection .....	115
7.3	Protein conjugation .....	121
7.3.1	Activation with SIDEA .....	121
7.3.2	CRM <sub>197</sub> conjugation.....	121
7.3.3	HSA conjugation .....	122
7.4	General methods for the characterization of Glycoconjugate .....	122
7.4.1	BCA.....	122
7.4.2	SDS-PAGE .....	123
8	Acknowledgement .....	124

9	References .....	126
10	Appendix.....	141





# 1 Immunology and carbohydrates

## 1.1 General overview: Innate and adaptive immune system

Affected children with severe combined immunodeficiencies (SCID) are born without a fully efficient immune system and mostly these new-borns die by the age of 1 year.<sup>1</sup> These diseases underline how important our immune system is and this system includes a collection of cells, chemicals and processes which protect the host from foreign antigens, such as microbes, viruses, parasites, cancer cells and toxins. The aim is the identification and a successful elimination, as well as any other kind of potential threat to the host, and the immune system comprises two distinct and interconnected arms, the innate immunity and the adaptive immunity (**Figure 1**).<sup>2</sup>

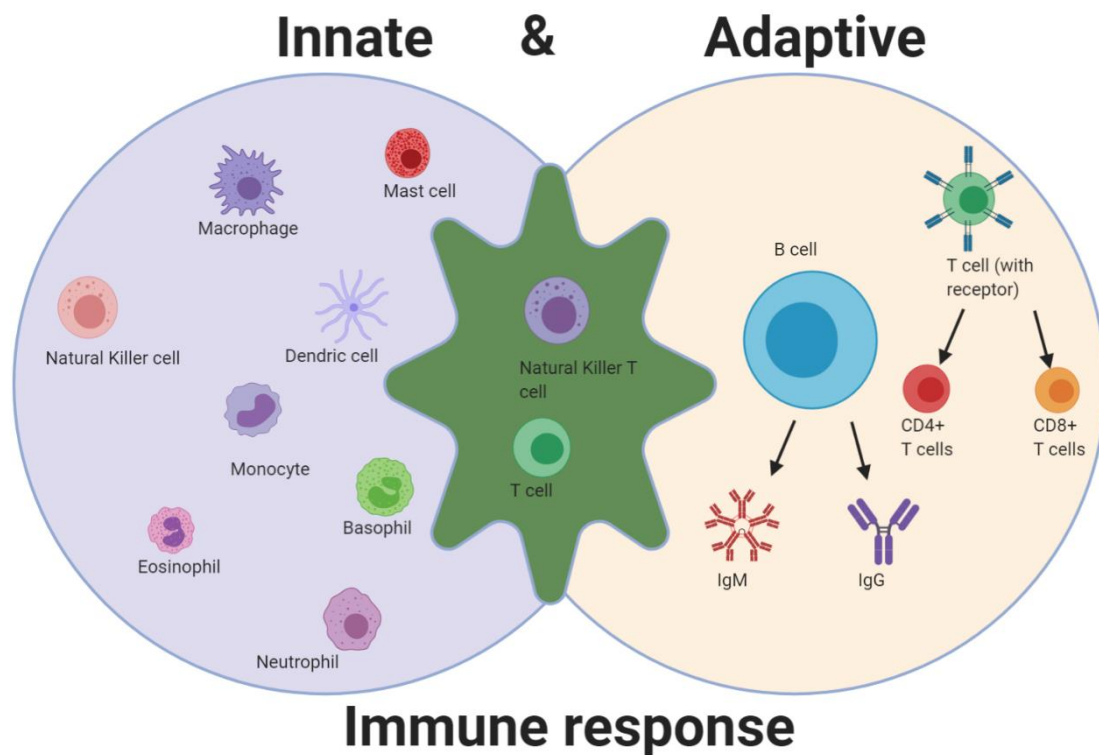


**Figure 1.** Our immune system represents many different cells and is divided in the innate and adaptive immune response. This figure shows the important cells of the innate (left) and of the adaptive system (right). The overlapping cells appearing in the two systems are marked in green.

Anatomical and physiological barriers are considered as first line of defence against pathogens and the immune system is part of it. Dendritic Cells (DC) belong to the innate immune response and are the most professional cells. APCs (Antigen-presenting cells) allow a continuous screening of the body by detecting and responding to Pathogen-Associated Molecular Patterns (PAMPs), structurally and chemically diverse compounds that are unique to foreign microorganisms, via a multiple set of Pathogen Recognition Receptors (PRRs), including peptidoglycan recognition proteins, scavenger

receptors, C-type lectin receptors typically containing a carbohydrate-binding domain (mannose-binding lectin, DC-SIGN), and Toll-like receptors (TLRs). The latter is a family of proteins able to recognize a huge variety of PAMPs, such as lipopolysaccharides (LPS) of Gram-negative bacteria or pathogen-associated glycolipids/lipoproteins.<sup>3,4</sup>

Besides DCs, several other cells are involved in the innate response: phagocytes (macrophages and neutrophils), mast cells, basophils, eosinophils, natural killer (NK) cells and innate lymphoid cells.<sup>3</sup> Within minutes after exposure of a pathogen, the innate immune system starts to generate co-stimulatory molecules (cytokines and chemokines), creating the pro-inflammatory context needed to trigger a proper and robust antigen-specific adaptive immune response.<sup>5</sup>

The adaptive immune response is mediated by B and T lymphocytes and recognizes pathogens with high affinity, providing the fine antigenic specificity required for complete elimination of the microorganism and the generation of the immunological memory. In the adaptive response T-cells are primed by APC (usually DCs, macrophages and B-cells). After antigen uptake (via PRRs) and its enzymatic degradation into the intracellular compartments, APCs translocate the resulting small peptide fragments to bind a group of proteins known as the major histocompatibility complex (MHC), to be eventually exposed on cell surface and presented to T-cell receptor (TCR) of T-cells. This crucial event, i.e. the ternary complex involving MHC, peptide fragments and TCR, is referred to as immunological synapse. In the immunological synapse, MHC molecules can present either endogenous (intracellular) peptides (MHC class I) or exogenous (extracellular) peptides (MHC class II). Depending on the antigen exposed on APC surface, the immunological synapse raises a complex cascade of events culminating in the activation and differentiation of T-cells into cytotoxic T lymphocytes (CTL or CD8+ cells) and/or T helper cells (TH or CD4+ cells). CTL are effector T-cells responsible for the cellular immunity, by destroying target cells infected by intracellular viruses and bacteria. Conversely, T-helper cells can not directly kill infected cells or clear pathogens, but stimulate the immune response by priming the maturation process of B-cells and driving their differentiation into plasma cells (antibody-forming cells) and memory B-cells (humoral immunity).<sup>3,4</sup>

Adaptive system, they represent 15% of peripheral blood leukocytes and they are defined by their production of immunoglobulin Ig (antibodies), which are B-cell antigen receptors. In total, there are five different isotypes of Ig: IgM, IgG, IgA, IgD and IgE, whereas some can be even further divided into subclasses. Furthermore, Ig molecules are proteins composed of two heavy (H) and two light (L) chains. In general, the adaptive system can take up to five days until its immune response depending on T-cells and B-cells succeed.<sup>5,6,7</sup>

In the first antigenic exposure plasma cells secrete low-affinity IgM-type antibodies and provoke mostly a modest and short-term immune response. Memory B-cells, however, survive for a long time in the body and respond rapidly (from two to three orders of magnitude higher) to subsequent exposures to the same pathogen by eliciting high-affinity IgG antibodies, thus conferring long-term protection to the host. Therefore, the production of high titres of IgG leads to the establishment of the immunological memory and represents the overall objective of the vaccination practice.<sup>8</sup>

## **1.2 Antigen depending immune response**

Bacteria are cause of several life-threatening diseases and our immune system is constantly active to protect our body against them. The activation of the immune response is triggered by recognition from APCs of antigens uniquely expressed on the pathogens surface (PAMPs), thus initiating the immune cascade which eventually leads to the identification and elimination of the disease-causing microorganism. More generally speaking, an antigen is any molecule which is identified by the immune system as foreign invader or as dangerous compound.<sup>9</sup> The immune system is very unique and can elicit a specific immune response to these antigens with the aim of defending the host and/or to generate long-term memory response for future recurrence. Antigens such as polysaccharides or proteins are divided into two groups: T-cell dependent (TD) and T-cell independent (TI) antigens.

Polysaccharides are T-cell independent antigens, which means that B cells are activated without any assistance neither from T-cells nor production of co-stimulatory proteins. Monomeric TI antigens are unable to activate B-cells, whereas polymeric TI antigens such as lipopolysaccharides can stimulate B-cells by cross-linking their B-cell receptors (BCR). In **Figure 2a** the process of B-cell activation with T-cell independent antigens such as polysaccharides is shown. After binding to the B-cell receptor, the B-cell is differentiated into plasma cells, and low affinity antibodies IgM are exclusively produced. No memory B-cells are generated within this mechanism of activation and no long-term protection to the host is evoked.<sup>10,11</sup>

T-cell dependent antigens such as proteins are different in their B-cell response- herein T cells are involved (**Figure 2b**). As described in 1.1, APCs like DCs have specific PRRs on their surface and these receptors such as TLR can intercept the antigen and promote its engulfment by the immature DC. After antigen take up and release of specific cytokines and chemokines, immature DCs are transformed into mature cells. Mature DCs migrate to the draining lymph nodes, where they stimulate naïve T-cells through the previously described immunological synapse. Whether MHCI or MHCII are used depends on the chemical properties of the antigen. Additionally, different immunological responses are induced and either cytotoxic CD8+ T cells (with MHC class I) or T helper cells CD4+ (with MHC class II) are

released. Hence, CD4<sup>+</sup> T cells provoke a conventional T-cell dependent immune response by interacting with B-cell through MHC class II complex and therefore, the B-cell becomes stimulated. Within this process their proliferation and most importantly, differentiation into plasma cells and memory B-cells emerge. Plasma cells are antibody producing cells (mainly low-affinity IgM antibodies) and are less favorite than memory B-cells as these cells survive for a long time and are important for a subsequent exposure of the antigen by forming high affinity IgG antibodies.<sup>10,12</sup>

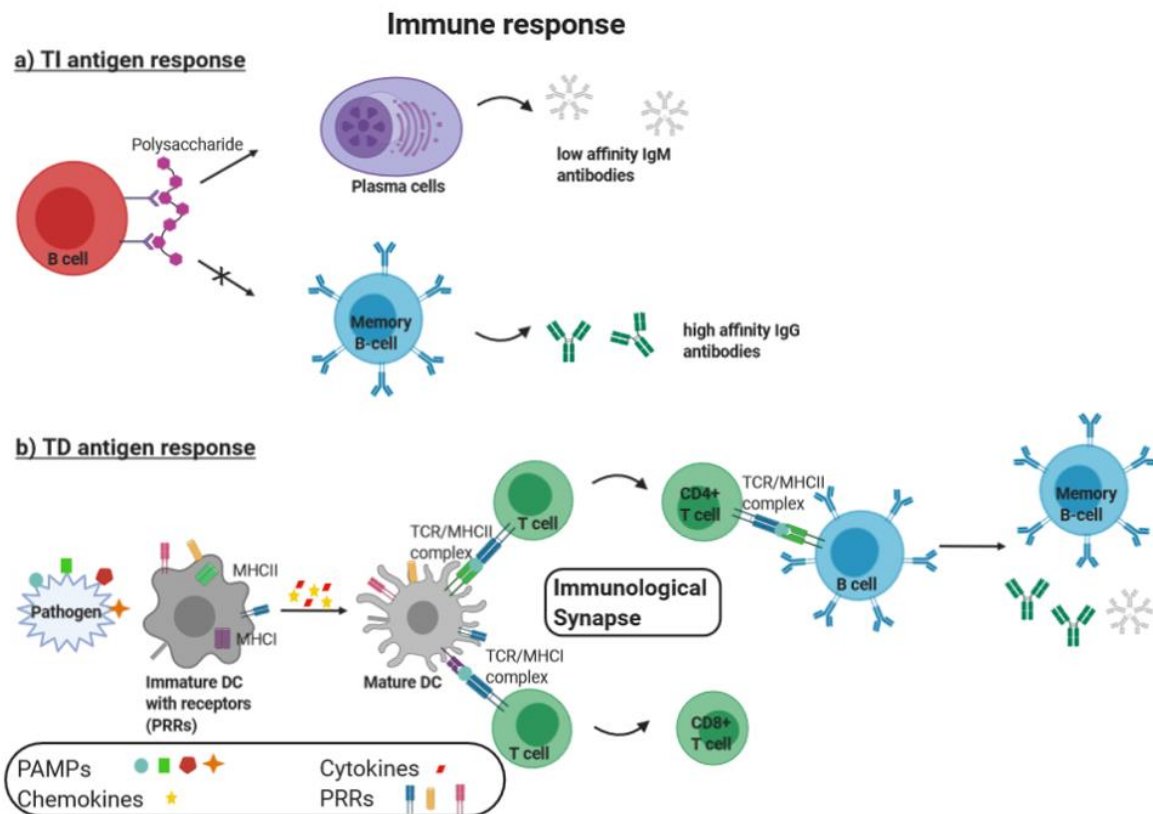


**Figure 2.** a) Simplified presentation of TI antigen response: The B-cell can recognize the TI antigen by its BCR and the B-cell is activated but only plasma cells eliciting low affinity antibodies (mostly IgM) are formed, whereas long-term memory B-cells are not produced. b) Simplified presentation of TD immune response. On the surface of a pathogen PAMPs can be recognized by PRR complexes on dendritic cells and specific cytokines and chemokines are released. Additionally, the dendritic cell is transformed to a mature DC. Within the MHC protein complex the T-cell can bind to the antigen and different immunological pathways can be activated. If the antigen is presented by MHCII complex, naïve T-cells are primed as CD4<sup>+</sup> T cells (T helper cells), which in turn start the maturation and proliferation of B-cells and ultimately leading to the production of memory B-cells and high affinity IgG antibodies.

Recent studies suggested that peptides are not the only existing T-cell epitopes (minimal portion of an antigen molecule needed to elicit a T cell-dependent immune response). Kasper et al. proposed a new model (*vide infra*), whereby not only peptide fragments, but also glycopeptides can be exposed by MHCII on APC surface.<sup>13</sup> Likewise, it was recently discovered some polysaccharides demonstrate a typical behaviour of TD antigens, as they were found capable of activating the immune system following uptake and processing from APCs. Although these polysaccharides are structurally diverse,

all of them contain both a positive and a negative charge within a single repeating unit and therefore, they are usually referred to as zwitterionic polysaccharides.<sup>14</sup>

### **1.3 Immunogenicity of glycoconjugate vaccines**

Carbohydrates are well-known and important for immune recognition. Polysaccharides uniquely expressed on the surface of pathogens are used as antigens for vaccines formulation since 1970s against *Streptococcus pneumoniae*, *Neisseria meningitidis* (groups A, C, Y and W) and *Haemophilus influenzae* infections. There is however, a general concern about carbohydrate-based vaccines. Since, most of the carbohydrates are T-cell independent immunogens, vaccines based on free and purified polysaccharides are poorly immunogenic in infants, young children and elderly (i.e. individuals with immature or compromised immune system). Polysaccharide-based vaccines induce only short-lasting antibody responses in adults and fail to generate conventional B-cell-mediated immunological memory in the population at risk. This can be circumvented by attaching the polysaccharide (or its fragment obtained by proper sizing of the native polysaccharide) to a protein carrier. In this way, TI antigens such as polysaccharides are transformed into TD antigens. This strategy opened a new era in the field of vaccinology. Glycoconjugate antigens are able to induce T-cell recruitment and immune memory B-cell proliferation, with the production of long-lasting IgG antibodies specifically directed towards the carbohydrate strictly associated to the pathogen. Today, all current polysaccharide vaccines licensed for use in children are glycoconjugates.<sup>15,16</sup>

Even if the first conjugate vaccine was licensed more than 30 years ago, we are still not able to fully explain the immune response to such glycoconjugates. Many scientists are investigating their mechanism of action, but little is known so far. Currently, it is stated that due to their hydrophilic character, polysaccharides are not able to enter the MHCII cavity, and consequently they cannot be efficiently presented to T-cells. Two different models to explain, how glycoconjugates can activate the adaptive immune system, will be briefly discussed herein.<sup>15,17</sup>

The traditional theory (**Figure 3a**) indicates that a B-cell binds through BCR the saccharide portion of the conjugate, afterwards the conjugate is internalized and processed. The glycoconjugate is taken into the endosome and the protein portion is digested by proteases to release peptide epitopes. These peptides bind to the MHCII complex to be presented to the receptor of CD4+ T cells in the context of the MHCII complex. This peptide-MHCII-activated T-cells complex releases cytokines to stimulate B-cell maturation and immunoglobulin class switching from IgM to IgG occurs. Studies have been carried out, but the mechanism is not confirmed. As the polysaccharides are covalently linked to the carrier protein, it is not known, if the environmental conditions in the endolysosome are sufficient to cleave the bond between the carbohydrate and the protein.<sup>17,18</sup>

The new model by Kasper (**Figure 3b**) proposes that glycoconjugate antigens raise carbohydrate-specific T cells clones called Tcarbs.<sup>19,13</sup> After saccharide recognition from BCR, the glycoconjugate is taken up and processed, giving rise to glycopeptide epitopes that can be detected by the Tcarb on the cell surface in association with MHCII. Recent studies showed that Tcarbs-mediated immune response yields protective immunity in controlled *in vivo* models through either depletion or adoptive transfer of Tcarbs. In addition, Kasper showed that three out of four glycoconjugate vaccines induced adaptive immune response regulated by Tcarbs. But still, the mode of action is not fully understood, and the characterization of more Tcarbs on different models or the structural requirements for MHCII-dependent carbohydrate presentation are under investigation.<sup>20</sup>

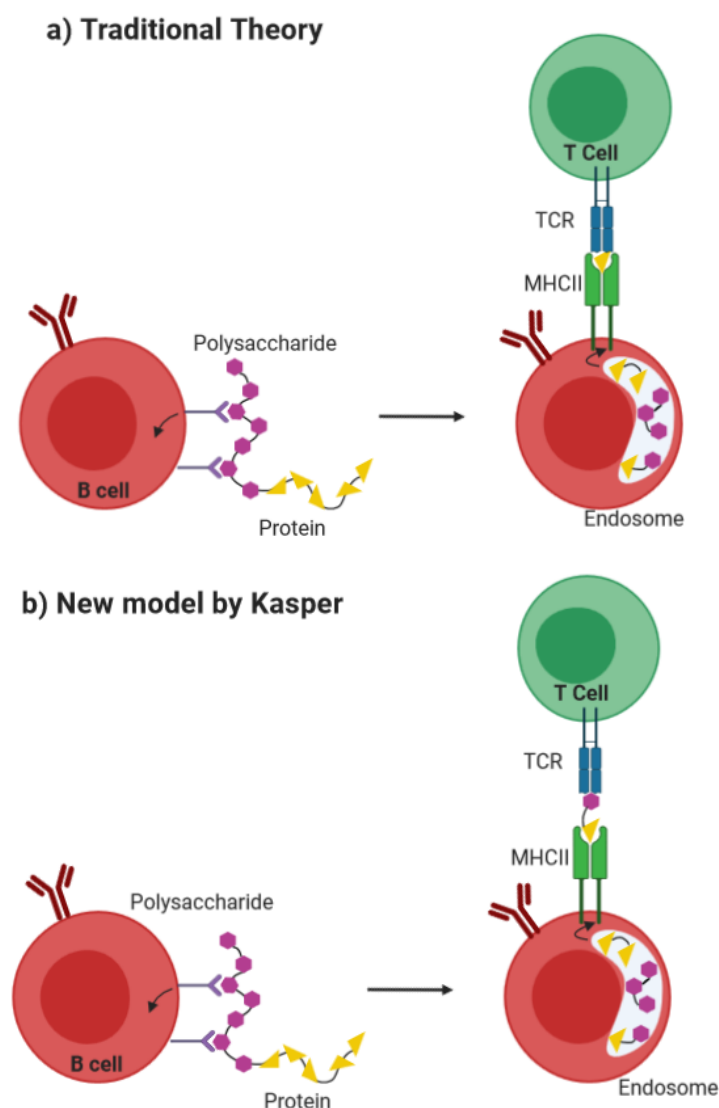


**Figure 3.** Simplified presentation of two different theories how glycoconjugate vaccines can activate B cells with the help of T-cells. a) Peptides can bind MHCII complex and the T cell. b) Small fragments containing carbohydrate and a peptide moiety are binding on the MHCII complex and the T-cell.

There are different variables which influence the immunogenicity of conjugated vaccines. The size and length of the saccharide moiety is one of the important factors which should be considered, because they have an influence on the presentation of the antigen/epitope to the immune system. Studies from Peeters et al. identified that a synthetic tetramer of *Haemophilus influenzae* type b capsular polysaccharide repeating unit, conjugated to a protein induced antibody levels comparable to the commercial Hib conjugate.<sup>21</sup> This observation was also confirmed by recent studies by Seeberger et al..<sup>22</sup> The ratio of polysaccharide and protein is a further crucial factor. Recent studies evidenced that these two parameters, i.e. the saccharide chain length and the sugar loading on the protein, are strictly interconnected. Kasper et al. studied the effect of the molecular size of the conjugate and the degree of polysaccharide: protein crosslinking. It was confirmed that for GBS (Group B streptococcus) type 3 conjugated to Tetanus Toxoid (TT) immunogenicity increased with molecular size of the polysaccharide and with the molecular size of the polysaccharide used for conjugation.<sup>23</sup> Furthermore, high crosslinking decreased the level of protective epitopes. Another important characteristic for the immunogenicity is the spacer, which is often used to link the polysaccharide to the protein carrier. Some studies suggest that a rigid spacer such as cyclohexyl maleimide may induce an anti-linker immunological response eliciting undesired antibodies, while the target epitope is ignored. The nature of the protein carrier plays also a key role. Multiple times it has been reported that a faster antibody response to a glycoconjugate can be induced, when mice or humans are primed with two different carrier proteins to those which had not been primed. Though this observation is not always noted, and it can also not be explained. Carrier proteins employed in currently licensed glycoconjugate vaccines are CRM<sub>197</sub> (cross-reacting material 197, a non toxic variant of the diphtheria toxin), tetanus toxoid (TT), diphtheria toxoid (DT), outer membrane protein complex and nontypeable *Haemophilus influenzae* protein D (PHiD). Nowadays, glycoconjugates use mostly CRM<sub>197</sub> or tetanus toxoid as carrier proteins.<sup>20,24</sup>

Costantino et al. reviewed the factors, which may induce immunogenicity of meningococcal vaccines. Besides the crucial variables mentioned above, the formulation of the vaccine is an additional parameter which might affect the immune response.<sup>25</sup>

## 2 Vaccines and its success

### 2.1 History of vaccines

In 1900, life expectancy in the U.S. was lower than 50 years old and often diseases such as pneumonia, influenzae, tuberculosis, diphtheria, smallpox, pertussis, measles and typhoid fever decreased the chance of survival and led to early mortality. A study between 1924 and 1988 describes that as a result of vaccination, many infections were prevented worldwide: 35 million cases of measles, 40 million cases of diphtheria, and a total number of 103 million cases of childhood diseases. In 2008, life expectancy increased to 78.7 years and heart diseases and cancer became the leading causes of death. Additionally, the highest decrease in mortality was seen for children and young adults, which were previously the most affected. Globally, we can say that vaccination, together with the hygiene practice and antibiotics improved our living standard tremendously. According to the World Health Organization (WHO) the development of vaccines saves every year more than 2.5 million people.<sup>26</sup>

In **Figure 4**, a brief history of the development of vaccines is summarized. Everything began with the first written record of immunity in 430 BCE during the plague of Athens in Greece. In *the History of the Peloponnesian War*, Thucydides described that a disease killed one-third of the population during the second year of war between Athens and Sparta.<sup>15</sup>

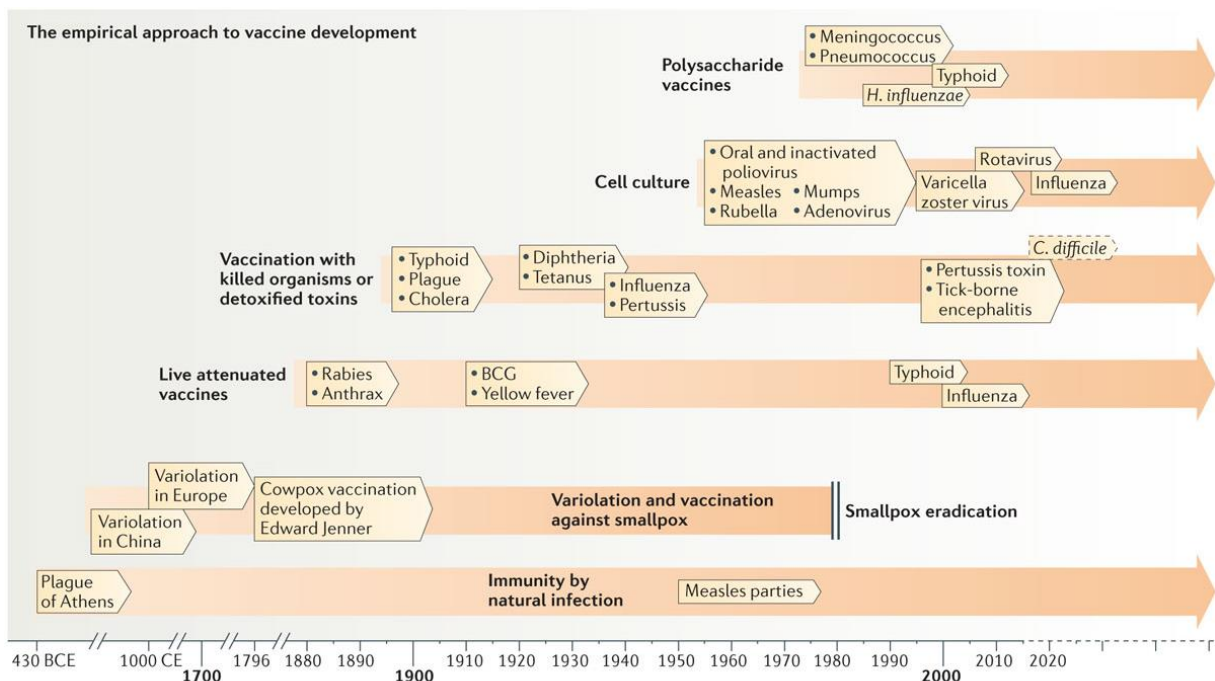


**Figure 4.** Development of different vaccine approaches in the historical timeline.<sup>15</sup>



The infection in Athens induced disorder for the law, women were not any longer obliged from their tight customs and people lost their religious belief. Thucydides reported also, that affected people never got the disease a second time. Still today, it is unknown whether the plague of Athens was caused by typhoid fever, epidemic typhus, bubonic plague, smallpox or even something else. The first report of an immunization being used to protect against infections comes from China in the tenth century. Chinese physicians found nasal inoculation of susceptible persons with material from smallpox lesions could raise immunity. Within this 'variolation' (Latin *varius* means spotted) pustules which were affected by a mild smallpox were dried and then blown into noses of infected people or were inoculated into scratched skin. The practice became known in several other regions, including Africa and India, prior to the 17<sup>th</sup> century and in western Europe variolation gained its popularity in the 18<sup>th</sup> century. After inoculation, children were mostly affected by severe symptoms which continued for the next seven to eight days with high fever, senseless speech and shooting pain in the armpits. When the variolation was successful individuals showed full protection against smallpox after 3 weeks. But this method was not safe and immunity was not assured, often people perished and it did not prevent the smallpox infection from spreading.<sup>15</sup>

In 1796, variolation was further improved by Edward Jenner, an English physician. He noticed that milkmaids, after exposed to cowpox, showed immunity to infections of smallpox. Using cowpox could achieve the same results in variolation, but with much less side effects. In a textbook of the 20<sup>th</sup> century the vaccination process is described as following:

*A spot, usually on the upper arm, is scraped by a lancet, so that the outer layers of the epidermis are removed; the spot is then rubbed with an ivory point, quill or tube, carrying the virus. A slight and usually unimportant illness or indisposition follows, and the arm is sore for a time, a characteristic scar remaining.*<sup>27</sup>

This is known as official birth for vaccination. The name vaccination comes from *vacca*, the Latin word for cow. But Edward Jenner was not aware of the origin of the infections and no mechanism of action of his vaccine was known to this time. This was changed by Robert Koch and Louis Pasteur, when discovered that infectious diseases are caused by microorganism. Pasteur was the first scientist developing attenuated vaccines by drying, heating, exposing them to oxygen or passing them in different animal hosts. The first human vaccine which was developed with this mechanism contained a rabies virus, which was grown in a rabbit spinal cord and attenuated by exposure to air. Even if the immunization process was not safe, the procedure became known and people from all over the world (e.g. Europe, Russia and U.S.) came to Pasteur to get vaccinated.<sup>15</sup>

A few years later, it was discovered that tetanus diphtheria is caused by bacteria, and Emil von Behring and Shibasaburo Kitasato made a breakthrough that serum of animals, which were inoculated, could protect humans from infections. Then an attenuated vaccine against tuberculosis with the commercial name Bacille Calmette-Guerin (BCG) was licensed. Up to this day, BCG is the only clinically vaccine against tuberculosis. In the early 1900s, attenuated vaccines became more popular and more of them were developed i.e. against typhoid fever, plague and cholera and a few decades later against pertussis. In 1924, Gaston Ramon in Paris and Alexander Glennie in London, published a chemical inactivation method of toxins and this led to the discovery of a vaccine against diphtheria and tetanus. These two vaccines are up to today still available and currently used. The influenzae virus was found to be grown in embryonated eggs and until now, this procedure is known to produce vaccines against influenzae. In the 1940s scientist discovered that viruses can be grown in *in vitro* cultures of animal cells and this breakthrough was followed by novel developments of many vaccines such as poliomyelitis, measles, mumps, rubella, varicella, hepatitis A.<sup>15,26</sup>

Smallpox infections are furthermore a perfect example of how effectively a vaccine can control an outbreak. Smallpox is caused by the variola virus which is a DNA virus of the genus *Orthopoxvirus*. After 10 to 14 days of incubation period, the infected individuals develop symptoms like fever, malaise and headache followed by a maculopapular rash. These lesions turn into pustular after one to two days. The mortality rate is about 30%, whereas most of the deaths occur during the second week post-infection. After developing a technique to produce a heat-stable, freeze-dried vaccine, the first large smallpox eradication effort was started in 1950 for the U.S. and later global eradication of smallpox was directed by D.A. Henderson. Even if in developing countries 80% of vaccine coverage was not achieved, a strategy called surveillance-containment or ring vaccination showed its success. Within this strategy cases of outbreaks were found and then individuals with possible contact became vaccinated. The World Health Organization declared the successful global eradication of smallpox in 1980.<sup>28</sup>

Until today many vaccines are developed and licensed on the market, but still some are used with old methods. Nevertheless, the development of vaccines constitutes an incontrovertible breakthrough in science and health. Due to the introduction of vaccines many diseases have been prevented, and the number of deadly infections has been reduced.

## **2.2 Different vaccine approaches**

The original idea of isolating, inactivating and injecting the microorganism by Jenner and Pasteur is currently obsolete and nowadays, new technologies are discovered to improve and to invent future vaccines. In 2.2 different technologies used for vaccine development are described.

### **2.2.1 Polysaccharide and Glycoconjugate vaccines**

The successful story of the antimicrobial vaccines based on polysaccharides began in 1917 by Dochez and Avery, when the capsular polysaccharide (CPS) of *Streptococcus pneumoniae* was isolated. Between 1923 and 1929 Avery and Heidelberger studied the CPS and understood its immunogenicity. In 1930, after injecting pure pneumococcal polysaccharides to patients, the first CPS-specific antibodies were discovered. Even when in the 40s carbohydrate-based vaccines were developed and licensed, the power of a vaccine was undervalued. Due to the introduction of new and effective drugs such as penicillin, chlortetracycline and chloramphenicol, the two vaccines lost their credits and no further research was performed. After emergence of antibiotic resistance, the idea of immunization with a vaccine caught on and new vaccines based on the CPS of bacteria were developed e.g. a vaccine targeting Hib. Even if carbohydrate-based vaccines showed good efficacy for individuals older than 5 years, poor immune response in newborns and children less than 5 years was observed. No high concentration of protective antibodies after a single dose in infants and young children was detected. For the Hib vaccine children less than 2 years and immune deficient people indicated some immunological disadvantages. This was even more concerning as Hib meningitis cases emerge at 3 months of age with a peak incidence at 9 months, meaning that the previous licensed vaccine was insufficient. These properties could be attributed to the use of polysaccharides as T-cell independent antigens.<sup>29,30,31</sup>

Already in 1929, Avery and Goebel indicated that the immunogenicity of the CPS could be enhanced by coupling the sugar moiety to a protein. A prepared protein conjugate of pneumococcus type 3 was successfully assembled and further studies showed poor immunogenicity in rabbits but specific antibodies after reinjection and challenge with type 3 pneumococci were found. Robbins and Schneerson assimilated this observation and developed a more efficient vaccine using the CPS of Hib coupled to tetanus toxoid as a carrier protein. With this approach the concentration of long-lived protective antibodies as well as an immunological memory in infants was improved. Soon, further vaccines targeting different bacteria were licensed.<sup>29,32</sup>

In 2000 the conjugated technology was further improved and a vaccine PCV7 (Prevenar) targeting *S. pneumoniae* and its seven serogroups (4, 6B, 9V, 14, 18C, 19F and 23F) was licensed. Prevenar is the first multivalent vaccine, i.e. directed against several serogroups and additionally, conjugated to a nontoxic mutant of diphtheria protein called CRM<sub>197</sub>. Prevenar is highly effective in children younger than 2 years, and infections caused by *S. pneumoniae* serotypes included in PCV7 were reduced after vaccination. Then, in 2010, PCV13 targeting six more serogroups of *S. pneumoniae* than PCV7 was licensed in the U.S. Nowadays, the 13-valent pneumococcal conjugate vaccine PCV13 is added in the routine national immunization programs of 138 countries according to the WHO. Additionally, other licensed glycoconjugate vaccines next to Hib and *S. pneumoniae* are *Neisseria meningitidis* and *Salmonella typhi* Vi. *Neisseria meningitidis* serotype A (MenA) is another successful example of the conjugated vaccine era. Before the introduction of a meningococcal vaccine (MenAfriVac), MenA was the leading cause of meningococcal meningitis in Africa. Due to this vaccine, meningococcal infections in the African meningitis belt were extremely decreased.<sup>31,33</sup>

There are different possibilities to obtain the desired polysaccharides. Traditionally, they are obtained through extraction from bacterial medium via growing on a specific media, harvesting and then several purification steps are necessary to obtain a pure CPS (**Figure 5**). Additionally, full length polysaccharides often undergo undesired partial hydrolysis (chemical or enzymatic).

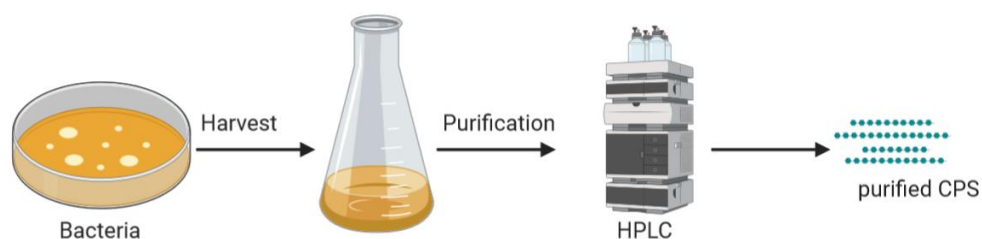


**Figure 5.** The way to obtain CPS extracted from the bacteria.

Poly/oligosaccharides from natural sources exist as heterogeneous mixtures of molecules with different degree of polymerization. These resulting oligosaccharides are size fractionated by SEC techniques and each pool is then chemically conjugated to the carrier protein.<sup>29</sup>

Even if the majority of licensed carbohydrate-based vaccines are developed using extracted polysaccharides coupled to a carrier protein, several issues are noted, especially in vaccine manufacture. The purification step is highly complicated as well as heterogeneity and traces of bacterial contaminants (e.g. endotoxins, variants containing non-protective epitopes) cannot be avoided.<sup>34</sup>

Hence, not all glycoconjugate vaccines are approved by the authorities (FDA or EMA). The yield of the conjugation and the polysaccharides conjugated to the carrier protein is often not consistent batch to batch. Moreover, the carrier protein and the linker may also be immunogenic and induce an immune response against oneself. Future vaccines will therefore avail themselves of new and more advanced techniques of molecular biology, alternative carriers and novel conjugation methods. This means new carbohydrate-based vaccines are under investigation (**Figure 6**).<sup>34,31</sup>

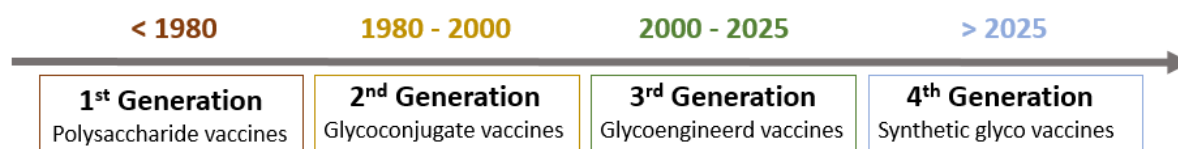


**Figure 6.** New vaccine approaches based on carbohydrates are under development.

In glycoengineered (3<sup>rd</sup> generation) vaccines two different ideas are studied. In the last decade, Protein Glycan Coupling technology (PGCT) has been developed and within this approach a E.coli cell is transformed with three plasmids in order to express the glycoconjugate protein in vivo. PGCT involves three stages, whereas in the first stage the desired glycan is expressed; in the second stage the carrier protein is designed and expressed and finally in the third stage the glycan is coupled to the protein.<sup>35</sup>

Another approach is called Generalized Modules for Membrane Antigens (GMMA), which simplify the purification of outer membrane antigens such as polysaccharides. GMMA can be used as a vehicle to deliver O-antigens to the immune system as the outside of GMMA mimic the bacterial surfaces with presentation of various exposed antigens. GMMA represent a technology with advantages such as low-cost, high-production yields and ease of technology transfer to the end manufacturer.<sup>36</sup>

Furthermore, methods in carbohydrate chemistry have improved in the last decade and making the development of synthetic carbohydrate-based vaccines a reality (4<sup>th</sup> generation). Novel glycosylation methods such as the formation of several new glycosidic linkages in one synthetic operation resulted in faster achievement of well-defined oligosaccharide-structures.<sup>37</sup> Furthermore, new approaches in automated synthetic systems such as ‘the glyconeer’ or the HPLC- assisted automated system will allow a faster synthesis of complex oligomers.<sup>38</sup> Now the approach has to be still improved as the automated system results in multi-milligram product insufficient for structural characterization.<sup>39,40</sup> Also, enzyme-catalysed oligosaccharide assembly is an interesting tool for future vaccine design. A combination of these modern techniques will provide powerful tools towards novel carbohydrate antigens.<sup>36</sup>

Vaccine candidates making use of synthetic antigens have a number of advantages. From the manufacturing point of view, shorter oligosaccharide fragments facilitate the production and especially the following purification and characterization procedures, resulting also in high reproducibility and batch-wise consistency. Furthermore, chemical modification of the polysaccharides can improve some characteristics such as stability issues.<sup>41</sup> Moreover, the synthetic manipulations enables the introduction of a linker with a functional group for further protein conjugation, leading to the development of new site-selective conjugation methods.<sup>36</sup>

Advances in the carbohydrate synthetic chemistry made it possible to synthesize complex oligosaccharides. In 2004, the first synthetic glycoconjugate vaccine targeting Hib (QuimiHib) was licensed. This vaccine is highly effective and safe in children (< 99% protective efficacy).<sup>42</sup>

Up to date, QuimiHib is still the only successful synthetic vaccine available on the market. Synthetic vaccines targeting *S.flexneri* type 2a O-PS (Pasteur Institute) and *S. pneumoniae* multivalent type 2, 3, 5, 8, 14 CPS (Max Planck Institutes) as well as the chemoenzymatic synthesis based vaccine against *N.meningitidis* serogroup X CPS (GSK-Hannover University) are currently in clinical trials or under development, and their safety and efficacy are being tested.<sup>36</sup>

Conjugate vaccines are not only studied as antimicrobial agents, but these vaccines also find application in non- infectious diseases such as cancer and Alzheimer. Vaccines for cancer are classified into prevention and therapeutic vaccines. In particular, cancer immunotherapy is mostly targeting surface proteins of cancer cells such as PD-L1, or new potential targets such as tumor-associated carbohydrate antigens (TACAs). TACAs are small oligosaccharides structurally related to blood group determinants and gangliosides. The idea is to use TACAs as target antigens in active immunization procedures. However, TACAs are poorly immunogenic, T-cell independent and their low level of expression in normal tissues is probably making them self-molecules, hence tolerated by the immune system. Several research groups are working to overcome these issues and to develop specific glycoconjugate vaccines with high effectiveness based on TACAs. Further applications of conjugate vaccines are against Alzheimer diseases and for drug abuse. These vaccines are now under development or in clinical trials.<sup>31,36</sup>

### **2.2.2 Recombinant DNA technology**

In recombinant vaccines multiple defined antigens in the pathogen are modified and a new genetic recombination is formed in the presence of an adjuvant or when the gene sequence is then expressed by plasmids or harmless bacteria/virus.<sup>43</sup>

The development of a vaccine against hepatitis B virus (HBV) emerged as a difficult task, because HBV cannot be cultivated in the laboratory and so the virus could not be grown and inactivated like in the original idea of Jenner. The scientist Hilleman developed a vaccine by purifying and inactivating virus-like particles (VLPs) which are present in the plasma of chronically infected individuals. The vaccine showed efficacy, but infected individuals were required to generate the vaccine. Then, recombinant DNA technology became available and scientist at the University of California in Berkeley cloned the gene which encodes the surface antigen of HBV in yeast. This breakthrough was responsible for the successful assembly of HBV antigens in VLPs which were antigenically identical to those from the infected individuals. This technique was further commercialized by Merck and GlaxoSmithKline and the HBV vaccine is the first example in which no microorganisms were cultivated. Nowadays, for the development human papilloma virus 16 (HPV 16) and HPV 18 causing cervical cancer, this method of recombinant VLPs is used. Moreover, VLPs found their application in many other research areas such as influenzae virus, respiratory syncytial virus (RSV), norovirus and parvovirus are currently in early-phase clinical studies. Furthermore, recombinant DNA technology is also used in the field of bacteriology to remove the toxicity from toxins. An example is the inactivated whole-cell pertussis vaccine, because of its real and purported side effects such as fever and encephalopathy. Using recombinant DNA technology, the pertussis toxin was detoxified by cloning and sequencing the operon of five genes. This operon is encoding the gene and then two amino acids in the active side of the toxin were selectively introduced. With this mutation the bacteria are not producing the pertussis toxin anymore and the vaccine became much safer. Clinical trials showed high efficacy and this formulation is tenfold more immunogenic than the one with a chemically detoxified toxin and additionally, long-term immunity was noticed.<sup>15</sup>

A huge advantage of recombinant vaccines is their purification, so that undesired contaminants are prevented, and a sufficient amount of antigen for the vaccine can be easily expressed.

### **2.2.3 A genome-based antigen approach called reverse vaccinology**

Another successful approach for the development of new vaccines is called 'reverse vaccinology'. In reverse vaccinology, the genome sequence of the pathogen is screened and possible proteins as antigens are predicted by computer analysis. This approach has its origin with *Neisseria meningitidis* serogroup B (MenB).<sup>44</sup>

MenB causes worldwide more than 50% of all meningococcus infection cases. Its capsular polysaccharide is composed of an ( $\alpha$ 2 $\rightarrow$ 8)-linked polysialic acid, which is also expressed on human glycoproteins, hence the immune system recognizes the polysaccharide as self-antigen and no antibodies are produced. After sequencing and analysing novel potential antigens based on a peptide structure, the antigens were cloned and expressed in *E.coli*. Within immunization studies, three antigens were selected and combined with outer membrane vesicles (OMV) to gain a stronger immune answer. Since 2013, this vaccine is the first example developed by reverse vaccinology and is very successful. Nowadays, other vaccine candidates against bacteria which showed antibiotic-resistance e.g. *Staphylococcus aureus* or many others use this genome-based antigen approach.<sup>15</sup>

In 2016, a new era of vaccinology was emerged: reverse vaccinology 2.0. Within this approach protective human antibodies are screened, different B-cells are sequenced and their corresponding antigen specificity and epitope are studied extensively.<sup>45</sup> One successful example which can be named here is the respiratory syncytial virus (RSV) fusion protein (F). Due to the reverse vaccinology 2.0 a more efficient antigen against this pneumovirus for further vaccine development was found in less than 5 years and its clinical trials are currently on-going.<sup>46</sup>

Another successful example concerns the development of a vaccine against the Human immunodeficiency virus (HIV). Therefore, germline-targeting (GT) antigens are needed and due to the potential of reverse vaccinology 2.0. these antigens are identified, characterized, and further human monoclonal antibodies produced by infected or vaccinated humans are used to design antigen-derived peptides. These peptides aim to tailor the antibody immune response and are currently under clinical investigation.<sup>47</sup>



### **3 The bacteria *Haemophilus Influenzae***

#### **3.1 General overview**

The bacteria *Haemophilus influenzae* (Hi) was first isolated from the sputum of individuals with influenza pneumonia during the influenza pandemic 1889-1892 by Robert Pfeiffer. Due to this observation it was misbelieved that the bacteria cause influenzae. Forty years later, the vital etiology of influenza became known. In 1920 the Society of American Bacteriologists renamed the bacteria *Haemophilus influenzae* to acknowledge the history of the first isolation (Greek: *haemophilus* means 'blood-loving').<sup>48</sup> Dr. Margaret Pittman identified capsulated and non-encapsulated strains in 1931 and capsulated ones can be further subdivided into 6 serotypes (a-f) according to the structural diversity of the capsular polysaccharide.<sup>49</sup>

However, *Haemophilus influenzae* is a facultative anaerobe and has an absolute requirement of the growth factors NAD (factor V) and a source of hem (factor X). Additionally, the bacteria *Haemophilus* only host humans and are present in the respiratory tract of more than 90% of the population older than 1 year, 49% of which are carrier of Hi and 6.6% are encapsulated. Interestingly, around 20% of infants are colonized in the first year of life, and this rises over time. More than 50% of children between 5 to 6 years are carrier of Hi and this outlook is growing. Furthermore, children are mostly colonized by more than one strain, whereas adults are mainly infected by one strain only.<sup>50</sup> Even if for most of the carrier the bacteria are not dangerous, for a small percentage they can be life threatening. Furthermore, also young children are carriers and this can lead to fast disease transmission (e.g. day care centres), as a single isolate can be passed to several individuals simultaneously. Normally, the bacteria are spread by airborne droplets and contact with secretions. However, infections caused by different serotypes or non-encapsulated remains a challenge.<sup>49</sup>

The epidemiology of Hi depends on a successful colonization of the nasopharynx to cause severe diseases. The time between infection and the appearance of symptoms is between two and ten days, but the correlation between carriage and disease developing is not understood. Three factors have been found to increase risk for development of severe symptoms: lack of antibodies, the size of bacterial inoculum and the presence of viral infections.<sup>51</sup>

The nasopharyngeal mucus, where Hi is attached, is also one of the first line of defence against pathogens. The human body has developed a system to protect the respiratory tract which is called 'mucociliary escalator'. Within this system, the cilia on the surface of epithelial cells move forward and backward and due to this controlled movement mucus and any bacteria trapped within are propelled out. The bacteria Hi can escape the escalator by its cytotoxic nature.<sup>49</sup>

In **Figure 7** the main stages for the development of invasive diseases are summarized.

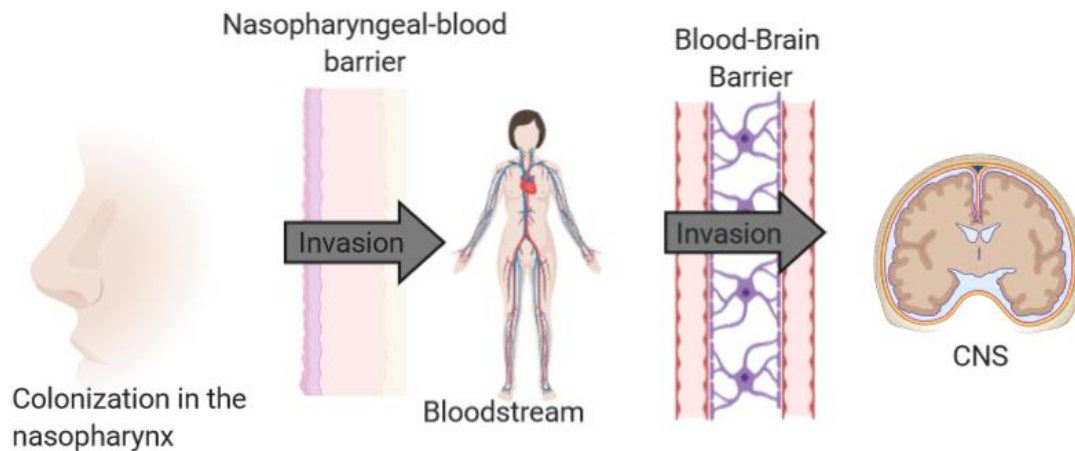


**Figure 7.** Development of invasive disease with *Haemophilus influenzae*.

Moreover, Hi is selectively linked to non-ciliated cells, and after passing tight junctions, the bacteria get access to the submucosa. Afterwards, the mucosal area is crossed, Hi is exposed in the bloodstream where also the corresponding host immune defence is present. The mechanism how Hi enters the subarachnoid space and then the central nervous system is unclear. Probably the port into the CNS is the choroid plexus.<sup>49</sup>

After entering into the bloodstream, the bacterium is exposed to the human immune system. Hi, as well as other bacteria, has however developed the so-called virulence factors to challenge and escape the immune system. The capsular polysaccharide, typically expressed by encapsulated strains, is one of the virulence factors. The capsular polysaccharide (CPS) of Hi is the major virulence factor for serotype b. This CPS is composed of linear teichoic acid containing ribose, ribitol and phosphate. This carbohydrate layer is on the outside of the bacteria surface, and its functions like resistance to desiccation, adherence, resistance to nonspecific and specific host immunity are important features as virulence factors. Another virulence factor is the pili, which is found in serotype b of the encapsulated and in almost half of the non-encapsulated strains. By binding to glycoproteins, pili can stimulate the attachment of bacterial cells to eukaryotic cells and cause agglutination of red blood cells.<sup>52</sup> Outer membrane proteins as well as lipopolysaccharides are also important virulence factors for Hi. In particular, Hi has six to eight outer membrane proteins and two of them have been studied as antigens in future vaccine design for non-typeable strains.<sup>53, 54</sup>

Within all these virulence factors, the bacterium challenges and tries to overcome the human immune system to cause mainly pneumonia and meningitis.

### 3.2 Diseases and their treatment

Hi pathologies are divided into invasive and non-invasive disease. Invasive diseases are defined as isolation of Hi from a sterile site such as blood, synovial fluid or cerebrospinal fluid and are mostly caused by encapsulated Hi strains. For non-invasive diseases, non-encapsulated Hi strains are responsible and Hi is isolated from non-sterile sites such as the external ear. Moreover, common medical conditions such as otitis media and sinusitis are mostly not life threatening.<sup>55,56</sup>

Serotype b (Hib) is the most virulent strain and it is responsible for the majority of serious invasive infections. Meningitis is an invasive disease caused by Hib and if untreated, it will lead to death. The most severe manifestation of Hib diseases is bacterial meningitis followed by pneumonia. But Hib can also cause other diseases such as septicaemia or epiglottitis. In the absence of vaccination, studies showed that Hib is the most common cause of bacterial meningitis in children under 5 years (**Figure 8**).<sup>57</sup>

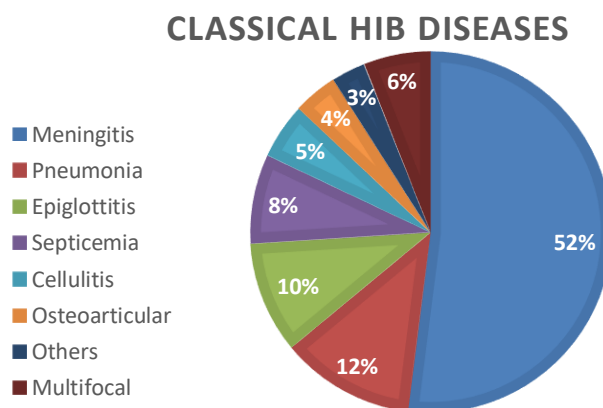


**Figure 8.** Classical Hib diseases worldwide (excluding nonbacteremic pneumonia).<sup>58</sup>

A post-vaccination study carried out between 2007 and 2014 in 12 European countries reported 10.624 cases of invasive *H.influenzae* disease. This is an annual notification rate of 0.6 cases/100.000, but by country the rate changed from 1.6 cases in Norway to 0.1 cases in Cyprus. In this study, also the clinical presentation was reported. Most of them had septicaemia (61%), bacterial pneumonia (18%), meningitis (9%), osteomyelitis (1%), meningitis and septicaemia (1%), cellulitis (1%), epiglottitis (1%) or other (8%).<sup>59</sup> Non-typeable strains are often associated with acute otitis in children and sinusitis in adults and children and pneumonia is often reported. But also invasive diseases are caused by non-typeable strains.<sup>60</sup>

Normally, *H.influenzae* is treated by oral antibiotics such as  $\beta$ -lactams, whereas some strains produce  $\beta$ -lactamase and then other antibiotics are given (e.g. cephalosporins, amoxicillin-clavulanic acid). In

Spain and Japan,  $\beta$ -lactamase negative, ampicillin-resistant strains are prevalent. So far, only a vaccine against serotype b is available, but further studies targeting NTHi are under development.<sup>61,62</sup>

### **3.3 Non-encapsulated species and their fear**

Non-typable or non-encapsulated *H. influenzae* (NTHi) strains lack the capsular polysaccharide layer as virulence factor. They are considered to be one of the most common commensal organisms which are colonizing the nasopharynx. Up to 20% of all infants within their first year of life are carriers of non-encapsulated strains and this number is increasing with age. After colonizing the nasopharynx, the bacteria can spread to the higher and lower respiratory tract and can cause inflammation and diseases. It is known that these strains are one of the major causes of respiratory tract infections, including acute otitis, cystic fibrosis and pneumonia as well as chronic bronchitis and chronic obstructive pulmonary disease (COPD) in the lower respiratory tract. According to Behrouzi et al. NTHi strains cause 20-30% of all episodes of acute otitis media and additionally, more than 40% of otitis media with effusion cases (chronic otitis media). For example, it is assumed that a higher density of colonization of the upper respiratory tract and the number of different isolates is linked to middle ear infections. Otherwise, studies about the role of NTHi in the upper airway microbiome are still ongoing as very little is known so far.<sup>63,64</sup>

Furthermore, NTHi strains show a high range of variability in their outer membrane proteins, to challenge additionally the host innate immune system.<sup>63,64</sup>

Studies showed that NTHi bacteria can play a role in the formation of biofilms in the respiratory tract of adults with COPD. In general, biofilms are an additional protection surrounding several bacterial cells of a polymer matrix attached to a solid surface. Within this biofilm, bacteria can develop antibiotic resistance.<sup>64</sup>

Despite of the constant rising number of infections, no vaccine targeting NTHi strains is on the market. As these strains vary, only few markers for targeting in vaccine development are known. Most of the studies focus on the immunogenic outer membrane proteins (OMP) as target such as P1, P2, P4 and P6. P2 is a potential candidate and animal studies confirmed these. Additionally, P2 has a high variability and antibodies showed high specificity. Another alternative candidate is to target protein D. Interestingly, Protein D, which is also a surface-exposed OMP, occurs in all *H. influenzae* strains (including encapsulated strains a-f). This feature makes protein D a very attractive vaccine candidate.<sup>63,64</sup>

### 3.4 Encapsulated strains

According to the capsular polysaccharide (CPS), the bacteria *Haemophilus influenzae* can be classified into 6 serotypes (a-f). These polysaccharides are located on the surface of a wide range of bacteria and are linked to the cell surface via covalent bond to phospholipid or lipid A molecules. Furthermore, their structure is organized in repeating units which can be substituted with organic and inorganic groups (e.g. phosphates). Some bacteria show a huge range of different serotypes: for example, more than 90 different serotypes have been classified for *Streptococcus pneumoniae*.<sup>54</sup>

The 6 different serotypes of *Haemophilus influenzae* are summarized in Table 1.

**Table 1.** Different CPS structures of *Haemophilus influenzae*.<sup>65,66</sup>

Type	CPS Structure	
a	4)-β-D-Glc-(1→4)-D-ribitol-5-(PO <sub>4</sub> →	
b	3)-β-D-Rib-(1→1)-D-ribitol-5-(PO <sub>4</sub> →	
c	4)-β-D-GlcNAc-(1→3)-α-D-Gal-1-(PO <sub>4</sub> )→	R: OAc (0.8), H (=0.2)
	3 ↑ R	
d	4)-β-D-GlcNAc-(1→3)-β-D-ManANAc-(1→	R: L-serine (0.41), L-threonine (0.14), L-alanine (0.41)
	6 ↑ R	
e	3)-β-D-GlcNAc-(1→4)-β-D-ManANAc-(1→	
e'	3)-β-D-GlcNAc-(1→4)-β-D-ManANAc-(1→	
	3 ↑ 2 β-D-fructose	
f	3)-β-D-GalNAc-(1→4)-α-D-GalNAc-l-(PO <sub>4</sub> →	
	3 ↑ OAc	

All the CPS consist of one disaccharide, which is linked in some strains through a phosphodiester to the next repeating unit. In serotype d and e' an additional cross-linkage to certain amino acids (L-serine, L-threonine or L-alanine) or to β-D-fructose is reported.

Serotype b in Hi is the most common and the most virulent one, followed by serotype a, which is more virulent than serotypes c-f.<sup>67</sup> Of all infections caused by *Haemophilus influenzae*, 95% were caused by type b, including cellulitis, septic arthritis, epiglottitis, pneumonia and meningitis. Especially young children between 4 months and 4 years are in high risk. Before the introduction of a vaccine against Hib, meningitis among children younger than 5 years was 54/100.000 in the United States and 23/100.000 in Europe.<sup>58</sup> The capsular polysaccharide of Hib is an important virulence factor and is composed of ribose-ribitol disaccharide linked via phosphodiester bond to the subsequent repeating unit. According to the WHO, Hib causes 7-8 million cases of pneumonia and hundreds of thousands of deaths, mainly in developing countries. The highest disease burden is known for children between 4 and 18 months of age. The number of (deadly) infections were highly reduced, when a vaccine became available and routine Hib vaccination of children was carried out.<sup>68</sup>

Nowadays, in the post-Hib conjugate vaccine era, non-Hib strains are the major cause of invasive Hi infections. A recent study showed that 69% of invasive *H. influenzae* disease in North American Arctic is caused by non-b.<sup>69</sup> Hia, Hie and Hif are the strains which are detected more frequently in certain populations.<sup>70</sup> Already in 1931, Margaret Pittman noted that a small percentage of infections were caused by Hia and Hif.<sup>71</sup> Sutton et al. showed further that Hia and Hif resist antibody-free complement-mediated bacteriolysis more than Hic, Hid and Hie strains.<sup>72</sup> Most of Hia infections are reported in the Aboriginal population in Northern America.<sup>73</sup>

Hia infections frequently occur in indigenous populations, and nowadays Hia is a leading cause of invasive *H. influenzae* disease in these populations. An outbreak was described in Alaska and data from the International Circumpolar Surveillance (ICS) program indicate an increasing number of Hia infections in Alaska as well as northern Canada.<sup>74,75</sup> Furthermore, cases described of Hia as well as of Hib are mostly affecting young children.<sup>69</sup>

A study in Europe between 1996 and 2006 was founded to investigate the epidemiology of invasive *H. influenzae* after the introduction of the glycoconjugate vaccine targeting Hib. Even after the introduction of the vaccine, infections are still mainly caused by Hib, followed by Hif and Hie. The clinical presentation of both the serotypes (Hie and Hif) is similar and comparable to non-typable Hi infections. Additionally, cases are mainly described in adults with underlying conditions.<sup>73</sup>

Infections caused by Hic and Hid are very rare suggesting that they may not be particularly virulent.<sup>73</sup>

No vaccine targeting other serotypes than Hib is currently on the market.

### 3.5 Hib and the story of a successful vaccine

The CPS is the most important virulence factor of Hib and can induce immunogenicity. The first polysaccharide vaccine against Hib was based on the CPS and was licensed in the 1990s. Even if the vaccine showed good immunogenicity in adults, low antibody titers in infants did not lead to immunization against Hib. Therefore, Robbins and Schneerson developed a conjugated vaccine targeting Hib by using tetanus toxoid as a carrier protein linked with a spacer to the extracted and purified CPS. As the Hib CPS has no reactive groups such as amino groups or carboxyl moieties which can be directly linked to a protein, the hydroxyls of the carbohydrate moiety were randomly activated with cyanogen bromide (CNBr) to be converted into the corresponding cyanate esters. Further elongation was achieved by introduction of a bifunctional spacer, adipic acid dihydrazide (ADH). Eventually, condensation to tetanus toxoid as a carrier protein was carried out via carbodiimide-mediated coupling to provide the first conjugate vaccine. Connaught Laboratories used a very similar protocol with diphtheria toxoid (DT) as a carrier protein. A clinical study in Finland showed that after three injections of Hib-DT to infants 80% protection against meningitis was observed. Hib-DT (ProHIBiT) was the first glycoconjugate vaccine and it was licensed in 1987 in the U.S. for immunization of 18-month-old children.<sup>29</sup>

A study carried out in the USA, Sweden and Finland showed effectiveness of the conjugated vaccine using TT as carrier protein instead of DT. The results are displayed in **Table 2**. Furthermore, Hib-TT stimulated a 10-fold higher antibody response when compared to Hib CPS vaccine and the highest antibody subclass was IgG1. It should also be noted that after a third injection a maximum antibody concentration was measured. The glycoconjugate vaccine coupled to DT was later withdrawn from the market, as Hib conjugate vaccines using tetanus toxoid, meningococcal outer membrane protein or CRM<sub>197</sub> were more efficient and higher levels of protective antibodies were observed.<sup>29,76</sup>

**Table 2.** Antibody response in infants who were vaccinated with the age of 3 months, 5 months and 7 months (USA), in Sweden with the age of 3 months, 5 months and 12 months and in Finland aged 2, 4 and 6 months.<sup>29</sup>

Study		µg Hib CPS antibody/ml of serum			
		Before injection	After injection		
Location, n	Carrier protein		First	Second	Third
USA, 77	TT	0.06	0.60	4.85	11.0
Sweden, 82	TT	0.08	0.47	3.71	12.6
Finland, 87	DT	0.07	0.07	0.42	-

The licensed vaccines using extracted Hib CPS such as Hib-TT were around five ribosyl-ribitol phosphate repeating units long. The manufacture process was adjusted to minimize purification and reaction steps. The enormous advances in carbohydrate synthetic chemistry made it possible a synthetic vaccine in 2004 (known with the tradename of Quimi-Hib<sup>®</sup>), a real breakthrough in the field. Quimi-Hib<sup>®</sup> is the result of a collaboration between Cuban and Canadian research teams. It was developed in Cuba using a one-step polycondensation reaction of ribosyl-ribitol phosphate repeating unit based on the *H*-phosphonate chemistry. After deprotection and purification, the oligomer with average seven repeating units (red in **Figure 9**) was conjugated to thiolated TT (green) through an *N*-hydroxysuccinimidyl 3-maleimidopropionate linker (blue). This vaccine is highly effective and totally safe in children (< 99% protective efficacy).<sup>42</sup>

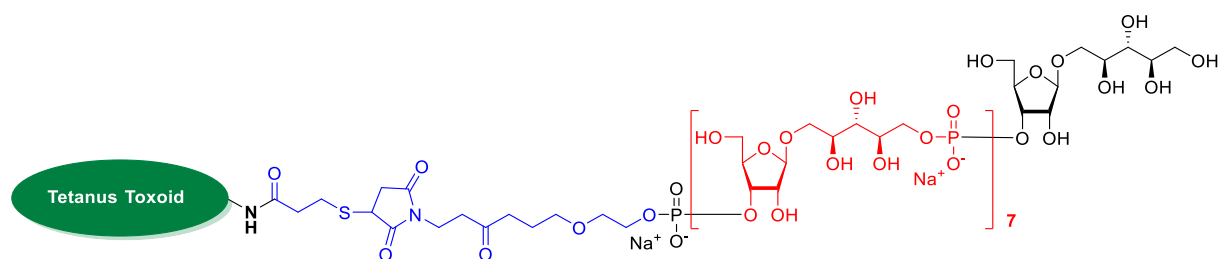


**Figure 9.** First synthetic vaccine Quimi-Hib against Hib is based on the CPS.

Up to date QuimiHib is still the only successful synthetic vaccine on the market, however the vaccine is not licensed everywhere.<sup>36</sup> In Europe, four different monovalent Hib conjugates containing the polyribosyl-ribitol phosphate (PRP) as antigen linked to a protein carrier are available on the market and they are all based on CPS extracted from the bacteria.<sup>77</sup> All four Hib vaccine types are highly efficient and reduced infections caused by Hib. PRP-OMPC vaccines have special use in populations at higher risk of early-onset disease e.g. Alaskans and Aboriginal Australians.<sup>34,78,79</sup>

Starting from 1990, the number of European countries with routine Hib immunization programs increased and demonstrated high efficacy against Hib disease after primary vaccination. In 1986, Finland was the first European country introducing a monovalent conjugate Hib vaccine, followed soon after by Iceland and other countries in Scandinavia. In 1993 the first combined vaccine DTPw with Hib was approved followed by DTPa/Hib in 1996. Now several hexavalent vaccines containing Hib are licensed in Europe mostly containing Hib-TT. From a missing booster campaign in the United Kingdom, we learned that a booster vaccination after a DTPa/Hib vaccine combination is necessary not to lose herd protection. This experience also underlines the importance of ongoing surveillance to identify and early detect new outbreaks.<sup>78</sup>



Before the introduction of a Hib vaccine, 23/100.000 cases of Hib meningitis were reported in Europe.<sup>58</sup> Owing to the success of the vaccine, infections caused by Hib decreased within the vaccine coverage in Europe.

In **Figure 10**, the notification rate in Europe by age is reported. While in the population older than 65 years no significant change was observed, young children below one year old avail oneself by the introduction of the vaccine and a rate of 0.29/100.000 for 2014 is reported. Furthermore, the average European coverage of three doses of any Hib vaccine was 85% in 2014.<sup>78</sup>

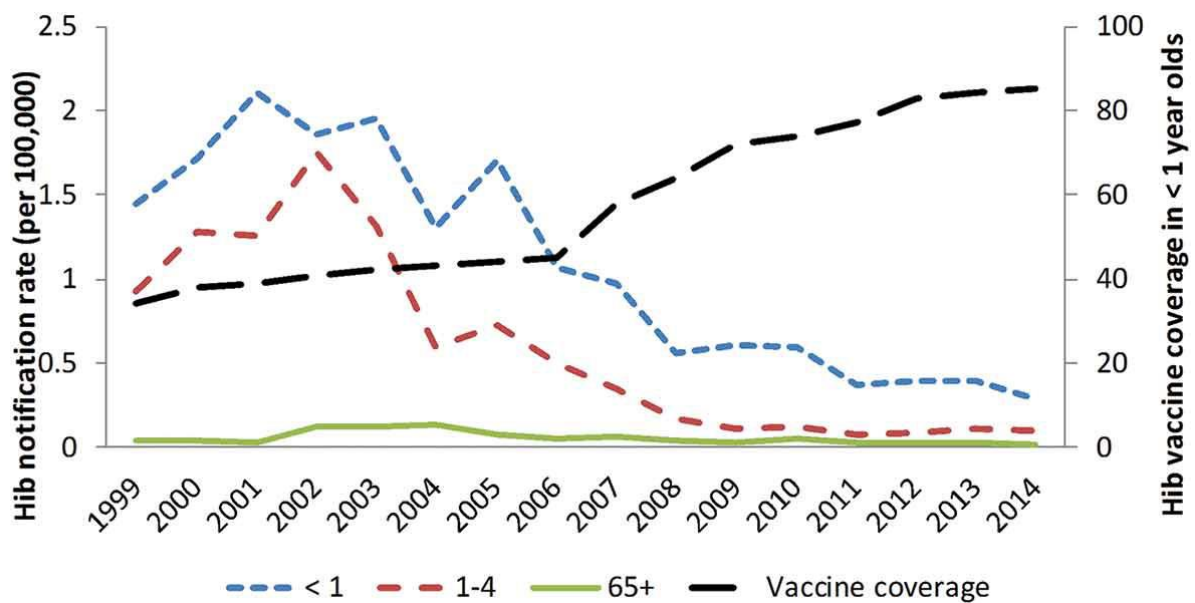


**Figure 10.** Notification rate of Hib infections by age distribution.<sup>78</sup>

The introduction of Hib vaccine was a wide success worldwide. A study in the U.S. showed that infections caused by Hib decreased from the pre-vaccination level of 41/100.000 children per year (1987) to 1/100.000 children per year (1997). Overall cases in the U.S. were lowered by 98% among children 4 years of age or younger. Before the introduction of a vaccine, 19.500 Hib cases were described in the U.S., and now only 300 cases are reported. It also has to be stated that in low income countries the Hib vaccine was later and slower introduced in the routine vaccination programs. This has been mostly due to high vaccine costs and underestimation of Hib disease. But when the vaccine was available, it also showed great effectiveness. Successful studies were also reported in Kenya, where the vaccination against Hib reduced the incidence of invasive disease by 88% within three years. In Bangladesh, the vaccination program prevented over one third of Hib pneumonia cases and more than 90% of meningitis cases. In Uganda, experts estimated that within four years after the introduction of the Hib vaccine, infection were weakened by 85%. Even if these studies show the high

efficacy of the conjugate-polysaccharide vaccine against Hib, the worldwide Hib vaccination coverage was described at only 28% in 2008. This value represents an increase from the 8% in 1999, but the global coverage is still low.<sup>58,80, 81</sup>

## 4 Studies towards a future vaccine targeting Hia

### 4.1 Increased cases of Hia and the theory of serotype replacement

While worldwide vaccination programs nearly declined infections caused by Hib, concerns were raised about a potential serotype replacement by non-type b strains. The rapid decline due to Hib vaccination might increase colonization by non-type b strains with the potential to become invasive. This phenomenon is known as serotype replacement and is discussed for *Haemophilus influenzae* type b. Especially, the increasing amount of cases reported by type a is noted (**Figure 11**).<sup>69</sup> Serotype a is the second most virulent strain of *Haemophilus influenzae* and can cause as Hib invasive diseases like meningitis, bacterial pneumonia and septic arthritis mainly in children below 5 years of age. As previously discussed, CPS is often considered as very important virulence factor of Hib and is used as antigen for the development for a vaccine. The CPS of Hia and Hib is very structurally similar, but no cross protection is observed. This means that vaccines based on the CPS of Hib cannot protect against infections caused by Hia.<sup>82</sup>

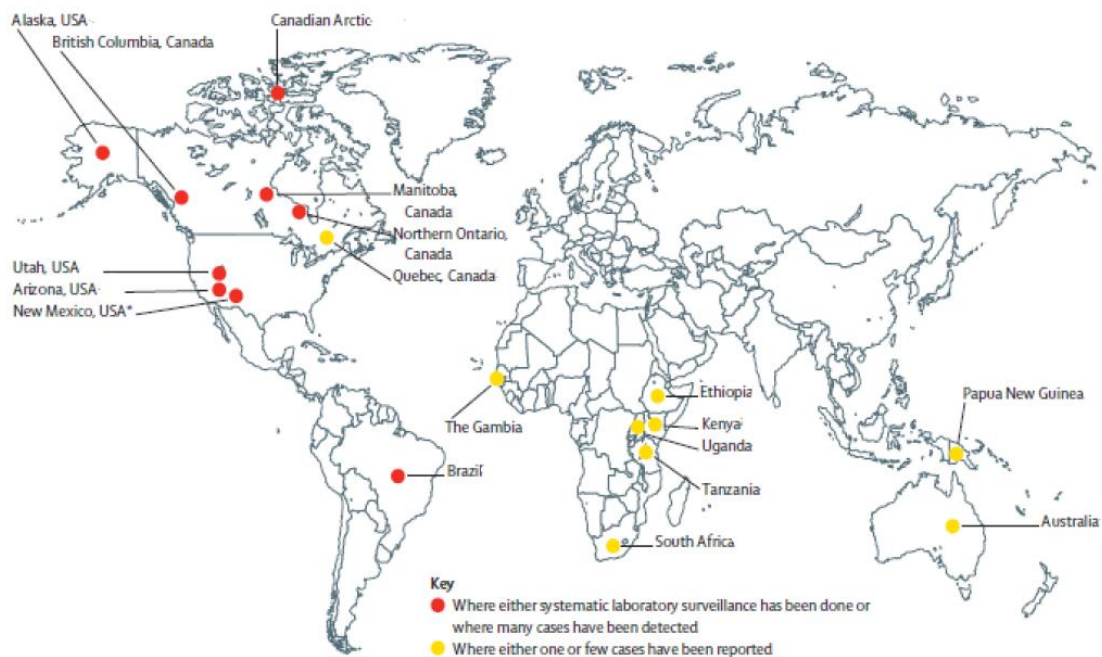


**Figure 11.** Worldwide distribution of invasive *Haemophilus influenzae* type a infections.<sup>83</sup>

In some North American Indigenous population infections caused by Hia are gradually increasing and have become now, in the post-Hib vaccine era, the new major cause of invasive disease. A study in Utah reported an annual incidence of invasive Hia disease increased from 0.8/100.000 (1996) in children and teens under the age of 18 years to 2.6/100.000 in 2008. Additionally, increasing incidence of invasive Hia disease are noted in Navajo and White Mountain Apache populations in southwestern USA and Alaska as well as in Northern Territories and western Provinces in Canada (Manitoba, Saskatchewan and British Columbia). Also, in Brazil and Papua New Guinea cases of invasive Hia disease are reported. Furthermore, up to now four outbreaks of invasive Hia disease are reported. Two of them in Alaska in 2003 and 2009-2011. In Nunavik, northern Canada, one was described in 2012-2013 and the fourth one was reported in New Mexico. In summary the cases of Hia are increasing and currently most of the cases are described in Indigenous people.<sup>82,83</sup>

The reason why indigenous individuals show a higher susceptibility for invasive Hia disease is unclear, but might include genetic, environmental and/or socioeconomic factors. Worldwide infections caused by Hia are still rare and data about serotype information are mostly missing in some countries. For example, in most of Asian and African countries systematic studies and serotype detections are missing, which makes it difficult to understand the exact number of cases caused by Hia.<sup>84</sup>

So far, no vaccine targeting Hia is on the market. However, a group of scientists are working already on a vaccine targeting Hia by using extracted polysaccharides from the bacteria. Cox et al., reported the preparation of the extracted CPS and the preparation of two glycoconjugate candidates. The polysaccharide was activated by oxidation of the vicinal hydroxyls of the ribitol that were further coupled to the carrier protein CRM<sub>197</sub> or to the protein D via direct reductive amination. No spacer to link protein and polysaccharide was used. Rabbits and mice models showed both promising outcomes, and antibodies which can facilitate bactericidal killing of Hia strains were detected. Interestingly, protein D conjugates generated an immune response to protein D in addition to the Hia CPS, but the resulting titers were smaller in comparison to CRM<sub>197</sub> conjugates. In the study from Cox et al. CRM<sub>197</sub> proved to be a more appropriate carrier protein compared to protein D, but further studies with different carrier proteins such as tetanus toxoid, diphtheria toxoid and Neisseria outer membrane protein complex are still missing.<sup>85,86</sup>

The ideal vaccine against the vast majority of Hi infections would be a bivalent formulation targeting both Hib and Hia, following the successful example of polyvalent vaccines against *Streptococcus pneumoniae*. Prevnar-13 is a conjugated vaccine targeting 13 different serogroups to provide comprehensive coverage of 85% of important pneumococcal serotypes.<sup>87</sup>

Moreover, extracted polysaccharides in vaccine manufacturing show some disadvantages and novel vaccine approaches are needed, such as synthetic vaccines. As far as we know, no synthetic vaccine targeting Hia is on the market nor under development.

## 4.2 State of the art synthesis of CPS of Hia fragments

The CPS structure of Hia was published in 1977 and studied by NMR by Branefors-Helander. The structure is composed of 4-O- $\beta$ -D-glucopyranosyl-D-ribitol residues joined through a phosphodiester between O-4 of the glucose and O-5 of the ribitol.<sup>88</sup> The structure shows high similarity to the CPS of Hib (**Figure 12**), but the synthesis of Hia is hardly studied compared to the well-known synthesis of Hib CPS.

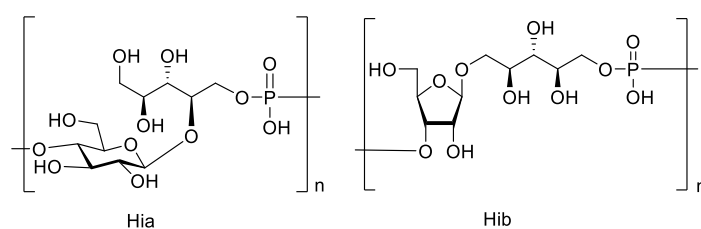
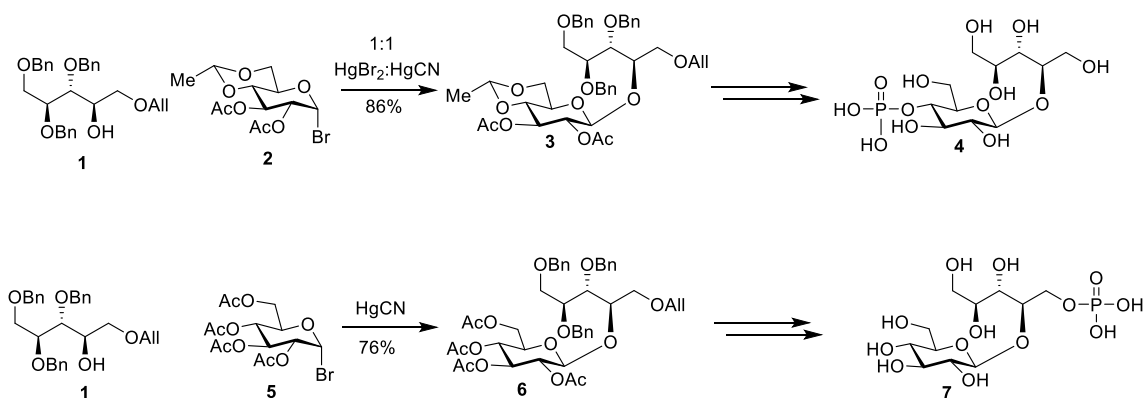


**Figure 12.** The CPS structure of Hia and Hib are highly similar.

More than 10 years after the paper of Branefors-Helander, a synthesis of repeating units with different positions of the phosphate was described (**Figure 12**).

The acceptor 5-O-allyl-1,2,3-tri-O-benzyl-D-ribitol **1** was synthesized starting from 2,3-O-isopropylidene- $\beta$ -D-ribofuranoside in a six-step synthesis. Glycosylation of acceptor **1** with a bromide donor **2** in the presence of 1:1 mercuric bromide-mercuric cyanide gave the desired disaccharide **3** in 86% yield. The phosphate moiety was introduced via diphenylphosphoro(1,2,4-triazolide) in good yields and after deprotection compound **4** was successfully obtained. Disaccharide **6** was synthesized by a similar approach using again a bromide donor with acceptor **1** in the presence of mercuric cyanide. Phosphorylation was obtained again using diphenylphosphoro(1,2,4-triazolide). Hence deprotection led to the final molecule **7**.<sup>89</sup>



**Scheme 1.** First and only synthesis for one repeating unit of Hia CPS published by Grzeszczyk in 1987.<sup>89</sup>

This is the only published synthesis of Hia CPS fragments to date, and due to the lack of orthogonal protecting groups further elongation and synthesis of longer fragments is not feasible using this approach. Furthermore, no linker for protein conjugation was introduced and no preliminary biological studies have been reported.

### 4.3 Prospects within this thesis

Seeberger et al. published recently a study explaining the correlation between oligosaccharide chain length and the immune response towards the CPS of Hib. The synthesis of well-defined oligosaccharides of up to 10 repeating units additionally modified with a linker and further conjugated to CRM<sub>197</sub> was reported.<sup>22</sup> The results indicated that four repeating units were sufficient to induce immunogenicity. The close structural resemblance of Hib and Hia CPS suggested that the two polysaccharides might have similar structure-immunogenicity relationship.

No synthesis of fragments longer than one repeating unit of Hia CPS has been reported as well as no epitope studies are known. Although the currently poor epidemiological relevance of Hia infections, the aforementioned phenomenon of the serotype replacement raised concerns that a vaccine targeting Hia might be needed in the future.

Our aim was to provide preliminary results for a CPS-based semi-synthetic glycoconjugate vaccine targeting Hia (**Figure 13**). We aimed to synthesize well defined oligosaccharides of the CPS of Hia with up to five repeating units using state of the art methodology.

The synthesis of our target oligomers was highly challenging and had to be planned in advance. For the disaccharide as repeating unit orthogonal protecting groups were studied and novel glycosylation approaches to join the ribitol (marked in blue, **Figure 13**) with the glucose moiety (marked in red) were reviewed. The phosphodiester (marked in green) combines two disaccharides and the coupling of two repeating units for the CPS of Hia had never been described in the literature. Furthermore, the oligosaccharides bear a linker (marked in orange) for further conjugation to a carrier protein.

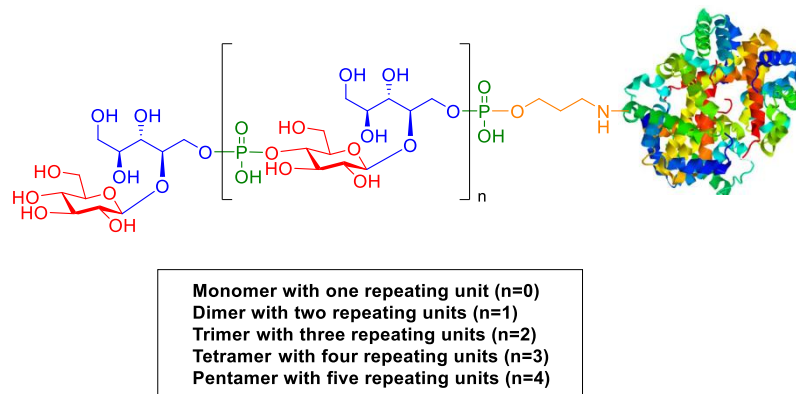


**Figure 13.** Our synthetic aim is the synthesis of different well-defined oligomers conjugated to a protein carrier with up to five repeating units.

The project was part of a European Training Network (ETN) funded in the framework of H2020 Marie Skłodowska-Curie ITN programme with the aim to rationally design well-defined and innovative glycoconjugate vaccines. In this project eight academic groups and two industrial partners were involved and within the project of the synthesis of Hia CPS fragments three partners are cooperating. The synthesis was carried out mostly at the University of Milan under the supervision of Prof. Luigi Lay and Dr. Laura Polito as well as at the Leiden University under the supervision of Dr. Jeroen Codée. The resulting oligomers were conjugated to a protein carrier (CRM<sub>197</sub>) and preliminary biological studies with the aim to identify the minimal protective epitope will be performed in cooperation with GSK (GSK Vaccines, Dr. Roberto Adamo and Dr. Maria R. Romano).

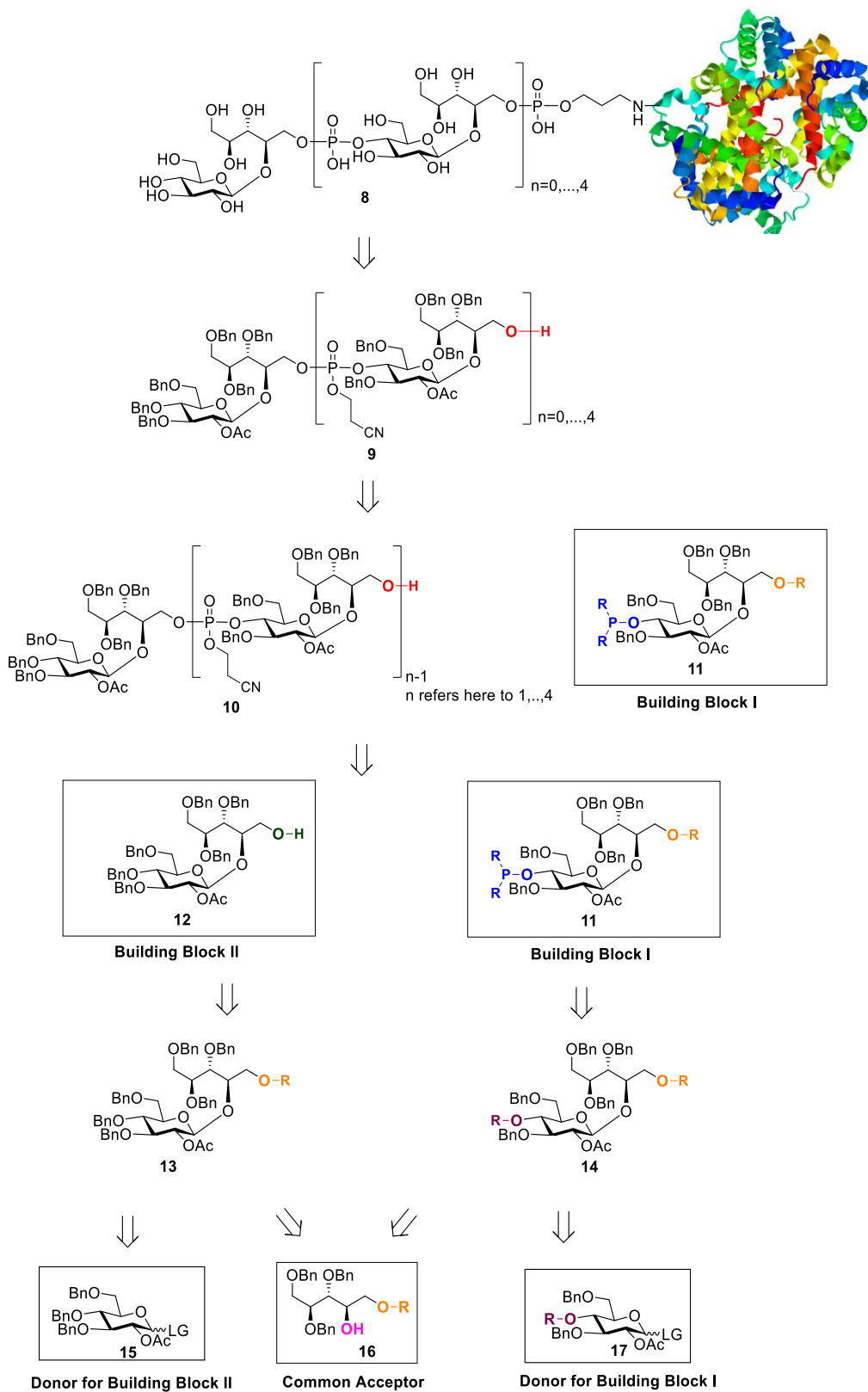
## 5 Our Synthetic approaches

### 5.1 Retrosynthetic Analysis

Initially, we designed a retrosynthetic approach for the preparation of different well-defined fragments of Hia CPS. The number of building blocks should be as little as possible to reduce the number of synthetic steps. In **Scheme 2**, the retrosynthesis to obtain defined fragments of the Hia CPS conjugated to a carrier protein is described.

Protein conjugation was achieved by using the amine function on the linker to covalently bind each fully deprotected oligomer to a protein carrier. Furthermore, the C3 linker was introduced using P(III)-chemistry on the protected oligomer **9**. In our approach we planned to obtain compound **9** with  $x$  repeating units ( $x = 1, \dots, 5$ ) from the previous oligomer **10** ( $n-1$ , whereas  $n$  refers to 1-4) using Building Block I (disaccharide **11**). Building Block I is an important intermediate, which will be required in every elongation step, and it has two important characteristics: the P(III) moiety on OH-4 coupled to glucose (marked in blue) and the easily removable temporary protecting group **R** on OH-1 at the ribitol (marked in orange). The elongation step can be iterated, until the desired chain length is achieved. For example, tetrasaccharide **9** ( $n = 2$ ) was obtained from coupling of Building Block I (**11**) with Building Block II (**12**), containing a free hydroxy group on the ribitol moiety (marked in green) suited for phosphodiester formation. Different coupling procedures using P(III)-chemistry were considered and are described in more detail in section **5.4.1**.

Both of the required Building Blocks are very similar and consist of a glucose 1,4  $\beta$ -linked to the ribitol moiety. In particular, Building Block II (**12**) can be referred to as “capping” residue, as it can be elongated only in the direction of the downstream residue of the growing oligosaccharide chain. The  $\beta$  configuration of the glycosidic linkage in disaccharides **13** (precursor of **12**) and **14** can be stereoselectively achieved by using donors **15** and **17** with participating groups on OH-2 (protected as acetyl ester). Since none of disaccharides **13** and **14** are reported in literature, different glycosylation approaches were explored with different leaving groups on the donor. Unlike donor **15**, donor **17** needs an orthogonal protecting group at OH-4 (a tert-butyldimethylsilyl ether, TBS, was used in our approach) for further selective introduction of the P(III) moiety (marked in purple). The synthetic scheme is completed by the ribitol acceptor **16**, bearing a temporary protection on the primary hydroxyl as triphenylmethyl ether (trityl, Tr) which is employed for the preparation of both disaccharides **13** and **14**. The synthesis of compound **16** is described for the first time in this thesis, while some intermediates for the preparation of glucose donors **15** and **17** are known and published procedures have been adapted from the literature.

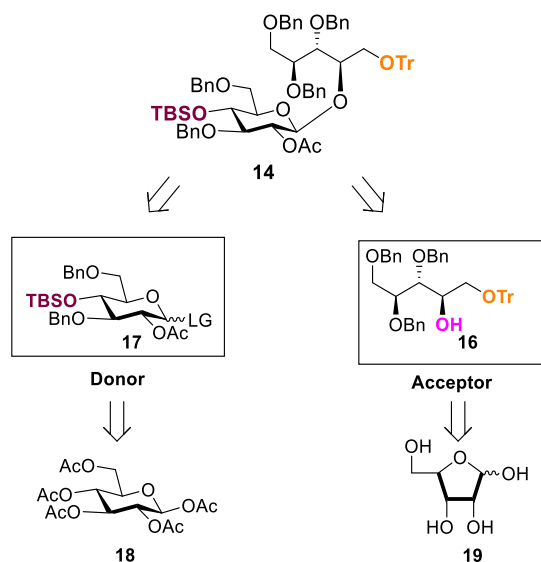


**Scheme 2.** Retrosynthesis of Hia CPS oligomers with different chain length conjugated to a carrier protein.



## 5.2 Synthesis of Disaccharide 14

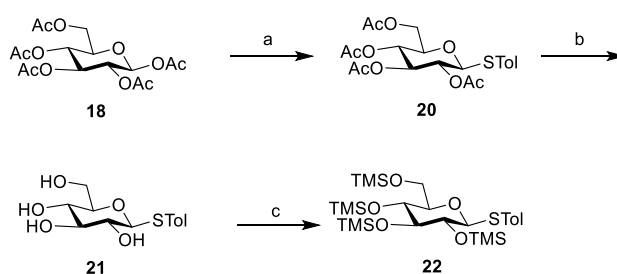
Disaccharide **14** is an important precursor of Building Block I. In this section a detailed synthesis of three different donors as well as the synthesis of acceptor **16** is described (**Scheme 3**). Furthermore, several reaction conditions for the glycosylation were screened to find the best approach.



**Scheme 3.** Retrosynthetic analysis of disaccharide **14**.

### 5.2.1 Synthesis of the Donors

The synthesis of three different donors for the preparation of disaccharide **14** is reported in this paragraph. All donors have two main features: a participating group (O-acetyl ester) to govern the stereochemistry in the glycosylation reaction and an orthogonal protecting group on O-4.

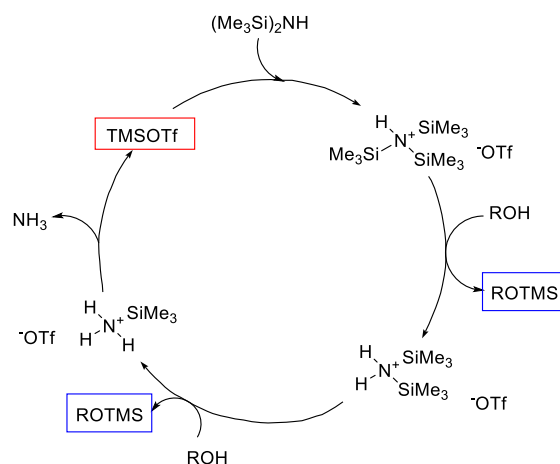


**Scheme 4.** Synthesis of **22**. Reagents and conditions: (a) *p*-Thiocrisol,  $\text{BF}_3 \times \text{Et}_2\text{O}$ , DCM,  $0^\circ\text{C} - \text{rt}$ , 2.5 h, 94% (b) NaOMe, MeOH, 17 h, quant., (c) TMSCl,  $\text{NEt}_3$ , DCM, 14 h, 65% or TMSOTf, HMDS, DCM, 2 h, 99%.

Peracetylated glucose **18** was used as commercially available and affordable starting material. Then, the thiol group was introduced at the anomeric position and after deacetylation and silylation compound **22** was obtained (**Scheme 4**). Two different procedures were studied for the obtainment of the silylated product **22**. At first, triethylamine and TMSCl were used but the formation of huge

quantities of salts as byproducts made the work-up challenging. Even buffering the silica in the chromatography with 1% of  $\text{NEt}_3$  could not prevent hydrolysis during the purification and the silylated compound **22** was obtained in a moderate yield of 65%.

In 2012, Wang et al. reported a new silylation methodology that reduces the amount of base and the formation of byproducts to a minimum using HMDS and TMSOTf.<sup>90</sup>



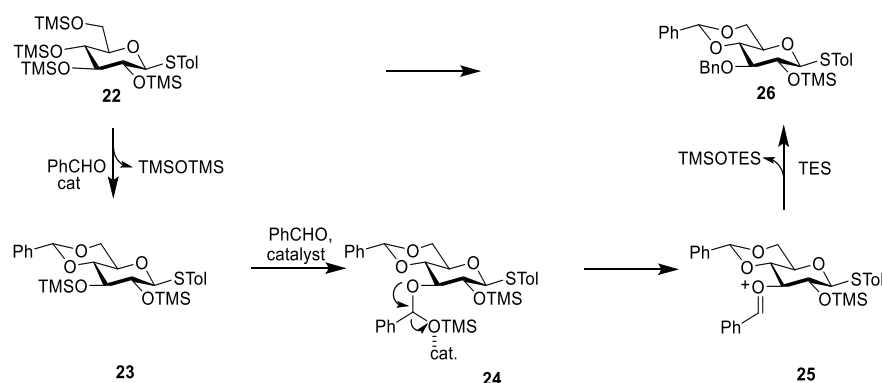
**Scheme 5.** Silylation mechanism using TMSOTf and HMDS.

HMDS is an inexpensive silylating agent and can be activated by TMSOTf in a catalytic cycle (**Scheme 5**). One equivalent of HMDS is capable to silylate two equivalents of hydroxy groups, resulting more convenient than the traditional method based on TMSCl. Furthermore, no large number of salts as byproducts is produced and the reaction time is shortened from hours to minutes. Only the evolution of ammonia appears but is needed to regenerate TMSOTf in the catalytic cycle.<sup>90</sup> Using this novel procedure we obtained **22** in 99% yield and no purification was necessary.

Compound **22** is an important intermediate and the TMS as temporary protecting groups play an essential role in the next regioselective one-pot reaction. TMS ethers are very acid sensitive and can be easily removed. Furthermore, O-TMS protection enhances the solubility in organic solvents compared to multiple hydroxy groups in compound **21**. Finally, TMS play a key role mediating O4,O6 arylidation and 3-OH regioselective reductive arylmethylation in certain reaction. These characteristics were employed in the next reaction.<sup>90</sup>

Recently, Beau et al. published a tandem catalytic reaction for a one-pot regioselective benzylation of glucopyranosides to minimize synthetic steps. The tandem process started from tetra-O-trimethylsilylated thioglucoside **22** and p-toluene 3-O-benzyl-4,6-O-benzylidene-2-O-trimethylsilyl-1-thio- $\beta$ -D-glucopyranoside **26** was achieved using  $\text{Cu}(\text{OTf})_2$  as catalyst, PhCHO and TES as reagents in DCM and ACN as solvent mixture.<sup>91</sup>

Several other catalysts are known for this reaction, such as  $\text{FeCl}_3 \cdot 6\text{H}_2\text{O}$  or  $\text{TMSOTf}$ .<sup>92</sup> Recently Beau et al. proposed a mechanism of this one-pot multistep protection protocol which is shown in **Scheme 6**.<sup>93</sup>

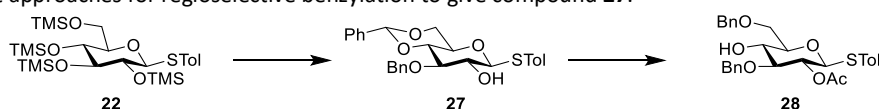


**Scheme 6.** Regioselective benzylation starting from **22** to obtain **26**.

The first catalytic step gives the 4,6-*O*-benzylidene intermediate **23** and  $\text{TMSOTMS}$  as a byproduct. The second catalytic cycle, in which the catalyst promotes the site selective formation of the open chain mixed acetal **24** at *O*-3 followed by formation of the oxonium species **25**. After reduction of the oxonium intermediate with  $\text{TES}$ , the benzylether **26** is produced giving  $\text{TMSOTES}$  as a byproduct. The remaining  $\text{TMS}$  group can be easily cleaved by  $\text{TBAF}$  or acidic conditions.

Our attempts using either  $\text{Cu}(\text{OTf})_2$  or  $\text{FeCl}_3 \cdot 6\text{H}_2\text{O}$  as catalyst,  $\text{PhCHO}$  and  $\text{TES}$  as reagents followed by treatment with  $\text{TBAF}$  are summarized in **Table 3**.

**Table 3.** Different approaches for regioselective benzylation to give compound **27**.

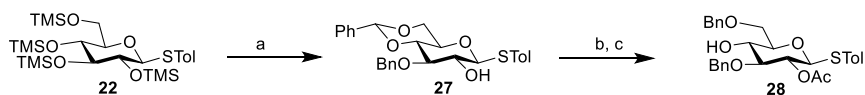


Attempt	catalyst	Reagents	Time	Yield
1	$\text{Cu}(\text{OTf})_2$ (0.01 eq)	$\text{PhCHO}$ (3 eq), $\text{TES}$ (1.1 eq)	45 min	-
2	$\text{FeCl}_3 \cdot 6\text{H}_2\text{O}$ (0.05 eq)	$\text{PhCHO}$ (3 eq), $\text{TES}$ (1.1 eq)	30 min	49%
3	$\text{FeCl}_3 \cdot 6\text{H}_2\text{O}$ (0.05 eq)	$\text{PhCHO}$ *(4 eq), $\text{TES}$ (1.1 eq)	60 min	57%

\*  $\text{PhCHO}$  was distilled;

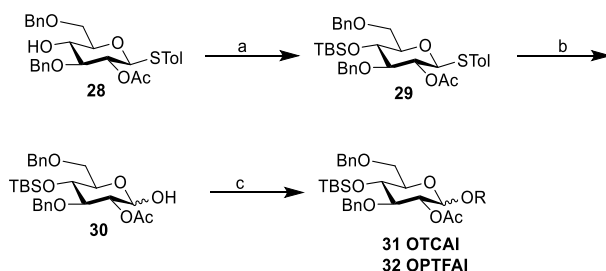
Apart from attempt 1, all approaches were performed using  $\text{FeCl}_3 \cdot 6\text{H}_2\text{O}$  as catalyst and more promising results were achieved. Furthermore, it was noticed that higher yields are reported when  $\text{PhCHO}$  was distilled and a yield of 57% after purification was obtained.

Compound **27** was further acetylated in quantitative yield and reductive opening of the benzylidene acetal gave **28** in 82% yield over two steps (**Scheme 7**). Overall, the three-steps conversion of compound **22** into alcohol **28** was achieved in 41% yield.



**Scheme 7.** Reagents and conditions: (a)  $\text{FeCl}_3 \times 6\text{H}_2\text{O}$ ,  $\text{PhCHO}$ , TES, DCM: ACN (4:1),  $0^\circ\text{C}$ – r.t., 2 h, then TBAF (b)  $\text{Ac}_2\text{O}$ , pyridine 17 h, (c) TFA, TES, DCM,  $0^\circ\text{C}$  – r.t., 17 h, 41% over three steps from **22**.

To obtain the first desired thioglycoside **29**, we silylated the remaining 4-OH with an orthogonal protecting group using TBSOTf and 2,6-Lutidine (**Scheme 8**).

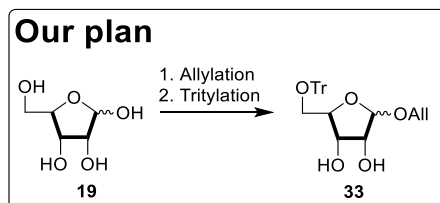


**Scheme 8.** Synthesis of thioglycoside **29** and imidate donors **31** and **32**. Reagents and conditions: (a) TBSOTf, 2,6-Lutidine, 3 h, 91%, (b) NBS, Aceton: water (9:1), 4 h, 63%, (c)  $\text{Cl}_3\text{CCN}$ , DBU, DCM, 1 h, 79% for **31** and  $\text{Cs}_2\text{CO}_3$ , NPhTFACI, DCM, 17 h, 95% for **32**.

To investigate the key glycosylation reaction, two alternative donors were prepared. Accordingly, the anomeric position of **29** was deprotected to obtain **30** using NBS in acetone/water, which gave only moderate yields. The reaction needed to be closely monitored as too many equivalents of NBS and a long reaction time led to the deprotection of the silyl group. Hence, the reaction was stopped after 4 h and 25% of the starting material **29** was recovered after purification by flash chromatography. As a last step the two different leaving groups were introduced giving imidate donors **31** and **32**. Even if our imidate donors are obtained as alpha/beta mixture and **32** even as a mixture of syn-anti epimers, no further characterization such as NMR studies at lower temperature were studied. Regardless of their configuration, the participation of the neighbouring group such as the acetyl group ensures the favoured beta glycosylation.

## 5.2.2 Acceptor

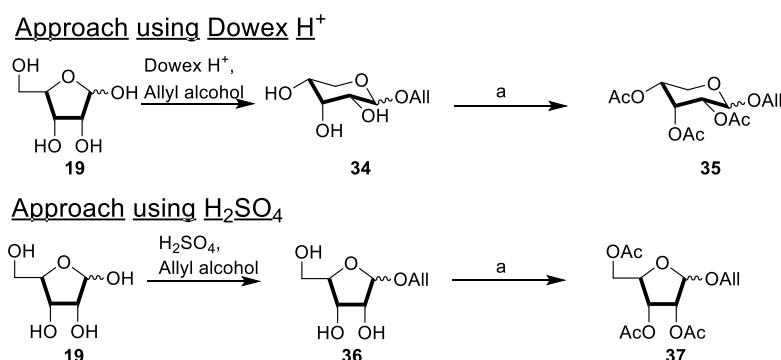
The synthesis of acceptor **16**, contained in both disaccharides **13** and **14**, will be discussed in this section. D-Ribose **19** was chosen as a cost effective starting material and the first step was a Fischer glycosylation with allyl alcohol followed by protection of the primary hydroxy group (Scheme 9).



**Scheme 9.** Our plan was to protect D-Ribose with an allyl followed by a trityl protecting group.

Two different procedures are well-known and mostly used to introduce an allyl group at the anomeric position. In the first approach ribose is treated with Dowex H<sup>+</sup> resin and allyl alcohol, whereas in the second approach H<sub>2</sub>SO<sub>4</sub> as acid promoter is used.<sup>94, 95</sup> After the allylation, the primary hydroxy group was provisionally protected using TrCl as orthogonal protecting group. Surprisingly, tritylation of the two crudes gave different outcomes (16% compared to 52%, **Scheme 11**) and two diverse molecules after the second step were obtained. Mass analysis showed the same mass, so we decided to investigate the results in more detail using NMR.

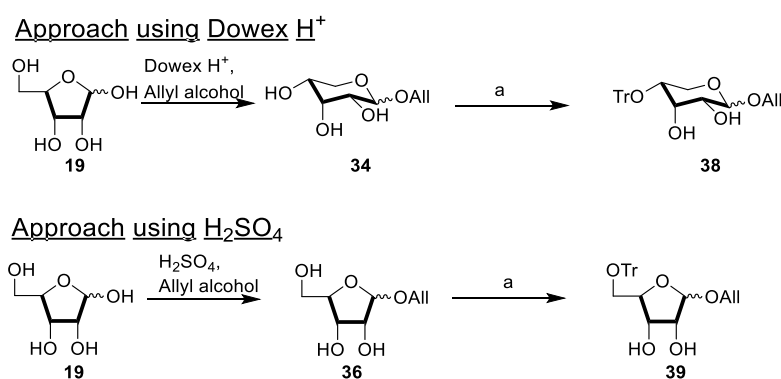
To study the different outcomes of the two common procedures, ribose was subjected to Fischer glycosylation using both conditions described above and performing, instead of the tritylation, the standard O-acetylation of the crudes (**Scheme 10**).



**Scheme 10.** Allylation studies using two different procedures followed by acetylation. Reagent and conditions: Dowex H<sup>+</sup>, allyl alcohol or H<sub>2</sub>SO<sub>4</sub>, allyl alcohol, (a) Ac<sub>2</sub>O, pyridine, 17 h.

Mass analysis of **35** and **37** showed again an identical result, but the NMR spectra were different and clearly indicated the formation of different molecules. After two-dimensional NMR experiments such as COSY, HSQC and HMBC, we identified different ring sizes. Using Dowex H<sup>+</sup> only the  $\alpha$ -isomer of the pyranose could be isolated, whereas using H<sub>2</sub>SO<sub>4</sub> we could isolate two anomeric isomers (coloured in green and red). Their NMR spectra are reported in **Figure 14**. After careful analysis of the NMR spectra, we concluded that the treatment of D-Ribose with Dowex H<sup>+</sup> and allyl alcohol provided the pyranose ring as major compound (compound **35**), whereas using H<sub>2</sub>SO<sub>4</sub> we obtained the furanoside **37** (**Scheme 11**). The major difference was seen in the H4 signal of the <sup>1</sup>H NMR. In the pyranose form the H4 is more downfield shifted compared to the furanose ring (**Figure 14**).

Based on this result, treatment of D-Ribose with Dowex H<sup>+</sup> and allyl alcohol followed by tritylation gave mostly the pyranoside **38**, while using H<sub>2</sub>SO<sub>4</sub> we obtained the desired furanoside **39** (**Scheme 11**).



**Scheme 11.** Alkylation of D-Ribose followed by tritylation. Reagent and conditions: Dowex H<sup>+</sup>, allyl alcohol or H<sub>2</sub>SO<sub>4</sub>, allyl alcohol, (a) TrCl, pyridine, 17 h, 60°C, 16% for **38** and 52% for **39**.

Moreover, considering the yields of the reactions, the results are in accordance with our hypothesis of the ring formation. Trityl is a well-known protecting group with a marked preference for primary hydroxy groups due to its steric hindrance. Hence, the low yield of 16% reported for the tritylation of **34** is intelligible. In order to determine if the outcome observed with ribose is a general behaviour with other monosaccharides, we treated several other aldopentoses with Dowex H<sup>+</sup> and H<sub>2</sub>SO<sub>4</sub> in allyl alcohol. However, different pentoses did not show the same trend in the generation of the furanose and pyranose ring.

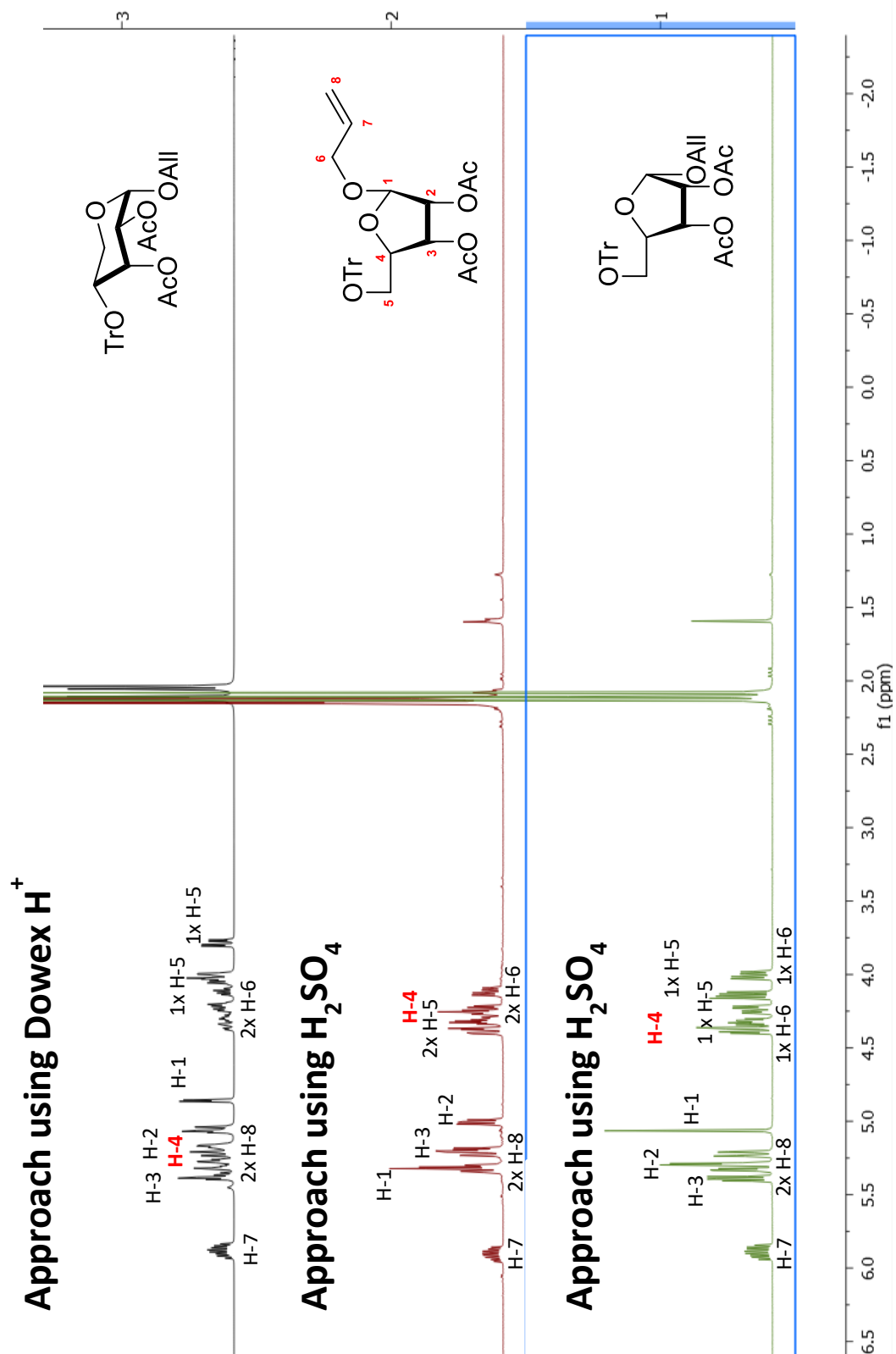
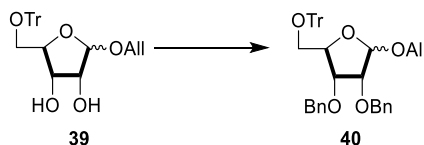


**Figure 14.** NMR results of two approaches to introduce an allyl protecting group at the anomeric position indicated different ring sizes. Using Dowex H<sup>+</sup> we mainly obtained the pyranose form, whereas the use of H<sub>2</sub>SO<sub>4</sub> in allyl alcohol gave the desired furanose form.

After investigating the first two steps in our acceptor synthesis, we proceeded with the protection of 2-OH and 3-OH (**Scheme 12**).

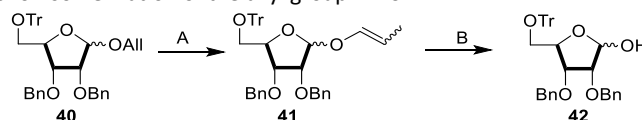


**Scheme 12.** Synthesis of **40**. Reagents and conditions: NaH, BnBr, DMF, 0°C- r.t., 2 h, 94 %.

Benzylation of furanoside **39** was carried out using standard conditions to obtain **40** in high yield. Additionally, after this step the anomeric mixture was for the first time separable by column chromatography.

As next step the allyl group was cleaved through isomerization to propenyl ether followed by cleavage using I<sub>2</sub> and water (**Table 4**).

**Table 4.** Different approaches for isomerization of the allyl group in **40**.

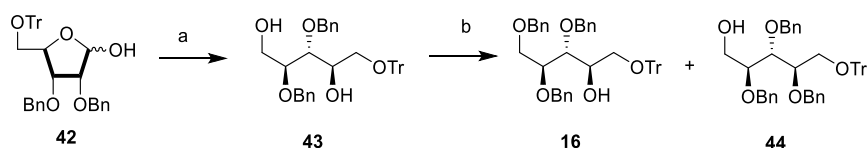


Attempt	Reagent A	Reagent B	Time A + B	Yield
1	[Ir(COD)(Ph <sub>2</sub> MeP) <sub>2</sub> PF <sub>6</sub>	I <sub>2</sub> /H <sub>2</sub> O	0.5 h + 15 min	94%
2	<i>t</i> -BuOK	I <sub>2</sub> /H <sub>2</sub> O	20 h + 15 min	92%

For the isomerization, a variety of catalysts are known such as rhodium and iridium catalysts, but with some of them up to 10% of the allyl ether is reduced to the undesired propyl ether. [Ir(COD)(Ph<sub>2</sub>MeP)<sub>2</sub>PF<sub>6</sub> is a well-known and effective catalyst, which can isomerize after hydrogen activation the allyl ether in high yields. Furthermore, with this approach the progress of the reaction can be easily monitored by NMR.<sup>96</sup> Treating **40** with the Ir-catalyst gave the desired isomerization product **41**, which was further cleaved by I<sub>2</sub>/H<sub>2</sub>O in a one pot reaction to give **42** in 94% yield over two steps. The unpleasant disadvantage using this method is that the Ir-catalyst is very expensive and 10 mol% of the catalyst for each reaction was required. Hence, we were looking for an isomerization strategy using more cost-effective reagents, that were further suitable for scale up synthesis. More than 50 years ago *t*-BuOK in DMSO was already used for isomerization of an allyl group and high yields were reported.<sup>97</sup> Use of *t*-BuOK and DMSO gave the desired intermediate **41** which was further treated with I<sub>2</sub>/H<sub>2</sub>O to obtain **42** in 92% yield over two steps. Both approaches gave the desired compound **41** in excellent yields. Isomerization reactions using the Ir-catalyst gave the desired intermediate in very



little time (<30 min), whereas *t*-BuOK reactions were carried out overnight and an additional work-up after the isomerization was required (**Table 4**). Both the isomerization reactions were checked via NMR for their progress, as the *R<sub>f</sub>* value of the propenyl and the allyl ether were identical. Nevertheless, the high costs of the Ir-catalyst favored the use of *t*-BuOK in this reaction.



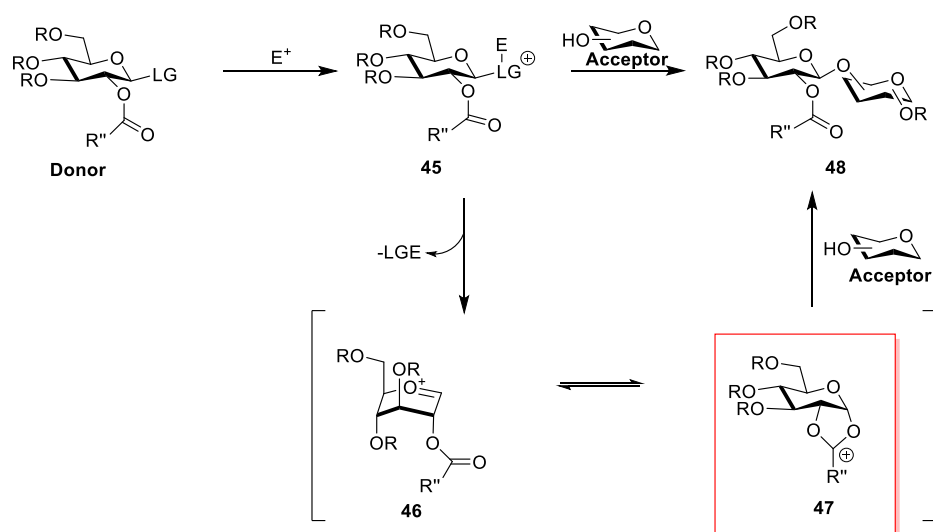
**Scheme 13.** Synthesis for acceptor **16**. Reagents and conditions: (a) NaBH<sub>4</sub>, EtOH, 15min, quant., (e) BnBr, Bu<sub>4</sub>NBr, 5% NaOH, DCM, 17h, 64%.

As next step, furanose **42** was reduced with NaBH<sub>4</sub> to give the ribitol **43** in excellent yields followed by a regioselective phase transfer benzylation to obtain **16** in 64% yield. However, 32% of the undesired isomer **44** was isolated as byproduct and fully characterized (**Scheme 13**).

### 5.2.3 Glycosylation approaches

The key reaction of carbohydrate chemistry is the glycosylation reaction which couples donor and acceptor via a glycosidic (mostly O-glycosidic) bond. Nowadays, although many different strategies are known and applied, the glycosylation reaction remains a difficult transformation. Its outcome is influenced by many different parameters, such as the nature of the leaving group on the glycosyl donor, the promoter (mostly a Lewis acid), the protecting groups on both reaction partners, solvent and temperature. In particular, the control of the stereoselectivity, *i.e.* the  $\alpha$  or  $\beta$  configuration of the newly formed glycosidic linkage, is still a challenge, and successful protocols must be established on a case-by-case basis. In a classical glycosylation reaction, the donor is equipped with an anomeric leaving group and the acceptor has an unprotected hydroxy group suited for a nucleophilic attack (**Scheme 14**). Typically, all the other functional groups are masked with temporary protecting groups which influence the reactivity of the donor and acceptor. Electron-donating groups such as benzyl groups increase the reactivity, while electron-withdrawing groups decrease the reactivity. Additionally, protecting groups can help to direct the stereochemistry.

Interaction of the promoter with the leaving group leads to the activated donor **45**, hence highly reactive intermediates are formed such as a flattened glycosyl cation stabilized via oxocarbenium cation **46** or, if the neighbouring group is an acyl, via bicyclic acyloxonium intermediate **47** (marked in red). Within a neighbouring group such as an acyl, the stereochemistry can be controlled, as the neighboring acyl group assists the departure of the activated leaving group to the formation of **48**. Therefore, the acceptor can only attack from the backside to form 1,2-trans glycosidic bonds corresponding to  $\beta$ -glycosides with glucosyl-type donors, while mannosyl-type donors deliver  $\alpha$ -glycosides.<sup>98</sup>



**Scheme 14.** Glycosylation mechanism leveraging the participating effect of the neighbouring group.

Due to the high reactivity of intermediates **46** and **47**, many other side reactions can occur during a glycosylation reaction, such as hydrolysis, elimination, cyclization, rearrangement, orthoester formation, etc. Beside using strictly anhydrous reaction conditions, donor hydrolysis can be inhibited by addition of molecular sieves in the reaction mixture. In general, novel glycosylation reactions need to be studied carefully and the leaving group, the nature of the promoter as well as the protecting groups are important characteristics which influence the result.<sup>99,100</sup>

Thioglycosides were introduced by Ferrier et al. in 1973 and since their introduction, these donors are widely used. Next to their relative ease of synthesis, they also show a highly stability and compatibility with several protection and deprotection conditions as well as their orthogonality of activation with several other glycosylation reactions. They are further applied in several novel one-pot oligosaccharide syntheses.<sup>101</sup>

Thioglycosides are activated using mild conditions such as metals salts like  $\text{Hg}^{2+}$ ,  $\text{Cu}^{2+}$  and  $\text{Ag}^+$  as well as organosulfur reagents (e.g. DMTST). Additionally, iodonium (di- $\gamma$ -collidine) perchlorate (IDCP), *N*-iodosuccinimide/triflic acid (NIS/TfOH) or NIS/TMSOTf are sources of highly thiophilic  $\text{I}^+$  and can activate thioglycosides. It is assumed that the activation is due to the iodination of the anomeric sulfur which leads to the departure of ISR and later to the corresponding disulfide RSSR and release of molecular iodine. The activation can also occur with bromonium sources (NBS). Crich et al. reported the activation of thioglycosides using 1-benzenesulfinyl piperidine (BSP)/ $\text{Tf}_2\text{O}$  in the presence of TTBP. This system allowed the difficult formation of a  $\beta$ -mannosidic linkage in excellent yield and stereoselectivity.<sup>102</sup> Within this activation protocol, the *S*-thiophenyl species is formed in situ at  $-60^\circ\text{C}$  and reacts further with the thioglycoside. This novel approach was further studied and other related activation systems including MPBT/  $\text{Tf}_2\text{O}$  or  $\text{Ph}_2\text{SO}/ \text{Tf}_2\text{O}$  were developed.<sup>101, 103,104,105</sup>

Glycosyl imidates represent another versatile set of glycosyl donors. In 1980 Schmidt et al. introduced trichloroacetimidates and since then, they are widely used. These donors require a Lewis acid such as TMSOTf or  $\text{BF}_3\cdot\text{Et}_2\text{O}$  for activation, and it is supposed that the Lewis acid coordinates to the nitrogen of the imidoyl leaving group and trichloroacetamide is formed. Since trichloroacetimidate has a lower basicity, the Lewis acid is released for the next catalytic cycle. More recently, *N*-phenyltrifluoroacetimidates (PTFAI) were introduced which can also be activated by a Lewis acid.<sup>106</sup> Various promoters have shown good results: TMSOTf,  $\text{I}_2\text{-TES}$ ,  $\text{Yb}(\text{OTf})_3$ , TBSOTf,  $\text{Bi}(\text{OTf})_3$  whereas the mechanisms are still under investigation. Additionally, trifluoroacetimidates are more stable and less reactive than trichloroacetimidates, due to the lower basicity of the nitrogen. Nowadays, both imidates are widely used and excellent yields are described in literature.<sup>103,107</sup>

For the synthesis of disaccharide **14**, three different donors were prepared: the thioglycoside **29**, the trichloroacetimidate **31** and the *N*-phenyl trifluoroacetimidate **32** (Figure 15). A participating group such as an acetyl group may lead selectively to the desired  $\beta$ -glycosidic bond due to the mechanism described above.

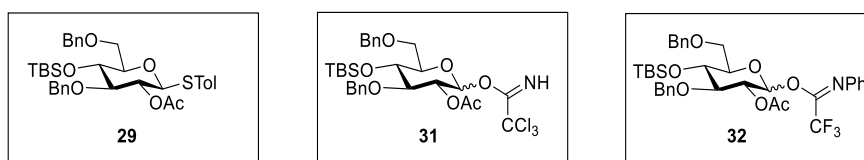
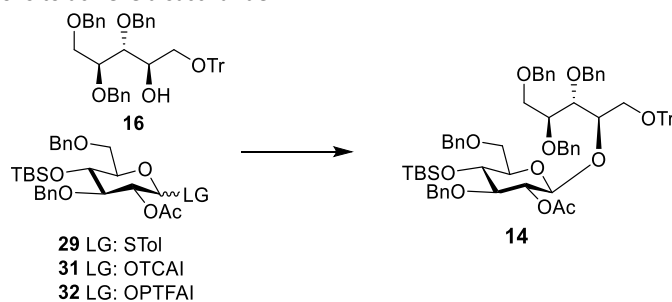


**Figure 15.** Three different donors were successfully synthesized.

**Table 5** reports different glycosylation conditions we applied with acceptor **16** to obtain the disaccharide **14**. In all attempts coevaporation of both reaction partners with toluene was performed to minimize the amount of water in the reaction as well as molecular sieves were used to decrease hydrolysis of the donor.

**Table 5.** Different glycosylation conditions to achieve disaccharide **14**.



Attempt	Donor	Temperature	MS 4 Å	Promotor	Yield
1	29	-40 °C	MS 4 Å	NIS (1.2 eq), TMSOTf (0.1 eq)	55%
2	29	-40°C	MS 4 Å	NIS (1.2 eq), TMSOTf (0.2 eq)	47%
3	29	-60°C	MS 4 Å	NIS (1.4 eq), TMSOTf (0.2 eq)	46%
4	29	-50°C	-	NIS (1.1 eq), TMSOTf (0.08 eq)	50%
5	29	-60 °C – r.t.	-	Ph <sub>2</sub> SO (2.8 eq), TTBP (3 eq), Tf <sub>2</sub> O (1.4 eq)	< 5%
6	29	-40°C	MS 4 Å	NIS (1.4 eq), AgOTf (0.2 eq)	-
7	31	-10°C – r.t.	MS 4 Å	TMSOTf (0.1 eq)	< 10%
8	32	-40°C	Not necessary after optimization	TMSOTf (0.05 eq)	82%

In the first attempt, the disaccharide **14** was successfully obtained in a moderate 55% yield from thioglycoside **29** activated by freshly crystallised NIS and TMSOTf at -40°C. The yield was not improved by increasing or decreasing the amount of the cat. amount of Lewis acid and using different reaction temperatures (attempts 1-4). Van der Marel et al. introduced the diphenylsulfoxide-triflic anhydride as successful promoter combination for thioglycosides. Disappointingly, using **29**, Ph<sub>2</sub>SO and Tf<sub>2</sub>O and additionally TTBP, the formation of the disaccharide **14** was obtained in less than 5% yield (attempt 5). Even a different well-known promoter system such as NIS/AgOTf was not giving any promising results of the glycosylation (attempt 6). After these attempts, we changed our strategy and studied the glycosylation using imidate donors **31** and **32**.

The 7th attempt describes the activation of trichloroacetimidate **31** with TMSOTf as Lewis acid. Unfortunately, only low yields (less than 10%) of the disaccharide were obtained, whereas other

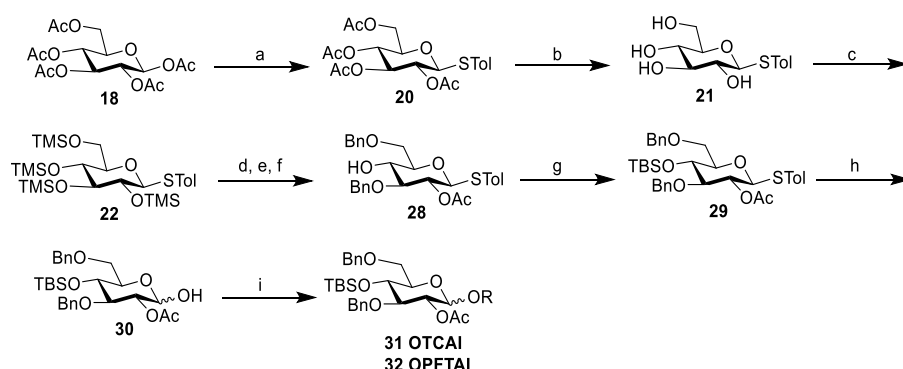
byproducts of the glycosylation were analyzed. Higher temperatures and the acidic conditions removed the trityl group of the acceptor.

Changing the imidate donor to **32** and using again TMSOTf as a promoter at  $-40^{\circ}\text{C}$  disaccharide **14** was achieved in a yield of up to 82% after purification (attempt 8). It should be noticed that the use of too many equivalents of Lewis acid (up to more than 0.3 eq) and long reaction time of the glycosylation led to deprotection of the acid sensitive trityl group on the acceptor. Furthermore, after optimizing of glycosylation conditions reported in Table 5 (attempt 8) no molecular sieves were needed. Only disaccharide **14** with a  $\beta$ -glycosidic bond was formed due to the participating group of the donor **32**.

### 5.2.4 Summary and conclusion

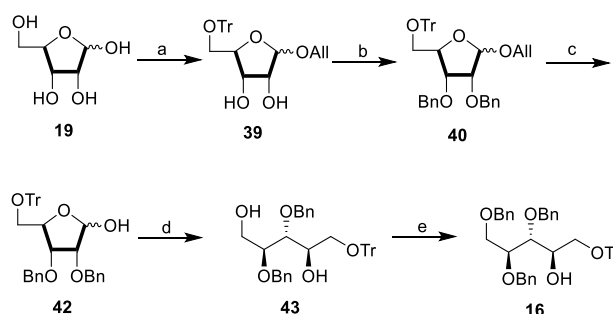
In section 5.2 the synthesis of three different donors (**29**, **31** and **32**) and of acceptor **16** as well as the coupling to disaccharide **14** are described.

Starting from peracetylated glucose and via multiple protections and deprotection steps, the silylated glycoside **22** was obtained using two different approaches. We then screened diverse catalysts to optimize the conditions of the regioselective one pot reaction leading to the benzylidene formation as well as the selective 3-O-benzylation. The use of  $\text{FeCl}_3 \times 6\text{H}_2\text{O}$  gave the best result. Then, acetylation and reductive opening of the benzylidene ring furnished **28** in good yields (41% over three steps). Finally, we introduced a silyl ether as orthogonal protection to obtain thioglycoside donor **29** in 7 steps from peracetylated glucose **18** in 35% overall yield. Next, compound **29** was hydrolysed and two different imidate donors, namely **31** and **32**, were obtained in 17% and 21% overall yield, respectively. The optimized synthesis of donors **29**, **31** and **32** is summarized in **Scheme 15**.



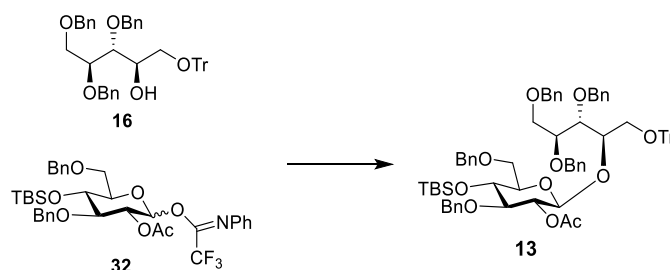
**Scheme 15.** Optimized synthesis of donors **29**, **31** and **32**. Reagents and conditions: (a) p-Thiocrisol,  $\text{BF}_3 \times \text{Et}_2\text{O}$ , DCM,  $0^{\circ}\text{C}$  – rt, 2.5 h, 94% (b) NaOMe, MeOH, 17 h, quant., (c) TMSOTf, HMDS, DCM, 2 h, 99%, (d)  $\text{FeCl}_3 \times 6 \text{H}_2\text{O}$ , PhCHO, TES, DCM: ACN (4:1),  $0^{\circ}\text{C}$ – r.t., 2 h, (e)  $\text{Ac}_2\text{O}$ , pyridine 17 h, (f) TFA, TES, DCM,  $0^{\circ}\text{C}$  – r.t., 17 h, 41% over three steps, (h) TBSOTf, 2,6-Lutidine, 3 h, 91%, (i) NBS, Aceton: water (9:1), 4 h, 63%, (j)  $\text{Cl}_3\text{CCN}$ , DBU, DCM, 1h, 79% for **31** and  $\text{Cs}_2\text{CO}_3$ , NPhTFACI, DCM, 17 h, 95% for **32**.

The synthesis of acceptor **16** is described in **Scheme 16**. Starting from D-Ribose **19**, we studied two different allylation procedures and we exposed the formation of two ring sizes. Using Dowex H<sup>+</sup> and allyl alcohol gave mostly the pyranoside ring, whereas H<sub>2</sub>SO<sub>4</sub> and allyl alcohol formed the desired furanoside, which was further tritylated giving compound **39**. Then, after benzylation, the allyl group was removed by isomerization followed by cleavage with I<sub>2</sub> and water (**42**). The propenyl ether was successfully synthesized by either using an Ir-catalyst or *t*-BuOK and both approaches gave similar high yields. As the Ir-catalyst is much more expensive, we decided to apply *t*-BuOK for the isomerization followed by the treatment with iodine and water. Ribose **42** was further reduced with NaBH<sub>4</sub> giving the ribitol **43**. As a last step in the acceptor synthesis, we employed a regioselective phase transfer benzylation of the primary hydroxyl to afford acceptor **16** in good yield. On the whole, the acceptor **16** was synthesized in 7-step in 29% overall yield.



**Scheme 16.** Synthesis of Acceptor **16**. Reagents and conditions: (a) i. Allyl alcohol, H<sub>2</sub>SO<sub>4</sub>, ii. TrCl, pyridine 80°C, 17 h, 52% over two steps, (b) NaH, BnBr, DMF, 0°C- r.t., 2 h, 94%, (c) i. *t*-BuOK, 4 h, DMSO, ii. I<sub>2</sub>, water, THF, 30 min, 92% over two steps, (d) NaBH<sub>4</sub>, EtOH, 15 min, quant., (e) BnBr, Bu<sub>4</sub>NBr, 5% NaOH, DCM, 17 h, 64%.

Even if all donors were studied in different glycosylation attempts, donor **32** and acceptor **16** reacted smoothly using TMSOTf as promoter at -40°C. The glycosylation reaction proceeded fast and in very good yields (82%). Furthermore, no molecular sieves were required after optimization (**Scheme 17**).

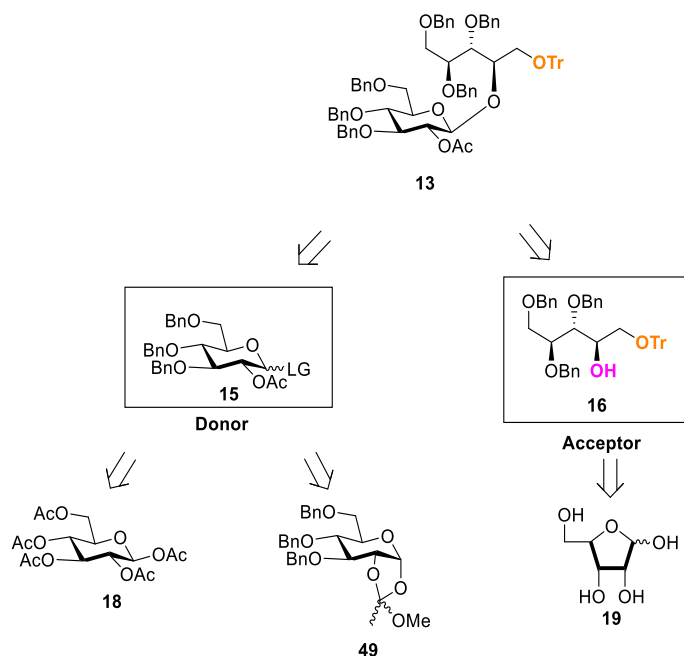


**Scheme 17.** Optimised glycosylation to obtain disaccharide **14**. Reagents and conditions: TMSOTf (0.05 eq), 30 min, DCM, -40°C, 82%.

The disaccharide **14** is an important intermediate in the preparation of Building Block I, which is further discussed in 5.4.

### 5.3 Synthesis of Disaccharide 13

Herein, the synthesis of disaccharide **13** is described. Different donors with different leaving groups were synthesized and tested in the coupling reaction with acceptor **16** (Scheme 18).

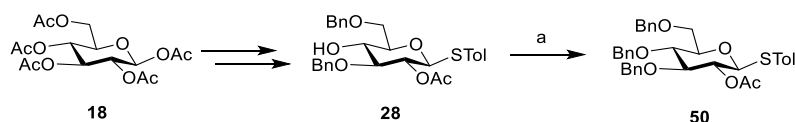


Scheme 18. Retrosynthesis of disaccharide **13**.

#### 5.3.1 Donor

The synthesis of an imidate donor as well as a thio-donor are described in this chapter. However, all donors are already reported in the literature and starting materials were affordable and commercially available.<sup>108, 109</sup>

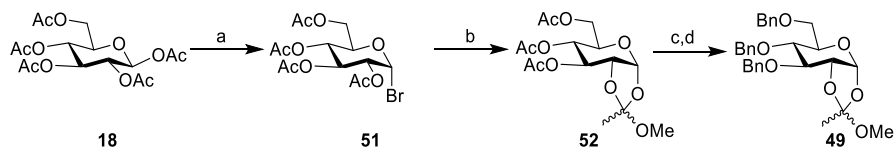
The thioglycoside **50** was gained using intermediate **28**, which was already available from the donor synthesis of disaccharide **14** described in detail in 5.2.1 (Scheme 19).



Scheme 19. Synthesis of Donor **50**. Reagents and conditions: (a) NaH, BnBr, DMF, 3 h, 56%.

The synthesis of imidate donor **57** started from cheap starting material **18**. The conversion of this compound into orthoester **49** is described in the literature and can be achieved by introduction of the orthoester ring on bromide **51**, followed by deacetylation and benzylation (Scheme 20).<sup>110</sup> However,

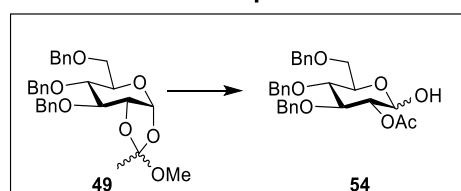
large quantities of compound **49** were already available in the lab of Prof. Lay and were used for the synthesis of hemiacetal **54** as described in **Scheme 21**.



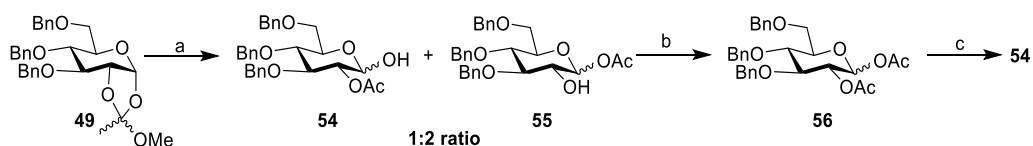
**Scheme 20.** Synthesis of orthoester **49**. Reagents and conditions: (a) 33% HBr in AcOH, (b) 2,6-lutidine, MeOH/CH<sub>2</sub>Cl<sub>2</sub> (c) MeONa, MeOH/CH<sub>2</sub>Cl<sub>2</sub>, (d) BnBr, NaH.<sup>110</sup>

As orthoesters are acid sensitive, this lability can be used to open the five membered ring and two different acids were explored with the aim to achieve selectively compound **54** (**Scheme 21**).

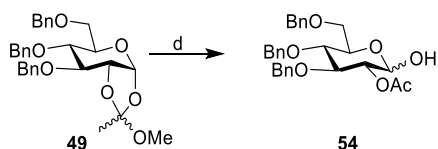
### Our plan



#### 1<sup>st</sup> approach using AcOH



#### 2<sup>nd</sup> approach using PTSA

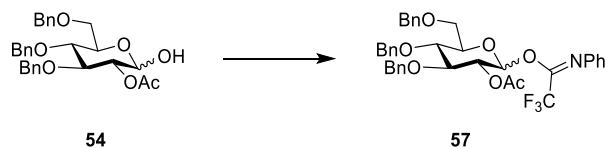


**Scheme 21.** Opening of the orthoester **49**: 1<sup>st</sup> approach: (a) 60% AcOH, 30 min, 1,4-Dioxane, (b) Ac<sub>2</sub>O, pyridine, 19 h, (c) NH<sub>2</sub>NH<sub>2</sub> AcOH (80%), MeOH, DMF, 19 h, 65% over three steps. 2<sup>nd</sup> approach: (d) PTSA, acetone:H<sub>2</sub>O 7:3, 45 min, 70%.

Using aq. AcOH (60%) gave a mixture of the two isomers **54** and **55** in the undesired ratio of 1:2 (**Scheme 21**). After acetylation of the crude and selective deacetylation of the anomeric position compound **54** was obtained in 65% overall yield over three steps. PTSA, which is also a mild acid and applied in opening of orthoesters, was used in the 2<sup>nd</sup> approach.<sup>111</sup> Using a mixture of PTSA and water gave **54** in a single step in 70% yield.



In both approaches the target intermediate **54** was successfully obtained and the yields were comparable. The use of PTSA, however, required only one step, and it was therefore preferred to continue the synthetic route. The next step was the preparation of the imidate donor **57** (Scheme 22).



**Scheme 22.** Synthesis of imidate donor **57**. Reagents and conditions:  $\text{Cs}_2\text{CO}_3$ , NPhTFACI, DCM, 17 h, quant.

Having **54** in our hands, the imidate donor **57** was successfully synthesized using common procedures. The  $^1\text{H-NMR}$  of **57** referred again to mixture of syn-anti epimers, but no further characterization was performed.

### 5.3.2 Glycosylation

As already described, almost each glycosylation reaction needs to be studied carefully and optimised. In order to obtain disaccharide **13**, acceptor **16** and two donors with different leaving groups were studied (**50** and **57**, shown in Figure 16).

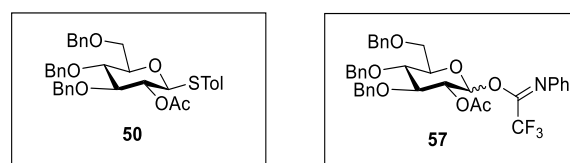
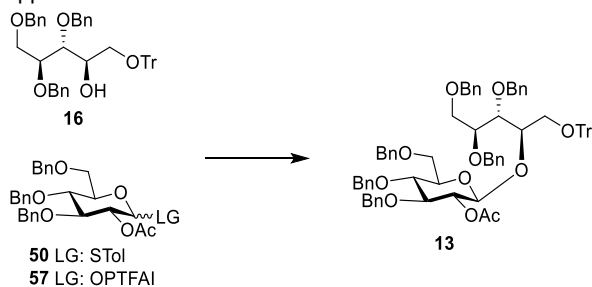


**Figure 16.** Two different donors were studied for the glycosylation.

The synthesis of acceptor **16** from ribose is described in detail in 5.2.2 and glycosylation attempts for disaccharide **13** are summarized in Table 6. As **13** is very similar to disaccharide **14** similar conditions such as equivalents of Lewis acid as well as different temperatures were screened.

To avoid hydrolysis during the glycosylation reaction, all attempts were carried out using molecular sieves, as well as all starting materials were coevaporated with toluene before use.

**Table 6.** Different glycosylation approaches to achieve disaccharide **13**.

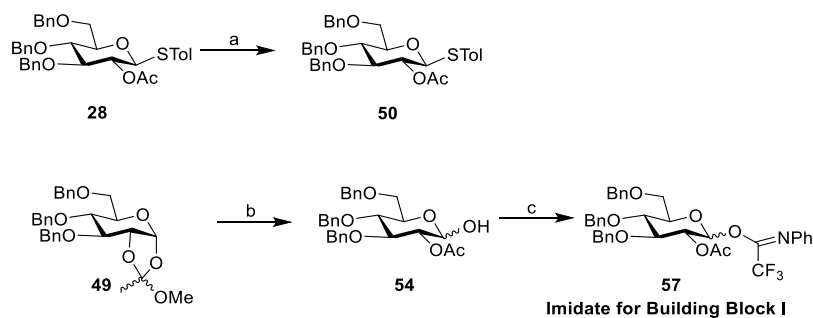


Attempt	Donor	Temperature	MS	Promoter	Yield
1	50	-60 to r.t.	MS 4A	NIS (1.2 eq), TMSOTf (0.2 eq)	52%
2	57	-40°C	MS 4A	TMSOTf (0.05 eq)	-
3	57	-40°C	MS 4A	TMSOTf (0.1 eq)	64%
4	57	-30°C	Not required after optimization	TMSOTf (0.07 eq)	76%

Donor **50** activated with NIS and TMSOTf from -60°C until rt gave successfully disaccharide **13** in moderate yield of 52% (**Table 6**). Interestingly, changing again to the imidate donor **57** we carried out more promising reactions. Whereas using the same glycosylation conditions (temperature and amount of Lewis acid) than for disaccharide **14**, resulted in no reaction (attempt 2), when we employed 0.1 eq of TMSOTf at -40°C the reaction proceeded well in 64% yield. This was even optimized by attempt 4 using 0.07 eq of TMSOTf at -30°C (76%) and even in this case the use of molecular sieves was not necessary. Glycosylation conditions with more than 0.07 eq of the Lewis acid TMSOTf resulted in deprotection of the acid sensitive trityl group and more byproducts were detected.

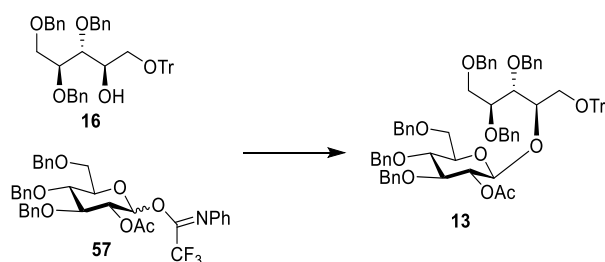
### 5.3.3 Summary and conclusion

The previous sections describe the synthesis of the donor as well as a successfully glycosylation to obtain disaccharide **13** (**Scheme 23**). The synthesis of thioglycoside **50** and the trifluoroacetimidate donor **57** is illustrated, using intermediates available in the lab of Prof. Luigi Lay. Furthermore, except of the participating group for a  $\beta$  glycosylation, no orthogonal protecting group for the donor of Building Block II was required. Thioglycoside **50** was achieved by benzylation of **28** and for the imidate donor **57** intermediate **49** was employed. For the opening of the orthoester ring of **49**, two different acids were tested. In particular, the use of PTSA enabled the opening of the orthoester in 70% yield, followed by the introduction of the imidate to provide donor **57**.



**Scheme 23.** Summarized synthesis of thioglycoside donor **50** and imidate donor **57**. Reagents and conditions: (a) PTSA, aceton:H<sub>2</sub>O 7:3, 45 min, 70%, (b) Cs<sub>2</sub>CO<sub>3</sub>, NPhTFACl, DCM, 17 h, quant.

The two different donors (**50** and **57**) were studied in different glycosylation conditions and the trifluoroacetimidate donor **57** gave better results. Using donor **57** and the previously described acceptor **16** in the presence of TMSOTf at -30°C gave the disaccharide **13** in high yields (76%) (**Scheme 24**).

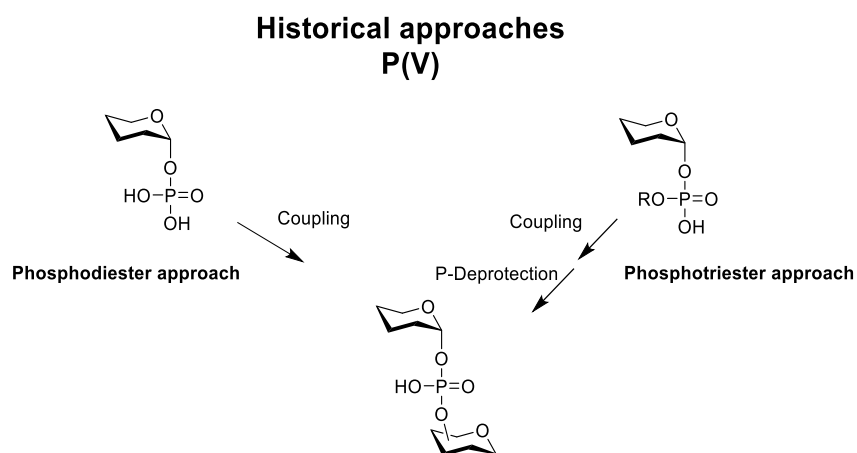


**Scheme 24.** Best glycosylation to obtain disaccharide **13**. Reagents and conditions: TMSOTf (0.07 eq), 30 min, DCM, -30°C.

Interestingly, for both disaccharides (**13** and **14**) the use of the trifluoroacetimidate donors with TMSOTf as a promoter afforded the best results in the glycosylation. This is not astonishing as both disaccharides are very similar and only the donors are slightly different. Donor **57** reacted at -30°C whereas donor **32** to obtain disaccharide **14** performed better at -40°C. Moreover, both thioglycoside donors **29** and **50** gave very similar yields in the glycosylation reactions (not more than 55%).

## 5.4 Preparation of the Oligomers

Four basic coupling procedures are known for the preparation of glycosyl phosphosaccharides, including phosphodiester, phosphotriester, phosphoramidite and hydrogenphosphonate (*H*-phosphonate) approaches. All these methodologies include a coupling step which involves a P-containing glycosyl building block acting as electrophile with the alcohol of the reaction partner working as a nucleophile. A variety of phosphosaccharides were synthesized within these approaches.



**Scheme 25.** Historical coupling approaches for the preparation of glycosyl phosphosaccharides.

The phosphodiester and phosphotriester methods are both based on P(V) chemistry and, until the introduction of the more modern approaches, represented the methodologies of choice for the synthesis of phosphosaccharides (**Scheme 25**). The phosphodiester approach uses only condensing agents for the coupling, such as dicyclohexylcarbodiimide (DCC). The reaction proceeds slowly and takes from 2 to 10 days, but the reaction time was reduced to 7 h by using 3-nitro-1-(2,4,6-triisopropylbenzenesulfonyl)-1,2,4-triazole (TPS-NT). However, only moderate yields (up to 69%) are typically obtained with this approach.

The phosphotriester method is characterised by the presence of an additional P-protecting group on the glycosyl phosphate compared to the phosphodiester approach (**Scheme 25**), and it was applied successfully in nucleotide chemistry. Additionally, higher yields in the condensation step are usually obtained. Using the phosphotriester method the first solid-phase synthesis of oligodeoxyribonucleotides was successfully accomplished, but unfortunately this approach showed to be less effective for the synthesis of glycosyl phosphosaccharides. Moreover, this methodology requires an additional second step to deprotect the phosphate ester after the coupling.<sup>112</sup>

Nowadays, the most common approaches are the *H*-phosphonate and the phosphoramidite methodologies.

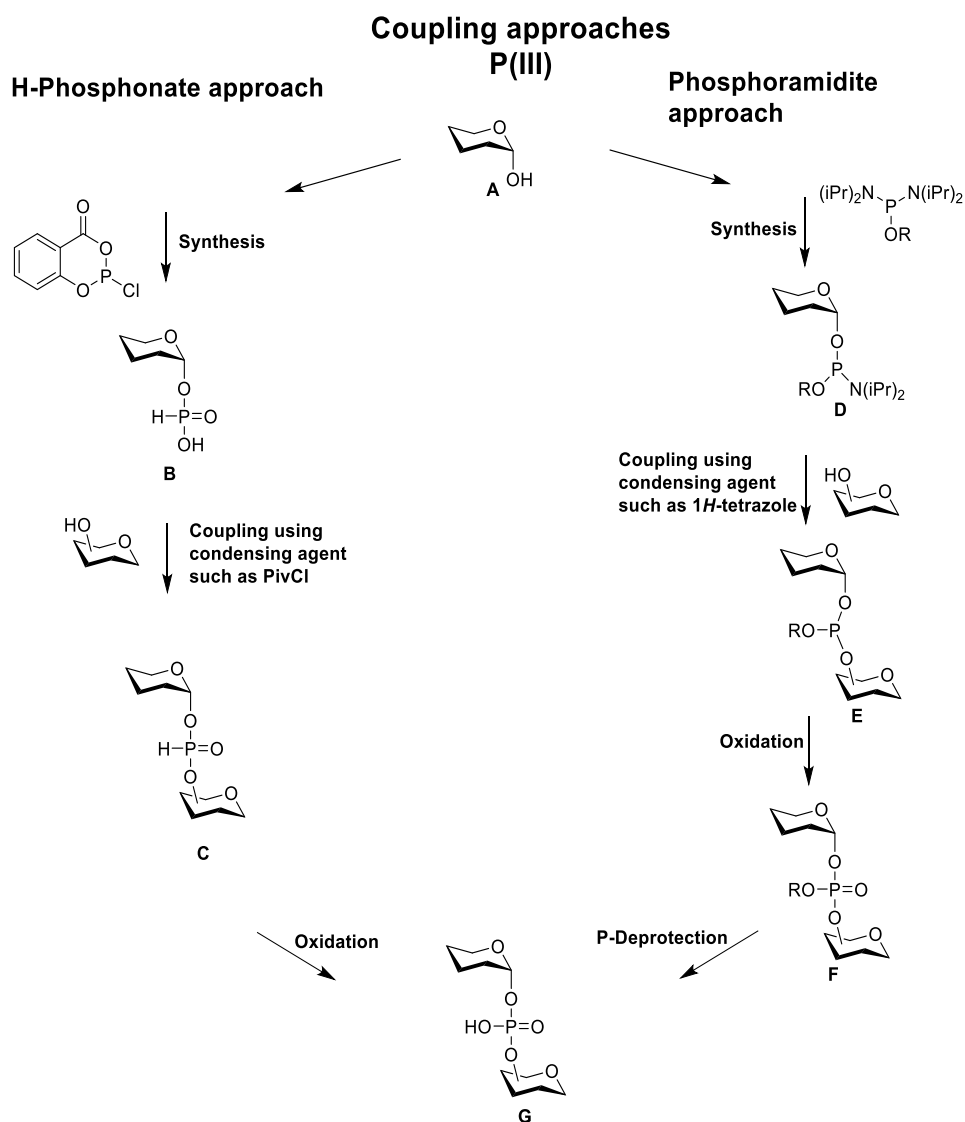
### 5.4.1 Phosphoramidite vs H-Phosphonate Methodology

Phosphoramidite and H-Phosphonate protocols are based on P(III) chemistry. Both procedures shown in detail in **Scheme 26** include two steps, the condensation followed by an oxidation to a phosphate.

*H*-Phosphonate method was first described by van Boom's group in the mid 1980s. Starting from commercially available reagents, such as salicylchlorophosphite, the desired *H*-phosphonate **B** can be obtained in good yields. The coupling step with a monohydroxy component in the presence of a condensing agent (typically pivaloyl chloride) is completed within 2-5 min and the resulting *H*-phosphonate diester **C** is further oxidized to the desired phosphodiester **G**. Since more than 30 years, this method has been applied in very successfully couplings such as the synthesis of glycosyl phosphates of *N*-acetyl- $\alpha$ -D-glucosamine as well as (1 $\rightarrow$ 6)-linked phosphodiester containing *N*-acetyl- $\alpha$ -D-mannosamine, which was not possible with the phosphoramidite approach.<sup>113</sup> The phosphoramidite approach is very similar but requires an additional protecting group that needs to be removed, but its presence can also facilitate the purification of the resulting phosphosaccharide.

The phosphoramidite approach was first described by Beaucage and Caruthers in 1980s.<sup>114</sup> The preparation of phosphoramidite intermediate **D** is easy and straightforward by using standard organic chemistry procedures. After coupling with a monohydroxy component using 1-*H* tetrazole as condensation agent, phosphite **E** is further oxidized (mostly in situ) to a phosphodiester **F**. After removing the additional protecting group **G** is obtained in high yields.<sup>114</sup> The phosphoramidite method found extensive application in the synthesis of biologically important nucleotides such as cytidine-5'-monophospho-*N*-acetylneuraminic acid (CMP-Neu5Ac).<sup>115</sup> Finally, the robustness of the phosphoramidite protocol is further proven by its effectiveness in the automated synthesis of oligonucleotides.<sup>112,116</sup>

Both approaches are very effective and result in high yields and even if the phosphoramidite requires three steps to obtain the phosphosaccharide (coupling, oxidation and deprotection, **Scheme 27**), due to its suitability for use in automated synthesis we decided to apply this protocol for our synthesis of Hia oligomers. However, before applying the automated synthesis to the preparation of Hia oligomers, the solution phase chemistry needs to be optimized. Each coupling cycle comprises three reaction steps: condensation, oxidation and deprotection for the following coupling cycle (**Scheme 27**).



**Scheme 26.** Comparison of H-Phosphonate and phosphoramidite approach as coupling methods.

Potential condensation reagents are shown in **Table 7**.

**Table 7.** Comparison of possible condensation reagents.<sup>117</sup>

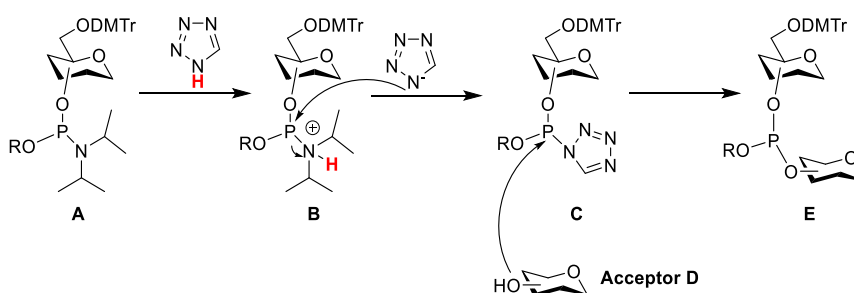
Name		pKa	Solubility in ACN
1 <i>H</i> -tetrazole		4.9	0.5 M
5-(ethylmercapto)-1 <i>H</i> -tetrazole		4.3	0.75 M
4,5-dicyanoimidazole		5.2	1.2 M
5-(benzylmercapto)-1 <i>H</i> -tetrazole		4.1	0.44 M

For the condensation step several activators are known such as 5-(benzylmercapto)-1*H*-tetrazole, 5-(ethylmercapto)-1*H*-tetrazole, 4,5-dicyanoimidazole and 1*H*-tetrazole (the most popular one). As shown in **Table 7**, 4,5-dicyanoimidazole (DCI) fully meets these requirements, thanks to its mild acidity and excellent solubility in ACN, even at low temperature. Additionally, previous studies showed that DCI promotes fast couplings with no observable side effects, and effective reactions with slight excess of phosphoramidite are reported.<sup>118</sup>

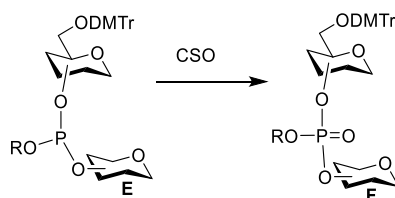
These activators are shown in **Table 7** and follow the same mechanism, which is exemplified in **Scheme 27** with 1*H*-tetrazole using *N,N*-diisopropylphosphoramidite.

### Phosphoramidite Approach

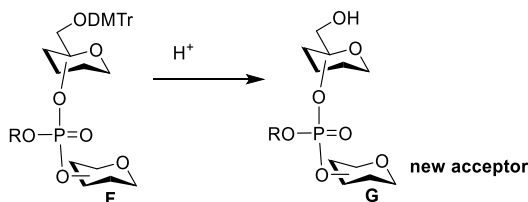
#### 1. Condensation



#### 2. Oxidation



#### 3. Preparation for a new cycle



**Scheme 27.** Phosphoramidite chemistry. Every coupling cycle consist of three different steps: Condensation, oxidation and deprotection for the following cycle.

After protonation of the diisopropylamino group in **A**, the hydroxy group on the 'acceptor **D**' can attack the phosphorous of the phosphoramidite **C** giving the phosphite triester **E**.<sup>119,117</sup>

The fluorenylmethyloxycarbonyl (Fmoc) and dimethoxytrityl (DMTr) are the temporary protecting groups most commonly used in automated synthesis. In particular, DMTr is acid labile and requires a strict control of the pH of the reaction medium to prevent its deprotection. For this reason, when using DMTr as a temporary protection the pKa of the activator is a key parameter, as well as the solubility in ACN, which is the most commonly used solvent for phosphoramidite couplings.<sup>117</sup>

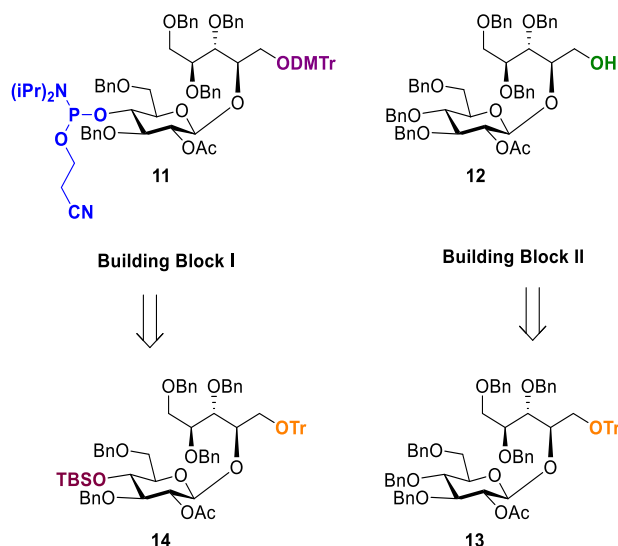
Next to the condensation step, the subsequent oxidation step also needed consideration. Iodine in aqueous pyridine is the most frequent reagent for the oxidation, but the formation of some undesired byproducts is reported. Furthermore, the use of aqueous basic conditions is unsuitable for some compounds. Several anhydrous methods have been developed and reported in literature, such as *m*-chloroperbenzoic acid (MCPBA) in DCM, *tert*-butyl hydroperoxide (TBHP)/toluene solution in acetonitrile, bis(trimethylsilyl)peroxide in DCM, dimethyldioxirane in DCM and (1S)-(+)-(10-camphorsulfonyl)oxaziridine (CSO) in acetonitrile. MCPBA is toxic and additionally generates *m*-chlorobenzoic acid during the oxidation which can cleave acid labile temporary protecting groups such as DMTr. TBHP, CSO and bis(trimethylsilyl)peroxide are all commercially available, even expensive, and the silylated peroxide is rather explosive.<sup>120</sup> We decided to employ CSO for the oxidation of **E** to **F**, due to its high solubility in ACN (**Scheme 27**). In this way, the oxidation could be performed at room temperature right after the condensation step in a one-pot reaction, obtaining satisfying reaction rates.

Finally, the coupling product is transformed into a new acceptor for an iterative cycle. In particular, the dimethoxytrityl group in **F** is cleaved under mild acid conditions to deliver a free hydroxy group in **G**, which can attack the phosphoramidite in the following condensation step in an additional cycle. The three-steps cycle can be repeated until the desired chain length is obtained. In an automated system, all three steps (condensation, oxidation, and deprotection of DMTr) are carried out iteratively, until the desired oligomer is achieved. On the contrary, in solution phase the product of each coupling is isolated and purified via silica gel chromatography followed by size exclusion.



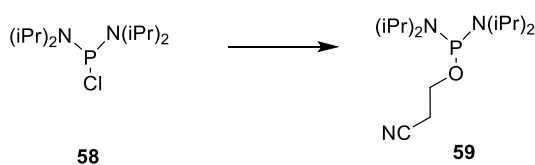
## 5.4.2 Synthesis of Oligomers: Approach I

For Approach I, we synthesized two different building blocks. Compound **11** (building block I) was prepared from disaccharide **14**, while compound **12** (building block II), representing the upstream residue of all oligomers, was synthesized from disaccharide **13** (Scheme 28).



**Scheme 28.** Retrosynthetic analysis for building blocks I and II.

Before starting to synthesize building block I, we prepared the phosphinite reagent **59**, which was required for the introduction of the phosphoramidite in intermediate **11**. Due to its high cost, phosphinite **59** was freshly prepared starting from cheap commercially available phosphine **58** (Scheme 29).



**Scheme 29.** Preparation of phosphinite **59**. Reagents and conditions: 3-Hydroxypropionitrile,  $\text{NEt}_3$ , 4 h,  $\text{Et}_2\text{O}$ , up to 70%.

Starting from phosphine **58** we generated the phosphinite **59** using triethylamine as a base and 3-Hydroxypropionitrile as temporary protecting group for the phosphinite.

Strictly dry conditions were applied, and molecular sieves were added to avoid formation of hydrolysis byproducts. Usually, the reaction proceeded within 4 h at room temperature. The reaction progress was checked every hour by  $^{31}\text{P}$ -NMR and a shift of the phosphorous signal indicated conversion to the phosphinite (**Figure 17**).

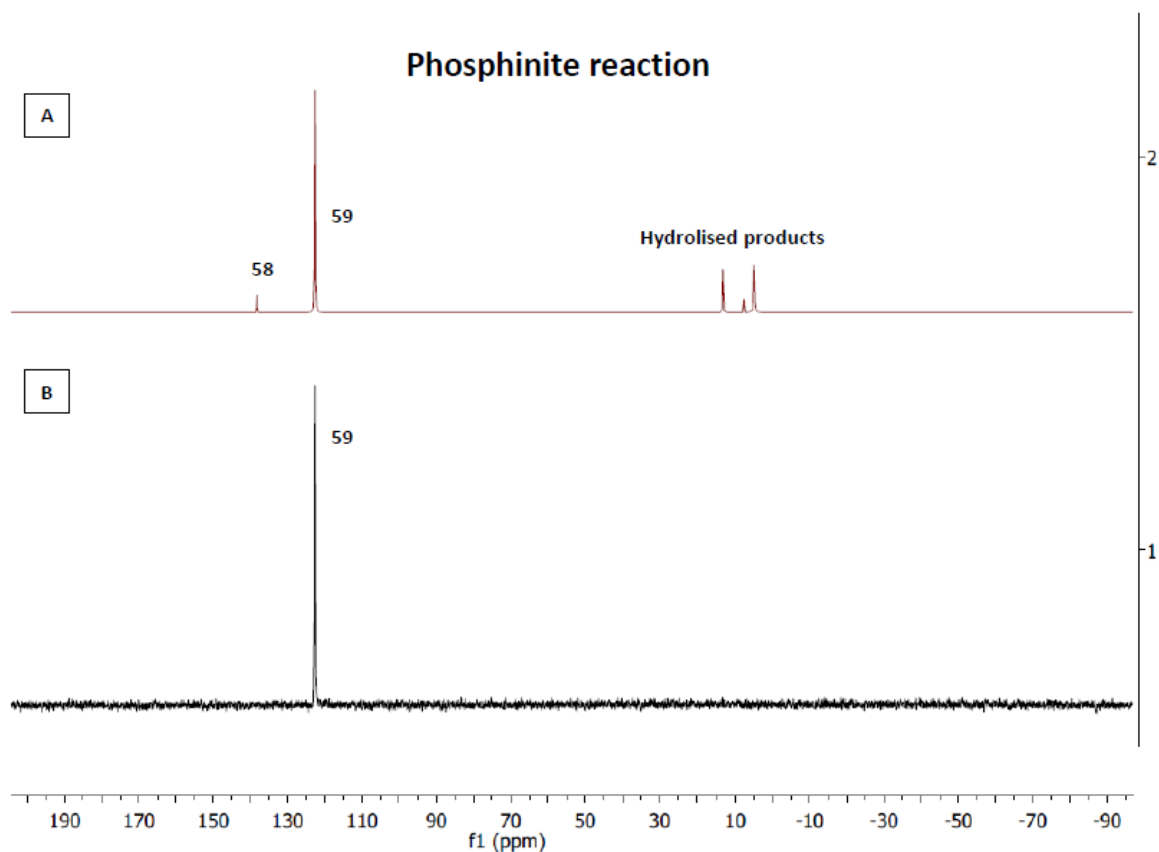
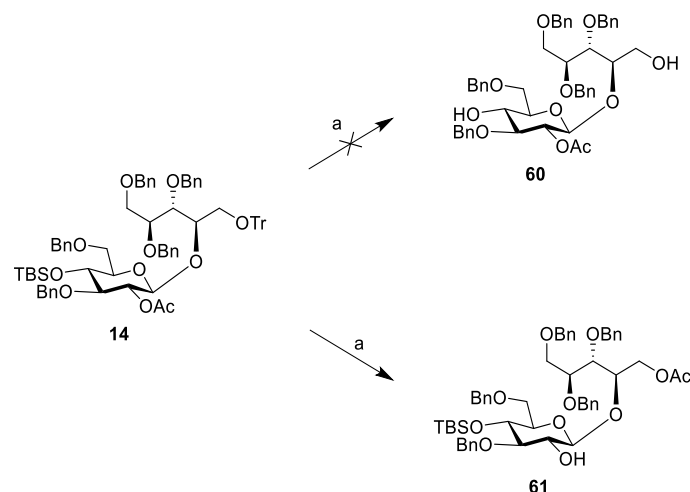


**Figure 17.** The reaction progress of the phosphinite synthesis was monitored by  $^{31}\text{P}$  NMR (A) and purification gave clean phosphinite (B).

Furthermore, as the product is highly labile under acidic conditions, deuterated acetone for NMR analysis was used as a solvent. Hydrolysis byproducts cannot be completely avoided during the reaction and after completion compound **59** was isolated and purified by short column chromatography with buffered  $\text{SiO}_2$  (100% Hex, 2%  $\text{NEt}_3$ ). It should be also noted that **59** was always used within 24 h after preparation for the synthesis of a phosphoramidite.

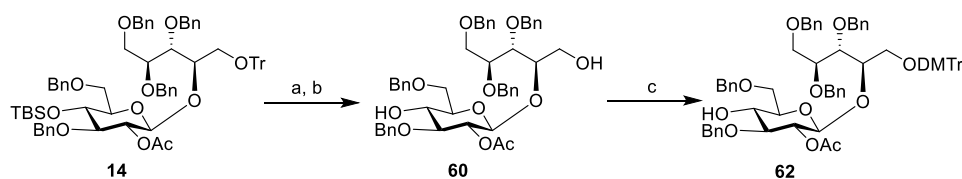
Disaccharide **14** was the precursor of building block I and has two important features: the phosphoramidite group (in blue) on the glucose moiety, and the dimethoxytrityl as temporary protecting group (in purple) on the ribitol. The dimethoxytrityl group is next to the protection group Fmoc a commonly used protecting group in the phosphoramidite couplings as well as in automated systems, but DmTr is highly acid labile. Hence, we introduced this orthogonal protecting group only a few steps before the coupling on our building block I.

To start the synthesis of building block I, the silyl and the trityl group were both deprotected in the following steps. As both protecting groups are acid labile, in theory they could be cleaved simultaneously using TFA (**Scheme 30**).



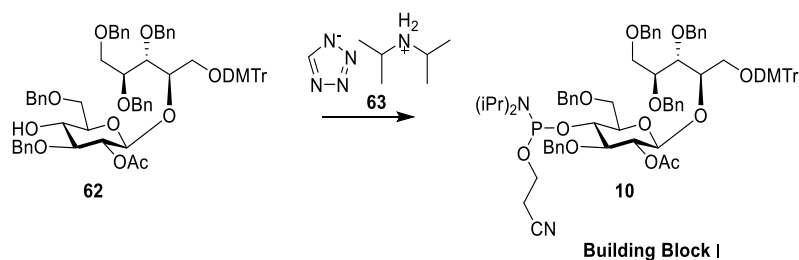
**Scheme 30.** Simultaneous deprotection of the silyl and trityl group. Reagents and conditions: (a) TFA, DCM, 17 h.

As the trityl group was more acid sensitive than TBS, its deprotection occurred faster delivering a primary hydroxy group. The reaction was stirred for more than 17 h and the formation of several products was observed by TLC. NMR analysis of the main product showed that the silyl ether was still in place, and probable intermolecular transesterification led to undesired product **61**. Due to this unexpected outcome, we applied a two-steps deprotection sequence to obtain **60** (**Scheme 31**).



**Scheme 31.** Synthesis of **62**. Reagents and conditions: (a) TBAF (1.0 M in THF), 20 min 0°C, THF, (b) TFA, 0°C – r.t., 40 min, DCM, (c) DMTrCl, TEA, 19 h, 80% over three steps.

First, the silyl ether was cleaved with 1 M TBAF in THF solution, followed by removal of the trityl group in acidic conditions to afford the desired alcohol **60**. After optimization, crude **60** was further treated with dimethoxytrityl chloride and  $\text{NEt}_3$  to yield **62** in 80% over three steps.

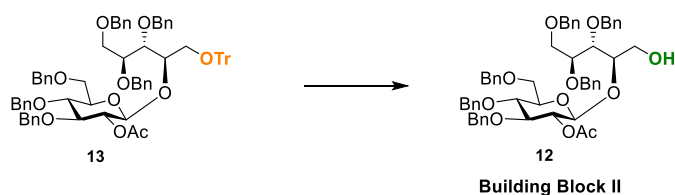


**Scheme 32.** Preparation of building block I. Reagents and conditions: Phosphinite **59**, tetrazolidine **63**, DCM, r.t. 95%.

Finally, building block I (*i.e.* phosphoramidite **10**) was obtained in excellent yields (95%) by reacting compound **62** with phosphinite **59** in the presence of tetrazolidine **63** (**Scheme 32**).

Compound **11** will be used as iteration block for subsequent elongations in the synthesis of Hia oligomers with different chain length.

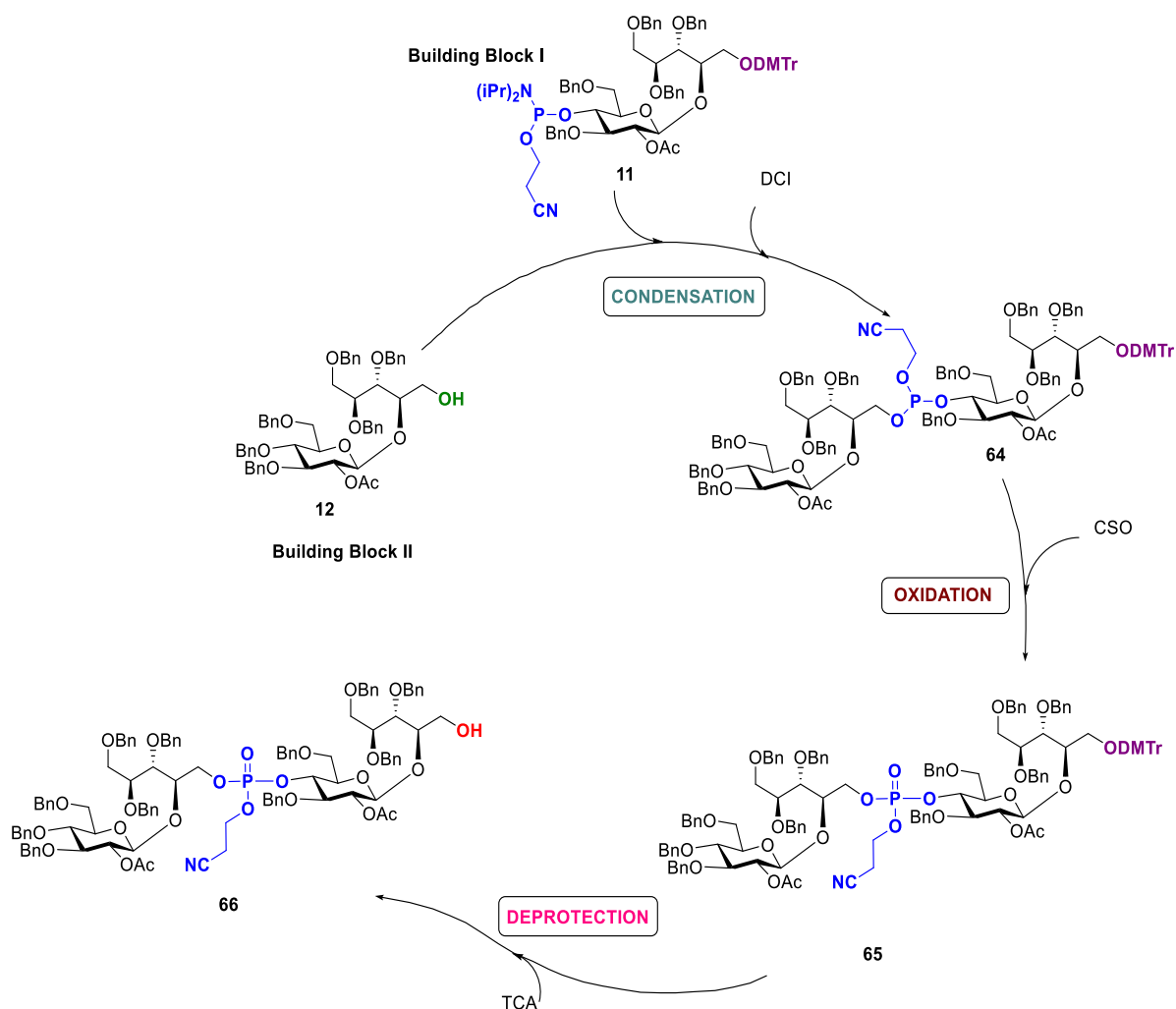
Having building block I in our hands, building block II (*i.e.* compound **12**) was prepared starting from disaccharide **13**. As mentioned above, building block II is the upstream residue of each final oligomer, as it will be coupled with the iteration block **11** for further elongation. Likewise, building block II will be coupled to the linker in the synthesis of the single repeating unit of Hia polysaccharide.



**Scheme 33.** Preparation of building block II. Reagents and conditions: TFA, DCM 0 °C- r.t, quant.

Deprotection of the trityl group using acidic conditions (TFA in DCM at 0°C) proceeded fast and in excellent yields (**Scheme 33**).

Each coupling consisted of a three steps sequence: condensation, oxidation and removal of the dimethoxytrityl protecting group. Previous studies with some already available intermediates in the Lab of Prof. Lay showed that it is key to perform the three steps in a row due to difficult separation of the intermediate after the oxidation to the phosphate. **Scheme 34** shows in detail the first coupling cycle to achieve dimer **66**.

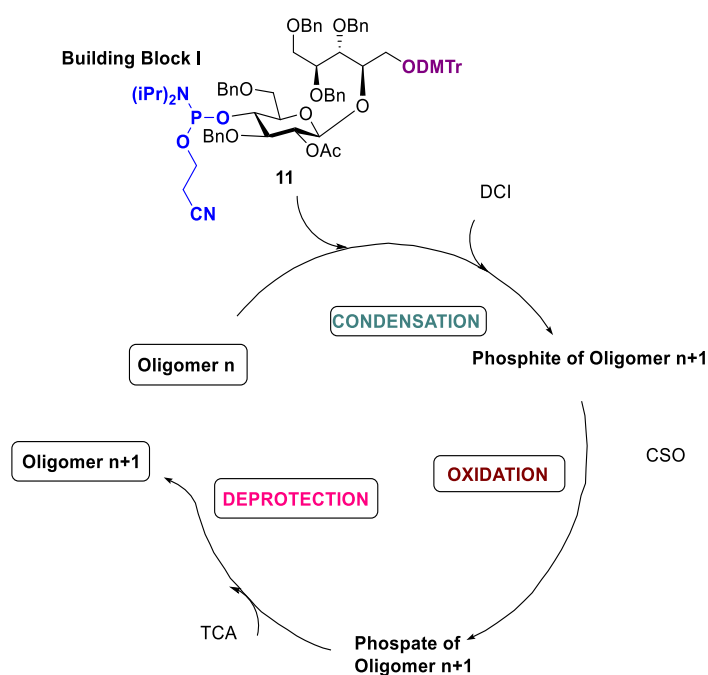


**Scheme 34.** Synthesis of dimer **66**. Reagents and conditions: DCl, DCM, MS 4 Å, then CSO, then TCA (0.18 M in DCM), DCM, 79%.

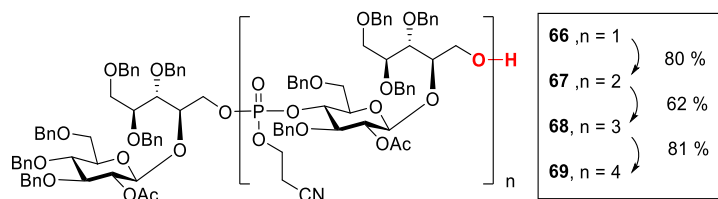
Molecular sieves were used to avoid hydrolysis byproducts and starting from building block II the condensation step was carried out with DCl and building block I. The resulting phosphite triester **64** was oxidized using CSO in a one pot-reaction giving **65**. The reaction was monitored by HPTLC, and the couplings proceeded fast in 2 h followed by the oxidation in 30 min. The molecular sieves were removed by filtration and an aqueous extraction was performed. Subsequently, deprotection of the dimethoxytrityl group was carried out after work-up with trichloroacetic acid (TCA). The reaction was quenched by MeOH/water and the dimer **66** was obtained in good yield (79%). All reactions are performed at r.t. and the condensation step was carried out under inert atmosphere.

In an additional cycle, dimer **66** can serve as a 'new' acceptor and was coupled to the bifunctional building block I (**11**). After condensation with DCI, oxidation with CSO and DMTr deprotection using TCA the trimer **67** was obtained. This procedure was iterated to obtain different oligomers up to the pentamer **69** as summarised in **Scheme 35**. After each cycle, the resulting oligomer was isolated and purified by silica gel and size exclusion chromatography (see Experimental Procedures). The success of the phosphoramidite approach was also proven by the high yields of each coupling step.

### General Oligomerization Procedure



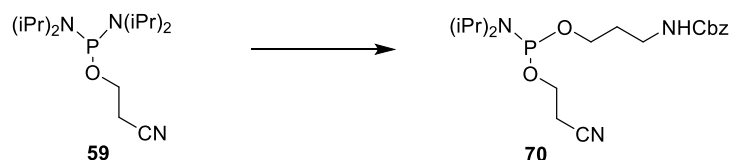
### Final Oligomers



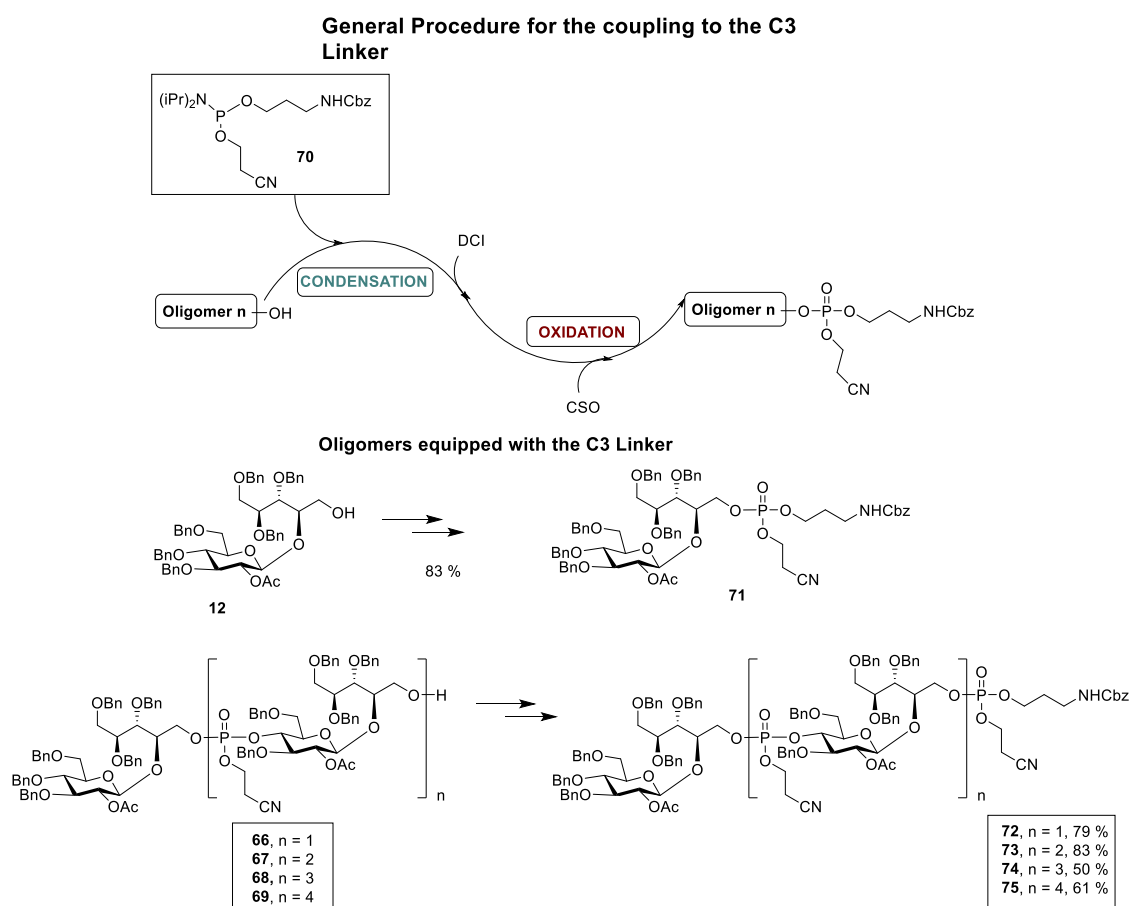
**Scheme 35.** General overview of our oligomerization procedure using phosphoramidite approach to obtain up to the pentamer. Reagents and conditions: DCI, DCM, MS 4 Å, then CSO, then TCA (0.18 M in DCM), DCM.

All our oligomers **66-69** were characterized by NMR studies and the corresponding mass experiment.

Having the oligomers **66-69** in our hands, the next step was the preparation of the linker and its coupling to our oligomers, once again using the phosphoramidite approach. Accordingly, phosphoramidite **70** was obtained in 82% yield from freshly prepared phosphinite **59** and 3-benzyloxycarbonylamino-1-propanol using tetrazolide salt **63** as activating agent (**Scheme 36**).



**Scheme 36.** Preparation of the phosphoramidite **70** with our C3 Linker. Reagents and conditions: 3-(Cbz-amino)-1-propanol, tetrazolide **63**, DCM, r.t. 82%.

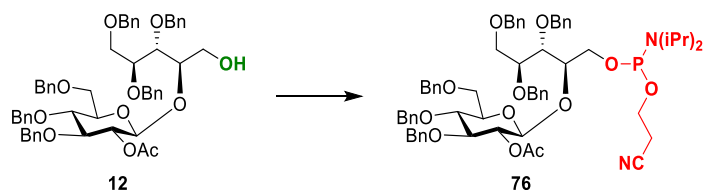


**Scheme 37.** General procedure for the coupling with the C3 Linker to our oligomers. Reagents and conditions: DCI, DCM, MS 4 Å, then CSO.

Our four oligomers **66-69**, as well as the monomer **12**, were functionalized with the C3 linker using phosphoramidite **70** as described in **Scheme 37**. The coupling reactions were carried out again using DCI as a condensing agent, followed by oxidation with CSO at room temperature in a one-pot reaction. Oligomers **71-75** were obtained in good to high yields.

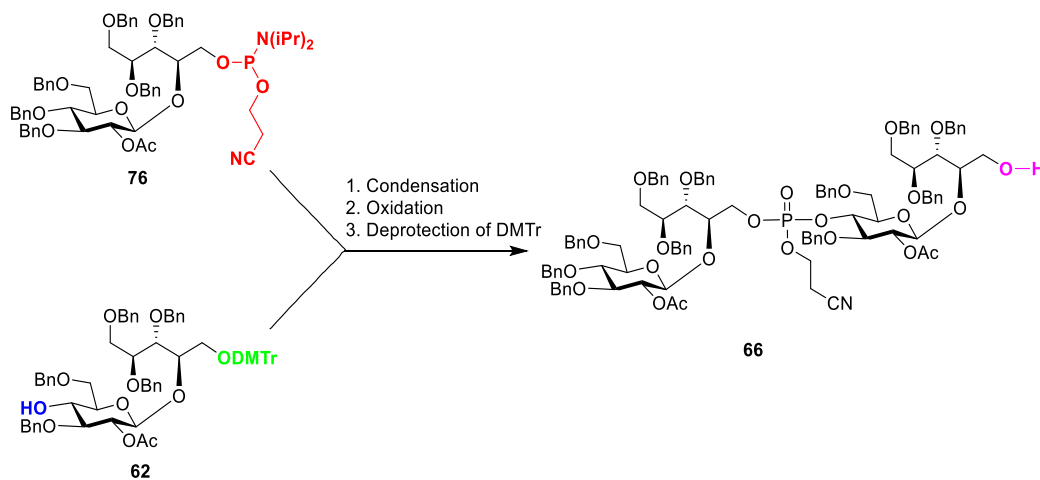
### 5.4.3 Coupling approach II

In addition to the methodology described in section 5.4.2, we also explored an alternative approach based on different building blocks for the synthesis of Hia oligomers. This strategy was tested in a new synthesis of dimer **66**. In particular, disaccharide phosphoramidite **76** was obtained from disaccharide **12**, while compound **59**, available from the approach described in 5.4.2, was used as acceptor. Phosphoramidite **76** was prepared from disaccharide **12** and phosphinite **59** in excellent yield (up to 98%) as previously reported (**Scheme 38**).



**Scheme 38.** Reagents and conditions: Phosphinite **59**, tetrazolid **63**, DCM, r.t., 3 h, 98%.

The major difference to the prior described coupling procedures were the nature of the building blocks. In this strategy, the bifunctional building block **62** serves as acceptor moiety (free 4-OH) with the dimethoxytrityl as a temporary protecting group. On the other hand, the phosphoramidite moiety is placed on the primary hydroxy group on disaccharide **76**.

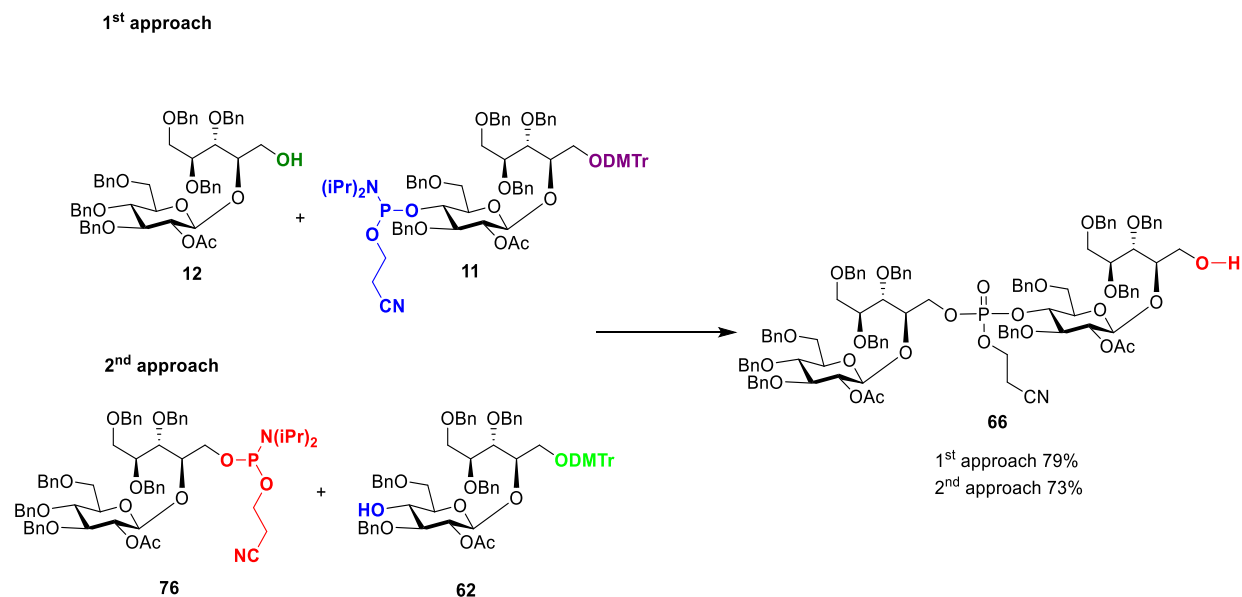


**Scheme 39.** Different coupling procedure was applied to achieve the dimer **66** using phosphoramidite **76** and acceptor **62**. Reagents and conditions: DCI, DCM, MS 4 Å, r.t., 1 h then CSO, 30 min, then TCA (0.18 M in DCM), DCM, 30 min, 73%.

The elongation strategy requires the introduction of the phosphoramidite group on the primary hydroxyl of the newly formed oligomer, followed by the subsequent coupling with acceptor **62**. The coupling was carried out using the same conditions previously described. In the condensation step we used DCI followed by an oxidation with CSO in a one pot-reaction (**Scheme 39**). The last step was the



dimethoxytrityl deprotection using acidic conditions to obtain dimer **66** in good yields (73%). In **Scheme 40** the two different approaches are summarized.



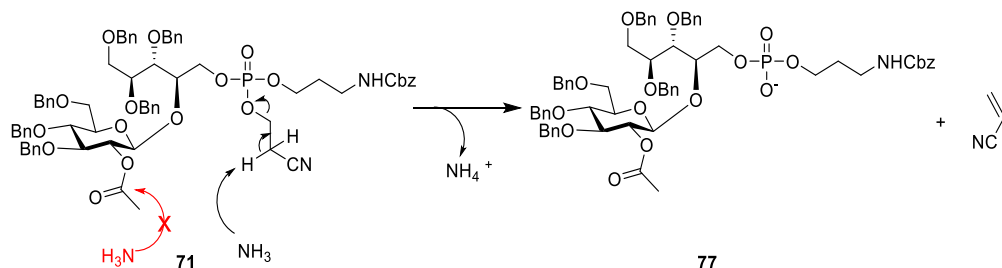
**Scheme 40.** Comparison of the two different coupling approaches.

Both phosphoramidite compounds **11** and **76** were synthesized and then coupled in high yields with the corresponding acceptor (**12** and **62**, respectively) using DCI and CSO for the oxidation.

Despite of the different structure of the building blocks, the dimer **66** was successfully achieved with both approaches in comparable yields (79% for 1<sup>st</sup> approach and 73% for the 2<sup>nd</sup> approach). After all, the 2<sup>nd</sup> approach leads to some disadvantages, so that we decided to apply the 1<sup>st</sup> approach. The synthesis of the dimer **66** is successfully achieved and to continue this method to attain the trimer **67**, the phosphoramidite building block needs to be prepared from the primary hydroxy group in **66** in an additional step. The dimer is already very precious, and reactions should be minimized. However, in the 1<sup>st</sup> approach, dimer **66** can be the new acceptor for the coupling to synthesize trimer **67** using **11** as bifunctional building block without any further changes and therefore, we decided to apply the 1<sup>st</sup> approach for our couplings.

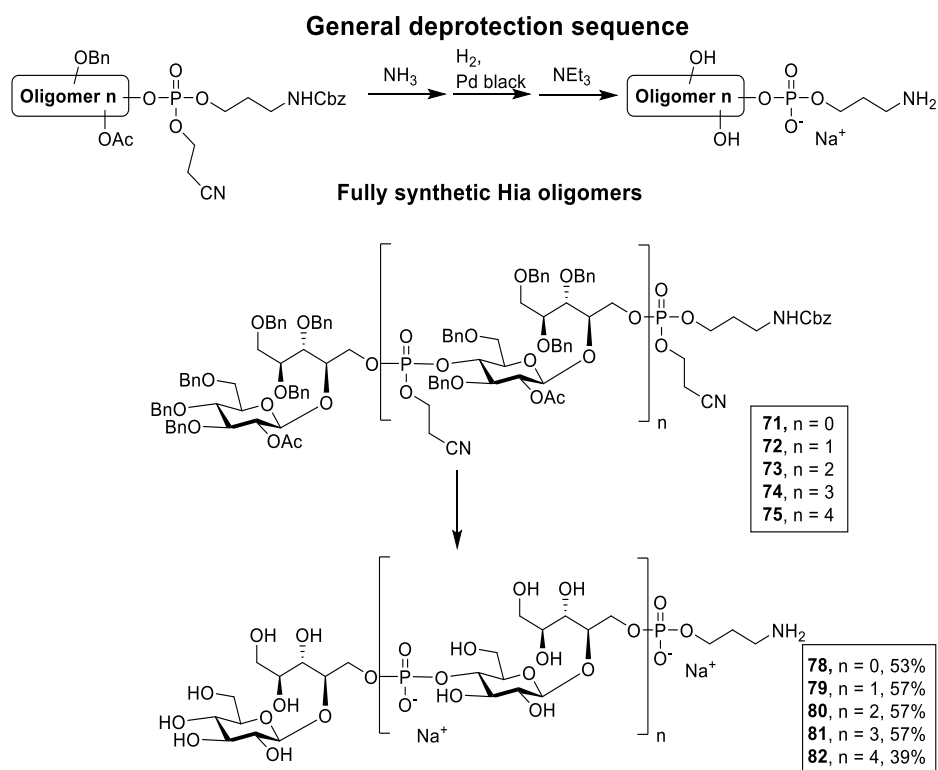
## 5.4.4 Deprotection of the oligomers

The full deprotection of the synthesized oligomers was carried out by removal of the cyanoethyl group to deliver the phosphate using basic conditions followed by hydrogenolysis of the remaining protecting groups. A common procedure to deprotect the cyanoethyl is 30-33% ammonia in aqueous solution which, according to the pH, should also deprotect the acetyl esters simultaneously.



**Scheme 41.** Mechanism of deprotection of the cyanoethyl group with ammonia. Under these conditions, however, complete removal of the acetyl esters was unsuccessful.

However, treating **71** with ammonia gave unfortunately **77**, with the acetyl group still partially remaining and even longer reaction time gave always a mixture of partially acetylated oligomers. The mechanism for the deprotection of the cyanoethyl group with ammonia is shown in **Scheme 41**.

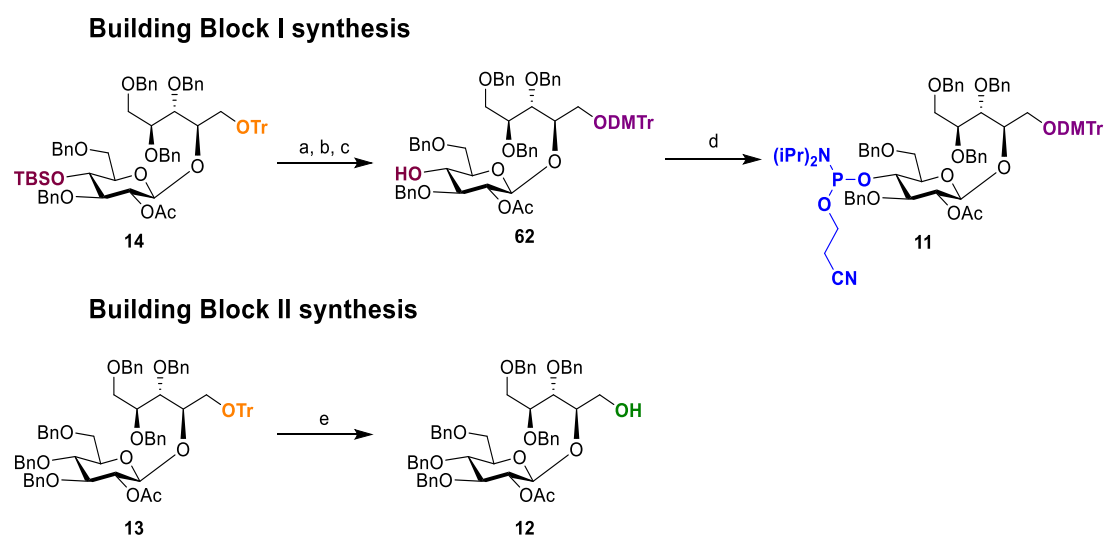


**Scheme 42.** General deprotection sequence to obtain final synthetic oligomers **78-82**. Reagents and conditions:  $\text{NH}_3$  (30-33%), dioxane, water, 18 h, then  $\text{H}_2$ , Pd black, AcOH, 2-4 days, then  $\text{NEt}_3$ , water, 24 h

Therefore, we decided to apply a different deprotection sequence. After treatment with ammonia and hydrogenolysis of the benzyl ethers and Cbz, full deacetylation was achieved using  $\text{NEt}_3$  and water. This deprotection sequence was successfully used on every oligomer giving five fully deprotected Hia oligomers with different chain length **78-82** (Scheme 42).

### 5.4.5 Summary and conclusion

Within this section we successfully described the application of the phosphoramidite approach to synthesize Hia oligomers with different chain length. First, the synthesis of building blocks **11** and **12** is reported starting from disaccharides **13** and **14** (Scheme 43).

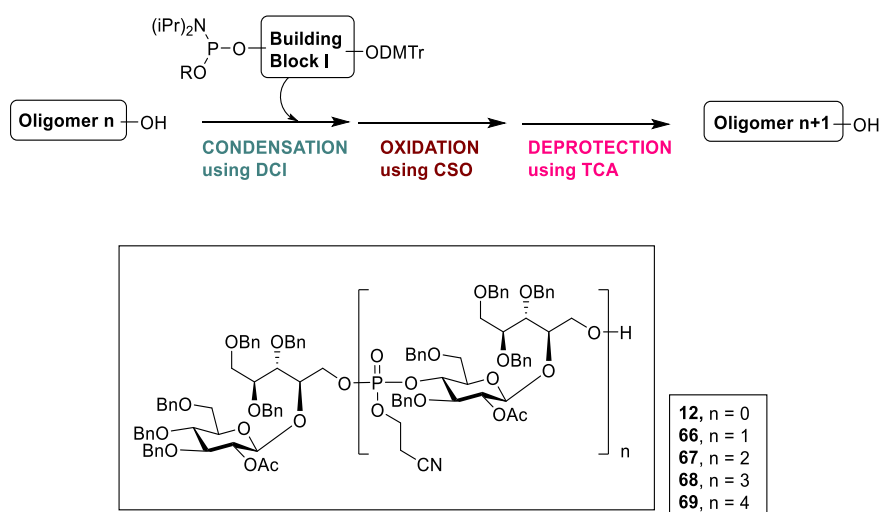


**Scheme 43.** Preparation of Building Block I and II. Reagents and conditions: (a) TBAF (1.0 M in THF), 20 min 0°C, THF, (b) TFA, 0°C – r.t., 40 min, DCM, (c) DMTrCl, TEA, 19 h, 80% over three steps, (d) Phosphinite **59**, tetrazolid salt **63**, DCM, r.t. 95%, (e) TFA, DCM 0 °C- r.t, quant.

Furthermore, the synthesis of dimer **66** was carried out using two building blocks **11** and **12**. The bifunctional building block **11** was required for each elongation step using **12** as the first corresponding acceptor. Of note, disaccharide **12** represents the repeating unit for the synthesis of Hia oligomers (Scheme 44).

The dimer can be then used in an iterative coupling as new acceptor using the general oligomerization sequence described before.

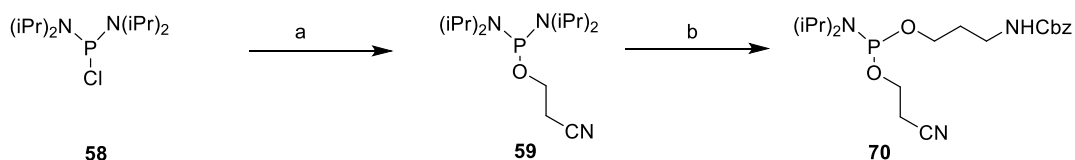
### General Oligomerization Sequence



**Scheme 44.** General oligomerization sequence applying phosphoramidite approach to achieve up to the pentamer **69**. Reagents and conditions: DCI, DCM, MS 4 Å, then CSO, then, TCA (0.18 M in DCM), DCM.

Every oligomerization cycle contains three steps: condensation using DCI and phosphoramidite **11**, oxidation with CSO and deprotection of the temporary protecting group. All condensation as well as oxidation reactions were carried out at room temperature and proceeded a couple of hours (condensation) and 30 min (oxidation). The last step was the deprotection of the dimethoxytrityl group using acidic conditions. After each cycle the oligomer was isolated, purified and the resulting compound was employed as new acceptor in the next iterative cycle. With this approach we obtained four oligomers with different chain length **66-69** in good yields of up to 80%.

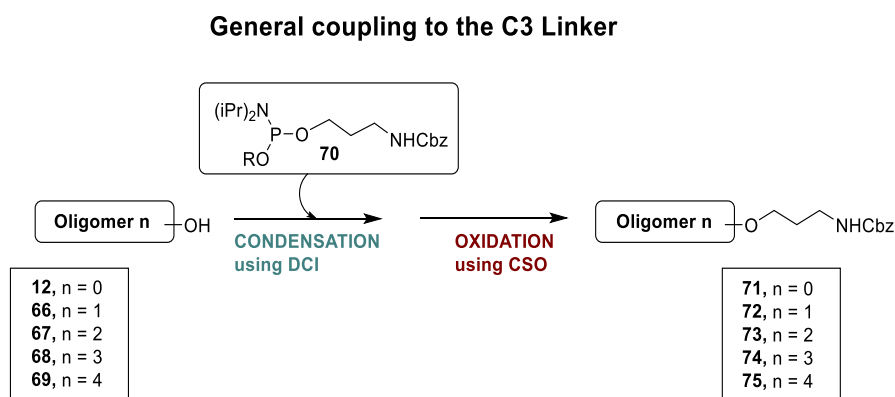
Furthermore, we described two different coupling approaches using the phosphoramidite methodology to achieve the dimer **66** (described in **5.4.2** and **5.4.3**). For both methods different building blocks were successfully synthesized. Additionally, both methods showed positive results and the yields for the dimer were comparable. However, the approach described in **5.4.3** showed some disadvantages as more synthetic steps are necessary for the iterative coupling. To achieve trimer **67**, the primary hydroxy group on the dimer **66** must be converted into a phosphoramidite and can be then coupled to the bifunctional building block **59**. Since the preparation of dimer **66** required several reaction steps, the least synthetic steps as possible should be performed on this precious intermediate. For this reason we decided to continue with the approach described in **5.4.2**.



**Scheme 45.** Preparation of the phosphoramidite **70**. Reagents and conditions: (a) 3-Hydroxypropionitrile,  $\text{NEt}_3$ , 4h,  $\text{Et}_2\text{O}$ , up to 70% (b) 3-(Cbz-amino)-1-propanol, tetrazolid salt **63**, DCM, r.t. 82%.

For further protein conjugation, we needed a linker on our oligomers using again the phosphoramidite approach for the coupling. At first, the phosphinite **59** was synthesized from the commercially available phosphine **58** followed by coupling with the C3 linker in good yields (**Scheme 45**).

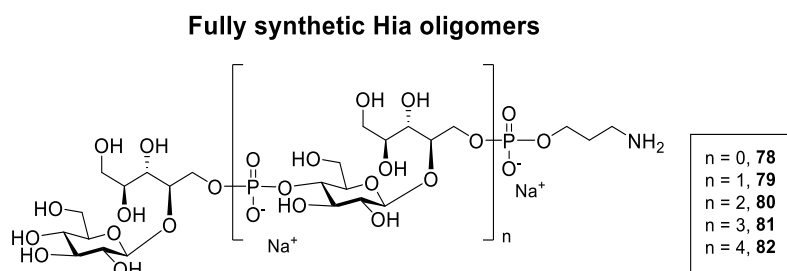
Then, for the coupling of the C3 linker we applied the same protocol of the phosphoramidite method which enabled the successful assembly of all oligomers (**Scheme 46**).



**Scheme 46.** General approach for coupling with the C3 Linker. Reagents and conditions: **70**, DCI, DCM, MS 4 Å, then CSO.

Our oligomers were coupled to the C3 Linker, using DCI for the condensation step followed by in-situ oxidation using CSO. We effectively obtained five oligomers (**71-75**) equipped with a linker for further protein conjugation.

As next step, a deprotection sequence was employed for each oligomer in order to obtain our fully deprotected oligomers (**Scheme 47**). At first, the deprotection of the cyanoethyl group as well as the acetyl groups were attempted using aqueous ammonia. Unfortunately, the acetyl groups were only partially deprotected with this procedure, therefore we applied the following sequence: Treatment with ammonia, hydrogenolysis followed by deacetylation using  $\text{NEt}_3$ . This deprotection scheme was employed for each oligomer (**71-75**) and we obtained after purification and cation exchange our final synthetic Hia oligomers (**78-82**).



**Scheme 47.** Overview of our synthetic deprotected oligomers bearing a linker.

## 5.5 Preparation of the Hia glycoconjugates

As next step all our well-defined oligomers were conjugated to a carrier protein and then further studied. Additionally, HSA-conjugates of the trimer and the pentamer were prepared as a control for future biological tests.

### 5.5.1 Carriers and their chemistry

Five different proteins for the protein conjugation are currently licensed: diphtheria toxoid, tetanus toxoid, CRM<sub>197</sub>, *Haemophilus* protein D and the outer membrane protein complex of serogroup B meningococcus (OMPC). In addition to these five protein carriers, others have been tested in preclinical studies and some are tested in clinical trials such as the recombinant non-toxic form of *Pseudomonas aeruginosa* exotoxin A. In order to select carriers for glycoconjugate vaccines a strong record of safety in conjugation with availability at industrial scale is essential and additionally, any toxic or enzymatic activity of the carrier should be removed before testing a protein as new carrier. Furthermore, manufacturability (yields, production cost and quality of the product) at large scale and according to cGMP are important requirements.<sup>121</sup>

Moreover, nanoparticle systems are also being studied to combine the multivalent presentation of carbohydrates with special physio-chemical properties of nanoparticle system.<sup>121</sup>

In order to link carbohydrates to the desired carrier protein, many approaches are nowadays known and summarized in **Figure 18**. Amino acid residues which are exposed on the protein surface and whose side chains have suitable functional groups such as primary amino groups of lysines and carboxylic groups of glutamic and aspartic acid residues are used for the covalent bond to the glycan. Carboxylic groups can react selectively with an amino or hydrazido linker attached to the sugar moiety by a carbodiimide mediated condensation. Lysines can be coupled using succinimido esters or cyano-esters, squarate, or by direct reductive amination.<sup>34, 121</sup>

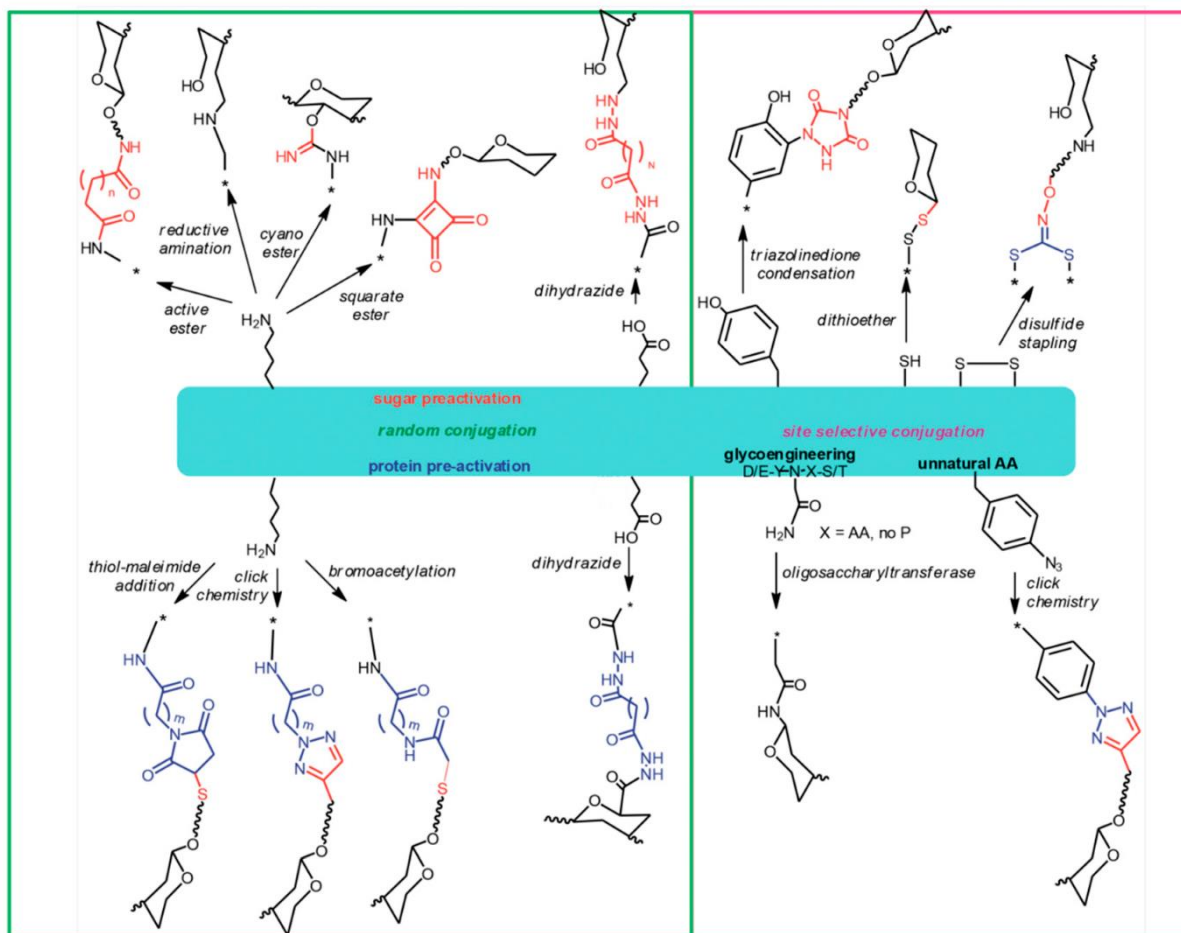


**Figure 18.** Different approaches are known to attach glycans to carrier proteins.<sup>121</sup>

The protein carrier can also be modified for conjugation using hydrazides, bromoacetyl groups or maleimido groups which are reacting with carboxyl groups, cyanoesters or thiol groups on the carbohydrate moiety. Additionally, azido groups can also be introduced into proteins for coupling to glycans with alkynes via cycloaddition. In general, conjugation using the upper described conditions results in a random ratio carbohydrate to protein as well as a random display on the surface of the protein. Currently, a technology known as “bioconjugation” is emerging and herein the glycosylation site is placed selectively on the carrier protein.<sup>121</sup>

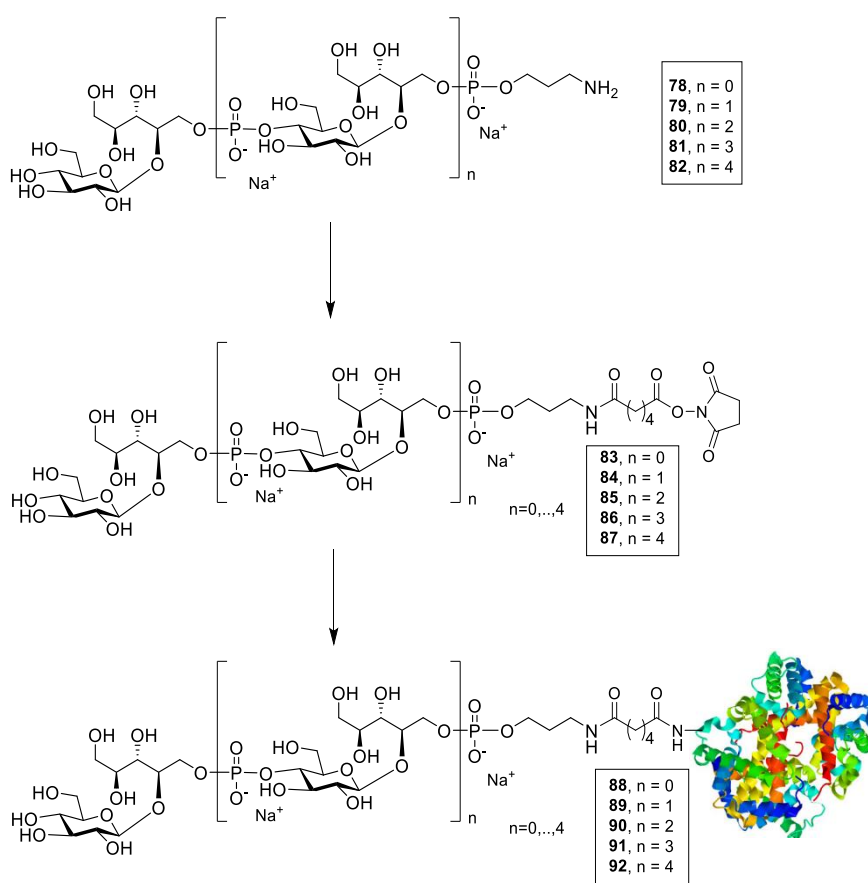
### 5.5.2 Pre-activation and Conjugation to CRM<sub>197</sub>

Cox et al. reported two studies in which the natural polysaccharide was activated by oxidation of the vicinal hydroxyls of the ribitol and then further coupled either to CRM<sub>197</sub> or to the protein D. CRM<sub>197</sub> showed more promising results, and therefore, we decided to couple **78-82** to CRM<sub>197</sub>.<sup>85,86</sup>

CRM<sub>197</sub> is a 58 kDa nontoxic mutant of diphtheria toxin with a substitution at position 52 from Glutamic amino acid to Glycine and hence, the protein does not require any chemical detoxification.<sup>122</sup>

Nowadays, CRM<sub>197</sub> can be either isolated from *Corynebacterium diphtheriae* C7(β197)tox(-) or produced by recombinant DNA techniques. Furthermore, CRM<sub>197</sub> as protein carrier is used widely for licensed Hib, multivalent meningococcal and pneumococcal conjugate vaccines as well as other vaccines in development. Furthermore, we decided to activate our linker with the active ester method and then lysine residues on the carrier protein CRM<sub>197</sub> are used for conjugation.

For the first step, we activated **78-82** using di-N-hydroxysuccinimidyl adipate linker in DMSO containing triethylamine and the resulting active esters **83-87** were analysed by NMR to check their activation rate (100%). Next, CRM<sub>197</sub> conjugation was achieved by targeting the most surface exposed lysine residues of the protein. In particular, overnight incubation of **83-87** with CRM<sub>197</sub> in a 75:1 (Trimer **85**, Tetramer **86** and Pentamer **87**) and a 50:1 (Monomer **83** and Dimer **84**) ratio resulted in the novel glycoconjugates **88-92**, which were further studied by SDS-PAGE and BCA analysis.



**Scheme 48.** Preactivation and conjugation of the oligomers with CRM<sub>197</sub>.



### 5.5.3 Analysis of glycoconjugates

The glycoconjugates **88-92** were characterized by SDS-PAGE to confirm the successful conjugation and to have preliminary data about their molecular weight and relative approximate sugar:protein ratio (**Figure 19**).

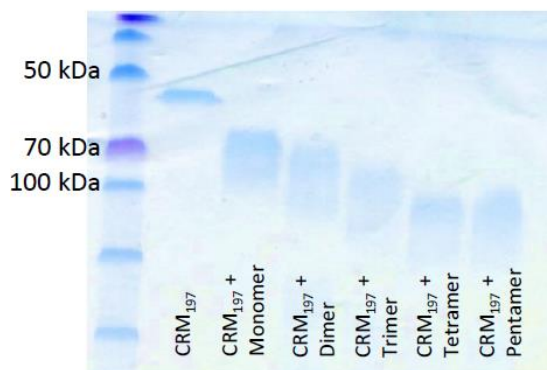


**Figure 19.** SDS-PAGE of the novel glycoconjugates.

The bicinchoninic acid (BCA) assay was first described by Smith et al. and the amount of protein can be quantified.<sup>123</sup> The assay depends on the conversion of  $\text{Cu}^{2+}$  to  $\text{Cu}^{+}$  under alkaline conditions and the resulting  $\text{Cu}^{+}$  is then detected by reaction with BCA as a complex is formed with an intense purple color. The protein content of unknown samples can be determined spectrophotometrically by comparison with known protein standards such as BSA.<sup>124</sup>

We were using the BCA assay to analyse the concentration of CRM<sub>197</sub> in our glycoconjugates and the results are shown in **Table 8**. High loading of oligomer on the protein shows successful conjugation approach and for every glycoconjugate a loading higher than 20 was observed, except of the trimer.

**Table 8.** Characteristics of the novel glycoconjugates

Glycoconjugate	Protein concentration (mg/ml)*	Saccharide/Protein ratio**
CRM <sub>197</sub> + Monomer	0.290	~ 25:1
CRM <sub>197</sub> + Dimer	0.534	~ 19:1
CRM <sub>197</sub> + Trimer	0.494	~ 13:1
CRM <sub>197</sub> + Tetramer	0.532	~ 25:1
CRM <sub>197</sub> + Pentamer	0.541	~ 20:1

\* protein concentration determined by BCA analysis \*\* Ratio was determined by SDS-PAGE and BCA analysis

Within the reported protocol, five well-defined glycoconjugates were successfully prepared and their MALDI analysis to confirm the conjugation loading will be carried out very soon due to temporary unavailability of the instrument.

## 6 Resume and Outline

Within this work, a successful synthetic route to achieve oligomers of Hia CPS with different chain lengths was reported. The synthesis of both disaccharide building blocks was carried out starting from ribose as acceptor and peracetylated glucose as donor on a multigram scale. Three different donors for building block I were successfully prepared. The overall yield of thiodonor **29** was 35%, whereas the two imidate donors, namely **31** and **32**, were obtained in 17% and 21% overall yield, respectively. The acceptor **16** for both building blocks was synthesized in 7 synthetic steps in 29% overall yield. The thiodonor **50** and the imidate donor **57** for building block II were prepared from already available intermediates. However, for both disaccharides **13** and **14**, different glycosylation reactions applying different donors, several Lewis acids as well as various reaction temperatures were screened. Eventually, the trifluoroacetimidate donors **32** and **57** activated by TMSOTf showed the best outcome of up to 82% (**14**) and 78% (**13**).

We decided to apply the well-known phosphoramidite approach for the assembly of the building blocks and our two disaccharides **13** and **14** were slightly modified giving the bifunctional building block **11** and the corresponding acceptor **12**. The bifunctional building block has the phosphoramidite moiety as well as a temporary protecting group (DMTr), which is easily removable in acidic conditions after each coupling cycle. The first coupling was carried out using DCI as coupling reagent and CSO for in-situ oxidation to the resulting phosphate. After deprotection of the DMTr group in acidic medium, dimer **66** was achieved in high yields (79%) and can be applied in an additional coupling cycle as new acceptor. Using the previously synthesized acceptor **66**, a new coupling sequence using DCI and CSO as well as deprotection conditions to remove DMTr gave trimer **67**. This approach was pursued to achieve tetramer **68** and pentamer **69**. All oligomers (**66-69**) as well as the monomer **12** were further coupled using the phosphoramidite approach to a C3 linker **70** with a protected amine function suited for conjugation to the carrier protein. After deprotection **78-82** were conjugated to CRM<sub>197</sub> taking advantage of a di-N-hydroxysuccinimidyl adipate linker. We successfully obtained five novel semisynthetic and well-defined Hia glycoconjugates (**88-92**).

With the ongoing cooperation with Andrew Cox (National Research Council Canada), Roberto Adamo and Maria R. Romano (both GSK Vaccines, Siena, Italy), immunization studies will be carried out and the efficacy of our novel glycoconjugates will be tested. In this cooperation, Andrew Cox will provide the native Hia CPS, which will be also conjugated to CRM<sub>197</sub> and used as a positive control. Furthermore, *in vivo* studies are planned to identify the minimal Hia glycoepitope with unconjugated synthetic oligosaccharides as well as glycoconjugates. Sera of immunised mice will be analysed by competitive ELISA. These studies will be carried out in the near future.

## 7 Experimental part

### 7.1 General experimental methods

All reagents were purchased from commercial suppliers and were used as supplied without further purification. Dry solvents such as DCM, MeOH, pyridine, toluene, DMF, ACN and THF were purchased from Sigma-Aldrich and were used without further purification. Non-anhydrous solvents were used from commercial suppliers.

Analytical thin-layer chromatography (TLC) was performed on Merck precoated 60F254 plates (0.25 mm), visualized by UV light at 254 nm and/or dipping the plates into stains:

- molybdc solution (21 g of  $(\text{NH}_4)_4\text{Mo}_4\text{O}_{24}$ , 1 g of  $\text{Ce}(\text{SO}_4)_2$ , 31 ml of  $\text{H}_2\text{SO}_4$  98%, 970 ml  $\text{H}_2\text{O}$ )
- sulphuric acid (50 ml of  $\text{H}_2\text{SO}_4$  98%, 450 ml of MeOH, 450 ml  $\text{H}_2\text{O}$ )
- ninhydrin (2.7 g of 2,2-dihydroxyindane-1,3-dione, 27 ml of AcOH, 900 ml of EtOH)

For some reactions High Performance Thin Layer Chromatography (HPTLC) (Merck precoated 60F254 plates 0.20mm) were used and correspondently pursued. Flash chromatography was performed using Silica gel ( $\text{SiO}_2$ , high-purity grade (Merck Grade 9385), pore size 60 Å, 230- 400 mesh particle size) from Sigma-Aldrich. Biotage SP1 system was used to purify some compounds. Normal phase Biotage SNAP cartridges (sizes from 3 g to 340 g, standard 50 µm silica) were employed.

Freeze-drying of aqueous solutions was performed using Lio5P Lypholizer.

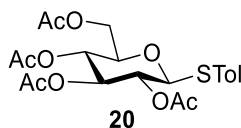
$^1\text{H}$ ,  $^{13}\text{C}$  and  $^{31}\text{P}$ -NMR spectra were obtained on a Bruker AMX 400 instrument (400,100.6 MHz and 162MHz for  $^1\text{H}$ ,  $^{13}\text{C}$  and  $^{31}\text{P}$ , respectively). All NMR measurements were performed at room temperature. The samples were prepared using deuterated solvents ( $\text{CDCl}_3$ ,  $\text{CD}_3\text{COCD}_3$ ,  $\text{D}_2\text{O}$  and  $\text{CD}_3\text{OD}$  from Sigma Aldrich or Eurisotop). Chemical shifts are reported in ppm and coupling constants (J) in Hz. According to Gottlieb and Nudelman, the chemical shifts were referenced to the residual proton in the solvent. (i.e.  $\text{CHCl}_3$ , 0.01% in 99.99%  $\text{CDCl}_3$ ). Multiplicities are abbreviated as: br (broad) s (singlet), d (doublet), t (triplet), hept (heptet), m (multiplet) or combinations thereof.  $^1\text{H}$ -NMR spectra were recorded for all the compounds. For unknown structures, characterization is reported by  $^1\text{H}$ -NMR,  $^{13}\text{C}$ -NMR and  $^{31}\text{P}$ -NMR. 2-dimensional NMR experiments (COSY, HSQC and HMBC) were used to better assign peaks to the structure.

Low resolution mass analysis was recorded in negative or positive mode on a Thermo Finnigan LCQ Advantage equipped with an ESI source. High resolution mass analyses were recorded on a Waters Micromass Q-ToF micro equipped with a LockSpray ESI source or on a Bruker Daltonics ICR-FTMS APEX II at C.I.G.A, University of Milan.

## 7.2 Experimental Synthetic Procedures

### 7.2.1 Synthesis of Donor for Building Block I

#### p-Methylphenyl 2,3,4,6-tetra-O-acetyl-1-thio-β-D-glucopyranoside 20



β-D-pentaacetylated glucose (5.0 g, 12.81 mmol) was dissolved in anhydrous DCM (25 ml) under N<sub>2</sub> atmosphere. Then p-Thiocresol (33.43 mmol) at 0°C and after 5 min BF<sub>3</sub>·OEt<sub>2</sub> (19.22 mmol) were added. After 2 h TLC showed full conversion (2:1 Hex:EtOAc) and the solvent was evaporated. The residue was dissolved in DCM and washed with NaHCO<sub>3</sub> (sat.), water and brine and dried over Na<sub>2</sub>SO<sub>4</sub>. The residue was dissolved in Hex:EtOAc 3:1 and recrystallized. The crystals were filtrated and the filtrate was purified by flash chromatography (7:3 Hex:EtOAc).

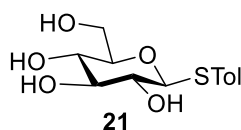
Yield: 5.5 g 94%

Rf: 0.30 (2:1 Hex:EtOAc)

The obtained analytical data are in agreement with those reported in literature.<sup>125</sup>

<sup>1</sup>H NMR (400 MHz, Chloroform-*d*) δ 7.51 – 7.32 (m, 2H), 7.12 (d, *J* = 7.9 Hz, 2H), 5.21 (t, *J* = 9.4 Hz, 1H, H-3), 5.02 (t, *J* = 9.8 Hz, 1H, H-4), 4.93 (dd, *J* = 10.1, 9.3 Hz, 1H, H-2), 4.63 (d, *J* = 10.0 Hz, 1H, H-1), 4.34 – 4.07 (m, 2H, 2x H6), 3.70 (ddd, *J* = 10.1, 4.9, 2.8 Hz, 1H, H-5), 2.09 (s, 3H, CH<sub>3</sub>), 2.08 (s, 3H, CH<sub>3</sub>), 2.01 (s, 3H, CH<sub>3</sub>), 1.98 (s, 3H, CH<sub>3</sub>).

p-Methylphenyl 1-thio-β-D-glucopyranoside **21**



**20** (2.78 g, 6.12 mmol) was dissolved in MeOH (30 ml) and NaOMe (0.612 mmol, solid) was added. The reaction was stirred overnight and after 14 h TLC showed full conversion (100% EtOAc). Ion exchange resin Dowex H<sup>+</sup> was added to neutralize the mixture and after filtration the solvent was evaporated.

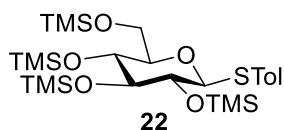
Yield: 1.82 g    100%

Rf: 0.26 (100% EtOAc)

The obtained analytical data are in agreement with those reported in literature.<sup>126</sup>

<sup>1</sup>H NMR (400 MHz, Deuterium Oxide) δ 7.57 – 7.49 (m, 2H), 7.33 – 7.26 (m, 2H), 4.75 (d, *J* = 9.9 Hz, 1H), 3.92 (dd, *J* = 12.5, 2.2 Hz, 1H), 3.74 (dd, *J* = 12.5, 5.6 Hz, 1H), 3.55 (t, *J* = 8.9 Hz, 1H), 3.49 (ddd, *J* = 9.8, 5.7, 2.2 Hz, 0H), 3.46 – 3.41 (m, 0H), 3.41 – 3.31 (m, 1H), 2.37 (s, 3H).

## p-Methylphenyl 2,3,4,6 tetra-O-trimethylsilyl-1-thio-β-D-glucopyranoside 22



### PROCEDURE 1

**21** (1.8 g, 6.286 mmol) was dissolved in anhydrous DCM (31 ml) under N<sub>2</sub> atmosphere and NEt<sub>3</sub> was added. The reaction mixture was cooled to 0°C and TMSCl (37.72 mmol) was added slowly. The mixture was allowed to warm to r.t.. After 14 h the solvent was removed and the residue was dissolved in hexane (20 ml). The mixture was filtered over celite to give a red brown oil.

The crude was purified via flash chromatography (12:1 Hex:EtOAc, 0.5% NEt<sub>3</sub>) to give a colourless oil.

Yield: 2.36 g 65%

### PROCEDURE 2

**21** (1.83 g, 6.391 mmol) was dissolved in anhydrous DCM (30 ml) under N<sub>2</sub> atmosphere. Then HMDS (14.06 mmol) was added and afterwards TMSOTf (0.639 mmol) was added slowly (NH<sub>3</sub> is produced). NH<sub>3</sub> was 'evaporated' using the pump during the reaction. After 2 h TLC (4:2 Hex:EtOAc) showed full conversion and water and DCM were added. The organic layers were washed with water and brine, then dried over Na<sub>2</sub>SO<sub>4</sub>.

Yield. 3.636 g 99%

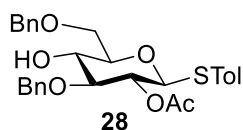
Rf: 0.40 (15:1 Hex:EtOAc)

No further purification was necessary.

The obtained analytical data are in agreement with those reported in literature.<sup>127</sup>

<sup>1</sup>H NMR (400 MHz, Chloroform-*d*) δ 7.43 (d, *J* = 8.2 Hz, 2H), 7.26 (CDCl<sub>3</sub>), 7.18 – 6.95 (m, 2H), 4.72 – 4.37 (m, 1H), 3.79 (dd, *J* = 11.2, 2.3 Hz, 1H), 3.63 (dd, *J* = 11.1, 6.2 Hz, 1H), 3.60 – 3.38 (m, 3H), 3.26 (dt, *J* = 5.1, 2.5 Hz, 1H), 2.32 (s, 3H), 0.24 (s, 9H), 0.17 (s, 9H), 0.16 (s, 9H), 0.11 (s, 9H).

p-Methylphenyl 2-O-acetyl-3,6-di-O-benzyl -1-thio-β-D-glucopyranoside 28



**22** (5.26 g, 9.15 mmol) was dissolved in anhydrous DCM (18.5 ml) under N<sub>2</sub> atmosphere. Then freshly distilled benzaldehyde (36.59 mmol) was added. After 1 h at r.t. the mixture was cooled to 0°C and a solution of FeCl<sub>3</sub>·6H<sub>2</sub>O in ACN (0.46 mmol in 4.5 ml) and TES (10.98 mmol) were added. The reaction was slowly warmed to r.t. The progress of the reaction was checked by TLC (R<sub>f</sub> 0.25 in 5:1 Hex:EtOAc). After 2 h the reaction was quenched by adding TBAF (1.0 M in THF). After 15 min, the reaction was diluted with EtOAc and the organic layer was washed with NaHCO<sub>3</sub> (sat.), brine and dried over Na<sub>2</sub>SO<sub>4</sub>.

The crude was used without any further purification. Pyridine (45 ml) and Ac<sub>2</sub>O (42.94 mmol) were added. The mixture was cooled to 0°C and DMAP (cat) was added. After 30 min at 0°C TLC showed complete conversion (R<sub>f</sub> 0.35 in 4:1 Hex:EtOAc). The reaction was quenched with MeOH and the solvent was removed. The residue was diluted with EtOAc and washed with NaHCO<sub>3</sub> (sat.), brine and dried over Na<sub>2</sub>SO<sub>4</sub>.

Afterwards, the intermediate (4.93 g) was dissolved in anhydrous DCM (48 ml) and cooled to 0°C under N<sub>2</sub> atmosphere. Then TES (48.66 mmol) and TFA (48.66 mmol) were added and after 10 min the ice bath was removed. The reaction showed full conversion after 17 h (TLC, 7:3 Hex:EtOAc) and the reaction was quenched with NaHCO<sub>3</sub> (sat.). The reaction was diluted with NaHCO<sub>3</sub> (sat.) and DCM. The organic layer was washed with NaHCO<sub>3</sub> (sat.), brine and dried over Na<sub>2</sub>SO<sub>4</sub>.

The product was purified via flash chromatography (8:2 Hex:EtOAc) to give a yellow oil.

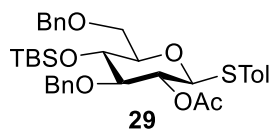
Yield: 1.888 g 41% over 4 steps

R<sub>f</sub>: 0.39 (7:3 Hex:EtOAc)

The obtained analytical data are in agreement with those reported in literature.<sup>128</sup>

<sup>1</sup>H NMR (400 MHz, Chloroform-*d*) δ 7.48–7.27 (m, 10H), 7.12–7.02 (m, 2H), 4.99 (dd, *J* = 10.0, 9.1 Hz, 1H), 4.74 (s, 2H), 4.70–4.43 (m, 3H), 3.78 (dd, *J* = 4.6, 1.4 Hz, 2H), 3.70 (dd, *J* = 9.6, 8.9 Hz, 1H), 3.56 (d, *J* = 9.0 Hz, 1H), 3.54–3.46 (m, 1H), 2.57 (s, OH), 2.32 (s, 3H), 2.06 (s, 3H).

p-Methylphenyl 2-O-acetyl-3,6-di-O-benzyl-4-O-tert-butylidimethylsilyl -1-thio-β-D-glucopyranoside **29**



**28** (0.846 g) was dissolved in anhydrous DCM (4 ml) under N<sub>2</sub> atmosphere and cooled to 0°C. Then fresh distilled 2,6 Lutidine (4.325 mmol) and TBSOTf (3.326 mmol) were added. After 17 h TLC (8:2 Hex:EtOAc) showed full conversion.

The reaction was diluted with DCM and washed with NaHCO<sub>3</sub> (sat.) and brine and dried over Na<sub>2</sub>SO<sub>4</sub>.

The product was purified by flash chromatography (6:1 Hex:EtOAc).

Yield: 904 mg 91%

Rf: 0.53 (4:1 Hex:EtOAc)

[α]<sub>D</sub><sup>32</sup> = + 26.2 (4.0 mg/ml)

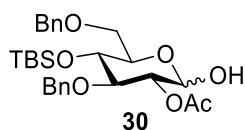
<sup>1</sup>H NMR (400 MHz, Chloroform-*d*) δ 7.52 – 7.37 (m, 2H, Ph), 7.40 – 7.15 (m, 10H, Ph), 7.13 – 6.80 (m, 2H, Ph), 5.01 (dd, *J* = 10.0, 9.0 Hz, 1H, H-2), 4.72 (d, *J* = 11.5 Hz, 1H, 1xCH<sub>2</sub>Ph), 4.64 (d, *J* = 11.6 Hz, 1H, 1xCH<sub>2</sub>Ph), 4.62 (d, *J* = 12.1 Hz, 1 H, 1xCH<sub>2</sub>Ph), 4.60 (d, *J* = 10.0 Hz, 1H, H-1), 4.51 (d, *J* = 11.9 Hz, 1H, 1xCH<sub>2</sub>Ph), 3.80 (dd, *J* = 10.7, 2.0 Hz, 1H, H-6), 3.71 – 3.56 (m, 2H, H-5, H-6), 3.56 – 3.45 (m, 2H, H-3, H-4), 2.29 (s, 3H, CH<sub>3</sub>), 1.92 (s, 3H, CH<sub>3</sub>), 0.85 (s, 9H, 3x CH<sub>3</sub>), 0.00 (s, 3H CH<sub>3</sub>), -0.03 (s, 3H, CH<sub>3</sub>).

<sup>13</sup>C NMR (101 MHz, CDCl<sub>3</sub>) δ 169.72 (C<sub>carbonyl</sub>), 138.55 (Ph-C<sub>quat</sub>), 138.36 (Ph-C<sub>quat</sub>), 137.86 (Ph-C<sub>quat</sub>), 132.72 (C<sub>arom</sub>), 129.70 (C<sub>arom</sub>), 128.44 (C<sub>arom</sub>), 127.71 (C<sub>arom</sub>), 127.61 (C<sub>arom</sub>), 127.56 (C<sub>arom</sub>), 127.39 (C<sub>arom</sub>), 86.45 (C-1), 85.12 (C-3 or C-4), 80.97 (C-3 or C-4), 77.48 (CDCl<sub>3</sub>), 77.16 (CDCl<sub>3</sub>), 76.84 (CDCl<sub>3</sub>), 75.35 (CH<sub>2</sub>Ph), 73.57 (CH<sub>2</sub>Ph), 72.38 (C-2), 71.08 (C-5), 69.58 (C-6), 26.06 (CH<sub>3</sub>), 21.26 (CH<sub>3</sub>), 21.15 (CH<sub>3</sub>), 18.11 (C<sub>quat</sub>), -3.69 (CH<sub>3</sub>), -4.62 (CH<sub>3</sub>).

HRMS (ESI+) *m/z* = [M + Na]<sup>+</sup> calculated for C<sub>35</sub>H<sub>46</sub>O<sub>6</sub>NaSi 645.2682; found 645.2676



2-O-acetyl-3,6-di-O-benzyl-4-O-tert-butyldimethylsilyl- D-glucopyranose 30



**29** (223 mg, 0.358 mmol) was dissolved in aceton (3.2 ml) and water (0.36 ml) and NBS (0.430 mmol) was added. After 1 h, 2 h, 3 h and 4 h NBS (0.086mmol x 4) was added and the reaction was monitored by TLC (8:2 Hex:EtOAc). Then a solution of sat. Na<sub>2</sub>S<sub>2</sub>O<sub>3</sub> was added and the reaction was diluted with EtOAc. The organic layer was washed with NaHCO<sub>3</sub> (sat.), brine and dried over Na<sub>2</sub>SO<sub>4</sub>. The product was purified via flash chromatography (8:2 Hex:EtOAc) to give the product and the starting material was recovered (0.0885 mmol, 25%).

Yield: 117 mg 63%

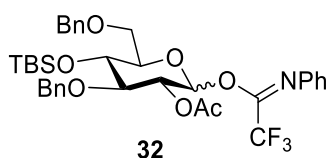
Rf: 0.19 (7:3 Hex:EtOAc)

<sup>1</sup>H NMR (400 MHz, Chloroform-*d*) δ 7.57 – 7.12 (m, 10H, 2 x Ph), 5.37 (t, *J* = 3.2 Hz, 1H, H-1β), 4.90 – 4.80 (m, 1H, H-2 α, H-2β), 4.81 – 4.69 (m, 2H, CH<sub>2</sub>Ph), 4.69 – 4.53 (m, 2H, 1x, CH<sub>2</sub>Ph, H-1α), 4.49 (dd, *J* = 12.3, 6.6 Hz, 1H, 1x CH<sub>2</sub>Ph), 4.04 (ddd, *J* = 9.3, 6.9, 2.1 Hz, 1H, H-5β), 3.93 – 3.80 (m, 2H, H-3β,OH), 3.75 – 3.60 (m, 2H, H-5α, 1xH6), 3.61 – 3.42 (m, 3H, H-3α, H-4α, H-4β, 1-H6), 1.86 (s, 3H), 0.81 (s, 3H, OAc), 0.81 (s, 9H, 3xCH<sub>3</sub>), -0.03 (s, 3H, CH<sub>3</sub>), -0.06 (s, 3H, CH<sub>3</sub>).

<sup>13</sup>C NMR (101 MHz, CDCl<sub>3</sub>) δ 171.23 (C<sub>carbonyl</sub>), 170.47 (C<sub>carbonyl</sub>), 139.00 (Ph-C<sub>quat</sub>), 138.54 (Ph-C<sub>quat</sub>), 137.89 (Ph-C<sub>quat</sub>), 133.12 (C<sub>arom</sub>), 129.72 (C<sub>arom</sub>), 128.52 (C<sub>arom</sub>), 128.42 (C<sub>arom</sub>), 128.34 (C<sub>arom</sub>), 127.95 (C<sub>arom</sub>), 127.83 (C<sub>arom</sub>), 127.52 (C<sub>arom</sub>), 127.33 (C<sub>arom</sub>), 127.10 (C<sub>arom</sub>), 126.95 (C<sub>arom</sub>), 95.70 (C-1), 90.34 (C-1), 83.24 (C-3α or C-4α), 80.14 (C-3β), 77.48 (CDCl<sub>3</sub>), 77.16 (CDCl<sub>3</sub>), 76.84 (CDCl<sub>3</sub>), 76.54 (C-3α or C-4α), 76.03 (or C-2α), 75.14 (CH<sub>2</sub>Ph), 74.23 (C-2β), 73.57 (CH<sub>2</sub>Ph), 73.39 (CH<sub>2</sub>Ph), 71.45 (C-4β), 71.56 (C-5β), 71.12 (C-5 α), 69.44 (C-6 β), 69.15 (C-6α), 25.99 (CH<sub>3</sub>), 20.90 (CH<sub>3</sub>), 18.08 (C<sub>quat</sub>), -3.70 (CH<sub>3</sub>), 4.75 (CH<sub>3</sub>).

HRMS (ESI+) *m/z* = [M + Na]<sup>+</sup> calculated for C<sub>28</sub>H<sub>40</sub>O<sub>7</sub>NaSi 539.2441; found 539.2441.

2-O-acetyl-3,6-di-O-benzyl-4-O-tert-butylidimethylsilyl -D-glucopyranosyl 1-( N-phenyl)- 2,2,2-trifluoroacetimidate) 32



**30** (1.79 g, 3.774 mmol) was dissolved in anhydrous DCM (11 ml) and cooled to 0°C under N<sub>2</sub> atmosphere. Then Cs<sub>2</sub>CO<sub>3</sub> (6.93 mmol) and 2,2,2-Trifluoro-N-phenylacetimidoyl Chloride (5.19 mmol) were added and slowly warmed to r.t. After 2 h Cs<sub>2</sub>CO<sub>3</sub> (3.456 mmol) and 2,2,2-Trifluoro-N-phenylacetimidoyl Chloride (2.595 mmol) were added again. The solvent was evaporated and the product was purified via flash chromatography (8:2 Hex:EtOAc with 0.1 % NEt<sub>3</sub>).

Yield: 2.2 g    92 %

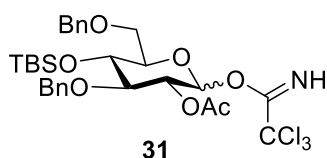
Rf: 0.42 (7:3 Hex:EtOAc)

<sup>1</sup>H NMR (400 MHz, Chloroform-*d*) δ 7.42 – 7.18 (m, 24H), 7.07 (td, *J* = 7.2, 1.4 Hz, 2H), 6.75 (t, *J* = 8.3 Hz, 4H), 5.22 (d, *J* = 7.8 Hz, 1H), 5.10 – 4.97 (m, 1H), 4.79 (d, *J* = 11.9 Hz, 1H), 4.76 – 4.56 (m, 4H), 4.50 (dd, *J* = 12.1, 2.8 Hz, 1H), 3.90 – 3.77 (m, 3H), 3.77 – 3.57 (m, 2H), 3.52 (t, *J* = 8.3 Hz, 2H), 1.90 (s, 3H), 1.82 (s, 3H), 0.85 (s, 6H), 0.82 (s, 12H).

<sup>13</sup>C NMR (101 MHz, CDCl<sub>3</sub>) δ 170.07, 169.30, 143.52, 138.78, 138.20, 129.29, 128.85, 128.59, 128.45, 127.70, 127.64, 127.54, 127.48, 127.36, 126.97, 124.49, 120.77, 119.56, 95.26, 83.23, 80.26, 77.50, 77.47 (CDCl<sub>3</sub>), 77.16 (CDCl<sub>3</sub>), 76.84 (CDCl<sub>3</sub>), 75.22, 74.91, 74.58, 73.40, 72.76, 72.15, 70.34, 68.75, 68.54, 26.08, 26.01, 20.80, 20.63, 18.12, -3.67, -3.83, -4.79.

HRMS (ESI+) *m/z* = [M + Na]<sup>+</sup> calculated for C<sub>36</sub>H<sub>44</sub>NO<sub>7</sub>NaF<sub>3</sub>Si 710.2737; found 710.2719.

2-O-acetyl-3,6-di-O-benzyl-4-O-tert-butylidimethylsilyl - D-glucopyranosyl 1-(2,2,2-chloro acetimidate) 31



**30** (0.072 g, 0.139 mmol) was dissolved in anhydrous DCM (1.4 ml) and  $\text{Cl}_3\text{CCN}$  (0.695 mmol) was added under  $\text{N}_2$  atmosphere. Then DBU (cat.) was added and the reaction turned red. After 1 h TLC (5:5 Hex:EtOAc) showed no starting material left and the solvent was evaporated. The product was purified via flash chromatography (8:2 Hex:EtOAc with 0.1 %  $\text{NEt}_3$ ).

Yield: 73 mg 79%

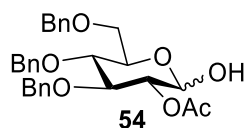
Rf: 0.82 (5:5 Hex:EtOAc)

$^1\text{H}$  NMR (400 MHz, Chloroform-*d*)  $\delta$  8.61 (s, 1H), 8.55 (s, 3H), 6.50 (d,  $J = 3.6$  Hz, 3H), 5.85 (d,  $J = 7.2$  Hz, 1H), 5.30 (dd,  $J = 8.0, 7.2$  Hz, 1H), 5.10 – 4.99 (m, 3H), 4.81 (d,  $J = 12.0$  Hz, 3H), 4.73 (d,  $J = 11.9$  Hz, 3H), 4.71 – 4.48 (m, 11H), 4.00 – 3.92 (m, 3H), 3.92 – 3.90 (m, 1H), 3.90 – 3.85 (m, 6H), 3.78 (dd,  $J = 10.5, 1.9$  Hz, 1H), 3.75 – 3.63 (m, 9H), 3.58 (t,  $J = 8.0$  Hz, 1H), 1.79 (s, 9H), 1.59 (s, 10H), 0.94 – 0.81 (m, 41H), 0.09 – -0.05 (m, 28H).

$^{13}\text{C}$  NMR (101 MHz,  $\text{CDCl}_3$ )  $\delta$  170.19, 169.30, 161.35, 161.21; 138.80, 138.29, 128.44, 128.43, 128.40, 127.77, 127.69, 127.65, 127.60, 127.48, 127.46, 96.15, 83.31, 80.23, 77.55, 77.48 ( $\text{CDCl}_3$ ), 77.16 ( $\text{CDCl}_3$ ), 76.84 ( $\text{CDCl}_3$ ), 75.17, 75.11, 76.84, 75.17, 75.11, 74.45, 73.41, 73.04, 72.01, 70.40, 70.29, 68.76, 68.51, 26.13, 26.04, 20.60, 18.15, -3.64, -4.78.

## 7.2.2 Synthesis of Donor for Building Block II

### 2-O-Acetyl-3,4,6-tri-O-benzyl-D-glucopyranose 54



#### Procedure 1

**49** (1 g, 1.974 mmol) was dissolved in 1,4 Dioxane (20 ml) and AcOH (60%, 39 ml) was added slowly. After 1 h TLC (1:1 Hex:EtOAc) showed full conversion and the solvent was evaporated and coevaporated with Tol. The crude was dissolved in pyridine (20 ml) and Ac<sub>2</sub>O (17.82 mmol) was added. The reaction was stirred for 17 h at r.t. and then the solvent was evaporated. The residue was dissolved in EtOAc and water and the organic layer was washed with NaHCO<sub>3</sub> (sat.) and brine and dried over Na<sub>2</sub>SO<sub>4</sub>.

The crude was dissolved in DMF (30 ml) and cooled to 0°C. Then a freshly prepared hydrazine acetate solution (7.722 mmol in MeOH) was added. The reaction was stirred for 17 h and slowly warmed to r.t. Then Et<sub>2</sub>O and NaHCO<sub>3</sub> (sat.) were added and the organic layer were washed with brine and dried over Na<sub>2</sub>SO<sub>4</sub>. The product was purified by flash chromatography (5:5 to 4:6 Hex:EtOAc).

Yield: 1.92 g 66% over three steps

#### Procedure 2

**50** (530 mg, 1.04 mmol) was dissolved in a solution 7:3 of acetone-H<sub>2</sub>O and PTSA (60 mg, 0.31 mmol) was added. After 0.75 h TLC (7: 3 Hex:EtOAc) showed full conversion and the reaction was quenched with NEt<sub>3</sub> until complete neutralization. The product was washed with EtOAc and brine, dried over Na<sub>2</sub>SO<sub>4</sub>, and concentrated in vacuo. The crude was purified via flash chromatography (5:5 Hex:EtOAc).

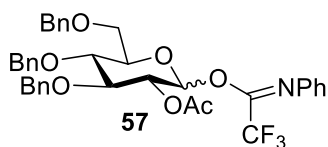
Yield: 360 mg 70%

Rf: 0.22 (5:5 Hex:EtOAc)

<sup>1</sup>H NMR (400 MHz, Chloroform-*d*) δ 7.41 – 7.23 (m, 13H, Ph), 7.24 – 7.09 (m, 2H, Ph), 5.42 (t, *J* = 3.4 Hz, 1H, H-1), 4.89 (ddd, *J* = 10.0, 3.7, 1.2 Hz, 1H, H-2), 4.88 – 4.75 (m, 2H, 1x CH<sub>2</sub>Ph), 4.77 – 4.67 (m, 1H, 1x CH<sub>2</sub>Ph), 4.69 – 4.55 (m, 2H, 2x CH<sub>2</sub>Ph), 4.58 – 4.48 (m, 2H, 2x CH<sub>2</sub>Ph), 4.14 – 4.01 (m, 2H, H-3, H-4), 3.72 (dt, *J* = 6.0, 1.6 Hz, 1H, 1xH-6), 3.73 – 3.64 (m, 2H, H-5, 1xH-6), 2.78 (dd, *J* = 3.4, 1.3 Hz, 1H, OH), 2.03 (s, 3H, CH<sub>3</sub>), 2.01 (s, 1H).

The obtained analytical data are in agreement with those reported in literature.<sup>129</sup>

2-O-Acetyl-3,4,6-tri-O-benzyl- D-glucopyranosyl 1-( N-phenyl)- 2,2,2-trifluoroacetimidate) 57



**54** (1.73 g, 3.512 mmol) was dissolved in anhydrous DCM (11 ml) and cooled to 0°C under N<sub>2</sub> atmosphere. Then Cs<sub>2</sub>CO<sub>3</sub> (7.024 mmol) and NPhTfACl (5.268 mmol) were added. TLC (6:4 Hex:EtOAc) showed full conversion after 2 h. The solvent was evaporated and the product was purified via flash chromatography (8:2 Hex:EtOAc + 0.1% NEt<sub>3</sub>).

Yield: 2.227 g 96%

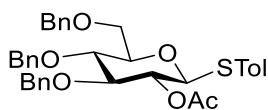
Rf: 0.51 (5:5 Hex:EtOAc)

HRMS (ESI+)  $m/z = [M + Na]^+$  calculated for C<sub>37</sub>H<sub>36</sub>NO<sub>7</sub>NaF<sub>3</sub> 686.2342; found 686.2333.

<sup>1</sup>H NMR (400 MHz, Chloroform-*d*) δ 7.52 – 7.37 (m, 1H), 7.38 – 7.22 (m, 14H), 7.21 – 6.92 (m, 4H), 6.94 – 6.59 (m, 2H), 5.63 (s, 1H), 5.23 (t, *J* = 8.5 Hz, 1H), 4.94 – 4.74 (m, 3H), 4.75 – 4.44 (m, 5H), 3.83 (t, *J* = 9.2 Hz, 1H), 3.80 – 3.33 (m, 3H).

<sup>13</sup>C NMR (101 MHz, CDCl<sub>3</sub>) δ 169.23, 138.13, 138.05, 137.91, 128.89, 128.59, 128.14, 128.05, 127.97, 127.85, 127.56, 124.57, 120.79, 119.52, 82.65, 77.48, 77.39, 77.38, 77.16, 76.84, 76.10, 75.19, 75.08, 73.62, 72.12, 68.24, 20.79.

**p-Methylphenyl 2-O-acetyl-3,4,6-tri-O-benzyl-1-thio-  $\beta$ -D-glucopyranoside 50**



**50**

**28** (2.154 g, 4.235 mmol) was dissolved in anhydrous DMF (14 mL) and cooled to 0°C under N<sub>2</sub> atmosphere. Then NaH (60% suspension, 8.470 mmol) and BnBr (8.470 mmol) were added. After 3 h reaction showed complete conversion (TLC 8:2 Hex:EtOAc) and MeOH was added to quench the reaction. The mixture was diluted with Et<sub>2</sub>O and the organic phase was washed with water, brine and then dried over Na<sub>2</sub>SO<sub>4</sub>. The product was purified via flash chromatography (8:2 to 7:3 Hex:EtOAc).

Yield: 1.43 g 56 %

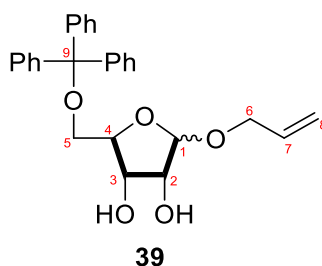
Rf: 0.33 (8:2 Hex:EtOAc)

The obtained analytical data are in agreement with those reported in literature.<sup>130</sup>

<sup>1</sup>H NMR (400 MHz, Chloroform-*d*)  $\delta$  7.46 – 7.37 (m, 2H), 7.37 – 7.23 (m, 10H), 7.19 (dd, *J* = 7.3, 2.2 Hz, 2H), 7.07 – 7.00 (m, 2H), 5.06 – 4.89 (m, 1H), 4.78 (dd, *J* = 11.1, 5.8 Hz, 2H), 4.66 (d, *J* = 11.3 Hz, 1H), 4.62 – 4.48 (m, 5H), 3.78 (dd, *J* = 11.1, 2.0 Hz, 1H), 3.72 (dd, *J* = 11.1, 4.7 Hz, 1H), 3.69 – 3.64 (m, 2H), 3.51 (ddt, *J* = 6.7, 4.8, 2.0 Hz, 1H), 2.29 (s, 3H), 2.00 (s, 3H).

## 7.2.3 Synthesis of Ribitol Acceptor

### Allyl 5-O-trityl- D-ribofuranoside 33



D-Ribose (5.0 g, 33.30 mmol) was dissolved in allyl alcohol (666.09 mmol) and cooled to 0°C. Then H<sub>2</sub>SO<sub>4</sub> was added slowly and after 1 h the reaction was warmed to r.t. After 5 h the reaction (TLC 10:7 CHCl<sub>3</sub>:MeOH) was neutralized with Amberlite (Na<sup>+</sup> form), filtered and the solvent was evaporated. The product was not purified.

The residue (4.56 g) was dissolved in anhydrous pyridine (60 ml) and TrCl (35.978 mmol) was added. The reaction was heated for 6 h at 60°C, then TrCl (20.8 mmol) was added again. The reaction was monitored by TLC (20:1 CHCl<sub>3</sub>: MeOH) and quenched with MeOH after 24 h. The solid was filtered off using celite. The solvent was evaporated and the residue was dissolved in EtOAc. The organic layer was washed with NaHCO<sub>3</sub> (sat.), brine and dried over Na<sub>2</sub>SO<sub>4</sub>. The product was purified via column chromatography (7:3 Hex:EtOAc).

Yield: 7.872 g 52% over two steps

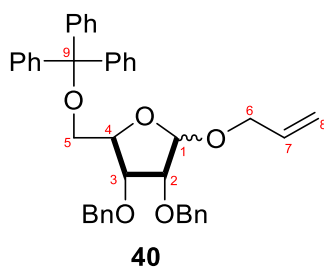
Rf: 0.62 (20:1 CHCl<sub>3</sub>:MeOH)

<sup>1</sup>H NMR (400 MHz, Chloroform-*d*) δ 7.48 – 7.32 (m, 5H, Trt-Ph), 7.31 – 7.09 (m, 10H, Trt-Ph), 5.94 – 5.82 (m, 1H, H-7α), 5.81 – 5.67 (m, 1H, H-7 β), 5.27 (dq, *J* = 17.2, 1.6 Hz, 1H, 1xH-8α), 5.23 – 5.02 (m, 4H, H-8β, 2x H-8α, H-1α), 4.95 (s, 1H, H-1β), 4.35 – 4.25 (m, 1H, 1x H-6α), 4.25 – 4.18 (m, 2H, H-2α, H-3β), 4.17 – 3.97 (m, 5H, 1x H-6β, 1x H-6α, H-4α, H-4β, H-2β), 3.90 (dtt, *J* = 12.7, 6.2, 1.9 Hz, 2H, H-3α, 1xH-6β), 3.41 – 3.19 (m, 3H, 1xH-5α, 2x H-5β), 3.10 (dd, *J* = 10.2, 3.9 Hz, 1H, 1xH-5α), 2.88 (d, *J* = 9.5 Hz, 1H, OH-α), 2.61 (s, 1H, OH-β), 2.53 (d, *J* = 8.7 Hz, 1H, OH-α), 2.33 (s, 1H, OH-β).

<sup>13</sup>C NMR (101 MHz, CDCl<sub>3</sub>) δ 143.85 (C<sub>quat</sub>), 143.85 (C<sub>quat</sub>), 134.06 (C7β), 128.82 (C7b), 128.00 (C<sub>arom</sub>), 127.23 (C<sub>arom</sub>), 127.19 (C<sub>arom</sub>), 117.96 (C8α), 117.53 (C8β), 106.36 (C1β), 101.21 (C1α), 86.85 (C9), 84.60 (C4α), 82.18 (C2β or C4β), 77.48 (CDCl<sub>3</sub>), 77.16 (CDCl<sub>3</sub>), 76.84 (CDCl<sub>3</sub>), 75.46 (C2β or C4β), 72.85 (C3β), 72.06 (C3α or C2α), 71.81 (C3α or C2α), 69.05 (C6α), 68.60 (C6β), 65.15 (C5β), 64.01 (C5α).

HRMS (ESI+) *m/z* = [M + Na]<sup>+</sup> calculated for C<sub>27</sub>H<sub>28</sub>O<sub>5</sub>Na 455.1834; found 455.1831.

## Allyl 2,3-di-O-benzyl-5-O-trityl- D-ribofuranoside 40



**39** (1.06 g, 2.451 mmol) was dissolved in anhydrous DMF (12 ml) and cooled to 0°C. Then NaH (60% suspension, 7.35 mmol) and BnBr (7.35 mmol) were added. The reaction was warmed slowly to r.t. over 18 h. The reaction was quenched with MeOH and diluted with Et<sub>2</sub>O and water. The organic layer was washed with NaHCO<sub>3</sub> (sat.) and brine and dried over Na<sub>2</sub>SO<sub>4</sub>. The product was purified via column chromatography (6:1 Hex:EtOAc).

Yield: 1.42 g 94%

Rf:  $\alpha$ -Isomer 0.66 (7:3 Hex:EtOAc),  $\beta$ -Isomer 0.74 (7:3 Hex:EtOAc)

$\alpha$ -Isomer  $[\alpha]_D^{32} = +59.2$  (4.5 mg/ml)  $\beta$ -Isomer  $[\alpha]_D^{33} = +17.2$  (6.2 mg/ml)

$\alpha$ : <sup>1</sup>H NMR (400 MHz, Chloroform-*d*)  $\delta$  7.36 – 7.06 (m, 25H, Ph), 5.92 (dddd,  $J = 17.0, 11.0, 6.5, 4.9$  Hz, 1H, H-7), 5.41 – 5.08 (m, 2H, 2xH-8), 5.04 (d,  $J = 4.1$  Hz, 1H, H-1), 4.71 – 4.40 (m, 4H, 2x CH<sub>2</sub>-Ph), 4.24 (dd,  $J = 13.4, 4.8$  Hz, 1H, 1xH-6), 4.18 (q,  $J = 3.9$  Hz, 1H, H-4), 4.10 (dd,  $J = 13.4, 6.6$  Hz, 1H, 1xH-6), 3.82 – 3.69 (m, 2H, H-2, H-3), 3.10 (dd,  $J = 10.1, 4.4$  Hz, 1H, 1xH-5), 2.92 (dd,  $J = 10.1, 3.8$  Hz, 1H, 1xH-5).

$\alpha$ : <sup>13</sup>C NMR (101 MHz, CDCl<sub>3</sub>)  $\delta$  143.92 (Trt-C<sub>quat</sub>), 138.44 (Ph-C<sub>quat</sub>), 138.11 (Ph-C<sub>quat</sub>), 138.11 (Ph-C<sub>quat</sub>), 134.96 (C7), 128.80 (C<sub>arom</sub>), 128.49 (C<sub>arom</sub>), 128.33 (C<sub>arom</sub>), 128.07 (C<sub>arom</sub>), 127.56 (C<sub>arom</sub>), 127.12 (C<sub>arom</sub>), 117.37 (C<sub>arom</sub>), 117.37 (C8), 100.13 (C1), 86.78 (C9), 82.28 (C4), 78.04 (C2), 77.48 (CDCl<sub>3</sub>), 77.16 (CDCl<sub>3</sub>), 76.84 (CDCl<sub>3</sub>), 75.83 (C3), 72.59 (CH<sub>2</sub>-Ph), 72.29 (CH<sub>2</sub>-Ph), 68.78 (C6), 64.14 (C5).

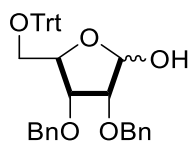
$\beta$ : <sup>1</sup>H NMR (400 MHz, Chloroform-*d*)  $\delta$  7.37 (d,  $J = 7.2$  Hz, 5H, Ph), 7.30 – 7.06 (m, 20H, Ph), 5.72 (ddt,  $J = 16.4, 10.9, 5.7$  Hz, 1H, H-7), 5.22 – 4.95 (m, 3H, 2xH-8, H-1), 4.68 – 4.47 (m, 2H, CH<sub>2</sub>Ph), 4.43 – 4.27 (m, 2H, CH<sub>2</sub>Ph), 4.25 (dt,  $J = 7.9, 4.1$  Hz, 1H, H-4), 4.16 – 4.03 (m, 2H, H-3, 1xH-6), 3.86 (dd,  $J = 19.8, 5.5$  Hz, 2H, H-2, 1xH-6), 3.24 (dd,  $J = 10.1, 3.6$  Hz, 1H, 1xH5), 3.05 (dd,  $J = 10.1, 4.7$  Hz, 1H, 1xH-5).

$\beta$ : <sup>13</sup>C NMR (101 MHz, CDCl<sub>3</sub>)  $\delta$  144.16 (Trt-C<sub>quat</sub>), 138.06 (Ph-C<sub>quat</sub>), 137.94 (Ph-C<sub>quat</sub>), 134.18 (C7), 128.87 (C<sub>arom</sub>), 128.51 (C<sub>arom</sub>), 128.42 (C<sub>arom</sub>), 128.06 (C<sub>arom</sub>), 127.89 (C<sub>arom</sub>), 127.77 (C<sub>arom</sub>), 127.03 (C<sub>arom</sub>), 117.49 (C8), 104.55 (C-1), 86.48 (C9), 80.72 (C4), 80.01 (C2), 78.40 (C3), 77.48 (CDCl<sub>3</sub>), 77.16 (CDCl<sub>3</sub>), 76.84 (CDCl<sub>3</sub>), 72.56 (CH<sub>2</sub>-Ph), 72.45 (CH<sub>2</sub>-Ph), 68.58 (C6), 64.19 (C-5).



HRMS (ESI+)  $m/z = [M + Na]^+$  calculated for  $C_{41}H_{40}O_5Na$  635.2773; found 635.2783.

**2,3-di-O-benzyl-5-O-trityl- D-ribofuranose 42**



**40** (8.58 g, 14.00 mmol) was dissolved in DMSO (28 ml) and tBuOK (30.80 mmol) was added. The reaction was stirred for 5 h and then diluted with EtOAc. The organic layer was washed with water, HCl (5 %) and brine and dried over  $Na_2SO_4$ . The product was not purified.

The crude was dissolved in THF (50 ml) and water (15 ml) and  $I_2$  (28.00 mmol) was added. After 30 min a solution of sat.  $Na_2S_2O_3$  was added. The organic layer was washed with  $NaHCO_3$  (sat.), brine and dried over  $Na_2SO_4$ . The product was purified via flash chromatography (7:3 Hex:EtOAc).

Yield: 6.71 g 84%

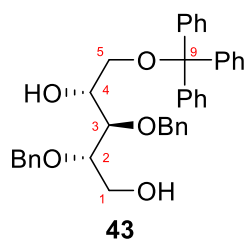
Rf: 0.29 (7:3 Hex:EtOAc)

$^1H$  NMR (400 MHz, Chloroform-*d*)  $\delta$  7.44 – 7.16 (m, 25H, Ph), 5.54 – 5.29 (m, 1H, H-1), 4.83 – 4.44 (m, 4H, 2x $CH_2$ Ph), 4.35 (dt,  $J = 4.8, 2.8$  Hz, 1H, H-4  $\alpha$ ), 4.32 – 4.25 (m, 2H, H-3 $\beta$ , H-4 $\beta$ ), 4.19 (d,  $J = 11.3$  Hz, 1H, OH,  $\alpha$ ), 4.01 (t,  $J = 4.5$  Hz, 1H, H-2  $\alpha$ ), 3.94 (dd,  $J = 4.9, 1.9$  Hz, 1H, H-3  $\alpha$ ), 3.92 – 3.86 (m, 1H, H-2 $\beta$ ), 3.44 (dd,  $J = 10.3, 2.9$  Hz, 1H, 1xH-5 $\beta$ ), 3.20 (dd,  $J = 10.2, 5.0$  Hz, 2H, 1xH-5  $\alpha$ , 1xH5 $\beta$ ), 3.10 (dd,  $J = 10.2, 3.6$  Hz, 1H, 1xH5  $\alpha$ ), 2.91 (d,  $J = 5.1$  Hz, OH- $\beta$ ).

$^{13}C$  NMR (101 MHz,  $CDCl_3$ )  $\delta$  143.78 (Trt- $C_{quat}$ ), 137.95 ( $\beta$ -Ph- $C_{quat}$ ), 137.75 ( $\beta$ -Ph- $C_{quat}$ ), 137.61 ( $\alpha$ -Ph- $C_{quat}$ ), 128.89 ( $C_{arom}$ ), 128.75 ( $C_{arom}$ ), 128.61 ( $C_{arom}$ ), 128.56 ( $C_{arom}$ ), 128.49 ( $C_{arom}$ ), 128.15 ( $C_{arom}$ ), 128.08 ( $C_{arom}$ ), 128.00 ( $C_{arom}$ ), 127.94 ( $C_{arom}$ ), 127.24 ( $C_{arom}$ ), 100.30 (C1- $\beta$ ), 96.32 (C1-  $\alpha$ ), 87.21 (C9), 87.00 (C9), 81.38 (C4-  $\alpha$ ), 80.97 (C4- $\beta$ ), 80.49 (C2- $\beta$ ), 78.10 (C2-  $\alpha$ ), 77.99 (C3-  $\alpha$ ), 77.48 ( $CDCl_3$ ), 77.16 ( $CDCl_3$ ), 77.41 (C3 $\beta$ ), 76.85 ( $CDCl_3$ ), 72.86 ( $CH_2$ -Ph-  $\alpha$ ), 72.61 ( $CH_2$ -Ph-  $\alpha$ ), 72.54 ( $CH_2$ -Ph- $\beta$ ), 72.41 ( $CH_2$ -Ph- $\beta$ ), 63.85 (C5-  $\alpha$ ), 63.61 (C5- $\beta$ )

HRMS (ESI+)  $m/z = [M + Na]^+$  calculated for  $C_{38}H_{36}O_5Na$  595.2460; found 595.2466.

### 2,3-di-O-benzyl-5-O-trityl- D-ribitol 43



**42** (6.71 g, 11.72 mmol) was dissolved in EtOH absolute (40 ml) and a solution of NaBH<sub>4</sub> (19.92 mmol in 20 ml of EtOH) was added. The reaction showed full conversion after 30 min and the pH was adjusted to pH =5 with a diluted solution of acetic acid in water. The organic layer was diluted with EtOAc and washed with water and brine and dried over Na<sub>2</sub>SO<sub>4</sub>.

Yield: 6.78 g    quant.

Rf: 0.29 (7:3 Hex:EtOAc)

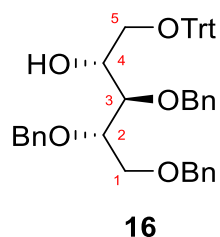
[α]<sub>D</sub><sup>33</sup> = + 15.4 (8.2 mg/ml)

<sup>1</sup>H NMR (400 MHz, Chloroform-*d*) δ 7.61 – 7.37 (m, 6H, Ph), 7.37 – 7.19 (m, 17H, Ph), 7.13 (dd, *J* = 6.6, 3.0 Hz, 2H, Ph), 4.83 – 4.31 (m, 4H, 2xCH<sub>2</sub>Ph), 4.02 (td, *J* = 6.6, 3.4 Hz, 1H., H-4), 3.93 – 3.66 (m, 4H, H-3, H-2, 2xH-1), 3.40 (dd, *J* = 9.7, 3.3 Hz, 1H, H-5), 3.30 (dd, *J* = 9.7, 6.6 Hz, 1H, H-5), 2.69 (s, 1H, OH), 2.36 (s, 1H, OH).

<sup>13</sup>C NMR (101 MHz, CDCl<sub>3</sub>) δ 143.89 (Trt-C<sub>quat</sub>), 138.13 (Ph-C<sub>quat</sub>), 137.99 (Ph-C<sub>quat</sub>), 128.84 (C<sub>arom</sub>), 128.62 (C<sub>arom</sub>), 128.48 (C<sub>arom</sub>), 128.18 (C<sub>arom</sub>), 128.02 (C<sub>arom</sub>), 127.92 (C<sub>arom</sub>), 127.27 (C<sub>arom</sub>), 127.09 (C<sub>arom</sub>), 87.00 (C9), 79.64 (C2 or C3), 79.41 (C2 or C3), 77.48 (CDCl<sub>3</sub>), 77.16 (CDCl<sub>3</sub>), 76.84 (CDCl<sub>3</sub>), 74.03 (CH<sub>2</sub>-Ph), 72.12 (CH<sub>2</sub>-Ph), 71.29 (C4), 64.83 (C5), 61.20 (C1).

HRMS (ESI+) *m/z* = [M + Na]<sup>+</sup> calculated for C<sub>38</sub>H<sub>38</sub>O<sub>5</sub>Na 597.2617; found 597.2627.

### 1,2,3-tri-*O*-benzyl-5-*O*-trityl- D-ribose **16**



**43** (195 mg, 0.334 mmol) was dissolved in DCM (3.4 ml) and BnBr (0.441 mmol) and Bu<sub>4</sub>NBr (0.068 mmol) were added. Afterwards 5 % of NaOH (800 μl) was added and the mixture was heated for 16 h at 50 °C. The reaction was monitored by TLC (3:1 Hex:EtOAc) and after 17 h no more starting material was observed. The reaction was diluted with DCM and the organic layer was washed with NaHCO<sub>3</sub> (sat.), brine and dried over Na<sub>2</sub>SO<sub>4</sub>. The product was purified by flash chromatography (8:2 Hex:EtOAc to 7:3 Hex:EtOAc).

Yield: 144 mg 64%

Rf: 0.24 (7:3 Hex:EtOAc)

[α]<sub>D</sub><sup>32</sup> = + 20.4 (2.9 mg/ml)

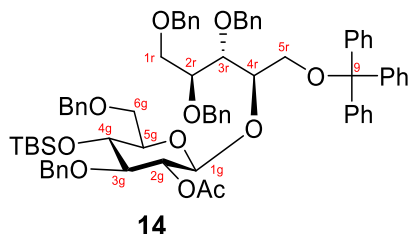
<sup>1</sup>H NMR (400 MHz, Chloroform-*d*) δ 7.48 – 7.33 (m, 6H, Ph), 7.32 – 7.12 (m, 22H, Ph), 7.01 (dd, *J* = 6.4, 2.9 Hz, 2H, Ph), 4.65 – 4.35 (m, 6H, 3xCH<sub>2</sub>Ph), 4.01 – 3.92 (m, 1H, H-4), 3.83 (q, *J* = 4.4 Hz, 1H, H-2), 3.79 – 3.69 (m, 2H, H-3, 1xH-1), 3.62 (dd, *J* = 10.3, 5.4 Hz, 1H, 1xH-1), 3.32 (dd, *J* = 9.6, 3.3 Hz, 1H, 1xH-5), 3.23 (dd, *J* = 9.6, 6.3 Hz, 1H, 1xH-5), 2.82 (d, *J* = 4.0 Hz, 1H, OH).

<sup>13</sup>C NMR (101 MHz, CDCl<sub>3</sub>) δ 144.04 (Trt-C<sub>quat</sub>), 138.54 (Ph-C<sub>quat</sub>), 138.37 (Ph-C<sub>quat</sub>), 138.28 (Ph-C<sub>quat</sub>), 128.87 (C<sub>arom</sub>), 128.50 (C<sub>arom</sub>), 128.43 (C<sub>arom</sub>), 128.32 (C<sub>arom</sub>), 128.06 (C<sub>arom</sub>), 127.94 (C<sub>arom</sub>), 127.81 (C<sub>arom</sub>), 127.74 (C<sub>arom</sub>), 127.63 (C<sub>arom</sub>), 127.13 (C<sub>arom</sub>), 86.79 (C9), 79.19 (C2 or C3), 79.05 (C2 or C3), 77.48 (CDCl<sub>3</sub>), 77.16 (CDCl<sub>3</sub>), 76.84 (CDCl<sub>3</sub>), 73.70 (CH<sub>2</sub>-Ph), 73.47 (CH<sub>2</sub>-Ph), 72.55 (CH<sub>2</sub>-Ph), 71.49 (C4), 69.73 (C1), 64.96 (C5).

HRMS (ESI+) *m/z* = [M + Na]<sup>+</sup> calculated for C<sub>45</sub>H<sub>44</sub>O<sub>5</sub>Na 687.3086; found 687.3091.

## 7.2.4 Synthesis of Disaccharides 13 and 14

### 4-O-(2-O-acetyl-3,6-di-O-benzyl-4-O-tert-butylidimethylsilyl-β-D-glucopyranosyl)-1,2,3,-tri-O-benzyl-5-O-trityl- D-ribose 14



Donor **32** (2.20 g, 3.20 mmol) and acceptor **16** (1.93 g, 2.90 mmol) were coevaporated with toluene 3 times and put on the vacuum line overnight. Furthermore, MS 4 Å were activated and DCM was dried with them for 2 h. Donor and acceptor were dissolved under Ar in dry DCM (19 ml) and cooled to -40°C. Then TMSOTf (0.146 mmol, 0.05 eq) was added slowly. After 10 min HPTLC (8:2 Hex:EtOAc) showed full conversion and the reaction was neutralized with  $\text{NET}_3$  and diluted with DCM. The organic layer was washed with  $\text{NaHCO}_3$  (sat.), brine and dried over  $\text{Na}_2\text{SO}_4$ .

The product was purified by flash chromatography (9:1 Hex:EtOAc).

Yield: 2.78 g 82%

Rf: 0.30 (4:1 Hex:EtOAc)

$[\alpha]_D^{33} = +4.5$  (3.9 mg/ml)

$^1\text{H}$  NMR (400 MHz, Chloroform-*d*)  $\delta$  7.49 – 7.36 (m, 6H, Ph), 7.36 – 7.15 (m, 32H, Ph), 7.14 – 7.06 (m, 2H, Ph), 5.11 (dd,  $J = 9.3, 7.9$  Hz, 1H, H-2g), 4.84 (d,  $J = 7.9$  Hz, 1H, H-1g), 4.78 – 4.64 (m, 2H, 2x  $\text{CH}_2\text{Ph}$ ), 4.60 (dd,  $J = 11.6, 7.8$  Hz, 2H, 2x  $\text{CH}_2\text{Ph}$ ), 4.54 – 4.46 (m, 2H, 2x  $\text{CH}_2\text{Ph}$ ), 4.46 – 4.38 (m, 3H, 3x  $\text{CH}_2\text{Ph}$ ), 4.34 (s, 1H, 1x  $\text{CH}_2\text{Ph}$ ), 4.35 – 4.23 (m, 1H, H-4r), 3.93 (dd,  $J = 6.2, 4.3$  Hz, 1H, H-3r), 3.74 – 3.62 (m, 4H, H-2r, 1xH-5r, H-4g, 1x H-6g), 3.56 (ddd,  $J = 12.5, 10.8, 6.0$  Hz, 3H, 2 xH-1r), 3.49 (dd,  $J = 9.3, 8.4$  Hz, 1H, H-6g), 3.45 – 3.36 (m, 3H, 2xH-5r, H-5g), 1.61 (s, 3H,  $\text{CH}_3$ ), 0.85 (s, 9H, 3x  $\text{CH}_3$ ), -0.02 (d,  $J = 1.1$  Hz, 6H, 2x  $\text{CH}_3$ ).

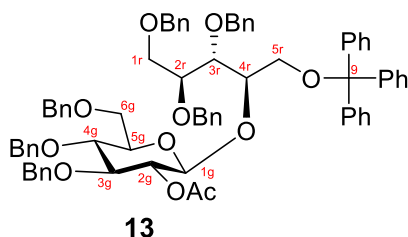
$^{13}\text{C}$  NMR (101 MHz,  $\text{CDCl}_3$ )  $\delta$  169.82 ( $\text{C}_{\text{carbonyl}}$ ), 144.09 ( $\text{Trt-C}_{\text{quat}}$ ), 139.12 ( $\text{Ph-C}_{\text{quat}}$ ), 138.83 ( $\text{Ph-C}_{\text{quat}}$ ), 138.80 ( $\text{Ph-C}_{\text{quat}}$ ), 138.61 ( $\text{Ph-C}_{\text{quat}}$ ), 138.52 ( $\text{Ph-C}_{\text{quat}}$ ), 128.98 ( $\text{C}_{\text{arom}}$ ), 128.40 ( $\text{C}_{\text{arom}}$ ), 128.38 ( $\text{C}_{\text{arom}}$ ), 128.25 ( $\text{C}_{\text{arom}}$ ), 128.23 ( $\text{C}_{\text{arom}}$ ), 128.07 ( $\text{C}_{\text{arom}}$ ), 127.90 ( $\text{C}_{\text{arom}}$ ), 127.64 ( $\text{C}_{\text{arom}}$ ), 127.48 ( $\text{C}_{\text{arom}}$ ), 127.45 ( $\text{C}_{\text{arom}}$ ), 127.38 ( $\text{C}_{\text{arom}}$ ), 127.29 ( $\text{C}_{\text{arom}}$ ), 127.10 ( $\text{C}_{\text{arom}}$ ), 100.14 ( $\text{C1g}$ ), 86.90 ( $\text{C9}$ ), 83.80 ( $\text{C3g}$ ), 79.40 ( $\text{C3r}$ ), 78.93 ( $\text{C2r}$ ), 77.95 ( $\text{C4r}$ ), 77.48 ( $\text{CDCl}_3$ ), 77.16 ( $\text{CDCl}_3$ ), 76.84 ( $\text{CDCl}_3$ ), 76.79 ( $\text{C5r}$ ), 74.93 ( $\text{CH}_2\text{-Ph}$ ), 73.94 ( $\text{C2g}$ ),

73.87 (CH<sub>2</sub>-Ph), 73.58 (CH<sub>2</sub>-Ph), 73.23 (CH<sub>2</sub>-Ph), 72.51 (CH<sub>2</sub>-Ph), 71.20 (C4g), 70.62 (C1r or C6g), 69.34 (C6g or C1r), 63.30 (C5r), 26.09 (CH<sub>3</sub>), 21.19 (CH<sub>3</sub>), -3.67 (CH<sub>3</sub>), -4.63 (CH<sub>3</sub>).

HRMS (ESI+)  $m/z = [M + Na]^+$  calculated for C<sub>73</sub>H<sub>82</sub>O<sub>11</sub>NaSi 1185.5524; found 1185.5555.

4-O-(2-O-acetyl-3,4,6-tri-O-benzyl-β-D-glucopyranosyl)-1,2,3-tri-O-benzyl-5-O-trityl-

D-ribose **13**



Donor **57** (1.475 g, 2.22 mmol) and acceptor **16** (1.334 g, 2.01 mmol) were coevaporated with toluene 3 times and put on the vacuum line overnight. Furthermore, MS 4Å were activated and DCM was dried with them.

Donor and acceptor were dissolved under Ar in dry DCM (13.4 ml) and cooled to -30°C. Then TMSOTf (0.141 mmol, 0.07 eq) was added slowly. After 10 min HPTLC (15:5 Hex:EtOAc) showed full conversion and the reaction was neutralized with NEt<sub>3</sub> and diluted with DCM.

The organic layer was washed with NaHCO<sub>3</sub> (sat.), brine and dried over Na<sub>2</sub>SO<sub>4</sub>.

The product was purified by flash chromatography (9:1 Hex:EtOAc).

Yield: 1.748 g 76%

Rf: 0.54 (7:3 Hex:EtOAc)

$[\alpha]_D^{33} = -3.4$  (7.4 mg/ml)

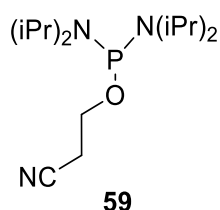
<sup>1</sup>H NMR (400 MHz, Chloroform-*d*) δ 7.40 – 7.29 (m, 6H, Ph), 7.30 – 7.07 (m, 36H, Ph), 7.02 (dd,  $J = 6.7, 2.9$  Hz, 2H, Ph), 5.01 (dd,  $J = 9.3, 8.0$  Hz, 1H, H-2g), 4.81 – 4.67 (m, 3H, H-1g, 2xCH<sub>2</sub>Ph), 4.62 (d,  $J = 11.5$  Hz, 1H, 1x CH<sub>2</sub>Ph), 4.51 (d,  $J = 12.1$  Hz, 3H, 3x CH<sub>2</sub>Ph), 4.48 – 4.38 (m, 2H, 2x CH<sub>2</sub>Ph), 4.38 – 4.31 (m, 3H, 3x CH<sub>2</sub>Ph), 4.25 (d,  $J = 11.8$  Hz, 1H, 1x CH<sub>2</sub>Ph), 4.20 (dt,  $J = 5.9, 3.8$  Hz, 1H, H-4r), 3.83 (dd,  $J = 6.2, 4.2$  Hz, 1H, H-3r), 3.70 – 3.54 (m, 6H, H-3g, H-4g, H-2r, 1xH-6g, 2xH-1r), 3.50 (dd,  $J = 10.8, 6.2$  Hz, 1H, 1xH-6g), 3.40 – 3.32 (m, 3H, H-5g, 2xH-1r), 1.59 (s, 3H, OAc).

$^{13}\text{C}$  NMR (101 MHz,  $\text{CDCl}_3$ )  $\delta$  169.78 ( $\text{C}_{\text{carbonyl}}$ ), 144.07 ( $\text{Trt-C}_{\text{quat}}$ ), 139.10 ( $\text{Ph-C}_{\text{quat}}$ ), 138.78 ( $\text{Ph-C}_{\text{quat}}$ ), 138.46 ( $\text{Ph-C}_{\text{quat}}$ ), 138.18 ( $\text{Ph-C}_{\text{quat}}$ ), 128.97 ( $\text{C}_{\text{arom}}$ ), 128.57 ( $\text{C}_{\text{arom}}$ ), 128.45 ( $\text{C}_{\text{arom}}$ ), 128.40 ( $\text{C}_{\text{arom}}$ ), 128.25 ( $\text{C}_{\text{arom}}$ ), 128.11 ( $\text{C}_{\text{arom}}$ ), 127.97 ( $\text{C}_{\text{arom}}$ ), 127.78 ( $\text{C}_{\text{arom}}$ ), 127.72 ( $\text{C}_{\text{arom}}$ ), 127.68 ( $\text{C}_{\text{arom}}$ ), 127.49 ( $\text{C}_{\text{arom}}$ ), 127.34 ( $\text{C}_{\text{arom}}$ ), 127.13 ( $\text{C}_{\text{arom}}$ ), 100.25 ( $\text{C1g}$ ), 83.23 ( $\text{C3g}$ ), 79.44 ( $\text{C3r}$ ), 78.87 ( $\text{C4g}$  or  $\text{C2r}$ ), 78.32 ( $\text{C4g}$  or  $\text{C2r}$ ), 78.16 ( $\text{C4r}$ ), 77.48 ( $\text{CDCl}_3$ ), 77.16 ( $\text{CDCl}_3$ ), 76.84 ( $\text{CDCl}_3$ ), 75.34 ( $\text{C5g}$ ), 75.11 ( $\text{CH}_2\text{-Ph}$ ), 73.74 ( $\text{CH}_2\text{-Ph}$ ), 73.58 ( $\text{C2g}$ ), 73.29 ( $\text{CH}_2\text{-Ph}$ ), 72.52 ( $\text{CH}_2\text{-Ph}$ ), 70.52 ( $\text{C6g}$ ), 69.03 ( $\text{C1r}$ ), 63.44 ( $\text{C5r}$ ), 21.19 ( $\text{CH}_3$ ).

HRMS (ESI+)  $m/z = [\text{M} + \text{Na}]^+$  calculated for  $\text{C}_{74}\text{H}_{74}\text{O}_{11}\text{Na}$  1161.5129; found 1161.5098.

## 7.2.5 Preparation of the Phosphinite

### 2-cyanoethyl N,N,N',N'-tetraisopropylphosphoramidite 59



Before reaction: Put every glassware in the oven and activate 4 Å MS (beats).

Chlorodiisopropylphosphine (500 mg, 1.874 mmol) was dissolved in  $\text{Et}_2\text{O}$  (9 ml) and MS 4 Å (500 mg) were added under Ar atmosphere. Then the mixture was cooled to  $0^\circ\text{C}$  and a solution of  $\text{NEt}_3$  (2.249 mmol) and 3-Hydroxypropionitril (2.249 mmol) in  $\text{Et}_2\text{O}$  (9 ml) was added very slowly. After 1h the icebath was removed and the mixture was stirred for 3h at r.t. Then the mixture was put on a column without any workup (100% Hex + 2%  $\text{NEt}_3$ ). The first 12 fractions were collected.

Yield: 405 mg 72%

$^1\text{H}$  NMR (400 MHz, Acetone- $d_6$ )  $\delta$  3.78 (dt,  $J = 7.2, 6.0$  Hz, 2H,  $-\text{CH}_2\text{-CH}_2\text{-CN}$ ), 3.60 (dp,  $J = 10.8, 6.8$  Hz, 4H, 4xCH), 2.74 (td,  $J = 6.0, 0.8$  Hz, 2H,  $\text{CH}_2\text{-CH}_2\text{-CN}$ ), 1.20 (dd,  $J = 8.0, 6.8$  Hz, 24H,  $\text{CH}_3$ ).

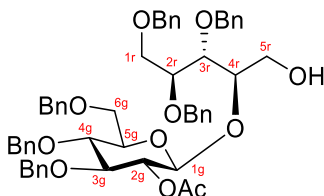
$^{31}\text{P}$  NMR (162 MHz, Acetone- $d_6$ )  $\delta$  122.78

The obtained analytical data are in agreement with those reported in literature.

## 7.2.6 Preparation of Building Blocks I and II

### 4-O-(2-O-acetyl-3,4,6-tri-O-benzyl-β-D-glucopyranosyl)- 1,2,3-tri-O-benzyl- D-ribose

**12**



**12**

**13** (664 mg, 0.583 mmol) was dissolved in DCM (3.9 ml) and cooled to 0°C. Then TFA (5.83 mmol) were added and stirred for 30 min at 0°C. The reaction was quenched by adding NaHCO<sub>3</sub> (sat.) and was diluted with DCM. The organic layer was washed with brine and dried over Na<sub>2</sub>SO<sub>4</sub>.

The product was purified by flash chromatography (7:3 Hex:EtOAc).

Yield 451 mg 86%

Rf: 0.36 (7:3 Hex:EtOAc)

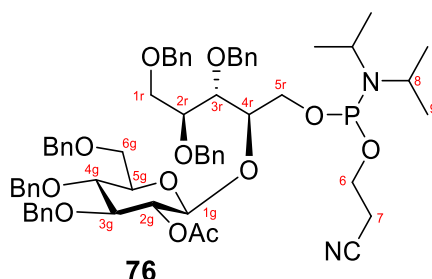
[α]<sub>D</sub><sup>33</sup> = + 7.4 (3.6 mg/ml)

<sup>1</sup>H NMR (400 MHz, Chloroform-*d*) δ 7.60 – 7.03 (m, 32H, Ph), 5.04 (dd, *J* = 9.3, 8.0 Hz, 1H, H-2g), 4.81 (d, *J* = 3.6 Hz, 1H, 1xCH<sub>2</sub>Ph), 4.78 (d, *J* = 3.3 Hz, 2H, 2xCH<sub>2</sub>Ph), 4.75 (d, *J* = 2.5 Hz, 1H, 1xCH<sub>2</sub>Ph), 4.74 – 4.64 (m, 2H, 2xCH<sub>2</sub>Ph), 4.64 – 4.59 (m, 2H, 3xCH<sub>2</sub>Ph), 4.59 – 4.51 (m, 3H, H-1g, 2xCH<sub>2</sub>Ph), 4.49 (s, 2H, 1xCH<sub>2</sub>Ph), 4.44 (d, *J* = 12.1 Hz, 1H, 1xCH<sub>2</sub>Ph), 4.01 (dt, *J* = 4.1, 2.6 Hz, 2H, H-3r, H-4r), 3.86 (td, *J* = 5.5, 3.0 Hz, 1H, H-2r), 3.79 – 3.61 (m, 9H, H-3g, H-4g, 2xH-6g, 2xH1r, 2xH5r), 3.44 (ddd, *J* = 9.6, 4.1, 2.2 Hz, 1H, H-5g), 2.48 (t, *J* = 6.4 Hz, 1H, OH), 1.95 (s, 3H, OAc).

<sup>13</sup>C NMR (101 MHz, CDCl<sub>3</sub>) δ 169.87 (C<sub>carbonyl</sub>), 138.49 (Ph-C<sub>quat</sub>), 138.34 (Ph-C<sub>quat</sub>), 138.27 (Ph-C<sub>quat</sub>), 138.06 (Ph-C<sub>quat</sub>), 128.58 (C<sub>arom</sub>), 128.49 (C<sub>arom</sub>), 128.46 (C<sub>arom</sub>), 128.18 (C<sub>arom</sub>), 128.07 (C<sub>arom</sub>), 128.00 (C<sub>arom</sub>), 127.95 (C<sub>arom</sub>), 127.88 (C<sub>arom</sub>), 127.83 (C<sub>arom</sub>), 127.77 (C<sub>arom</sub>), 127.71 (C<sub>arom</sub>), 100.67 (C1g), 83.04 (C3g), 80.11 (C3r, C4r), 80.03 (C2r, C4r), 78.31 (C2r), 78.03 (C4g), 77.48 (CDCl<sub>3</sub>), 77.16 (CDCl<sub>3</sub>), 76.84 (CDCl<sub>3</sub>), 75.30 (C5g), 75.18 (CH<sub>2</sub>-Ph), 74.44 (CH<sub>2</sub>-Ph), 73.69 (CH<sub>2</sub>-Ph), 73.67 (CH<sub>2</sub>-Ph), 73.53 (C2g), 72.61 (CH<sub>2</sub>-Ph), 69.88 (C6g), 68.89 (C1r), 61.66 (C5r), 21.06 (CH<sub>3</sub>).

HRMS (ESI+) *m/z* = [M + Na]<sup>+</sup> calculated for C<sub>55</sub>H<sub>60</sub>O<sub>11</sub>Na 919.4033; found 919.4031.

4-O-(2-O-acetyl-3,4,6-tri-O-benzyl-β-D-glucopyranosyl)-1,2,3-tri-O-benzyl-5-O-[(N,N-diisopropylamino) O-2-cyanoethyl-phosphoramidite]-D-ribose **76**



**12** (270 mg, 0.301 mmol) was dissolved in DCM (2.5 ml) under N<sub>2</sub> atmosphere. Then the phosphoramidite (0.3 M of the phosphoramidite in DCM, 0.602 mmol) and the tetrazolide **63** (0.361 mmol) were added. The reaction was stirred for 3 h at r.t. and then diluted with DCM and washed with (sat.) NaHCO<sub>3</sub>: brine (1:1) and dried over Na<sub>2</sub>SO<sub>4</sub>. The product was purified by flash chromatography (8:2 Hex:EtOAc 0.5% NEt<sub>3</sub>).

Yield: 326 mg 98%

Rf: 0.64 (6:4 Hex:EtOAc)

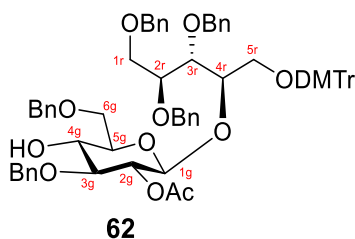
<sup>1</sup>H NMR (400 MHz, Acetone-*d*<sub>6</sub>) δ 7.48 – 7.13 (m, 29H, Ph), 4.99 (ddd, *J* = 9.2, 7.9, 4.6 Hz, 1H, H-2g), 4.87 (dd, *J* = 8.0, 1.5 Hz, 1H, H-1g), 4.85 – 4.70 (m, 5H, 5xCH<sub>2</sub>Ph), 4.70 – 4.60 (m, 3H, 3xCH<sub>2</sub>Ph), 4.58 (d, *J* = 2.6 Hz, 1H, 1xCH<sub>2</sub>Ph), 4.57 – 4.52 (m, 2H, 2xCH<sub>2</sub>Ph), 4.52 – 4.43 (m, 1H, 1xCH<sub>2</sub>Ph), 4.32 (dq, *J* = 6.6, 3.3 Hz, 1H, H-4r), 4.08 – 3.59 (m, 12H, 2xCH, 2x H-1r, H-3g, H-4g, 2xH-6g, H-2r, H-3r, 2xH-5r, 2xH-6, 2xH-8), 3.55 (tdd, *J* = 6.9, 5.3, 3.2 Hz, 1H, H-5g), 2.83 – 2.75 (m, 2H, 2x H-7), 2.05 (dq, *J* = 4.3, 2.2 Hz, 15H, Aceton, OAc), 1.29 – 1.10 (m, 12H, 4xH-9).

<sup>13</sup>C NMR (101 MHz, Acetone) δ 206.09 (Aceton), 169.95 (C<sub>carbonyl</sub>), 139.91 (Ph-C<sub>quat</sub>), 139.73 (Ph-C<sub>quat</sub>), 139.51 (Ph-C<sub>quat</sub>), 129.06 (C<sub>arom</sub>), 128.98 (C<sub>arom</sub>), 128.81 (C<sub>arom</sub>), 128.63 (C<sub>arom</sub>), 128.60 (C<sub>arom</sub>), 128.38 (C<sub>arom</sub>), 128.11 (C<sub>arom</sub>), 128.03 (C<sub>arom</sub>), 101.57 (C1-g), 101.49 (C1-g), 83.80 (C-3g), 83.62 (C3-g), 80.55 (C2-r, C3-r or C4-g), 80.39 (C2-r, C3-r or C4-g), 79.68 (C2-r, C3-r or C4-g), 79.62 (C2-r, C3-r or C4-g), 79.50 (C2-r, C3-r or C4-g), 79.43 (C2-r, C3-r or C4-g), 79.25 (C2-r, C3-r or C4-g), 79.16 (C2-r, C3-r or C4-g), 79.07 (C2-r, C3-r or C4-g), 76.00 (C5-g), 75.48 (CH<sub>2</sub>-Ph), 75.38 (CH<sub>2</sub>-Ph), 74.44 (CH<sub>2</sub>-Ph), 74.35 (CH<sub>2</sub>-Ph), 74.27 (C2-g), 73.99, 73.75, 72.96, 72.90, 71.09 (C6-g), 69.80 (C1-r), 64.78 (d, *J* = 4.6 Hz, C5-r), 64.63 (d, *J* = 4.6 Hz, C5-r), 60.24 – 59.14 (m, C6), 43.74 (t, *J* = 13.2 Hz, C8), 30.42 (Aceton), 30.22 (Aceton), 30.03 (Aceton), 29.84 (Aceton), 29.65 (Aceton), 29.46 (Aceton), 29.26 (Aceton), 25.20 (C9), 25.14 (C9), 25.07 (C9), 24.96 (C9), 24.92 (C9), 21.43 (CH<sub>3</sub>), 20.85 (t, *J* = 6.8 Hz, C7).

<sup>31</sup>P NMR (162 MHz, Acetone) δ 147.76, 147.24.



4-O-(2-O-acetyl-3,6-di-O-benzyl-β-D-glucopyranosyl)- 1,2,3,-tri-O-benzyl-5-O-[bis(4-methoxyphenyl)(phenyl)]- D-ribose **62**



**14** (0.227 g, 0.195 mmol) was dissolved in THF (2 ml) and cooled to 0°C. Then TBAF (1M in THF, 0.975 mmol) were added. The reaction was stirred for 30 min at 0°C and another 30 min at r.t. Then NaHCO<sub>3</sub> (sat.) and DCM were added. The organic layer was washed with brine and dried over Na<sub>2</sub>SO<sub>4</sub>. No purification was performed.

The crude was dissolved in DCM (1.5 ml) and cooled to 0°C. Then TFA (3.9 mmol) were added and after 30 min TLC showed full conversion. The reaction was diluted with DCM and the organic layer were washed with NaHCO<sub>3</sub> (sat.), brine and dried over Na<sub>2</sub>SO<sub>4</sub>. No purification was performed.

The residue was dissolved in anhydrous DCM (2 ml) under N<sub>2</sub>-atmosphere and cooled to 0°C. Then NEt<sub>3</sub> (0.293 mmol) and DMTrCl (0.293 mmol) were added and the reaction was stirred for 17 h. Afterwards the reaction was diluted with DCM and water was added. The organic layer was washed with brine and dried over Na<sub>2</sub>SO<sub>4</sub>. The product was purified by flash chromatography (7:3 Hex:EtOAc + 0.1 % of NEt<sub>3</sub>)

Yield: 170 mg 80 % over three steps

Rf: 0.40 (6:4 Hex:EtOAc)

[α]<sub>D</sub><sup>33</sup> = + 11.0 (5.5 mg/ml)

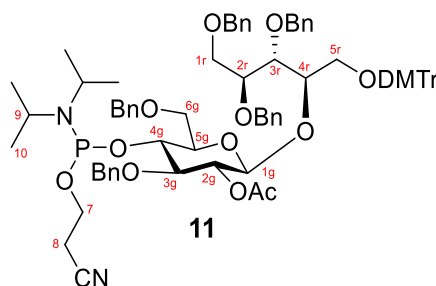
<sup>1</sup>H NMR (400 MHz, Chloroform-*d*) δ 7.41 (dt, *J* = 8.0, 1.6 Hz, 2H, Ph), 7.37 – 7.14 (m, 36H, Ph), 7.13 – 7.00 (m, 2H, Ph), 6.74 (dq, *J* = 8.9, 1.7 Hz, 4H, Ph), 5.03 (ddd, *J* = 9.5, 8.0, 1.5 Hz, 1H, H-2g), 4.87 – 4.70 (m, 3H, H-1g, 2x CH<sub>2</sub>Ph), 4.61 (dd, *J* = 11.9, 1.4 Hz, 1H, 1x CH<sub>2</sub>Ph), 4.58 – 4.33 (m, 7H, 7x CH<sub>2</sub>Ph), 4.19 (dd, *J* = 5.6, 2.8 Hz, 1H, H-4r), 3.85 (ddd, *J* = 6.1, 4.4, 1.5 Hz, 1H, H-3r), 3.80 – 3.28 (m, 15H, H-3g, H-4g, 2x H-6, H-4r, 2x H-1r, 2x H-5r, 2xOMe), 2.87 (s, 1H, OH), 2.04 (d, *J* = 1.5 Hz, 3H, CH<sub>3</sub>).

<sup>13</sup>C NMR (101 MHz, CDCl<sub>3</sub>) δ 169.72 (C<sub>carbonyl</sub>), 158.54 (Ph-C<sub>quat</sub>), 158.53 (Ph-C<sub>quat</sub>), 145.01 (Ph-C<sub>quat</sub>), 139.01 (Ph-C<sub>quat</sub>), 138.72 (Ph-C<sub>quat</sub>), 138.66 (Ph-C<sub>quat</sub>), 138.53 (Ph-C<sub>quat</sub>), 137.74 (Ph-C<sub>quat</sub>), 136.13 (Ph-C<sub>quat</sub>), 130.30 (C<sub>arom</sub>), 130.27 (C<sub>arom</sub>), 128.38 (C<sub>arom</sub>), 128.36 (C<sub>arom</sub>), 128.24 (C<sub>arom</sub>), 128.20 (C<sub>arom</sub>), 127.90 (C<sub>arom</sub>), 127.86 (C<sub>arom</sub>), 127.84 (C<sub>arom</sub>), 127.78 (C<sub>arom</sub>), 127.62 (C<sub>arom</sub>), 127.60 (C<sub>arom</sub>), 127.47 (C<sub>arom</sub>), 127.41 (C<sub>arom</sub>), 127.33 (C<sub>arom</sub>), 126.84 (C<sub>arom</sub>), 113.14, 100.07 (C1-g), 86.36 (C<sub>quat</sub>), 82.53 (C3-g), 79.23 (C3-r),

78.68 (C2-r), 77.92 (C4-r), 77.48 (CDCl<sub>3</sub>), 77.16 (CDCl<sub>3</sub>), 76.84 (CDCl<sub>3</sub>), 74.32 (CH<sub>2</sub>-Ph), 73.89 (CH<sub>2</sub>-Ph), 73.74 (CH<sub>2</sub>-Ph), 73.57 (CH<sub>2</sub>-Ph), 73.21 (CH<sub>2</sub>-Ph), 73.13 (CH<sub>2</sub>-Ph), 72.92 (CH<sub>2</sub>-Ph), 72.37 (CH<sub>2</sub>-Ph), 70.96 (C6-g or C1-r), 70.35 (C6-g or C1-r), 63.20 (C-5r), 55.28 (OMe), 21.15 (CH<sub>3</sub>).

HRMS (ESI+)  $m/z = [M + Na]^+$  calculated for C<sub>69</sub>H<sub>72</sub>O<sub>13</sub>Na 1131.4871; found 1131.4860.

4-O-{2-O-acetyl-3,6-di-O-benzyl-4-O-[(N,N,-diisopropylamino) O-2-cyanoethyl-phosphoramidite]-β-D-glucopyranosyl}- 1,2,3,-tri-O-benzyl-5-O-[bis(4-methoxyphenyl)(phenyl)]- D-ribose **11**



**59** (392 mg, 0.359 mmol) was dissolved in DCM under N<sub>2</sub> atmosphere. Then a solution of the phosphoramidite (0.718 mmol, 0.3 M in DCM) was added followed by addition of the tetrazolid **63** (0.466 mmol). The reaction turned white-pink. After 3 h 0.5 eq of the phosphoramidite was added again (0.180 mmol) and the reaction was warmed to 30 °C. After 6 h TLC showed full conversion (6:4 Hex:EtOAc) and DCM was added. The organic layer was washed with (sat.) NaHCO<sub>3</sub>: brine (1:1) and dried over Na<sub>2</sub>SO<sub>4</sub>. The product was purified by flash chromatography (8:2 Hex:EtOAc + 0.5 % NEt<sub>3</sub>).

Yield: 448 mg 95%

Rf: 0.49 (7:3 Hex:EtOAc)

<sup>1</sup>H NMR (400 MHz, Chloroform-*d*) δ 7.61 – 7.38 (m, 2H, Ph), 7.39 – 7.06 (m, 36H, Ph), 6.84 – 6.57 (m, 4H, Ph), 5.11 (ddd,  $J = 12.6, 9.5, 7.9$  Hz, 1H, H-2g), 4.92 – 4.74 (m, 2H, H-1g, 1xCH<sub>2</sub>Ph), 4.69 (d,  $J = 11.2$  Hz, 1H, 1xCH<sub>2</sub>Ph), 4.67 – 4.39 (m, 7H, 7xCH<sub>2</sub>Ph), 4.34 (dt,  $J = 12.5, 4.6$  Hz, 2H, H-2r, 1xCH<sub>2</sub>Ph), 3.92 (ddd,  $J = 15.1, 8.3, 4.1$  Hz, 2H, H-3r, 1xHx5r), 3.87 – 3.49 (m, 12H, OMe, 2x CH, H-3g, H-4g, 2xH-7, 2xH-6g, 1xH-5r?), 3.49 – 3.34 (m, 2H, 2xH-1r), 2.34 (q,  $J = 6.4$  Hz, 1H, 1xHx8), 2.22 – 1.97 (m, 3H, 3xH-8), 1.66 (d,  $J = 13.7$  Hz, 3H, CH<sub>3</sub>), 1.26 – 1.06 (m, 12H, CH<sub>3</sub>).

<sup>13</sup>C NMR (101 MHz, CDCl<sub>3</sub>) δ 169.75, 169.69, 158.53, 145.10, 139.13, 138.80, 138.70, 138.61, 138.39, 136.22, 130.34, 128.44, 128.37, 128.23, 128.10, 127.98, 127.88, 127.74, 127.70, 127.62, 127.47, 127.38, 127.27, 126.82, 117.72, 113.16, 100.05, 99.91, 86.31, 83.48, 82.59, 79.35, 78.91, 78.16, 77.90, 77.48 (CDCl<sub>3</sub>), 77.16 (CDCl<sub>3</sub>), 76.84 (CDCl<sub>3</sub>), 75.95, 74.71, 74.66, 73.86, 73.63, 73.57, 73.55, 73.39,

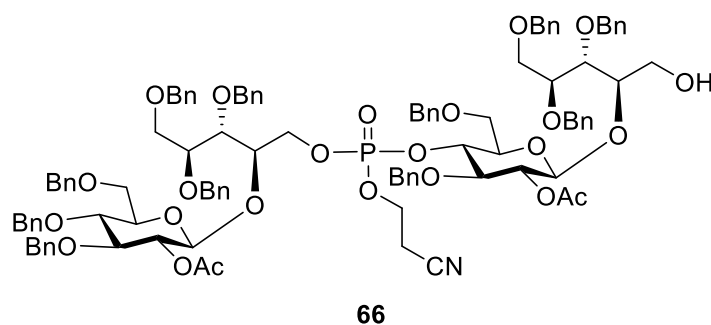
73.24, 73.07, 72.87, 72.48, 70.58, 70.52, 69.72, 69.35, 63.04, 58.99, 58.76, 58.49, 58.24, 55.31, 43.72, 43.59, 43.45, 43.32, 29.84, 24.85, 24.77, 24.60, 21.14, 20.13, 20.06, 19.94, 19.87.

$^{31}\text{P}$  NMR (162 MHz,  $\text{CDCl}_3$ )  $\delta$  152.34, 150.58.

HRMS (ESI+)  $m/z = [\text{M} + \text{Na}]^+$  calculated for  $\text{C}_{78}\text{H}_{89}\text{N}_2\text{O}_{14}\text{NaP}$  1331.5949; found 1331.6008.

## 7.2.7 Different Oligomerization Approach

### Dimer 66



#### Procedure I

Before reaction: **62** and phosphoramidite **76** were both coevaporated with ACN and put on the pump overnight. Furthermore MS 3 A were freshly activated.

**62** (330 mg, 0.302 mmol) was dissolved in ACN (1.5 ml) and DCI (0.362 mmol) and MS 3 A were added under Ar atmosphere. After 30 min a solution of the phosphoramidite **76** (0.400 mmol in ACN 800  $\mu\text{l}$  + 200  $\mu\text{l}$  + 300  $\mu\text{l}$  + 200  $\mu\text{l}$ ) were added. The reaction was monitored by HPTL (11.5: 8.5 Hex:EtOAc). After 1 h CSO (0.604 mmol) were added and stirred for 15 min. Then the MS were filtered off and the reaction was diluted with DCM. The organic layer was washed with (sat.)  $\text{NaHCO}_3$ : brine (1:1) and dried over  $\text{Na}_2\text{SO}_4$ . The crude was again dissolved in DCM (3 ml) and TCA (0.906 mmol, 0.18 M in DCM) was added. After 30 min the reaction was quenched by adding water. The organic phase was diluted with DCM and washed with (sat.)  $\text{NaHCO}_3$ : brine (1:1) and dried over  $\text{Na}_2\text{SO}_4$ . The product was purified by Biotage.

#### Biotage conditions

Cartridge	SNAP KP-Sil25g
Flow-rate	30 ml/min
Solvent A	n-Hexane
Solvent B	Ethyl acetate
Max. Fraction Volume	15 ml

## Gradient

	<b>Solvents</b>	<b>Mix</b>	<b>Length in column volume (CV)</b>
<b>1</b>	A/B	40%-80%	10.0 CV
<b>2</b>	A/B	80%-82%	0.1 CV
<b>3</b>	A/B	82%-100%	1.0 CV
<b>4</b>	A/B	100%	2.0 CV

Yield: 399 mg 73 %

Rf: 0.37 (4:6 Hex:EtOAc)

### **7.2.8 General Coupling Procedure**

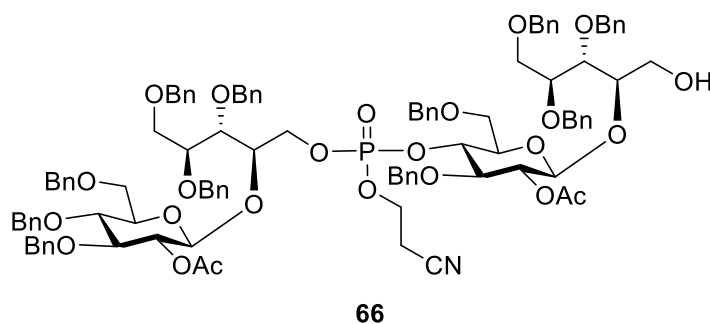
#### Procedure II

Before reaction: 'acceptor' and phosphoramidite were both coevaporated with ACN and put on the pump overnight. Furthermore MS 3 A were freshly activated.

The 'acceptor' was dissolved in ACN (0.1M) and DCI and MS 3 A were added under Ar atmosphere. After 30 min a solution of the phosphoramidite in ACN was added. The reaction was monitored by HPTLC and after consumption of the starting materials CSO was added and stirred for additional 15 min. Then the MS were filtered off and diluted with DCM. The organic layer was washed with (sat.) NaHCO<sub>3</sub>: brine (1:1) and dried over Na<sub>2</sub>SO<sub>4</sub>. The crude was again dissolved in DCM and TCA (0.18 M in DCM) was added. After 30 min the reaction was quenched by adding water and MeOH. The organic phase was diluted with DCM and washed with (sat.) NaHCO<sub>3</sub>: brine (1:1) and dried over Na<sub>2</sub>SO<sub>4</sub>.

The product was purified by Biotage (and Sephadex LH-20 (DCM:MeOH 2:8)

## Dimer 66



**12** (100 mg, 0.111 mmol) was coupled with phosphoramidite **11** (0.123 mmol in ACN 800  $\mu$ l + 200  $\mu$ l) using DCI (0.144 mmol) and CSO (0.222 mmol) followed by deprotection of DMTr with TCA (0.333 mmol, 0.18 M in DCM). The product was purified by Biotage.

### Biotage conditions

Cartridge	SNAP KP-Sil25g
Flow-rate	30 ml/min
Solvent A	n-Hexane
Solvent B	Ethyl acetate
Max. Fraction Volume	10 ml

### Gradient

	Solvents	Mix	Length in column volume (CV)
<b>1</b>	A/B	30%-68%	7.6 CV
<b>2</b>	A/B	68%	1.0 CV
<b>3</b>	A/B	68-70%	0.3 CV
<b>4</b>	A/B	70-100%	1.0 CV
<b>5</b>	A/B	100%	2 CV

Yield: 160 mg 79 %

Rf: 0.37 (4:6 Hex:EtOAc)

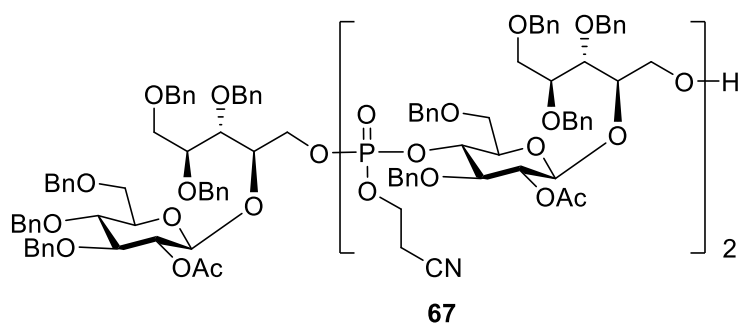
$^1\text{H}$  NMR (400 MHz, Chloroform-*d*)  $\delta$  7.42 – 7.21 (m, 54H), 5.21 – 5.00 (m, 2H), 4.92 – 4.68 (m, 8H), 4.69 – 4.39 (m, 17H), 4.39 – 4.27 (m, 1H), 4.28 – 4.20 (m, 1H), 4.19 – 4.12 (m, 1H), 4.12 – 3.90 (m, 4H), 3.90 – 3.57 (m, 14H), 3.45 (ddt,  $J = 12.9, 9.6, 4.1$  Hz, 2H), 3.38 – 3.29 (m, 1H), 2.56 (d,  $J = 13.8$  Hz, 1H), 2.36 (q,  $J = 5.7$  Hz, 1H), 2.20 (dt,  $J = 17.1, 6.2$  Hz, 1H), 2.04 (s, 3H), 2.00 (s, 3H), 1.50 – 1.24 (m, 5H).

$^{13}\text{C}$  NMR (101 MHz,  $\text{CDCl}_3$ )  $\delta$  169.97, 169.74, 169.59, 138.77 (Ph- $\text{C}_{\text{quat}}$ ), 138.56 (Ph- $\text{C}_{\text{quat}}$ ), 138.40 (Ph- $\text{C}_{\text{quat}}$ ), 138.28 (Ph- $\text{C}_{\text{quat}}$ ), 138.18 (Ph- $\text{C}_{\text{quat}}$ ), 137.93 (Ph- $\text{C}_{\text{quat}}$ ), 137.84 (Ph- $\text{C}_{\text{quat}}$ ), 128.28 ( $\text{C}_{\text{arom}}$ ), 128.21 ( $\text{C}_{\text{arom}}$ ), 128.14 ( $\text{C}_{\text{arom}}$ ), 127.93 ( $\text{C}_{\text{arom}}$ ), 127.83 ( $\text{C}_{\text{arom}}$ ), 127.60 ( $\text{C}_{\text{arom}}$ ), 127.51 ( $\text{C}_{\text{arom}}$ ), 116.71, 116.52, 101.17 (d,  $J = 14.6$  Hz, H-1g), 100.42 (d,  $J = 21.7$  Hz, H-1g), 82.87, 82.74, 80.91, 80.09, 79.98, 79.29, 79.19, 78.91, 78.84, 78.42, 78.32, 77.99, 77.87, 77.48 ( $\text{CDCl}_3$ ), 77.16 ( $\text{CDCl}_3$ ), 76.84 ( $\text{CDCl}_3$ ), 75.27, 75.21, 74.99, 74.90, 74.38, 73.90, 73.64, 73.55, 73.45, 73.35, 72.71, 72.60, 72.47, 72.33, 69.72, 69.54, 68.83, 68.63, 68.27, 68.16, 62.28, 62.23 (C-7), 61.42 (C-7), 46.77, 32.01, 29.78, 29.45, 22.78, 21.18, 21.12 (CH<sub>3</sub>), 20.90 (CH<sub>3</sub>), 19.30 (d,  $J = 6.3$  Hz, C8), 18.99 (d,  $J = 6.7$  Hz, C8).

$^{31}\text{P}$  NMR (162 MHz, Chloroform-*d*)  $\delta$  -2.39, -2.55.

HRMS (ESI+)  $m/z = [\text{M} + \text{Na}]^+$  calculated for  $\text{C}_{106}\text{H}_{116}\text{NO}_{24}\text{NaP}$  1840.7523; found 1840.7468.

### Trimer **67**



**66** (161 mg, 0.089 mmol) was coupled with phosphoramidite **11** (0.118 mmol in ACN 200  $\mu\text{l}$ +200  $\mu\text{l}$  + 100  $\mu\text{l}$  + 100  $\mu\text{l}$ ) using DCI (0.107 mmol) and CSO (0.604 mmol) followed by deprotection of DMTr with TCA (0.267 mmol, 0.18 M in DCM). The product was purified by Biotage.

#### Biotage conditions

Cartridge	SNAP KP-Sil25g
Flow-rate	33 ml/min
Solvent A	n-Hexane
Solvent B	Ethyl acetate
Max. Fraction Volume	10 ml

## Gradient

	<b>Solvents</b>	<b>Mix</b>	<b>Length in column volume (CV)</b>
<b>1</b>	A/B	45%-67%	5.8 CV
<b>2</b>	A/B	67%	1.0 CV
<b>3</b>	A/B	67%-75%	2.1 CV
<b>4</b>	A/B	75%-100%	1 CV
<b>5</b>	A/B	100%	5 CV

Yield: 198 mg 80 %

Rf: 0.43 (4:6 Hex:EtOAc)

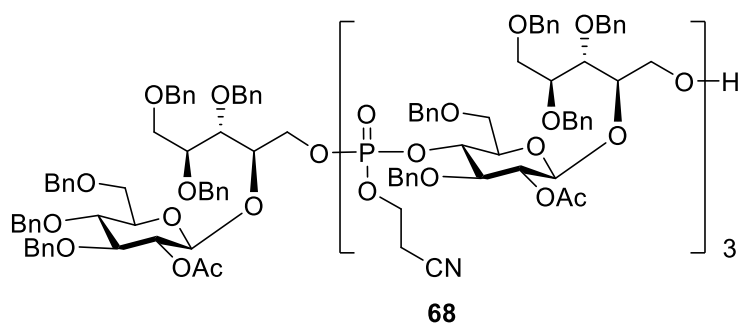
$^1\text{H}$  NMR (400 MHz, Chloroform-*d*)  $\delta$  7.63 – 6.90 (m, 85H), 5.15 – 4.93 (m, 3H), 4.83 – 4.31 (m, 32H), 4.26 (td,  $J = 12.0, 9.7, 3.6$  Hz, 4H), 4.16 (qd,  $J = 6.8, 3.6$  Hz, 1H), 4.12 – 4.05 (m, 1H), 4.05 – 3.96 (m, 1H), 3.97 – 3.82 (m, 2H), 3.81 – 3.44 (m, 9H), 3.45 – 3.32 (m, 2H), 3.26 (dd,  $J = 9.7, 4.0$  Hz, 1H), 2.46 (q,  $J = 6.6$  Hz, 1H), 2.27 (dt,  $J = 9.6, 6.3$  Hz, 1H), 2.02 – 1.93 (m, 9H).

$^{13}\text{C}$  NMR (101 MHz,  $\text{CDCl}_3$ )  $\delta$  170.06, 169.82, 169.65, 169.57, 169.43, 138.81, 138.73, 138.61, 138.48, 138.33, 138.19, 138.06, 137.97, 137.87, 128.48, 128.40, 128.08, 128.00, 127.92, 127.84, 127.76, 127.68, 127.62, 116.79, 116.72, 116.61, 101.18, 100.60, 100.34, 82.95, 82.80, 80.92, 80.76, 80.64, 80.28, 80.15, 80.04, 79.34, 79.22, 79.16, 78.90, 78.60, 78.52, 78.32, 78.03, 77.99, 77.91, 77.48 ( $\text{CDCl}_3$ ), 77.16 ( $\text{CDCl}_3$ ), 76.84 ( $\text{CDCl}_3$ ), 75.57, 75.52, 75.31, 75.14, 75.07, 74.94, 74.44, 74.36, 74.16, 73.96, 73.53, 73.50, 73.40, 72.76, 72.65, 72.53, 72.42, 72.35, 69.78, 69.61, 68.88, 68.70, 68.28, 68.22, 62.38, 62.25, 61.46, 29.83, 21.18, 20.96, 19.32, 19.09, 19.03, 18.96.

$^{31}\text{P}$  NMR (162 MHz,  $\text{CDCl}_3$ )  $\delta$  -1.70, -1.72, -1.75, -1.79, -1.82, -1.97, -2.00.

HRMS (ESI+)  $m/z = [\text{M} + \text{Na}]^+$  calculated for  $\text{C}_{157}\text{H}_{172}\text{N}_2\text{O}_{37}\text{NaP}_2$  2762.1012; found 2762.0999.

### Tetramer **68**



**67** (98 mg, 0.036 mmol) was coupled with phosphoramidite **11** (0.047 mmol in ACN 200  $\mu$ l + 100  $\mu$ l + 100  $\mu$ l) using DCI (0.043 mmol) and CSO (0.072 mmol) followed by deprotection of DMTr with TCA (0.108 mmol, 0.18 M in DCM). The product was purified by Biotage and additionally with Sephadex LH-20 (8:2 MeOH:DCM).

#### Biotage conditions

Cartridge	SNAP Ultra 10g
Flow-rate	17 ml/min
Solvent A	n-Hexane
Solvent B	Ethyl acetate
Max. Fraction Volume	7 ml

#### Gradient

	Solvents	Mix	Length in column volume (CV)
<b>1</b>	A/B	20%-50%	4.0 CV
<b>2</b>	A/B	50%-79%	6.8 CV
<b>3</b>	A/B	79%-80%	0.9 CV
<b>4</b>	A/B	80%	1.0 CV
<b>5</b>	A/B	80-100%	0.5 CV
<b>6</b>	A/B	100%	4.9%

Yield: 82 mg 62 %

Rf: 0.25 (3:7 Hex:EtOAc)

$^1\text{H}$  NMR (400 MHz, Chloroform-*d*)  $\delta$  7.43 – 7.12 (m, 105H), 5.06 (dp,  $J$  = 16.5, 8.4 Hz, 4H), 4.86 – 4.33 (m, 42H), 4.28 (p,  $J$  = 6.6 Hz, 5H), 4.19 (td,  $J$  = 7.2, 6.2, 2.7 Hz, 1H), 4.15 – 3.98 (m, 3H), 3.90 (dq,  $J$  = 20.0, 6.2 Hz, 6H), 3.84 – 3.48 (m, 28H), 3.47 – 3.34 (m, 3H), 3.28 (dq,  $J$  = 7.3, 3.9, 3.0 Hz, 1H), 2.48 (q,  $J$  = 6.3 Hz, 1H), 2.27 (dp,  $J$  = 11.2, 5.5 Hz, 2H), 2.20 – 2.04 (m, 2H), 2.05 – 1.89 (m, 12H).

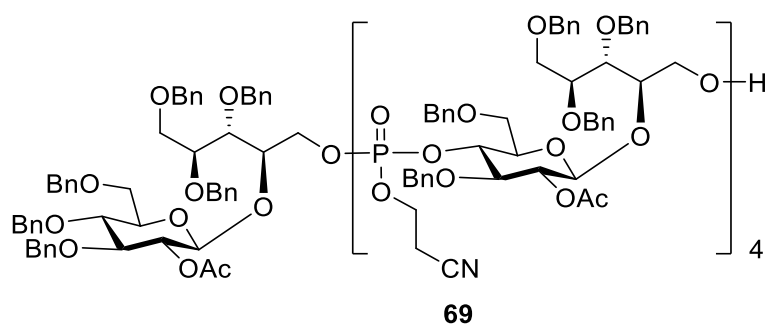


$^{13}\text{C}$  NMR (101 MHz,  $\text{CDCl}_3$ )  $\delta$  170.02, 169.79, 169.75, 169.62, 169.57, 138.83, 138.81, 138.72, 138.63, 138.60, 138.50, 138.36, 138.18, 138.13, 138.05, 137.97, 137.87, 128.57, 128.52, 128.47, 128.44, 128.41, 128.36, 128.08, 128.05, 128.01, 127.90, 127.81, 127.76, 127.71, 127.68, 127.63, 127.59, 116.75, 116.70, 116.67, 116.60, 116.56, 116.39, 101.16, 100.37, 82.96, 82.82, 80.95, 80.19, 80.07, 78.35, 78.00, 77.48 ( $\text{CDCl}_3$ ), 77.16 ( $\text{CDCl}_3$ ), 76.84 ( $\text{CDCl}_3$ ), 75.33, 75.11, 75.01, 74.93, 74.42, 74.15, 73.99, 73.95, 73.69, 73.60, 73.52, 73.50, 73.47, 73.39, 72.79, 72.65, 72.54, 72.46, 72.36, 72.33, 69.85, 69.82, 69.79, 69.66, 68.96, 68.91, 68.34, 68.29, 68.26, 68.18, 62.25, 21.09, 19.31, 19.23, 19.10, 19.05, 18.98, 18.96.

$^{31}\text{P}$  NMR (162 MHz,  $\text{CDCl}_3$ )  $\delta$  -2.38, -2.45, -2.57, -2.65, -2.69.

HRMS (ESI+)  $m/z = [M + 2\text{Na}]^+$  calculated for  $\text{C}_{208}\text{H}_{227}\text{N}_3\text{O}_{50}\text{Na}_2\text{P}_3$  3705.4321; found 3705.4507.

### Pentamer **69**



**68** (150 mg, 0.041 mmol) was coupled with phosphoramidite **11** (0.049 mmol in ACN 200  $\mu\text{l}$  + 200  $\mu\text{l}$  + 180  $\mu\text{l}$ ) using DCI (0.057 mmol) and CSO (0.082 mmol) followed by deprotection of DMTr with TCA (0.205 mmol, 0.18 M in DCM). The product was purified by Biotage and additionally with Sephadex LH-20 (8:2 MeOH:DCM).

### Biotage conditions

Cartridge	SNAP KP-Sil10g
Flow-rate	15 ml/min
Solvent A	n-Hexane
Solvent B	Ethyl acetate
Max. Fraction Volume	5 ml

## Gradient

	<b>Solvents</b>	<b>Mix</b>	<b>Length in column volume (CV)</b>
<b>1</b>	A/B	50%-70%	1.5 CV
<b>2</b>	A/B	70%-85%	8.0 CV
<b>3</b>	A/B	85%-100%	2.0 CV
<b>4</b>	A/B	100%	2.0 CV

Yield: 153 mg 81 %

Rf: 0.50 (2:8 Hex:EtOAc)

<sup>1</sup>H NMR (400 MHz, Chloroform-*d*) δ 8.20 – 6.81 (m, 146H), 5.27 – 4.92 (m, 5H), 4.87 – 4.33 (m, 32H), 4.34 – 4.14 (m, 6H), 4.14 – 3.96 (m, 2H), 3.99 – 3.83 (m, 7H), 3.82 – 3.48 (m, 22H), 3.47 – 3.32 (m, 5H), 3.32 – 3.22 (m, 1H), 2.55 – 2.42 (m, 1H), 2.34 – 2.21 (m, 2H), 2.21 – 2.06 (m, 1H), 2.08 – 1.87 (m, 15H).

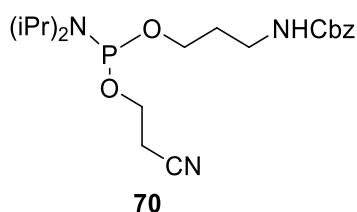
<sup>13</sup>C NMR (101 MHz, CDCl<sub>3</sub>) δ 170.03, 169.79, 169.68, 169.56, 169.54, 169.41, 138.80, 138.71, 138.62, 138.60, 138.47, 138.41, 138.39, 138.33, 138.27, 138.25, 138.06, 137.99, 137.97, 137.92, 128.55, 128.49, 128.46, 128.43, 128.37, 128.09, 128.06, 127.99, 127.91, 127.86, 127.83, 127.80, 127.76, 127.72, 127.68, 127.65, 127.61, 116.89, 116.75, 116.55, 101.51, 101.44, 101.34, 101.23, 101.17, 82.94, 82.80, 81.02, 80.85, 80.72, 79.36, 79.20, 78.98, 78.60, 78.51, 78.43, 78.35, 78.26, 78.08, 77.99, 77.90, 77.48 (CDCl<sub>3</sub>), 77.16 (CDCl<sub>3</sub>), 76.84 (CDCl<sub>3</sub>), 75.23, 75.12, 75.08, 75.03, 74.99, 74.95, 74.92, 74.29, 74.23, 73.99, 73.95, 73.86, 73.60, 73.59, 73.55, 73.48, 73.45, 73.43, 73.40, 72.69, 72.61, 72.56, 72.53, 72.49, 72.47, 72.36, 72.25, 72.23, 72.21, 72.18, 72.15, 69.79, 69.61, 69.53, 69.48, 69.43, 68.89, 68.71, 68.35, 68.31, 68.26, 68.21, 68.19, 68.16, 68.02, 68.00, 67.95, 67.94, 67.92, 67.89, 62.31, 62.26, 62.21, 62.01, 61.96, 29.83, 21.25, 21.17, 21.06, 20.98, 20.94, 20.90, 19.34, 19.27, 19.03, 18.95.

<sup>31</sup>P NMR (162 MHz, CDCl<sub>3</sub>) δ -2.39, -2.44, -2.47, -2.51, -2.55, -2.57, -2.59, -2.62, -2.65, -2.69.

HRMS (ESI+)  $m/z$  = [M + 3Na]<sup>+</sup> calculated for C<sub>259</sub>H<sub>282</sub>N<sub>4</sub>O<sub>63</sub>Na<sub>3</sub>P<sub>4</sub> 4648.7629; found 4648.7876.

## 7.2.9 Coupling to the Linker

### 7.2.9.1 Preparation of the Linker-Containing Phosphoramidite



3-(Cbz-amino)-1-propanol was coevaporated with toluene and dissolved in DCM (1 ml) under Ar atmosphere. Then a solution of the phosphoramidite **55** (1.228 mmol in 3 ml DCM) and tetrazolide **63** were added. The reaction was stirred for 4 h and then a solution of NaHCO<sub>3</sub> (sat.) and brine (1:1) were added. The organic layers were washed with NaHCO<sub>3</sub> (sat.) and brine (1:1) and dried over Na<sub>2</sub>SO<sub>4</sub>. The product was purified by flash chromatography to give the product **70**.

Yield: 273 mg 82 %

Rf: 0.44 (5:5 Hex:EtOAc)

<sup>1</sup>H NMR (400 MHz, Acetone-*d*<sub>6</sub>) δ 7.52 – 7.24 (m, 5H, Ph), 6.29 (s, 1H, NH), 5.06 (d, *J* = 3.0 Hz, 2H, CH<sub>2</sub>Ph), 4.03 – 3.53 (m, 6H, 2xCH, 2xH-3, 2xH-4), 3.28 (q, *J* = 6.6 Hz, 2H, 2xH-1), 2.74 (t, *J* = 6.0 Hz, 2H, 2xH-5), 2.05 (p, *J* = 2.2 Hz, Aceton), 1.83 (p, *J* = 6.5 Hz, 2H, 2xH-2), 1.19 (dd, *J* = 6.8, 3.4 Hz, 12H, 4xCH<sub>3</sub>).

<sup>13</sup>C NMR (101 MHz, Acetone) δ 206.26 (Aceton), 157.31 (C<sub>carbonyl</sub>), 138.75 (Ph-C<sub>quat</sub>), 129.36 (C<sub>arom</sub>), 128.82 (C<sub>arom</sub>), 128.74 (C<sub>arom</sub>), 119.15 (CN), 66.56 (CH<sub>2</sub>-Ph), 62.26 (d, *J* = 17.4 Hz, C3), 59.64 (d, *J* = 18.3 Hz, C4), 43.94 (d, *J* = 12.4 Hz, CH), 39.11 (C1), 32.46 (d, *J* = 7.2 Hz, C2), 30.60 (Aceton), 30.41 (Aceton), 30.22 (Aceton), 30.03 (Aceton), 29.83 (Aceton), 29.64 (Aceton), 29.45 (Aceton), 25.13 (CH<sub>3</sub>), 25.06 (CH<sub>3</sub>), 20.95 (d, *J* = 6.7 Hz, C5).

<sup>31</sup>P NMR (162 MHz, Acetone) δ 147.17.

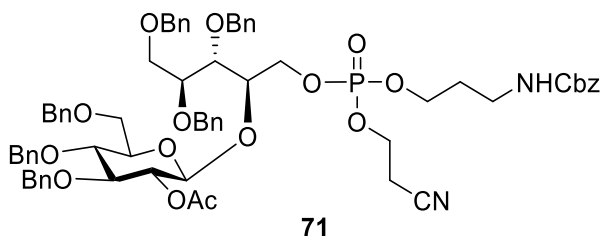
HRMS (ESI+) *m/z* = [M + Na]<sup>+</sup> calculated for C<sub>20</sub>H<sub>32</sub>N<sub>3</sub>O<sub>4</sub>NaP 432.2028; found 432.2029.

### 7.2.9.2 General Procedure for the Coupling with the Linker

Before reaction: 'acceptor' and phosphoramidite-Linker were both coevaporated with ACN and put on the pump overnight. Furthermore MS 3 A were freshly activated.

Acceptor was dissolved in ACN and MS 3 A and DCI were added under Ar atmosphere. After 15 min a solution of the phosphoramidite in ACN (0.1 M in ACN) was added. After full conversion of the starting material CSO (2 eq) was added and the the reaction was stirred for additional 15 min. The mixture was filtered through a pad of celite and then washed with NaHCO<sub>3</sub> (sat.) and brine (1:1) solution and dried over Na<sub>2</sub>SO<sub>4</sub>. The crude was purified by flash chromatography.

#### Monomer **71**



**12** (0.117 mmol) was coupled with the linker **70** (0.152 mmol) using DCI (0.152 mmol) and CSO (0.234 mmol) as reported in the general procedure.

The product was purified by Biotage.

#### Biotage conditions

Cartridge	SNAP KP-Sil10g
Flow-rate	15 ml/min
Solvent A	n-Hexane
Solvent B	Ethyl acetate
Max. Fraction Volume	5 ml

#### Gradient

	Solvents	Mix	Length in column volume (CV)
<b>1</b>	A/B	40%-70%	10 CV
<b>2</b>	A/B	70%-72%	2.9 CV
<b>3</b>	A/B	72%-100%	0.4 CV
<b>4</b>	A/B	100%	5.8 CV

Yield. 118 mg 83 %

Rf: 0.44 (2:8 Hex:EtOAc)

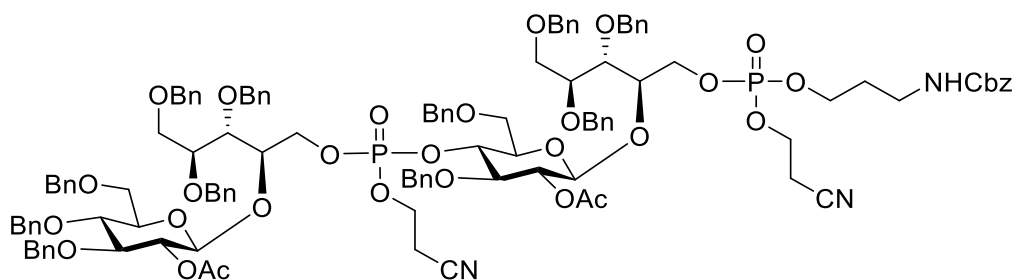
$^1\text{H}$  NMR (400 MHz, )  $\delta$  7.42 – 7.14 (m, 36H, Ph), 5.11 (d,  $J$  = 2.1 Hz, 2H,  $2\times\text{CH}_2\text{Ph}$ ), 5.06 (ddd,  $J$  = 9.0, 7.9, 3.5 Hz, 1H, H-2g), 4.91 – 4.65 (m, 7H,  $5\times\text{CH}_2\text{Ph}$ ), 4.68 – 4.55 (m, 3H,  $5\times\text{CH}_2\text{Ph}$ ), 4.57 – 4.37 (m, 3H,  $4\times\text{CH}_2\text{Ph}$ ), 4.39 – 4.23 (m, 3H, H-4r,  $2\times\text{H}5\text{r}$ ), 4.23 – 3.96 (m, 7H, H-3r,  $2\times\text{H}-7$ ,  $2\times\text{H}-9$ ), 3.84 (tdd,  $J$  = 5.4, 3.1, 2.0 Hz, 1H, H-4r), 3.80 – 3.59 (m, 7H, H-3g, H-4g,  $2\times\text{H}-6\text{g}$ ,  $2\times\text{H}-1\text{r}$ ), 3.47 (ddd,  $J$  = 9.3, 4.2, 2.1 Hz, 1H, H-5g), 3.25 (s, 2H,  $2\times\text{H}11$ ), 2.66 – 2.45 (m, 2H,  $2\times\text{H}-8$ ), 2.02 (s, 3H, OAc), 1.82 (q,  $J$  = 6.1 Hz, 2H,  $2\times\text{H}-10$ ).

$^{13}\text{C}$  NMR (101 MHz,  $\text{CDCl}_3$ )  $\delta$  169.96 ( $\text{C}_{\text{carbonyl}}$ ), 156.57 ( $\text{C}_{\text{carbonyl}}$ ), 138.63 (Ph- $\text{C}_{\text{quat}}$ ), 138.54 (Ph- $\text{C}_{\text{quat}}$ ), 138.39 (Ph- $\text{C}_{\text{quat}}$ ), 138.27 (Ph- $\text{C}_{\text{quat}}$ ), 138.10 (Ph- $\text{C}_{\text{quat}}$ ), 128.62 ( $\text{C}_{\text{arom}}$ ), 128.54 ( $\text{C}_{\text{arom}}$ ), 128.45 ( $\text{C}_{\text{arom}}$ ), 128.13 ( $\text{C}_{\text{arom}}$ ), 128.04 ( $\text{C}_{\text{arom}}$ ), 127.94 ( $\text{C}_{\text{arom}}$ ), 127.83 ( $\text{C}_{\text{arom}}$ ), 127.74 ( $\text{C}_{\text{arom}}$ ), 127.68 ( $\text{C}_{\text{arom}}$ ), 101.46 (C1g), 82.95 (C3g), 82.91 (C3r and C4r), 79.22 (C3r and C4r), 78.27 (C2r), 78.01 (C4g), 77.48 ( $\text{CDCl}_3$ ), 77.16 ( $\text{CDCl}_3$ ), 76.84 ( $\text{CDCl}_3$ ), 75.19 (C5g), 75.08 ( $\text{CH}_2\text{-Ph}$ ), 74.05 ( $\text{CH}_2\text{-Ph}$ ), 73.63 (C2g), 73.56 ( $\text{CH}_2\text{-Ph}$ ), 73.48 ( $\text{CH}_2\text{-Ph}$ ), 72.44 ( $\text{CH}_2\text{-Ph}$ ), 69.71 (C6g), 69.01 (C1r), 68.07 (C5r), 66.73 ( $\text{CH}_2\text{-Ph}$ ), 65.74 (C9), 61.98 (C7), 37.26 (C11), 30.40 (C10), 29.83 (C10), 21.10 ( $\text{CH}_3$ ), 19.60 (C8).

$^{31}\text{P}$  NMR (162 MHz,  $\text{CDCl}_3$ )  $\delta$  -1.14, -1.32.

HRMS (ESI+)  $m/z$  =  $[\text{M} + \text{Na}]^+$  calculated for  $\text{C}_{69}\text{H}_{77}\text{N}_2\text{O}_{16}\text{NaP}$  1243.4908; found 1243.4948.

### Dimer 72



### 72

**66** (0.081 mmol) was coupled with the linker **70** (0.106 mmol) using DCI (0.097 mmol) and CSO (0.162 mmol) as reported in the general procedure.

The product was purified by Biotage.

### Biotage conditions

Catridge	SNAP KP-Sil10g
Flow-rate	15 ml/min
Solvent A	n-Hexane
Solvent B	Ethyl acetate
Max. Fraction Volume	5 ml

### Gradient

	Solvents	Mix	Length in column volume (CV)
1	A/B	40%-60%	2.0 CV
2	A/B	60%-80%	7.9 CV
3	A/B	80%	2.8 CV
4	A/B	80%-85%	1.0 CV
5	A/B	85%-100%	1.0 CV
6	A/B	100%	5.9 CV

Yield: 138 mg 79 %

Rf: 0.51 (4:1 Hex:EtOAc)

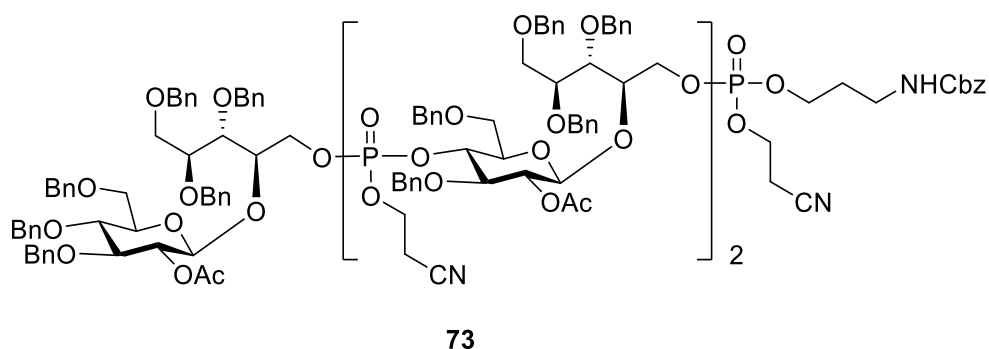
<sup>1</sup>H NMR (400 MHz, )  $\delta$  7.98 – 6.84 (m, 67H), 5.25 – 5.09 (m, 1H), 5.08 – 4.84 (m, 5H), 4.78 – 4.13 (m, 31H), 4.12 – 3.73 (m, 9H), 3.73 – 3.42 (m, 14H), 3.42 – 3.32 (m, 1H), 3.28 (t,  $J$  = 6.6 Hz, 1H), 3.13 (hept,  $J$  = 8.8, 7.0 Hz, 3H), 2.41 (dt,  $J$  = 12.2, 6.1 Hz, 2H), 2.21 (q,  $J$  = 6.0 Hz, 1H), 2.04 (dt,  $J$  = 17.3, 6.2 Hz, 1H), 1.99 – 1.81 (m, 7H).

<sup>13</sup>C NMR (101 MHz, CDCl<sub>3</sub>)  $\delta$  170.05, 169.80, 169.73, 169.62, 138.79, 138.44, 138.24, 138.02, 137.92, 128.64, 128.50, 128.44, 128.21, 128.05, 127.92, 127.84, 127.78, 127.73, 127.68, 127.63, 116.76, 116.64, 116.57, 101.36, 101.22, 82.93, 82.80, 80.95, 80.81, 79.80, 79.73, 79.64, 79.56, 79.34, 79.16, 78.68, 78.60, 78.41, 78.34, 78.12, 77.99, 77.91, 77.48 (CDCl<sub>3</sub>), 77.16 (CDCl<sub>3</sub>), 76.84 (CDCl<sub>3</sub>), 75.35, 75.29, 75.08, 75.04, 74.96, 74.28, 74.00, 73.60, 73.45, 73.42, 72.63, 72.49, 72.37, 69.76, 69.50, 68.89, 68.31, 68.18, 68.08, 66.73, 65.72, 62.35, 62.31, 62.25, 62.00, 30.42, 30.37, 21.25, 21.17, 20.97, 19.62, 19.58, 19.37, 19.31, 19.05, 18.99.

<sup>31</sup>P NMR (162 MHz, CDCl<sub>3</sub>)  $\delta$  -1.09, -1.33, -2.39, -2.54, -2.58.

HRMS (ESI+)  $m/z$  = [M + Na]<sup>+</sup> calculated for C<sub>120</sub>H<sub>133</sub>N<sub>3</sub>O<sub>29</sub>NaP<sub>2</sub> 2164.8398; found 2164.8384.

### Trimer 73



**67** (0.018 mmol) was coupled with the linker **70** (0.023mmol) using DCI (0.022 mmol) and CSO (0.036 mmol) as reported in the general procedure.

The product was purified by Biotage.

#### Biotage conditions

Cartridge	SNAP KP-Sil10g
Flow-rate	15 ml/min
Solvent A	n-Hexane
Solvent B	Ethyl acetate
Max. Fraction Volume	7 ml

#### Gradient

	Solvents	Mix	Length in column volume (CV)
<b>1</b>	A/B	70%-100%	10.0 CV
<b>2</b>	A/B	100%	5.0 CV

Yield: 46 mg 83 %

Rf: 0.50 (9:14 Hex:EtOAc)

$^1\text{H}$  NMR (400 MHz, Chloroform-*d*)  $\delta$  7.44 – 7.12 (m, 83H), 5.33 – 5.20 (m, 1H), 5.17 – 4.96 (m, 5H), 4.87 – 4.23 (m, 39H), 4.24 – 3.84 (m, 12H), 3.85 – 3.34 (m, 21H), 3.27 (dp,  $J$  = 18.6, 6.7, 4.5 Hz, 3H), 2.52 (p,  $J$  = 6.2 Hz, 2H), 2.28 (p,  $J$  = 5.8, 5.2 Hz, 2H), 2.24 – 1.90 (m, 12H).

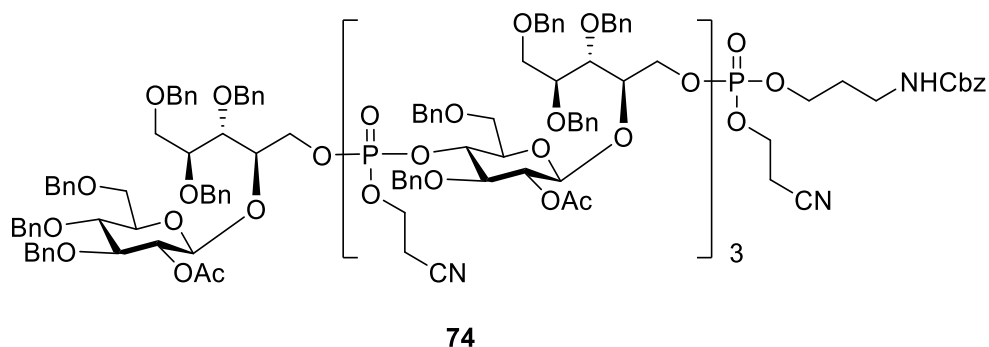
$^{13}\text{C}$  NMR (101 MHz,  $\text{CDCl}_3$ )  $\delta$  195.62, 170.07, 170.03, 169.83, 169.82, 169.75, 169.73, 169.72, 169.63, 169.59, 169.57, 169.46, 169.45, 156.54, 138.77, 138.67, 138.57, 138.45, 138.39, 138.31, 138.26, 138.25, 138.01, 137.97, 137.88, 136.69, 128.62, 128.56, 128.48, 128.45, 128.41, 128.35, 128.19, 128.05, 128.01, 127.98, 127.90, 127.82, 127.77, 127.75, 127.71, 127.66, 127.59, 116.84, 116.79, 116.76, 116.74, 116.71, 116.63, 101.46, 101.37, 101.29, 101.24, 101.14, 100.10, 82.91, 82.76, 80.76,

80.62, 79.72, 79.71, 79.63, 79.62, 79.54, 79.29, 79.11, 79.01, 78.98, 78.96, 78.93, 78.89, 78.60, 78.58, 78.49, 78.38, 78.27, 78.23, 78.09, 78.05, 77.96, 77.87, 77.48 (CDCl<sub>3</sub>), 77.16 (CDCl<sub>3</sub>), 76.84 (CDCl<sub>3</sub>), 75.28, 75.23, 75.11, 75.01, 74.94, 74.92, 74.90, 74.22, 74.18, 74.11, 74.07, 74.02, 73.97, 73.93, 73.63, 73.57, 73.51, 73.44, 73.38, 72.73, 72.71, 72.61, 72.43, 72.32, 69.80, 69.72, 69.70, 69.60, 69.51, 69.45, 69.42, 68.94, 68.90, 68.86, 68.78, 68.65, 68.63, 68.38, 68.31, 68.26, 68.19, 68.17, 68.12, 68.06, 68.04, 66.71, 65.75, 65.70, 65.65, 62.40, 62.35, 62.29, 62.24, 62.19, 62.02, 61.99, 61.94, 37.17, 37.15, 32.05, 31.56, 30.43, 30.40, 30.37, 30.34, 29.82, 29.74, 29.48, 29.28, 29.07, 21.24, 21.16, 21.11, 21.05, 20.99, 20.94, 19.64, 19.60, 19.57, 19.53, 19.35, 19.33, 19.31, 19.28, 19.24, 19.06, 19.00, 18.99, 18.94.

<sup>31</sup>P NMR (162 MHz, CDCl<sub>3</sub>) δ -1.08, -1.33, -2.36, -2.47, -2.63, -2.67.

HRMS (ESI+) *m/z* = [M + Na]<sup>+</sup> calculated for C<sub>171</sub>H<sub>189</sub>N<sub>4</sub>O<sub>42</sub>NaP<sub>3</sub> 3086.1887; found 3086.1917.

#### Tetramer **74**



**68** (0.013 mmol) was coupled with the linker **70** (0.036 mmol) using DCI (0.019 mmol) and CSO (0.026 mmol) as reported in the general procedure.

The product was purified by Biotage and size exclusion LH-20 (MeOH:DCM 8:2).

#### Biotage conditions

Cartridge	SNAP KP-Sil10g
Flow-rate	15 ml/min
Solvent A	n-Hexane
Solvent B	Ethyl acetate
Max. Fraction Volume	5 ml



## Gradient

	<b>Solvents</b>	<b>Mix</b>	<b>Length in column volume (CV)</b>
<b>1</b>	A/B	70%-90%	9.0 CV
<b>2</b>	A/B	90%-100	0.5 CV
<b>3</b>	A/B	100%	4.8 CV

Yield: 26 mg 50%

Rf: 0.46 (9:14 Hex:EtOAc)

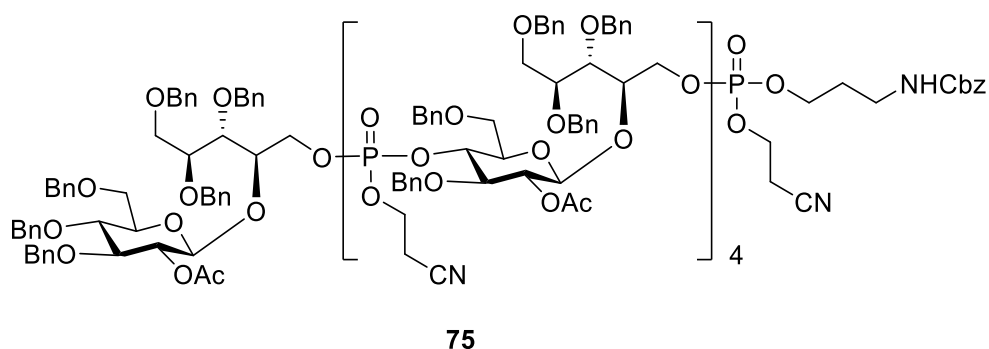
$^1\text{H}$  NMR (400 MHz, )  $\delta$  7.62 – 6.96 (m, 103H), 5.24 (dd,  $J$  = 16.3, 7.1 Hz, 1H), 5.17 – 4.94 (m, 6H), 4.89 – 4.22 (m, 53H), 4.22 – 3.12 (m, 43H), 2.65 – 2.43 (m, 2H), 2.40 – 2.20 (m, 2H), 2.12 (ddt,  $J$  = 17.1, 12.0, 6.2 Hz, 2H), 2.07 – 1.88 (m, 13H).

$^{13}\text{C}$  NMR (101 MHz,  $\text{CDCl}_3$ )  $\delta$  138.85, 138.83, 138.73, 138.64, 138.63, 138.55, 138.52, 138.50, 138.46, 138.44, 138.41, 138.38, 138.35, 138.31, 138.23, 138.07, 138.04, 128.64, 128.58, 128.58, 128.55, 128.49, 128.47, 128.43, 128.38, 128.22, 128.21, 128.21, 128.09, 128.05, 128.03, 128.00, 127.95, 127.92, 127.90, 127.86, 127.84, 127.79, 127.75, 127.69, 127.65, 127.62, 101.40, 101.33, 101.18, 100.13, 82.98, 82.83, 80.98, 80.81, 79.40, 79.27, 79.20, 78.37, 78.30, 78.01, 77.48 ( $\text{CDCl}_3$ ), 77.16 ( $\text{CDCl}_3$ ), 76.84 ( $\text{CDCl}_3$ ), 75.09, 75.03, 74.95, 74.91, 74.10, 74.05, 74.01, 73.97, 73.68, 73.62, 73.57, 73.48, 73.45, 73.42, 72.67, 72.63, 72.48, 72.43, 72.41, 72.37, 72.35, 69.86, 69.83, 69.69, 69.65, 69.59, 69.56, 69.51, 68.95, 68.91, 68.85, 68.31, 68.28, 68.25, 68.18, 68.09, 66.74, 65.74, 62.42, 62.38, 62.33, 62.31, 62.26, 62.22, 62.05, 62.02, 62.00, 61.97, 37.25, 37.24, 29.84, 21.26, 21.18, 21.14, 21.07, 21.00, 19.67, 19.64, 19.60, 19.33, 19.27, 19.05, 19.04, 18.97.

$^{31}\text{P}$  NMR (162 MHz,  $\text{CDCl}_3$ )  $\delta$  -1.08, -1.33, -2.37, -2.45, -2.60, -2.67.

HRMS (ESI+)  $m/z$  =  $[\text{M} + \text{Na}]^+$  calculated for  $\text{C}_{222}\text{H}_{245}\text{N}_5\text{O}_{55}\text{NaP}_4$  4007.5376; found 4007.5422.

### Pentamer **75**



**69** (0.012 mmol) was coupled with the linker **70** (0.019 mmol) using DCI (0.019 mmol). After 2 h the linker **66** (0.012 mmol) was added again and after 5 h the reaction was oxidized using CSO (0.036 mmol) as reported in the general procedure.

The product was purified by Biotage and size exclusion LH-20 (MeOH:DCM 8:2).

#### Biotage conditions

Cartridge	SNAP KP-Sil10g
Flow-rate	15 ml/min
Solvent A	n-Hexane
Solvent B	Ethyl acetate
Max. Fraction Volume	5 ml

#### Gradient

	Solvents	Mix	Length in column volume (CV)
<b>1</b>	A/B	70%-90%	1.5 CV
<b>2</b>	A/B	90%-100%	0.5 CV
<b>3</b>	A/B	100%	2.0 CV

Yield: 36 mg 61%

Rf: 0.62 (9:14 Hex:EtOAc)

<sup>1</sup>H NMR (400 MHz, Chloroform-*d*)  $\delta$  7.56 – 7.02 (m, 118H), 5.24 (dt,  $J$  = 13.4, 6.0 Hz, 1H), 5.17 – 4.94 (m, 6H), 4.92 – 4.35 (m, 52H), 4.29 (dtd,  $J$  = 15.7, 11.4, 6.4 Hz, 8H), 4.24 – 3.98 (m, 8H), 3.90 (dtt,  $J$  = 19.7, 11.3, 4.6 Hz, 8H), 3.84 – 3.47 (m, 28H), 3.45 – 3.33 (m, 1H), 3.35 – 3.10 (m, 4H), 2.52 (p,  $J$  = 6.1 Hz, 2H), 2.27 (p,  $J$  = 8.0, 7.3 Hz, 2H), 2.11 (dtt,  $J$  = 9.8, 6.5, 3.8 Hz, 2H), 2.08 – 1.90 (m, 15H).

<sup>13</sup>C NMR (101 MHz, CDCl<sub>3</sub>)  $\delta$  169.71, 169.60, 138.83, 138.72, 138.63, 138.51, 138.50, 138.36, 138.30, 128.63, 128.57, 128.53, 128.47, 128.43, 128.37, 128.21, 128.08, 128.04, 127.92, 127.83, 127.78,

127.72, 127.68, 127.64, 127.60, 116.84, 116.76, 116.74, 101.38, 101.33, 101.31, 101.16, 82.97, 82.82, 80.82, 79.39, 79.21, 78.29, 78.00, 77.48 (CDCl<sub>3</sub>), 77.16 (CDCl<sub>3</sub>), 76.84 (CDCl<sub>3</sub>), 75.02, 74.94, 74.05, 74.00, 73.95, 73.93, 73.61, 73.45, 73.40, 72.79, 72.66, 72.57, 72.41, 72.36, 72.34, 69.85, 69.68, 69.63, 69.58, 68.96, 68.84, 68.69, 68.40, 68.38, 68.35, 68.30, 68.28, 68.22, 68.14, 68.12, 66.77, 66.74, 66.72, 65.78, 65.72, 62.46, 62.43, 62.38, 62.32, 62.25, 62.22, 62.04, 62.01, 61.99, 61.97, 37.27, 37.24, 21.17, 21.06, 19.66, 19.59, 19.56, 19.39, 19.32, 19.29, 19.08, 19.03.

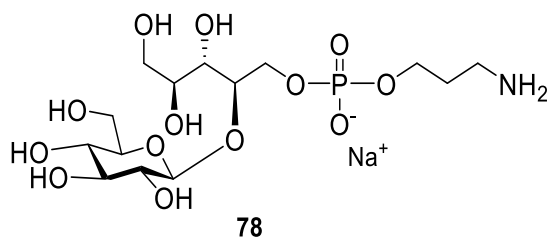
<sup>31</sup>P NMR (162 MHz, CDCl<sub>3</sub>) δ -1.07, -1.09, -1.31, -1.34, -2.37, -2.39, -2.41, -2.44, -2.46, -2.51, -2.54, -2.57, -2.59, -2.62, -2.64, -2.68.

HRMS (ESI+)  $m/z = [M + Na]^+$  calculated for C<sub>274</sub>H<sub>305</sub>N<sub>6</sub>O<sub>67</sub>NaP<sub>5</sub> 4928.8866; found 4928.9087.

### **7.2.10 General Procedure for Deprotection**

Starting material was dissolved in Dioxane and NH<sub>3</sub> (aqueous solution 30-33 %, 1 ml for 10 μmol of starting material) and stirred for 18 h. Then the solvent was evaporated and the residue was coevaporated three times with milliQ H<sub>2</sub>O. Afterwards the sugar was dissolved in dioxane:water mixture and eluted through a column containing Dowex Na<sup>+</sup> cation-exchange resin (type: 50WX8 Na<sup>+</sup> form, stored on a 0.5 M NaOH in H<sub>2</sub>O, flushed with MilliQ H<sub>2</sub>O and MeOH before use). After the ion exchange the sugar was dissolved in 1,4-Dioxane:milli Q H<sub>2</sub>O (until completely dissolved) and 3-4 drops of glacial AcOH were added. The mixture was purged with Ar and afterwards, a scup of Pd black was added. The reaction was purged again with Ar and after a few minutes the atmosphere was exchanged to H<sub>2</sub>. The reaction was stirred for 2-4 days. Then the mixture was filtrated through a syringe containing a frit and concentrated in vacuo. The residue was dissolved in 2 mL of milliQ H<sub>2</sub>O and 50 μl of NEt<sub>3</sub> were added. The reaction was stirred for 24 h to give the fully deprotected products. The drude was purified by size exclusion chromatography (Toyopearl HW-40) and the pure compounds were dissolved in MilliQ H<sub>2</sub>O, eluted through a column containing Dowex Na<sup>+</sup> cation-exchange resin (type: 50WX8 Na<sup>+</sup> form, stored on a 0.5 M NaOH in H<sub>2</sub>O, flushed with MilliQ H<sub>2</sub>O and MeOH before use) and lyophilized.

### Monomer **78**



**71** (0.025 mmol) was deprotected using the general deprotection procedure.

Yield: 6.0 mg 53%

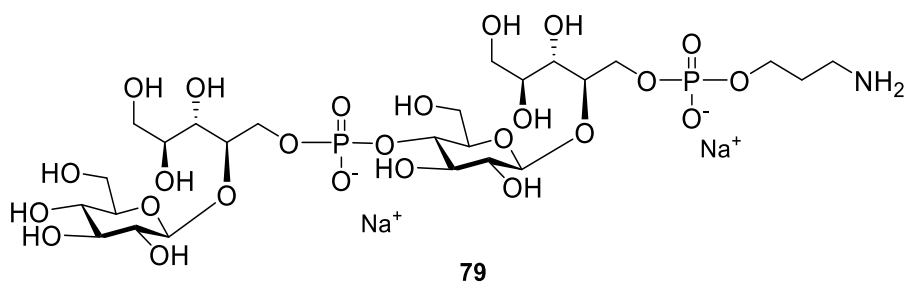
$^1\text{H}$  NMR (400 MHz, Deuterium Oxide)  $\delta$  4.68 (d,  $J = 7.8$  Hz, 1H, H-1g), 4.17 (ddt,  $J = 8.5, 5.6, 3.0$  Hz, 2H, H5r), 4.14 – 4.06 (m, 1H), 4.03 (q,  $J = 6.0$  Hz, 2H), 3.98 – 3.89 (m, 2H), 3.87 (dt,  $J = 4.4, 2.5$  Hz, 1H), 3.85 (dd,  $J = 2.7, 0.9$  Hz, 1H), 3.74 (dd,  $J = 12.4, 5.5$  Hz, 1H), 3.66 (dd,  $J = 12.3, 7.3$  Hz, 1H), 3.57 – 3.38 (m, 3H), 3.33 (dd,  $J = 9.4, 7.9$  Hz, 1H), 3.17 (t,  $J = 7.2$  Hz, 2H, CH<sub>2</sub>-Linker), 2.04 (p,  $J = 6.6$  Hz, 2H, CH<sub>2</sub>-Linker).

$^{13}\text{C}$  NMR (101 MHz, D<sub>2</sub>O)  $\delta$  102.00, 78.72 (d,  $J = 7.4$  Hz), 75.49, 75.33, 72.96, 71.41, 71.06, 69.29, 64.34 (d,  $J = 5.1$  Hz), 63.02 (d,  $J = 5.7$  Hz), 62.26, 60.35, 36.82, 27.27.

$^{31}\text{P}$  NMR (162 MHz, D<sub>2</sub>O)  $\delta$  0.85.

HRMS (ESI-)  $m/z = [\text{M}]^+$  calculated for C<sub>14</sub>H<sub>29</sub>NO<sub>13</sub>P 450.1377; found 450.1373.

### Dimer **79**



**72** (0.025 mmol) was deprotected using the general deprotection procedure.

Yield: 7.0 mg 57%

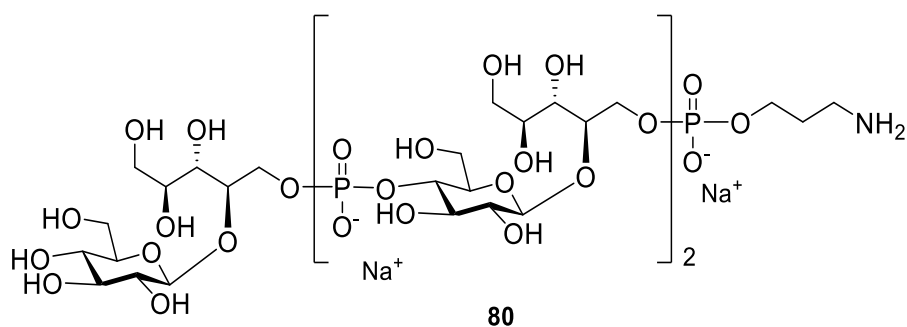
$^1\text{H}$  NMR (400 MHz, Deuterium Oxide)  $\delta$  4.70 (dd,  $J = 7.9, 5.9$  Hz, 2H, H-1g), 4.30 – 4.21 (m, 1H, H5r), 4.21 – 3.99 (m, 6H), 3.99 – 3.78 (m, 10H), 3.78 – 3.61 (m, 5H), 3.62 – 3.44 (m, 2H), 3.45 – 3.38 (m, 2H), 3.38 – 3.27 (m, 1H), 3.18 (t,  $J = 7.2$  Hz, 2H, CH<sub>2</sub>-Linker), 2.04 (p,  $J = 7.3, 6.9$  Hz, 2H).

$^{13}\text{C}$  NMR (101 MHz, D<sub>2</sub>O)  $\delta$  102.27, 102.18, 79.05 (dd,  $J = 12.2, 7.8$  Hz), 75.73, 75.60, 74.95, 74.91, 74.82, 74.05, 74.00, 73.28, 73.15, 71.67, 71.62, 71.44, 71.33, 69.56, 65.39 – 64.83 (m), 64.81 – 64.48 (m), 63.31 (d,  $J = 5.2$  Hz), 62.54, 60.62, 60.47, 37.10, 27.62, 27.54.

$^{31}\text{P}$  NMR (162 MHz, D<sub>2</sub>O)  $\delta$  1.25, 0.80.

HRMS (ESI-)  $m/z = [\text{M}]^+$  calculated for C<sub>25</sub>H<sub>48</sub>NO<sub>25</sub>Na<sub>2</sub>P<sub>2</sub> 870.1786; found 870.1784.

### Trimer **80**



**73** (0.025 mmol) was deprotected using the general deprotection procedure.

Yield: 8.9 mg 57%

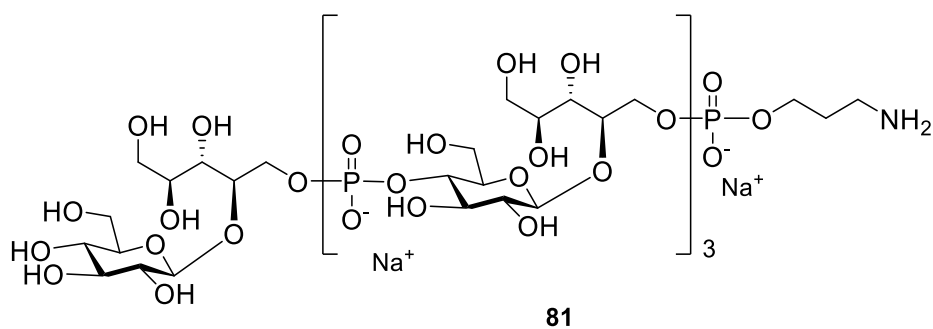
$^1\text{H}$  NMR (400 MHz, Deuterium Oxide)  $\delta$  4.74 – 4.62 (m, 3H, H-1g), 4.25 (dd,  $J$  = 10.2, 6.2 Hz, 2H, H5r), 4.21 – 3.61 (m, 31H), 3.44 – 3.26 (m, 4H), 3.17 (t,  $J$  = 7.2 Hz, 2H, CH<sub>2</sub>-Linker), 2.03 (p,  $J$  = 6.5 Hz, 2H, CH<sub>2</sub>-Linker).

$^{13}\text{C}$  NMR (101 MHz, D<sub>2</sub>O)  $\delta$  102.00, 101.94, 101.90, 78.91, 78.90, 78.86, 78.83, 78.79, 78.73, 78.73, 78.65, 75.47, 75.34, 74.69, 74.64, 74.60, 74.56, 74.53, 73.85, 73.83, 73.81, 73.79, 73.78, 73.75, 73.02, 72.93, 72.93, 72.88, 71.41, 71.35, 71.18, 71.16, 71.07, 69.31, 64.78, 64.73, 64.72, 64.70, 64.69, 64.68, 64.68, 64.61, 64.35, 64.32, 64.32, 64.30, 63.11, 63.06, 62.29, 60.36, 60.20, 60.20, 60.15, 36.83, 27.36, 27.29.

$^{31}\text{P}$  NMR (162 MHz, D<sub>2</sub>O)  $\delta$  0.84, 0.37.

HRMS (ESI-)  $m/z$  =  $[\text{M}]^+$  calculated for C<sub>36</sub>H<sub>68</sub>NO<sub>37</sub>Na<sub>3</sub>P<sub>3</sub> 1268.2376; found 1268.2367.

Tetramer **81**



**74** (0.025 mmol) was deprotected using the general deprotection procedure.

Yield: 4.26 mg 57%

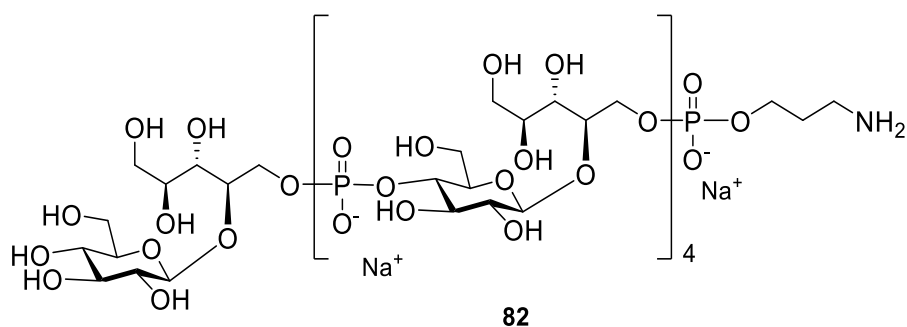
$^1\text{H}$  NMR (400 MHz, Deuterium Oxide)  $\delta$  4.74 – 4.66 (m, 4H, H-1g), 4.25 (t,  $J$  = 8.2 Hz, 3H, H5r), 4.22 – 3.28 (m, 50H), 3.17 (t,  $J$  = 7.2 Hz, 2H, CH<sub>2</sub>-Linker), 2.04 (p,  $J$  = 6.7 Hz, 2H, CH<sub>2</sub>-Linker).

$^{13}\text{C}$  NMR (101 MHz, D<sub>2</sub>O)  $\delta$  102.25, 79.15, 75.73, 75.60, 74.91, 74.80, 74.02, 73.29, 73.20, 71.61, 71.44, 71.34, 69.57, 64.91, 63.32, 62.55, 60.62, 60.47, 37.11, 27.56.

$^{31}\text{P}$  NMR (162 MHz, D<sub>2</sub>O)  $\delta$  0.86, 0.39.

HRMS (ESI-)  $m/z$  =  $[\text{M}]^+$  calculated for C<sub>47</sub>H<sub>88</sub>NO<sub>49</sub>Na<sub>4</sub>P<sub>4</sub> 1666.2966; found 1666.2983.

Pentamer **82**



**75** (0.025 mmol) was deprotected using the general deprotection procedure.

Yield: 3.25 mg 39%

$^1\text{H}$  NMR (400 MHz, Deuterium Oxide)  $\delta$  4.70 – 4.60 (m, 5H, H-1g), 4.28 – 3.23 (m, 59H), 3.14 (t,  $J$  = 7.2 Hz, 2H,  $\text{CH}_2$ -Linker), 2.00 (p,  $J$  = 6.6 Hz, 2H,  $\text{CH}_2$ -Linker).

$^{13}\text{C}$  NMR (101 MHz,  $\text{D}_2\text{O}$ )  $\delta$  102.25, 79.11, 79.04, 75.73, 75.60, 74.88, 74.77, 74.08, 73.28, 73.19, 71.60, 71.42, 71.33, 69.56, 64.95, 64.61, 63.33, 62.54, 60.62, 60.42, 37.08, 27.61, 27.54.

$^{31}\text{P}$  NMR (162 MHz,  $\text{D}_2\text{O}$ )  $\delta$  0.83, 0.34.

HRMS (ESI-)  $m/z$  =  $[\text{M}]^+$  calculated for  $\text{C}_{58}\text{H}_{113}\text{NO}_{61}\text{P}_5$  1954.4459; found 1954.4484.



## 7.3 Protein conjugation

### 7.3.1 Activation with SIDEA

The lyophilized polysaccharides were dissolved in water and DMSO, followed by addition of  $\text{NEt}_3$  (5 eq) and SIDEA (12 eq). The reaction was stirred for 3 h, then transferred to a 15 mL Falcon tube, 5 mL of cold EtOAc was added and the mixture was cooled to  $0^\circ\text{C}$ . After 30 min a suspension was formed and the Falcon was further centrifuged for 10 min ( $4^\circ\text{C}$ , 4500 r/min). The solvent was taken out and the remaining suspension was again dissolved with EtOAc (5 mL) and centrifuged. The washing step was repeated for 10 times and finally the remaining solid was frozen and lyophilized.

**Table 9.** Summarized conditions for the activation using SIDEA

Oligomer	$\mu\text{mol}$	DMSO	Water
Monomer (n = 0)	3.1	180 $\mu\text{l}$	20 $\mu\text{l}$
Dimer (n = 1)	3.1	180 $\mu\text{l}$	20 $\mu\text{l}$
Trimer (n = 2)	1.9	270 $\mu\text{l}$	30 $\mu\text{l}$
Tetramer (n = 3)	1.9	270 $\mu\text{l}$	30 $\mu\text{l}$
Pentamer (n = 4)	2.1	270 $\mu\text{l}$	30 $\mu\text{l}$
Trimer * (n = 2)	2.5	270 $\mu\text{l}$	30 $\mu\text{l}$
Pentamer * (n = 4)	1.9	270 $\mu\text{l}$	30 $\mu\text{l}$

Trimer \* and Pentamer \* were used for further HSA conjugation

### 7.3.2 CRM<sub>197</sub> conjugation

The activated oligomers were conjugated to CRM<sub>197</sub> in sodium phosphate 1 M pH 7.2 at a protein concentration of 42.6 mg/mL, using a molar ratio of 75:1 saccharide to protein (Trimer, Tetramer and Pentamer) and a ratio of 50:1 (Monomer and Dimer), which were assessed by SDS page gel electrophoresis and purified by dialysis against a 10kDa MW cutoff membrane.

### 7.3.3 HSA conjugation

The activated Trimer\* and Pentamer\* were conjugated to HSA in a sodium phosphate 1 M pH 7.2 at a protein concentration of 30.0 mg/mL using a molar ratio of 75:1 saccharide to protein. The glycoconjugates were further studied by SDS Page and purified by dialysis against a 10kDa MW cutoff membrane.

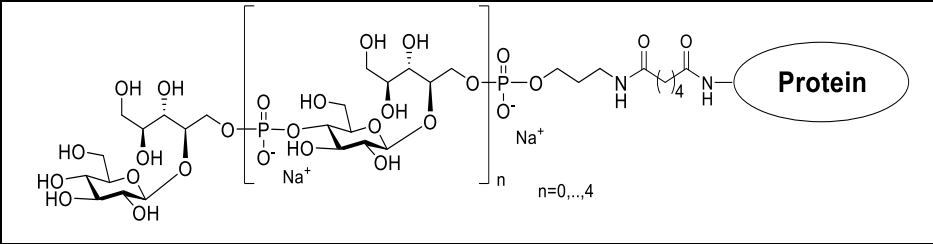
## 7.4 General methods for the characterization of Glycoconjugate

### 7.4.1 BCA

The quantification of the total protein amount was performed by micro BCA (Thermo Scientific). A 2 mg/mL solution of serum bovine albumin (BSA) was used to create a calibration curve in the range 5-20  $\mu\text{g/mL}$ . Samples with unknown protein concentration were diluted with MilliQ water in order to obtain sample protein concentration in the range of the calibration curve with a final volume of 500  $\mu\text{L}$ . The micro BCA reagent was prepared according to manufacturer instructions and 500  $\mu\text{L}$  of the prepared BCA reagent was added to each sample. The mixture was further incubated for 1 h at 60°C and the absorbance at 562 nm was measured by spectrophotometer for each sample. Within these data, the protein concentration was recalculated.

**Table 10.** Total amount of protein in all glycoconjugates analysed by BCA.

Oligomer	Total protein mg/mL
CRM <sub>197</sub> -Monomer (n = 0)	0.290
CRM <sub>197</sub> -Dimer (n = 1)	0.534
CRM <sub>197</sub> -Trimer (n = 2)	0.494
CRM <sub>197</sub> - Tetramer (n = 3)	0.532
CRM <sub>197</sub> -Pentamer (n = 4)	0.541
HSA-Trimer (n = 2)	0.902
HSA-Pentamer (n = 4)	0.685



### **7.4.2 SDS-PAGE**

Sodium Dodecyl Sulfate- Polyacrylamide gel electrophoresis (SDS-PAGE) was performed on 3-8% pre-casted polyacrylamide gel (NuPAGE®Invitrogen) using tris acetate as running buffer (NuPAGE®Invitrogen). 7 µg of protein were loaded for each sample. After electrophoretic running with a voltage of 150V for 45 min, the gel was stained with blue Coomassie.

## **8 Acknowledgement**

I spent my last three years at the University of Milan and I loved this adventure. I have super good memories when I think about Milan, Lay's Lab, all the aperitivi and my Italian friends. This thesis would have not been possible with the support and encouragement of many people.

First of all, I would like to thank Prof. Luigi Lay for his trust and confidence over the past years. Luigi is an exceptional chemist with an immense knowledge in the fields of immunology, carbohydrate chemistry and organic chemistry. I learnt so many techniques and methods from him. During the synthetic work, I often faced some challenges and he was always there for some suggestions and his door was always open. He gave me fruitful advices whenever needed and we discussed many scientific points. Furthermore, he gave me the possibility to decide on my own and I could try my own ideas. Thank you so much for everything you did. I had a perfect PhD period and I really appreciated your supervision. Thank you and Grazie!

Additionally, Laura Polito was next to Prof. Luigi Lay always around and helped out. Next to her work, she mostly took over some administrative work and I really appreciate it. Furthermore, she was always keen to publish some reviews about nanoparticles. Thanks, Laura for being there and your advices throughout my PhD period.

Thanks also to Dr. Jeroen Codee, Dr. Roberto Adamo and Dr. Maria R. Romano for your kind and valuable advices during my secondments at the Leiden University and GSK Siena. Thanks also to all the Glycovax consortium members for your guidance through the last years and your useful suggestions. Thanks to the network GLYCOVAX, I had a perfect time in our Glycovax meetings and the evenings/nights. Even if I joined your group later, you welcomed me warm and friendly as new member. Thanks also to Linda and Jacopo who helped me a lot during my secondments in Siena and Leiden. Thanks guys!

No words will describe how thankful I am about my labmates in the group of Prof. Luigi Lay. I would have not managed all the problems without you. Even if the group changed a lot in the last three years, the motivation and kindness remained the same. Our lunches and coffee breaks were always full of jokes, good food (especially from Cri), and we laughed so much! The group was not only full of chemists but also full of my friends. We organized a lot of things outside from the lab (Beach Volley, Aperitivo, Dinner, Oktoberfest, Paris, ...) and I am sure that I will miss this time a lot!

Cinzia, I learnt so many things from you. You are a perfect teacher, and every lab can be more than happy to have you! You also forced the other colleagues to speak more and more English- Thank you!!

Meni, Andrea, Riccardo, Alessandro, Musa, Guiseppe, Olimpia, Aurelio; thanks a lot for everything.

I guess with supervising not only the students can learn but also the supervisor- Davide and Marco my two bachelor students. You were both amazing and you taught me a lot. Thank you!

Ludo, I still remember the first months when I started and you were already in Milan. Thanks to you I did not feel lonely surrounded by all the Italians and the Italian language! Additionally, you always helped me out in our Glycovax meeting! Thanks and Merci!

Cri, I can not tell you how much I am thankful. I am more than happy that we became friends! You are such a strong and exceptional chemist. I think I never saw someone who is motivated to start a column on Friday at 6.00pm except of you! But you were also always smily and kind; and you helped me sooo often with some Italian stuff! Thanks for everything! Grazie!

Ruth, we were not only labmates but also flatmates and I have to say I am quite happy that you decided to come to Milan for your PhD! You are a strong woman and I am happy that we became friends! I will miss our dinners, our talks and your tasty tortilla. Thanks also for reading my thesis and giving me some super useful suggestions! I m super looking forward to you and your family in your typical dresses! Don't forget the flowers in your hair! Thanks for everything and enjoy the chemistry (or not)!

Laura P., Sofia and Laura L., it was really nice to share the Central Lab with you. Your positive mood was always catching, and I had always a good time with you. Additionally, it was nice to see how much your English improved and how much carbohydrate chemistry you learnt! Thanks for cheering me up and always making me smile!

Marco, the best Italian cook, you are just amazing. Your redwine potatoes are incredible tasty- and they can be a perfect side dish next to nothing :D Next to your qualities as a cook, your knowledge of chemistry is astonishing. I will miss our daily conversations about dry solvents; reaction progress and work-ups. You are a perfect friend and I will miss our meetings upstairs. Thanks for being such a perfect friend to me!

Valentina, you are soooo incredible strong and always in good mood! It is super nice having you around and as a friend. Thanks for your dinners, pizza, your incredible chocolate cake and being my friend!

Adrian, I know that our relationship was never straightforward! Thank you so much for making us possible, your constant support and your continuous love. Danke!

The biggest thank will go to my incredible family- my sisters and my parents. I am so happy to be part of this family. Without you, my way would have been different. You always encouraged me even when I had my own ideas and you motivated me to go on. Your constant support and your deep love made this possible! Tausend Dank.

## 9 References

- (1) Rivers, L.; Gaspar, H. B. Severe Combined Immunodeficiency: Recent Developments and Guidance on Clinical Management. *Arch. Dis. Child.* **2015**, *100* (7), 667–672. <https://doi.org/10.1136/archdischild-2014-306425>.
- (2) Warrington, R.; Watson, W.; Kim, H. L.; Antonetti, F. R. An Introduction to Immunology and Immunopathology. *Allergy Asthma. Clin. Immunol.* **2011**, *7 Suppl 1* (Suppl 1), S1–S1. <https://doi.org/10.1186/1710-1492-7-S1-S1>.
- (3) Warrington, R.; Watson, W.; Kim, H. L.; Antonetti, F. R. An Introduction to Immunology and Immunopathology. *Allergy Asthma. Clin. Immunol.* **2011**, *7 Suppl 1* (Suppl 1), S1–S1. <https://doi.org/10.1186/1710-1492-7-S1-S1>.
- (4) Cancogni, D.; Fusari, M.; Poggi, N.; Lay, L. Major Advances in the Development of Synthetic -Based Vaccines. In *Polysaccharides*; Ramawat, K. G., Mérillon, J.-M., Eds.; Springer International Publishing: Cham, 2014; pp 1–45. [https://doi.org/10.1007/978-3-319-03751-6\\_65-1](https://doi.org/10.1007/978-3-319-03751-6_65-1).
- (5) Turvey, S. E.; Broide, D. H. Innate Immunity. *J. Allergy Clin. Immunol.* **2010**, *125* (2 Suppl 2), S24–S32. <https://doi.org/10.1016/j.jaci.2009.07.016>.
- (6) Schroeder Jr, H. W.; Cavacini, L. Structure and Function of Immunoglobulins. *J. Allergy Clin. Immunol.* **2010**, *125* (2 Suppl 2), S41–S52. <https://doi.org/10.1016/j.jaci.2009.09.046>.
- (7) Chaplin, D. D. Overview of the Immune Response. *J. Allergy Clin. Immunol.* **2010**, *125* (2), S3–S23. <https://doi.org/10.1016/j.jaci.2009.12.980>.
- (8) Goins, C. L.; Chappell, C. P.; Shashidharamurthy, R.; Selvaraj, P.; Jacob, J. Immune Complex-Mediated Enhancement of Secondary Antibody Responses. *J. Immunol.* **2010**, *184* (11), 6293–6298. <https://doi.org/10.4049/jimmunol.0902530>.
- (9) Morelli, L.; Poletti, L.; Lay, L. Carbohydrates and Immunology: Synthetic Oligosaccharide Antigens for Vaccine Formulation. *European J. Org. Chem.* **2011**, *2011* (29), 5723–5777. <https://doi.org/10.1002/ejoc.201100296>.
- (10) Chaplin, D. D. Overview of the Immune Response. *J. Allergy Clin. Immunol.* **2010**, *125* (2), S3–S23. <https://doi.org/10.1016/j.jaci.2009.12.980>.

- (11) Pollard, A. J.; Perrett, K. P.; Beverley, P. C. Maintaining Protection against Invasive Bacteria with Protein–Polysaccharide Conjugate Vaccines. *Nat. Rev. Immunol.* **2009**, *9* (3), 213–220. <https://doi.org/10.1038/nri2494>.
- (12) Morelli, L.; Poletti, L.; Lay, L. Carbohydrates and Immunology: Synthetic Oligosaccharide Antigens for Vaccine Formulation. *European J. Org. Chem.* **2011**, *2011* (29), 5723–5777. <https://doi.org/10.1002/ejoc.201100296>.
- (13) Avci, F. Y.; Li, X.; Tsuji, M.; Kasper, D. L. A Mechanism for Glycoconjugate Vaccine Activation of the Adaptive Immune System and Its Implications for Vaccine Design. *Nat. Med.* **2011**, *17* (12), 1602–1609. <https://doi.org/10.1038/nm.2535>.
- (14) Avci, F. Y.; Kasper, D. L. How Bacterial Carbohydrates Influence the Adaptive Immune System. *Annu. Rev. Immunol.* **2010**, *28* (1), 107–130. <https://doi.org/10.1146/annurev-immunol-030409-101159>.
- (15) De Gregorio, E.; Rappuoli, R. From Empiricism to Rational Design: A Personal Perspective of the Evolution of Vaccine Development. *Nat. Rev. Immunol.* **2014**, *14* (7), 505–514. <https://doi.org/10.1038/nri3694>.
- (16) Klein Klouwenberg, P.; Bont, L. Neonatal and Infantile Immune Responses to Encapsulated Bacteria and Conjugate Vaccines. *Clin. Dev. Immunol.* **2008**, *2008*, 628963. <https://doi.org/10.1155/2008/628963>.
- (17) Rappuoli, R.; De Gregorio, E. A Sweet T Cell Response. *Nat. Med.* **2011**, *17* (12), 1551–1552. <https://doi.org/10.1038/nm.2587>.
- (18) Avci, F. Y.; Kasper, D. L. How Bacterial Carbohydrates Influence the Adaptive Immune System. *Annu. Rev. Immunol.* **2010**, *28* (1), 107–130. <https://doi.org/10.1146/annurev-immunol-030409-101159>.
- (19) Sun, X.; Stefanetti, G.; Berti, F.; Kasper, D. L. Polysaccharide Structure Dictates Mechanism of Adaptive Immune Response to Glycoconjugate Vaccines. *Proc. Natl. Acad. Sci.* **2019**, *116* (1), 193–198. <https://doi.org/10.1073/pnas.1816401115>.
- (20) Avci, F.; Berti, F.; Dull, P.; Hennessey, J.; Pavliak, V.; Prasad, A. K.; Vann, W.; Wacker, M.; Marcq, O. Glycoconjugates: What It Would Take To Master These Well-Known yet Little-Understood Immunogens for Vaccine Development. *mSphere* **2019**, *4* (5). <https://doi.org/10.1128/mSphere.00520-19>.

- (21) Peeters, C. C.; Evenberg, D.; Hoogerhout, P.; Käyhty, H.; Saarinen, L.; van Boeckel, C. A.; van der Marel, G. A.; van Boom, J. H.; Poolman, J. T. Synthetic Trimer and Tetramer of 3-Beta-D-Ribose-(1-1)-D-Ribitol-5-Phosphate Conjugated to Protein Induce Antibody Responses to Haemophilus Influenzae Type b Capsular Polysaccharide in Mice and Monkeys. *Infect. Immun.* **1992**, *60* (5), 1826–1833.
- (22) Baek, J. Y.; Geissner, A.; Rathwell, D. C. K.; Meierhofer, D.; Pereira, C. L.; Seeberger, P. H. A Modular Synthetic Route to Size-Defined Immunogenic Haemophilus Influenzae b Antigens Is Key to the Identification of an Octasaccharide Lead Vaccine Candidate. *Chem. Sci.* **2018**, *9* (5), 1279–1288. <https://doi.org/10.1039/C7SC04521B>.
- (23) Wessels, M. R.; Paoletti, L. C.; Guttormsen, H. K.; Michon, F.; D’Ambra, A. J.; Kasper, D. L. Structural Properties of Group B Streptococcal Type III Polysaccharide Conjugate Vaccines That Influence Immunogenicity and Efficacy. *Infect. Immun.* **1998**, *66* (5), 2186–2192.
- (24) Costantino, P.; Rappuoli, R.; Berti, F. The Design of Semi-Synthetic and Synthetic Glycoconjugate Vaccines. *Expert Opin. Drug Discov.* **2011**, *6* (10), 1045–1066. <https://doi.org/10.1517/17460441.2011.609554>.
- (25) Bröker, M.; Berti, F.; Costantino, P. Factors Contributing to the Immunogenicity of Meningococcal Conjugate Vaccines. *Hum. Vaccin. Immunother.* **2016**, *12* (7), 1808–1824. <https://doi.org/10.1080/21645515.2016.1153206>.
- (26) Rappuoli, R.; Pizza, M.; Del Giudice, G.; De Gregorio, E. Vaccines, New Opportunities for a New Society. *Proc. Natl. Acad. Sci.* **2014**, *111* (34), 12288–12293. <https://doi.org/10.1073/pnas.1402981111>.
- (27) The Human Mechanism, Its Physiology and Hygiene and the Sanitation of Its Surroundings. *Nature* **1907**, *75* (1944), 318–319. <https://doi.org/10.1038/075318b0>.
- (28) Belongia, E. A.; Naleway, A. L. Smallpox Vaccine: The Good, the Bad, and the Ugly. *Clin. Med. Res.* **2003**, *1* (2), 87–92. <https://doi.org/10.3121/cm.1.2.87>.
- (29) Robbins, J. B.; Schneerson, R. Polysaccharide-Protein Conjugates: A New Generation of Vaccines. *J. Infect. Dis.* **1990**, *161* (5), 821–832. <https://doi.org/10.1093/infdis/161.5.821>.



- (30) Macleod, C. M.; Hodges, R. G.; Heidelberger, M.; Bernhard, W. G. PREVENTION OF PNEUMOCOCCAL PNEUMONIA BY IMMUNIZATION WITH SPECIFIC CAPSULAR POLYSACCHARIDES. *J. Exp. Med.* **1945**, 82 (6), 445–465.
- (31) Mettu, R.; Chen, C.-Y.; Wu, C.-Y. Synthetic Carbohydrate-Based Vaccines: Challenges and Opportunities. *J. Biomed. Sci.* **2020**, 27 (1), 9. <https://doi.org/10.1186/s12929-019-0591-0>.
- (32) Micoli, F.; Adamo, R.; Costantino, P. Protein Carriers for Glycoconjugate Vaccines: History, Selection Criteria, Characterization and New Trends. *Molecules* **2018**, 23 (6), 1451. <https://doi.org/10.3390/molecules23061451>.
- (33) Micoli, F.; Del Bino, L.; Alfini, R.; Carboni, F.; Romano, M. R.; Adamo, R. Glycoconjugate Vaccines: Current Approaches towards Faster Vaccine Design. *Expert Rev. Vaccines* **2019**, 18 (9), 881–895. <https://doi.org/10.1080/14760584.2019.1657012>.
- (34) Costantino, P.; Rappuoli, R.; Berti, F. The Design of Semi-Synthetic and Synthetic Glycoconjugate Vaccines. *Expert Opin. Drug Discov.* **2011**, 6 (10), 1045–1066. <https://doi.org/10.1517/17460441.2011.609554>.
- (35) Kay, E.; Cuccui, J.; Wren, B. W. Recent Advances in the Production of Recombinant Glycoconjugate Vaccines. *npj Vaccines* **2019**, 4 (1), 16. <https://doi.org/10.1038/s41541-019-0110-z>.
- (36) Micoli, F.; Del Bino, L.; Alfini, R.; Carboni, F.; Romano, M. R.; Adamo, R. Glycoconjugate Vaccines: Current Approaches towards Faster Vaccine Design. *Expert Rev. Vaccines* **2019**, 18 (9), 881–895. <https://doi.org/10.1080/14760584.2019.1657012>.
- (37) Huang, X.; Huang, L.; Wang, H.; Ye, X.-S. Iterative One-Pot Synthesis of Oligosaccharides. *Angew. Chemie Int. Ed.* **2004**, 43 (39), 5221–5224. <https://doi.org/10.1002/anie.200460176>.
- (38) Pistorio, S. G.; Nigudkar, S. S.; Stine, K. J.; Demchenko, A. V. HPLC-Assisted Automated Oligosaccharide Synthesis: Implementation of the Autosampler as a Mode of the Reagent Delivery. *J. Org. Chem.* **2016**, 81 (19), 8796–8805. <https://doi.org/10.1021/acs.joc.6b01439>.

- (39) Panza, M.; Pistorio, S. G.; Stine, K. J.; Demchenko, A. V. Automated Chemical Oligosaccharide Synthesis: Novel Approach to Traditional Challenges. *Chem. Rev.* **2018**, *118* (17), 8105–8150. <https://doi.org/10.1021/acs.chemrev.8b00051>.
- (40) Plante, O. J.; Palmacci, E. R.; Seeberger, P. H. Automated Solid-Phase Synthesis of Oligosaccharides. *Science* (80-. ). **2001**, *291* (5508), 1523–1527. <https://doi.org/10.1126/science.1057324>.
- (41) Gao, Q.; Tontini, M.; Brogioni, G.; Nilo, A.; Filippini, S.; Harfouche, C.; Polito, L.; Romano, M. R.; Costantino, P.; Berti, F.; Adamo, R.; Lay, L. Immunoactivity of Protein Conjugates of Carba Analogues from *Neisseria Meningitidis* A Capsular Polysaccharide. *ACS Chem. Biol.* **2013**, *8* (11), 2561–2567. <https://doi.org/10.1021/cb400463u>.
- (42) Verez-Bencomo, V.; Fernández-Santana, V.; Hardy, E.; Toledo, M. E.; Rodriguez, M. C.; Heynngnezz, L.; Rodriguez, A.; Baly, A.; Herrera, L.; Izquierdo, M.; Villar, A.; Valdés, Y.; Cosme, K.; Deler, M. L.; Montane, M.; Garcia, E.; Ramos, A.; Aguilar, A.; Medina, E.; Toraño, G.; Sosa, I.; Hernandez, I.; Martinez, R.; Muzachio, A.; Carmenates, A.; Costa, L.; Cardoso, F.; Campa, C.; Diaz, M.; Roy, R. A Synthetic Conjugate Polysaccharide Vaccine Against *Haemophilus Influenzae* Type B. *Science* (80-. ). **2004**, *305* (5683), 522–525. <https://doi.org/10.1126/science.1095209>.
- (43) Nascimento, I. P.; Leite, L. C. C. Recombinant Vaccines and the Development of New Vaccine Strategies. *Brazilian J. Med. Biol. Res. = Rev. Bras. Pesqui. medicas e Biol.* **2012**, *45* (12), 1102–1111. <https://doi.org/10.1590/s0100-879x2012007500142>.
- (44) Rappuoli, R. Reverse Vaccinology. *Curr. Opin. Microbiol.* **2000**, *3* (5), 445–450. [https://doi.org/https://doi.org/10.1016/S1369-5274\(00\)00119-3](https://doi.org/https://doi.org/10.1016/S1369-5274(00)00119-3).
- (45) Rappuoli, R.; Bottomley, M. J.; D’Oro, U.; Finco, O.; De Gregorio, E. Reverse Vaccinology 2.0: Human Immunology Instructs Vaccine Antigen Design. *J. Exp. Med.* **2016**, *213* (4), 469–481. <https://doi.org/10.1084/jem.20151960>.
- (46) Andreano, E.; D’Oro, U.; Rappuoli, R.; Finco, O. Vaccine Evolution and Its Application to Fight Modern Threats. *Front. Immunol.* **2019**, *10*, 1722. <https://doi.org/10.3389/fimmu.2019.01722>.

- (47) Andreano, E.; D'Oro, U.; Rappuoli, R.; Finco, O. Vaccine Evolution and Its Application to Fight Modern Threats. *Front. Immunol.* **2019**, *10*, 1722. <https://doi.org/10.3389/fimmu.2019.01722>.
- (48) Slack, M. P. E. 31 - Haemophilus: Respiratory Infections; Meningitis; Chancroid. In *Medical Microbiology*; Greenwood, D., Barer, M., Slack, R., Irving, W. B. T.-M. M. (Eighteenth E., Eds.; Churchill Livingstone: Edinburgh, 2012; pp 324–330. <https://doi.org/https://doi.org/10.1016/B978-0-7020-4089-4.00046-9>.
- (49) High, N. J.; Fan, F.; Schwartzman, J. D. Chapter 97 - Haemophilus Influenzae; Tang, Y.-W., Sussman, M., Liu, D., Poxton, I., Schwartzman, J. B. T.-M. M. M. (Second E., Eds.; Academic Press: Boston, 2015; pp 1709–1728. <https://doi.org/https://doi.org/10.1016/B978-0-12-397169-2.00097-4>.
- (50) King, P. Haemophilus Influenzae and the Lung. *Clin. Transl. Med.* **2012**, *1* (1), 10. <https://doi.org/10.1186/2001-1326-1-10>.
- (51) Stephens, D. S.; Farley, M. M. Pathogenic Events During Infection of the Human Nasopharynx with Neisseria Meningitidis and Haemophilus Influenzae. *Rev. Infect. Dis.* **1990**, *13* (1), 22–33. <https://doi.org/10.1093/clinids/13.1.22>.
- (52) King, P. Haemophilus Influenzae and the Lung. *Clin. Transl. Med.* **2012**, *1* (1), 10. <https://doi.org/10.1186/2001-1326-1-10>.
- (53) Kostyanev, T. S.; Sechanova, L. P. Virulence Factors and Mechanisms of Antibiotic Resistance of Haemophilus Influenzae. *Folia Med. (Plovdiv)*. **2012**, *54* (1), 19–23.
- (54) Taylor, C. M.; Roberts, I. S. Capsular Polysaccharides and Their Role in Virulence. In *Contributions to Microbiology*; 2005; Vol. 12, pp 55–66. <https://doi.org/10.1159/000081689>.
- (55) Rubach, M. P.; Bender, J. M.; Mottice, S.; Hanson, K.; Weng, H. Y. C.; Korgenski, K.; Daly, J. A.; Pavia, A. T. Increasing Incidence of Invasive Haemophilus Influenzae Disease in Adults, Utah, USA. *Emerg. Infect. Dis.* **2011**, *17* (9), 1645–1650. <https://doi.org/10.3201/eid1709.101991>.
- (56) Murphy, T. F.; Faden, H.; Bakaletz, L. O.; Kyd, J. M.; Forsgren, A.; Campos, J.; Virji, M.; Pelton, S. I. Nontypeable Haemophilus Influenzae as a Pathogen in Children. *Pediatr. Infect. Dis. J.* **2009**, *28* (1), 43–48.

- (57) Watt, J. P.; Levine, O. S.; Santosham, M. Global Reduction of Hib Disease: What Are the next Steps? Proceedings of the Meeting: Scottsdale, Arizona, September 22-25, 2002. *J. Pediatr.* **2003**, *143* (6), 163–187. [https://doi.org/10.1067/S0022-3476\(03\)00576-6](https://doi.org/10.1067/S0022-3476(03)00576-6).
- (58) Peltola, H. Worldwide Haemophilus Influenzae Type b Disease at the Beginning of the 21st Century: Global Analysis of the Disease Burden 25 Years after the Use of the Polysaccharide Vaccine and a Decade after the Advent of Conjugates. *Clin. Microbiol. Rev.* **2000**, *13* (2), 302–317. <https://doi.org/10.1128/cmr.13.2.302-317.2000>.
- (59) Whittaker, R.; Economopoulou, A.; Dias, J. G.; Bancroft, E.; Ramliden, M.; Celentano, L. P.; Disease, E. C. for D. P. and C. C. E. for I. H. influenzae. Epidemiology of Invasive Haemophilus Influenzae Disease, Europe, 2007-2014. *Emerg. Infect. Dis.* **2017**, *23* (3), 396–404. <https://doi.org/10.3201/eid2303.161552>.
- (60) Nizet, V.; Colina, K. F.; Almquist, J. R.; Rubens, C. E.; Smith, A. L. A Virulent Nonencapsulated Haemophilus Influenzae. *J. Infect. Dis.* **1996**, *173* (1), 180–186. <https://doi.org/10.1093/infdis/173.1.180>.
- (61) García-Cobos, S.; Campos, J.; Lázaro, E.; Román, F.; Cercenado, E.; García-Rey, C.; Pérez-Vázquez, M.; Oteo, J.; de Abajo, F. Ampicillin-Resistant Non-Beta-Lactamase-Producing Haemophilus Influenzae in Spain: Recent Emergence of Clonal Isolates with Increased Resistance to Cefotaxime and Cefixime. *Antimicrob. Agents Chemother.* **2007**, *51* (7), 2564–2573. <https://doi.org/10.1128/AAC.00354-07>.
- (62) Hasegawa, K.; Kobayashi, R.; Takada, E.; Ono, A.; Chiba, N.; Morozumi, M.; Iwata, S.; Sunakawa, K.; Ubukata, K.; Meningitis, on behalf of the W. G. of the N. S. for B. High Prevalence of Type b  $\beta$ -Lactamase-Non-Producing Ampicillin-Resistant Haemophilus Influenzae in Meningitis: The Situation in Japan Where Hib Vaccine Has Not Been Introduced. *J. Antimicrob. Chemother.* **2006**, *57* (6), 1077–1082. <https://doi.org/10.1093/jac/dkl142>.
- (63) King, P. T.; Sharma, R. The Lung Immune Response to Nontypeable Haemophilus Influenzae. *J. Immunol. Res.* **2015**, *2015*, 706376. <https://doi.org/10.1155/2015/706376>.
- (64) Behrouzi, A.; Vaziri, F.; Rahimi-Jamnani, F.; Afrough, P.; Rahbar, M.; Satarian, F.; Siadat, S. D. Vaccine Candidates against Nontypeable Haemophilus Influenzae: A

- Review. *Iran. Biomed. J.* **2017**, *21* (2), 69–76.  
<https://doi.org/10.18869/acadpub.ibj.21.2.69>.
- (65) Jin, Z.; Romero-steiner, S.; Carlone, G. M.; Robbins, J. B.; Schneerson, R. Minireview Haemophilus Influenzae Type a Infection and Its Prevention □. *Infect Immun* **2007**, *75* (6), 2650–2654. <https://doi.org/10.1128/IAI.01774-06>.
- (66) Egan, W.; Fai-Po, T.; Climenson, P. A.; Schneerson, R. Structural and Immunological Studies of the Haemophilus Influenzae Type c Capsular Polysaccharide. *Carbohydr. Res.* **1980**, *80* (2), 305–316. [https://doi.org/https://doi.org/10.1016/S0008-6215\(00\)84869-7](https://doi.org/https://doi.org/10.1016/S0008-6215(00)84869-7).
- (67) Zwahlen, A.; Kroll, J. S.; Rubin, L. G.; Moxon, E. R. The Molecular Basis of Pathogenicity in Haemophilus Influenzae: Comparative Virulence of Genetically-Related Capsular Transformants and Correlation with Changes at the Capsulation Locus Cap. *Microb. Pathog.* **1989**, *7* (3), 225–235.  
[https://doi.org/https://doi.org/10.1016/0882-4010\(89\)90058-2](https://doi.org/https://doi.org/10.1016/0882-4010(89)90058-2).
- (68) WHO | Haemophilus Influenzae Type b (Hib). *WHO* **2014**.
- (69) Bruce, M. G.; Deeks, S. L.; Zulz, T.; Navarro, C.; Palacios, C.; Case, C.; Hemsley, C.; Hennessy, T.; Corriveau, A.; Larke, B.; Sobel, I.; Lovgren, M.; Debyle, C.; Tsang, R.; Parkinson, A. J. Epidemiology of Haemophilus Influenzae Serotype a, North American Arctic, 2000-2005. *Emerg. Infect. Dis.* **2008**, *14* (1), 48–55.  
<https://doi.org/10.3201/eid1401.070822>.
- (70) Ulanova, M.; Tsang, R. S. W. Invasive Haemophilus Influenzae Disease: Changing Epidemiology and Host–Parasite Interactions in the 21st Century. *Infect. Genet. Evol.* **2009**, *9* (4), 594–605. <https://doi.org/https://doi.org/10.1016/j.meegid.2009.03.001>.
- (71) Pittman, M. Variation and Type Specificity in the Bacterial Species Haemophilus Influenzae. *J. Exp. Med.* **1931**, *53* (4), 471–492. <https://doi.org/10.1084/jem.53.4.471>.
- (72) Sutton, A.; Schneerson, R.; Kendall-Morris, S.; Robbins, J. B. Differential Complement Resistance Mediates Virulence of Haemophilus Influenzae Type B. *Infect. Immun.* **1982**, *35* (1), 95–104.
- (73) Ladhani, S.; Slack, M. P. E.; Heath, P. T.; Gottberg, A. von; Chandra, M.; Ramsay, M. E. Invasive Haemophilus Influenzae Disease, Europe, 1996–2006. *Emerg. Infect. Dis.*

- J.* **2010**, *16* (3), 455. <https://doi.org/10.3201/eid1603.090290>.
- (74) Millar, E. V.; O'Brien, K. L.; Watt, J. P.; Lingappa, J.; Pallipamu, R.; Rosenstein, N.; Hu, D.; Reid, R.; Santosham, M. Epidemiology of Invasive Haemophilus Influenzae Type A Disease among Navajo and White Mountain Apache Children, 1988–2003. *Clin. Infect. Dis.* **2005**, *40* (6), 823–830. <https://doi.org/10.1086/428047>.
- (75) Hammitt, L. L.; Block, S.; Hennessy, T. W.; DeByle, C.; Peters, H.; Parkinson, A.; Singleton, R.; Butler, J. C. Outbreak of Invasive Haemophilus Influenzae Serotype a Disease. *Pediatr. Infect. Dis. J.* **2005**, *24* (5).
- (76) van den Biggelaar, A. H. J.; Pomat, W. S. Immunization of Newborns with Bacterial Conjugate Vaccines. *Vaccine* **2013**, *31* (21), 2525–2530. <https://doi.org/https://doi.org/10.1016/j.vaccine.2012.06.019>.
- (77) Wang, S.; Tafalla, M.; Hanssens, L.; Dolhain, J. A Review of Haemophilus Influenzae Disease in Europe from 2000–2014: Challenges, Successes and the Contribution of Hexavalent Combination Vaccines. *Expert Rev. Vaccines* **2017**, *16* (11), 1095–1105. <https://doi.org/10.1080/14760584.2017.1383157>.
- (78) Wang, S.; Tafalla, M.; Hanssens, L.; Dolhain, J. A Review of Haemophilus Influenzae Disease in Europe from 2000–2014: Challenges, Successes and the Contribution of Hexavalent Combination Vaccines. *Expert Rev. Vaccines* **2017**, *16* (11), 1095–1105. <https://doi.org/10.1080/14760584.2017.1383157>.
- (79) Singleton, R.; Hammitt, L.; Hennessy, T.; Bulkow, L.; DeByle, C.; Parkinson, A.; Cottle, T. E.; Peters, H.; Butler, J. C. The Alaska Haemophilus Influenzae Type b Experience: Lessons in Controlling a Vaccine-Preventable Disease. *Pediatrics* **2006**, *118* (2), e421--e429. <https://doi.org/10.1542/peds.2006-0287>.
- (80) Bärnighausen, T.; Bloom, D. E.; Canning, D.; Friedman, A.; Levine, O. S.; O'Brien, J.; Privor-Dumm, L.; Walker, D. Rethinking the Benefits and Costs of Childhood Vaccination: The Example of the Haemophilus Influenzae Type b Vaccine. *Vaccine* **2011**, *29* (13), 2371–2380. <https://doi.org/https://doi.org/10.1016/j.vaccine.2010.11.090>.
- (81) Vella, M.; Pace, D. Glycoconjugate Vaccines: An Update. *Expert Opin. Biol. Ther.* **2015**, *15* (4), 529–546. <https://doi.org/10.1517/14712598.2015.993375>.

- (82) Tsang, R. S. W.; Ulanova, M. The Changing Epidemiology of Invasive Haemophilus Influenzae Disease: Emergence and Global Presence of Serotype a Strains That May Require a New Vaccine for Control. *Vaccine* **2017**, *35* (33), 4270–4275. <https://doi.org/https://doi.org/10.1016/j.vaccine.2017.06.001>.
- (83) Ulanova, M.; Tsang, R. S. W. Haemophilus Influenzae Serotype a as a Cause of Serious Invasive Infections. *Lancet Infect. Dis.* **2014**, *14* (1), 70–82. [https://doi.org/10.1016/S1473-3099\(13\)70170-1](https://doi.org/10.1016/S1473-3099(13)70170-1).
- (84) Ulanova, M.; Tsang, R. S. W. Haemophilus Influenzae Serotype a as a Cause of Serious Invasive Infections. *Lancet Infect. Dis.* **2014**, *14* (1), 70–82. [https://doi.org/10.1016/S1473-3099\(13\)70170-1](https://doi.org/10.1016/S1473-3099(13)70170-1).
- (85) Cox, A. D.; Williams, D.; Cairns, C.; St. Michael, F.; Fleming, P.; Vinogradov, E.; Arbour, M.; Masson, L.; Zou, W. Investigating the Candidacy of a Capsular Polysaccharide-Based Glycoconjugate as a Vaccine to Combat Haemophilus Influenzae Type a Disease: A Solution for an Unmet Public Health Need. *Vaccine* **2017**, *35* (45), 6129–6136. <https://doi.org/https://doi.org/10.1016/j.vaccine.2017.09.055>.
- (86) Cox, A. D.; Barreto, L.; Ulanova, M.; Bruce, M. G.; Tsang, R.; contributors, C. Developing a Vaccine for Haemophilus Influenzae Serotype a: Proceedings of a Workshop. *Can. Commun. Dis. Rep.* **2017**, *43* (5), 89–95. <https://doi.org/10.14745/ccdr.v43i05a02>.
- (87) Gruber, W. C.; Scott, D. A.; Emini, E. A. Development and Clinical Evaluation of Prevnar 13, a 13-Valent Pneumococcal CRM197 Conjugate Vaccine. *Ann. N. Y. Acad. Sci.* **2012**, *1263* (1), 15–26. <https://doi.org/10.1111/j.1749-6632.2012.06673.x>.
- (88) Branefors-Helander, P.; Erbing, C.; Kenne, L.; Lindberg, B. The Structure of the Capsular Antigen from Haemophilus Influenzae Type A. *Carbohydr. Res.* **1977**, *56* (1), 117–122. [https://doi.org/https://doi.org/10.1016/S0008-6215\(00\)84242-1](https://doi.org/https://doi.org/10.1016/S0008-6215(00)84242-1).
- (89) Grzeszczyk, B.; Banaszek, A.; Zamojski, A. The Synthesis of Two Repeating Units of Haemophilus Influenzae Type a Capsular Antigen. *Carbohydr. Res.* **1988**, *175* (2), 215–226. [https://doi.org/https://doi.org/10.1016/0008-6215\(88\)84144-2](https://doi.org/https://doi.org/10.1016/0008-6215(88)84144-2).

- (90) Joseph, A. A.; Verma, V. P.; Liu, X.-Y.; Wu, C.-H.; Dhurandhare, V. M.; Wang, C.-C. TMSOTf-Catalyzed Silylation: Streamlined Regioselective One-Pot Protection and Acetylation of Carbohydrates. *European J. Org. Chem.* **2012**, 2012 (4), 744–753. <https://doi.org/10.1002/ejoc.201101267>.
- (91) Français, A.; Urban, D.; Beau, J. Tandem Catalysis for a One-Pot Regioselective Protection of Carbohydrates : The Example of Glucose \*\*. *Angew. Chem. Int. Ed.* **2007**, 46 (45), 8662–8665.
- (92) Bourdreux, Y.; Lemétais, A.; Urban, D.; Beau, J.-M. Iron(III) Chloride-Tandem Catalysis for a One-Pot Regioselective Protection of Glycopyranosides. *Chem. Commun.* **2011**, 47 (7), 2146–2148.
- (93) Gouasmat, A.; Lemétais, A.; Solles, J.; Bourdreux, Y.; Beau, J.-M. Catalytic Iron(III) Chloride Mediated Site-Selective Protection of Mono- and Disaccharides and One Trisaccharide. *European J. Org. Chem.* **2017**, 2017 (23), 3355–3361. <https://doi.org/10.1002/ejoc.201700538>.
- (94) Pichavant, L.; Guillermain, C.; Duchiron, S.; Coqueret, X. Compared Reactivity of Allyl Ribosides in UV-Initiated Free Radical Copolymerization with Acceptor Monomers. *Biomacromolecules* **2009**, 10 (2), 400–407. <https://doi.org/10.1021/bm8011677>.
- (95) Motoyama, K.; Mitsuyasu, R.; Akao, C.; Tanaka, T.; Ohyama, A.; Sato, N.; Higashi, T.; Arima, H. Design and Evaluation of Thioalkylated Mannose-Modified Dendrimer (G3)/ $\alpha$ -Cyclodextrin Conjugates as Antigen-Presenting Cell-Selective siRNA Carriers. *AAPS J.* **2014**, 16 (6), 1298–1308. <https://doi.org/10.1208/s12248-014-9665-9>.
- (96) Oltvoort, J. J.; Van Boeckel, C. A. A.; De Koning, J. H.; Van Boom, J. H. Use of the Cationic Iridium Complex 1,5-Cyclooctadiene-Bis[Methyldiphenylphosphine]-Iridium Hexafluorophosphate in Carbohydrate Chemistry: Smooth Isomerization of Allyl Ethers to 1-Propenyl Ethers. *Synthesis (Stuttg.)* **1981**, 1981 (04), 305–308. <https://doi.org/10.1055/s-1981-29429>.
- (97) Gigg (née Cunningham), J.; Gigg, R. The Allyl Ether as a Protecting Group in Carbohydrate Chemistry. *J. Chem. Soc. C* **1966**, No. 0, 82–86. <https://doi.org/10.1039/J39660000082>.



- (98) Guo, J.; Ye, X. Protecting Groups in Carbohydrate Chemistry: Influence on Stereoselectivity of Glycosylations. *Molecules* **2010**, *15* (10), 7235–7265. <https://doi.org/10.3390/molecules15107235>.
- (99) Mydock, L. K.; Demchenko, A. V. Mechanism of Chemical O-Glycosylation: From Early Studies to Recent Discoveries. *Org. Biomol. Chem.* **2010**, *8* (3), 497–510. <https://doi.org/10.1039/B916088D>.
- (100) Ranade, S. C.; Demchenko, A. V. Mechanism of Chemical Glycosylation: Focus on the Mode of Activation and Departure of Anomeric Leaving Groups. *J. Carbohydr. Chem.* **2013**, *32* (1), 1–43. <https://doi.org/10.1080/07328303.2012.749264>.
- (101) Codée, J. D. C.; Litjens, R. E. J. N.; van den Bos, L. J.; Overkleeft, H. S.; van der Marel, G. A. Thioglycosides in Sequential Glycosylation Strategies. *Chem. Soc. Rev.* **2005**, *34* (9), 769–782. <https://doi.org/10.1039/B417138C>.
- (102) Crich, D.; Smith, M. 1-Benzenesulfinyl Piperidine/Trifluoromethanesulfonic Anhydride: A Potent Combination of Shelf-Stable Reagents for the Low-Temperature Conversion of Thioglycosides to Glycosyl Triflates and for the Formation of Diverse Glycosidic Linkages. *J. Am. Chem. Soc.* **2001**, *123* (37), 9015–9020. <https://doi.org/10.1021/ja0111481>.
- (103) Ranade, S. C.; Demchenko, A. V. Mechanism of Chemical Glycosylation: Focus on the Mode of Activation and Departure of Anomeric Leaving Groups. *J. Carbohydr. Chem.* **2013**, *32* (1), 1–43. <https://doi.org/10.1080/07328303.2012.749264>.
- (104) Lian, G.; Zhang, X.; Yu, B. Thioglycosides in Carbohydrate Research. *Carbohydr. Res.* **2015**, *403*, 13–22. <https://doi.org/https://doi.org/10.1016/j.carres.2014.06.009>.
- (105) Codée, J. D. C.; Litjens, R. E. J. N.; den Heeten, R.; Overkleeft, H. S.; van Boom, J. H.; van der Marel, G. A. Ph<sub>2</sub>SO/Tf<sub>2</sub>O: A Powerful Promotor System in Chemoselective Glycosylations Using Thioglycosides. *Org. Lett.* **2003**, *5* (9), 1519–1522. <https://doi.org/10.1021/ol034312t>.
- (106) Yu, B.; Tao, H. Glycosyl Trifluoroacetimidates. Part 1: Preparation and Application as New Glycosyl Donors. *Tetrahedron Lett.* **2001**, *42* (12), 2405–2407. [https://doi.org/https://doi.org/10.1016/S0040-4039\(01\)00157-5](https://doi.org/https://doi.org/10.1016/S0040-4039(01)00157-5).

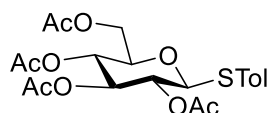
- (107) Das, R.; Mukhopadhyay, B. Chemical O-Glycosylations: An Overview. *ChemistryOpen* **2016**, *5* (5), 401–433. <https://doi.org/doi:10.1002/open.201600043>.
- (108) Fürstner, A.; Konetzki, I. A Practical Synthesis of  $\beta$ -d-Mannopyranosides. *Tetrahedron Lett.* **1998**, *39* (32), 5721–5724. [https://doi.org/https://doi.org/10.1016/S0040-4039\(98\)01163-0](https://doi.org/https://doi.org/10.1016/S0040-4039(98)01163-0).
- (109) Sun, J.; Han, X.; Yu, B. First Total Synthesis of Caminoside A, an Antimicrobial Glycolipid from Sponge. *Synlett* **2005**, *2005* (03), 437–440. <https://doi.org/10.1055/s-2004-837221>.
- (110) Feng, Z.-L.; Wu, S.-P.; Li, W.-H.; Guo, T.-T.; Liu, Q.-C. Concise Synthesis and Antidiabetic Effect of Three Natural Triterpenoid Saponins Isolated from *Fadogia Ancylyantha* (Makoni Tea). *Helv. Chim. Acta* **2015**, *98* (9), 1254–1266. <https://doi.org/10.1002/hlca.201500061>.
- (111) Richichi, B.; Luzzatto, L.; Notaro, R.; Marca, G. la; Nativi, C. Synthesis of the Essential Core of the Human Glycosylphosphatidylinositol (GPI) Anchor. *Bioorg. Chem.* **2011**, *39* (2), 88–93. <https://doi.org/https://doi.org/10.1016/j.bioorg.2010.12.002>.
- (112) Nikolaev, A. V; Botvinko, I. V; Ross, A. J. Natural Phosphoglycans Containing Glycosyl Phosphate Units: Structural Diversity and Chemical Synthesis. *Carbohydr. Res.* 2007, pp 297–344. <https://doi.org/10.1016/j.carres.2006.10.006>.
- (113) Westerduin, P.; Veeneman, G. H.; van der Marel, G. A.; van Boom, J. H. Synthesis of the Fragment GlcNAc- $\alpha$ (1 $\rightarrow$ p $\rightarrow$ 6)-GlcNAc of the Cell Wall Polymer of *Staphylococcus Lactis* Having Repeating N-Acetyl-D-Glucosamine Phosphate Units. *Tetrahedron Lett.* **1986**, *27* (51), 6271–6274. [https://doi.org/https://doi.org/10.1016/S0040-4039\(00\)85450-7](https://doi.org/https://doi.org/10.1016/S0040-4039(00)85450-7).
- (114) Beaucage, S. L.; Caruthers, M. H. Deoxynucleoside Phosphoramidites—A New Class of Key Intermediates for Deoxypolynucleotide Synthesis. *Tetrahedron Lett.* **1981**, *22* (20), 1859–1862. [https://doi.org/https://doi.org/10.1016/S0040-4039\(01\)90461-7](https://doi.org/https://doi.org/10.1016/S0040-4039(01)90461-7).
- (115) Kondo, H.; Ichikawa, Y.; Wong, C. H. SS-Sialyl Phosphite and Phosphoramidite: Synthesis and Application to the Chemoenzymic Synthesis of CMP-Sialic Acid and Sialyl Oligosaccharides. *J. Am. Chem. Soc.* **1992**, *114* (22), 8748–8750.

<https://doi.org/10.1021/ja00048a085>.

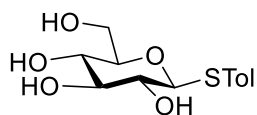
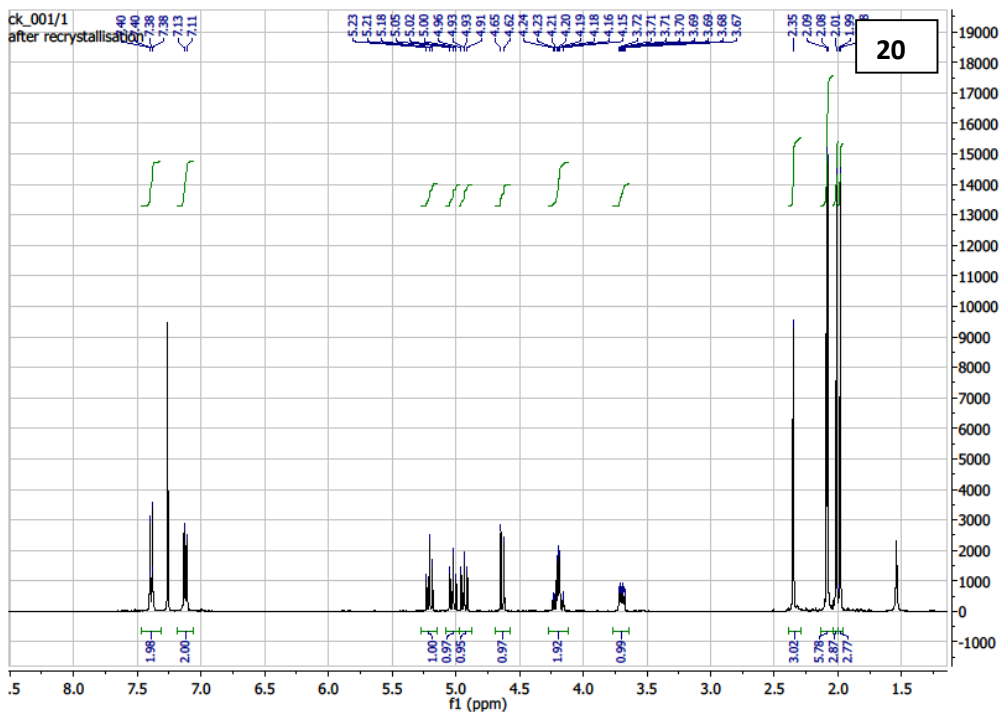
- (116) Lashkari, D. A.; Hunicke-Smith, S. P.; Norgren, R. M.; Davis, R. W.; Brennan, T. An Automated Multiplex Oligonucleotide Synthesizer: Development of High-Throughput, Low-Cost DNA Synthesis. *Proc. Natl. Acad. Sci. U. S. A.* **1995**, *92* (17), 7912–7915. <https://doi.org/10.1073/pnas.92.17.7912>.
- (117) Welz, R.; Müller, S. 5-(Benzylmercapto)-1H-Tetrazole as Activator for 2'-O-TBDMS Phosphoramidite Building Blocks in RNA Synthesis. *Tetrahedron Lett.* **2002**, *43* (5), 795–797. [https://doi.org/10.1016/S0040-4039\(01\)02274-2](https://doi.org/10.1016/S0040-4039(01)02274-2).
- (118) Vargeese, C.; Carter, J.; Yegge, J.; Krivjansky, S.; Settle, A.; Kropp, E.; Peterson, K.; Pieken, W. Efficient Activation of Nucleoside Phosphoramidites with 4,5-Dicyanoimidazole during Oligonucleotide Synthesis. *Nucleic Acids Res.* **1998**, *26* (4), 1046–1050. <https://doi.org/10.1093/nar/26.4.1046>.
- (119) Russell, M. A.; Laws, A. P.; Atherton, J. H.; Page, M. I. The Mechanism of the Phosphoramidite Synthesis of Polynucleotides. *Org. Biomol. Chem.* **2008**, *6* (18), 3270–3275. <https://doi.org/10.1039/B808999J>.
- (120) Kataoka, M.; Hattori, A.; Okino, S.; Hyodo, M.; Asano, M.; Kawai, R.; Hayakawa, Y. Ethyl(Methyl)Dioxirane as an Efficient Reagent for the Oxidation of Nucleoside Phosphites into Phosphates under Nonbasic Anhydrous Conditions. *Org. Lett.* **2001**, *3* (6), 815–818. <https://doi.org/10.1021/ol000364w>.
- (121) Micoli, F.; Adamo, R.; Costantino, P. Protein Carriers for Glycoconjugate Vaccines: History, Selection Criteria, Characterization and New Trends. *Molecules* **2018**, *23* (6), 1451. <https://doi.org/10.3390/molecules23061451>.
- (122) Giannini, G.; Rappuoli, R.; Ratti, G. The Amino-Acid Sequence of Two Non-Toxic Mutants of Diphtheria Toxin: CRM45 and CRM197. *Nucleic Acids Res.* **1984**, *12* (10), 4063–4069. <https://doi.org/10.1093/nar/12.10.4063>.
- (123) Smith, P. K.; Krohn, R. I.; Hermanson, G. T.; Mallia, A. K.; Gartner, F. H.; Provenzano, M. D.; Fujimoto, E. K.; Goetze, N. M.; Olson, B. J.; Klenk, D. C. Measurement of Protein Using Bicinchoninic Acid. *Anal. Biochem.* **1985**, *150* (1), 76–85. [https://doi.org/10.1016/0003-2697\(85\)90442-7](https://doi.org/10.1016/0003-2697(85)90442-7).

- (124) Walker, J. M. The Bicinchoninic Acid (BCA) Assay for Protein Quantitation. *Methods Mol. Biol.* **1994**, 32, 5–8. <https://doi.org/10.1385/0-89603-268-X:5>.
- (125) Mukhopadhyay, B.; Kartha, K. P. R.; Russell, D. A.; Field, R. A. Streamlined Synthesis of Per-O-Acetylated Sugars, Glycosyl Iodides, or Thioglycosides from Unprotected Reducing Sugars1. *J. Org. Chem.* **2004**, 69 (22), 7758–7760. <https://doi.org/10.1021/jo048890e>.
- (126) Weng, S.-S.; Lin, Y.-D.; Chen, C.-T. Highly Diastereoselective Thioglycosylation of Functionalized Peracetylated Glycosides Catalyzed by MoO<sub>2</sub>Cl<sub>2</sub>. *Org. Lett.* **2006**, 8 (24), 5633–5636. <https://doi.org/10.1021/ol062375g>.
- (127) Wang, C.; Kulkarni, S. S.; Lee, J.; Luo, S.; Hung, S. Regioselective One-Pot Protection of Glucose. *Nat Protoc* **2008**, 3 (1), 97–113.
- (128) Wang, C.-C.; Lee, J.-C.; Luo, S.-Y.; Kulkarni, S. S.; Huang, Y.-W.; Lee, C.-C.; Chang, K.-L.; Hung, S.-C. Regioselective One-Pot Protection of Carbohydrates. *Nature* **2007**, 446 (7138), 896–899.
- (129) Fascione, M. A.; Turnbull, W. B. Benzyne Arylation of Oxathiane Glycosyl Donors. *Beilstein J. Org. Chem.* **2010**, 6 (19).
- (130) Chayajarus, K.; Chambers, D. J.; Chughtai, M. J.; Fairbanks, A. J. Stereospecific Synthesis of 1,2-Cis Glycosides by Vinyl-Mediated IAD. *Org. Lett.* **2004**, 6 (21), 3797–3800. <https://doi.org/10.1021/ol048427o>.

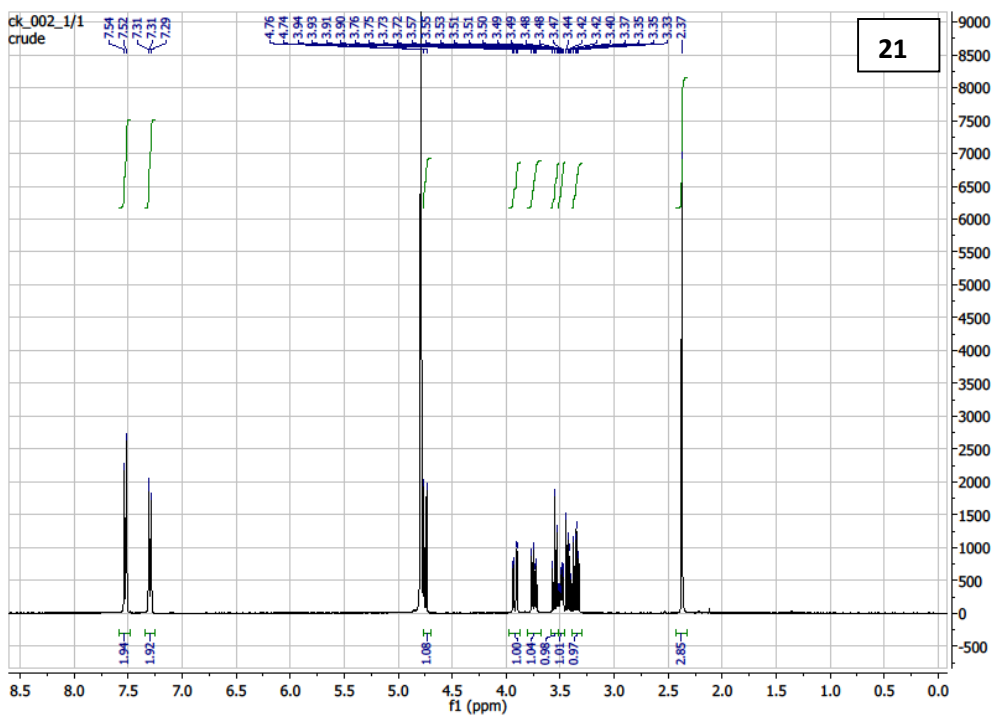
# 10 Appendix

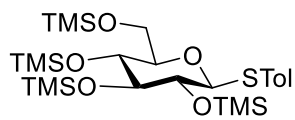


20

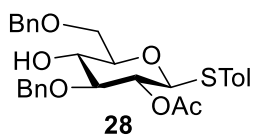
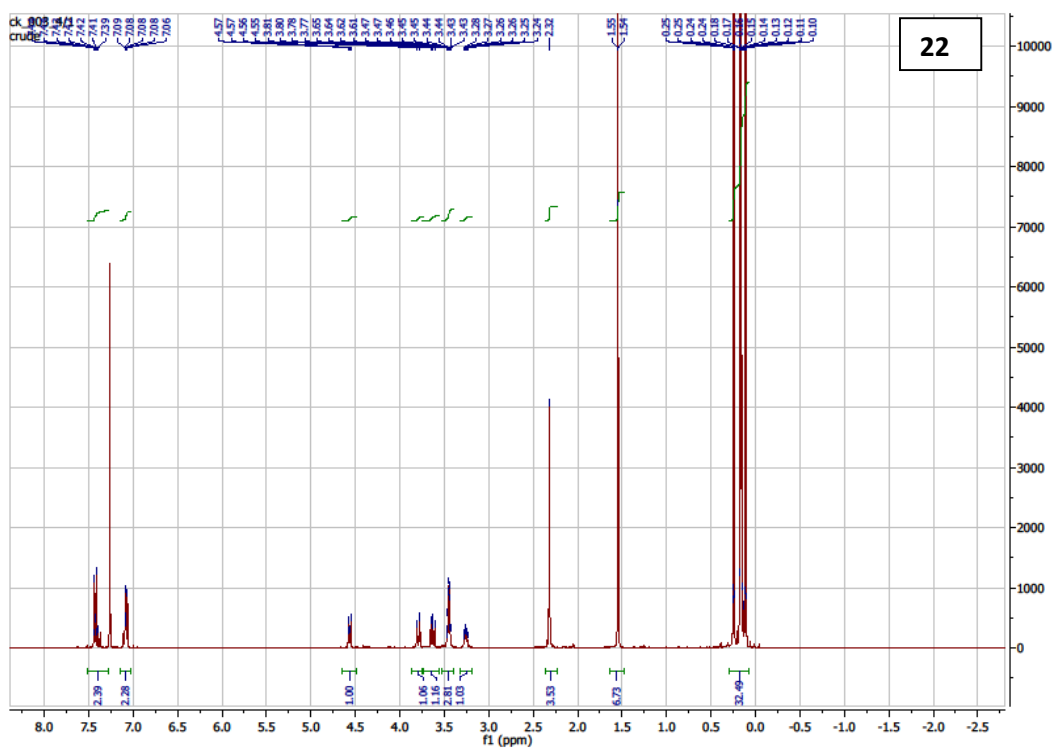


21

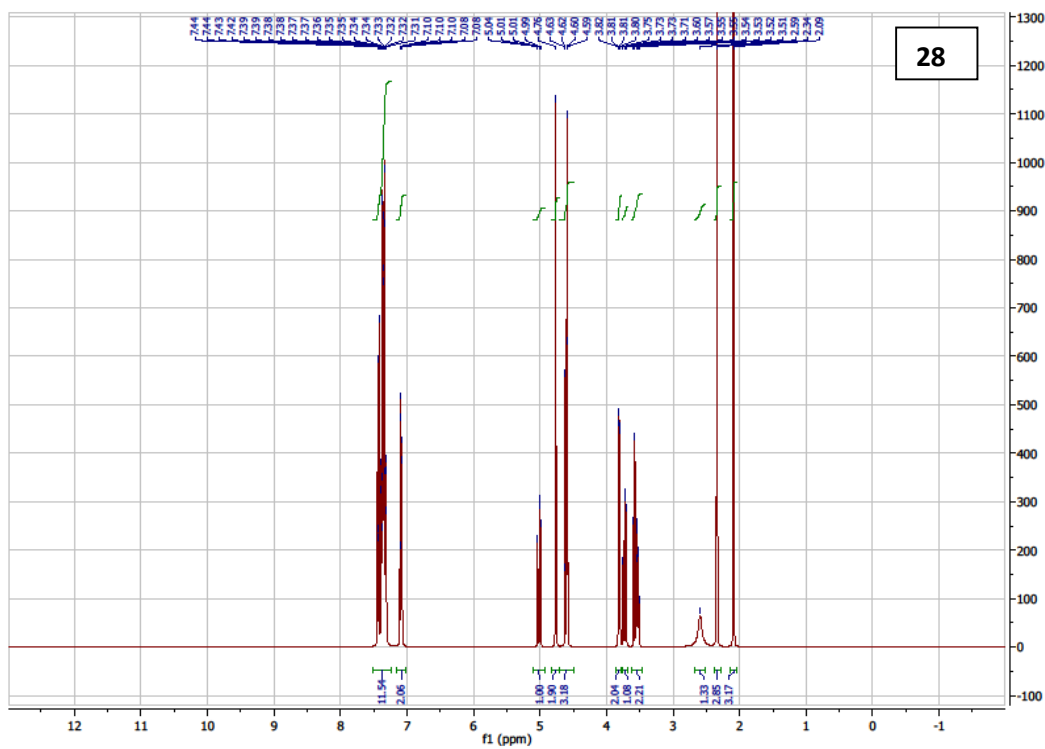


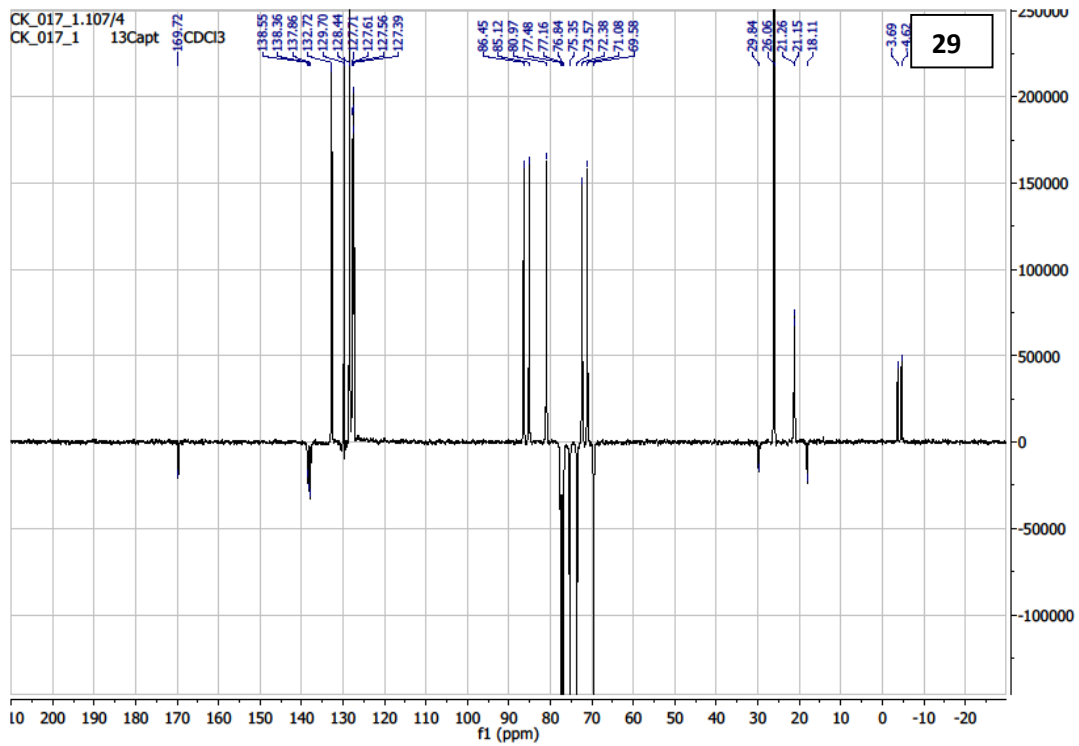
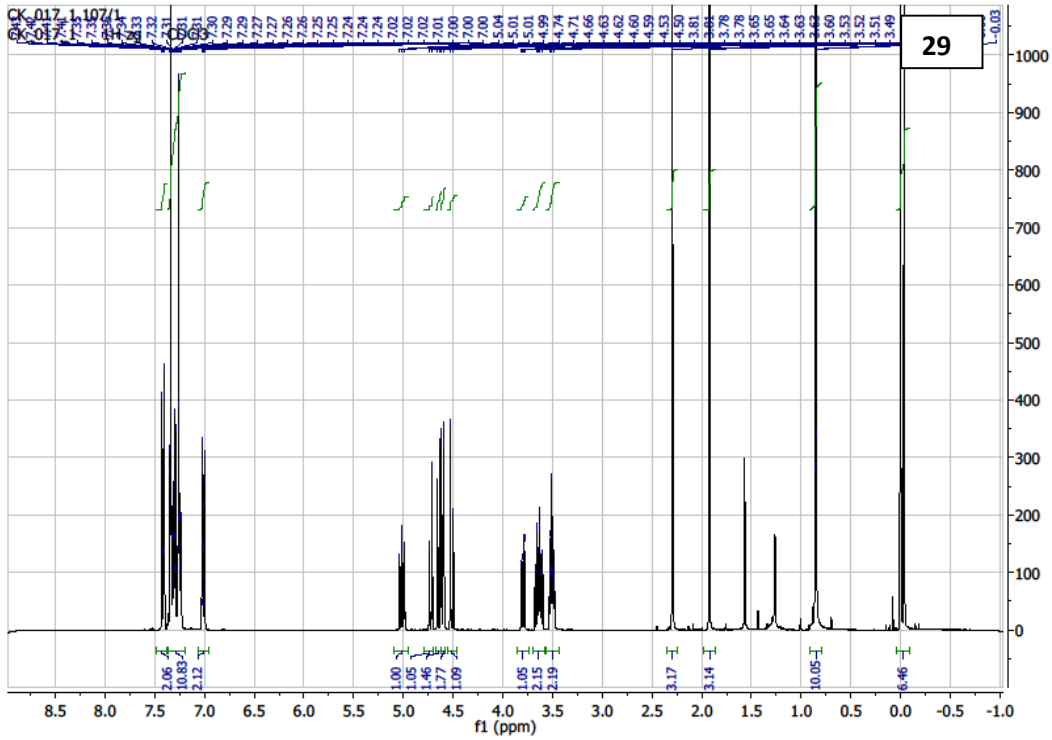
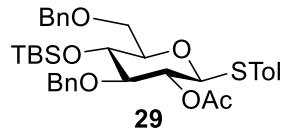


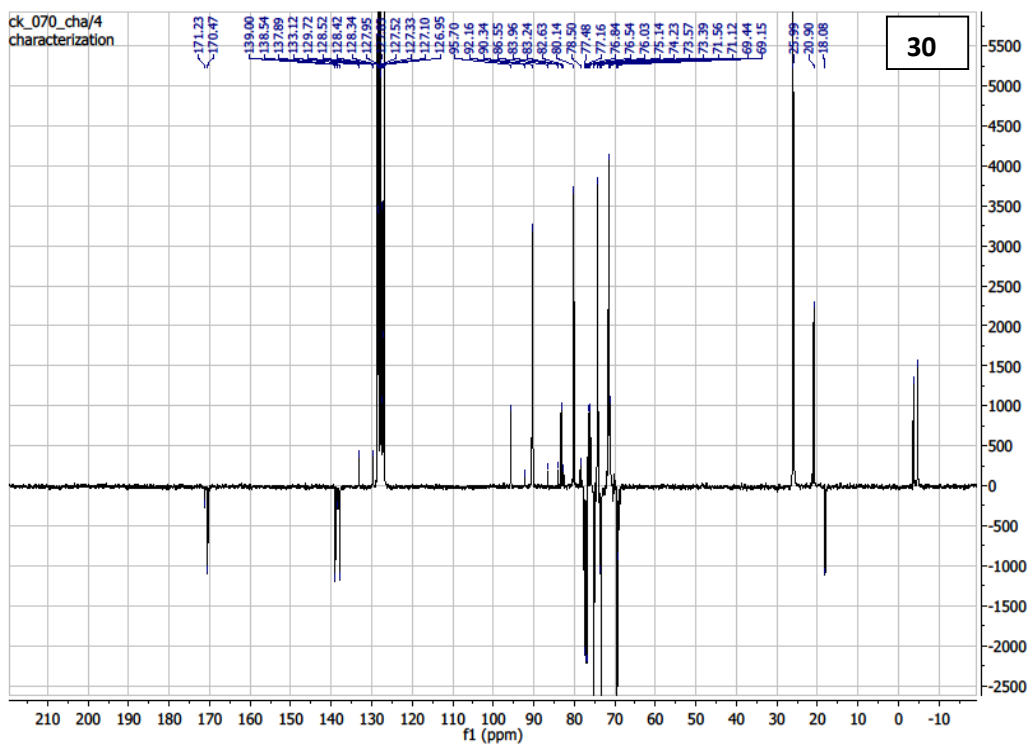
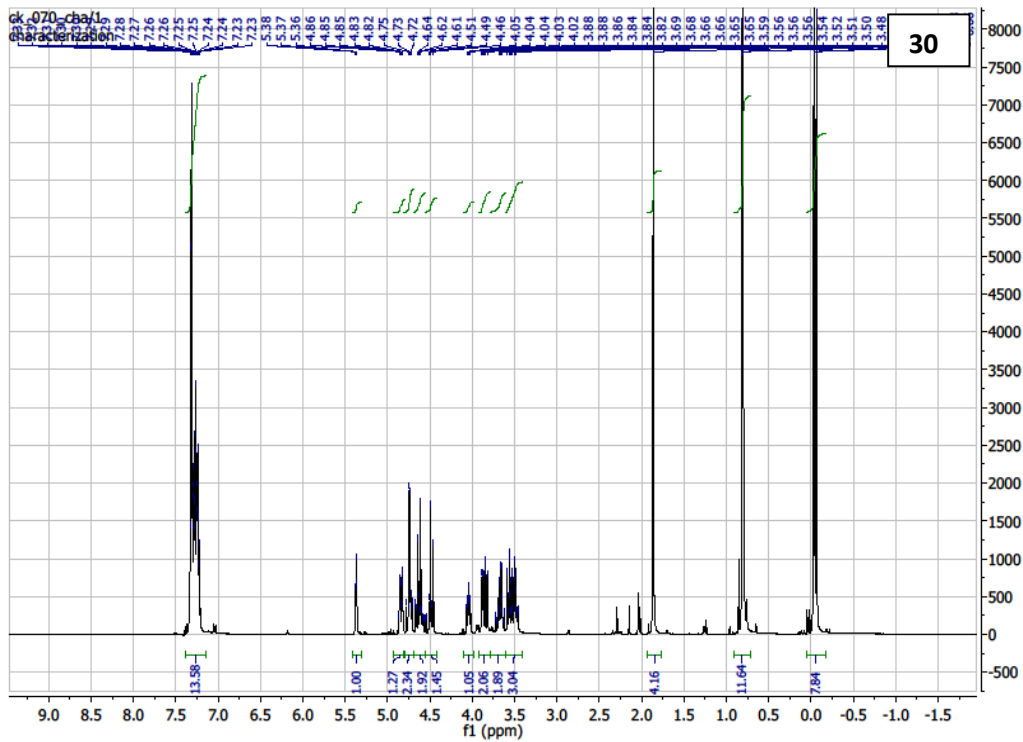
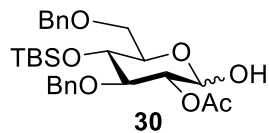
22



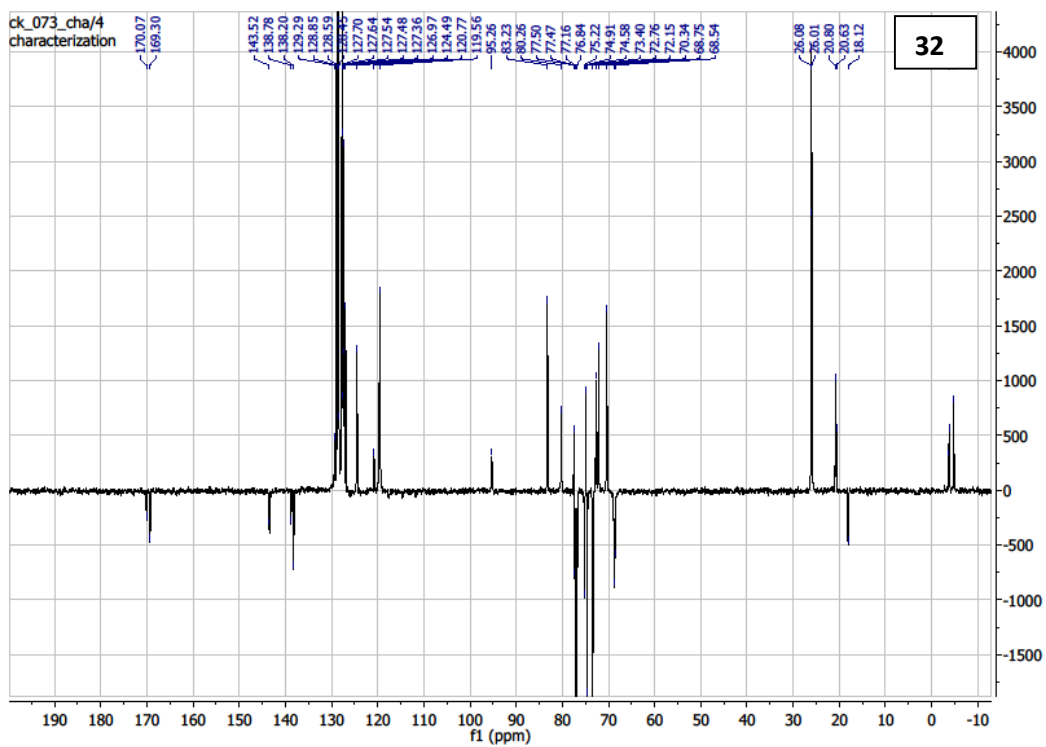
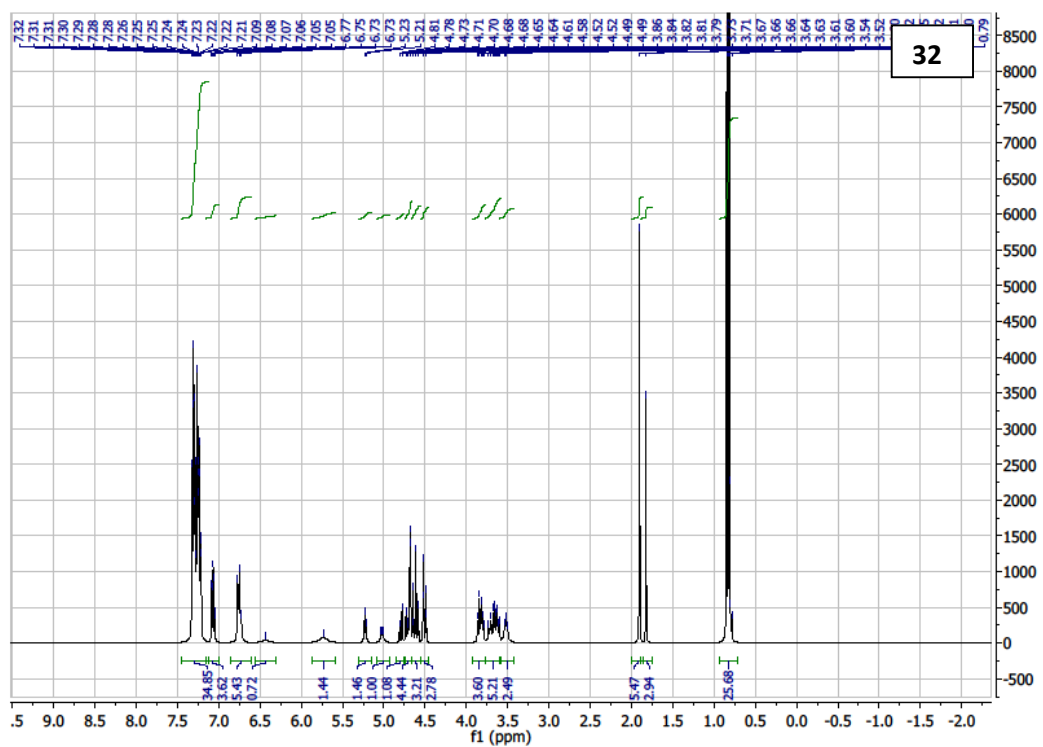
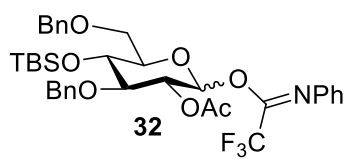
28

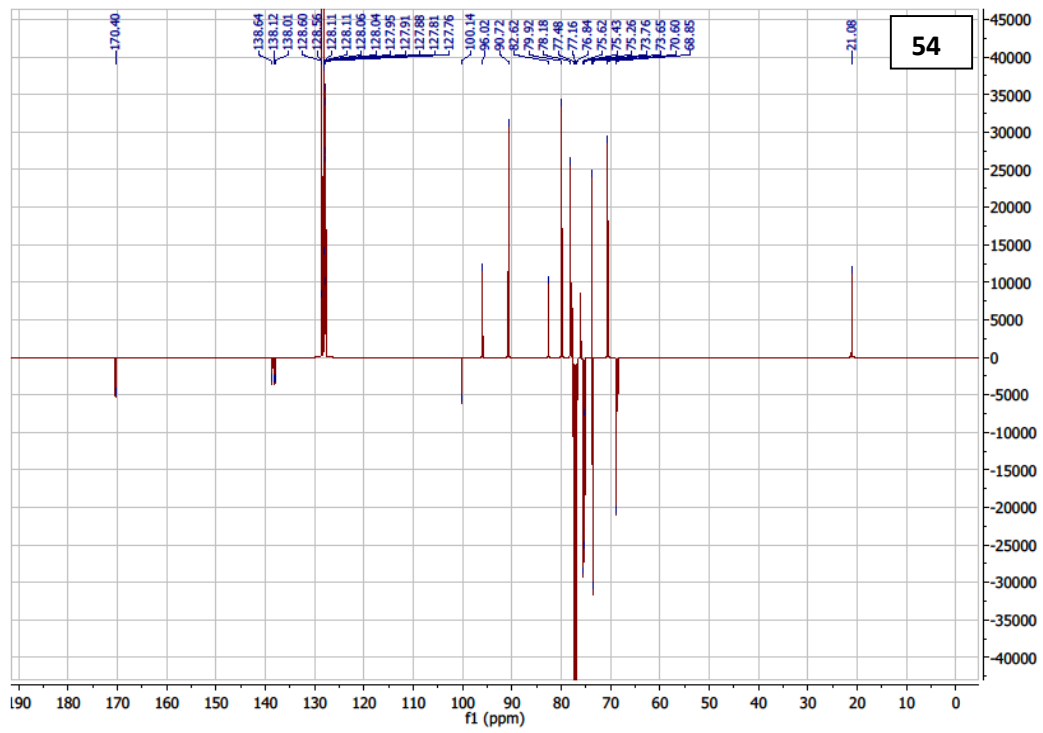
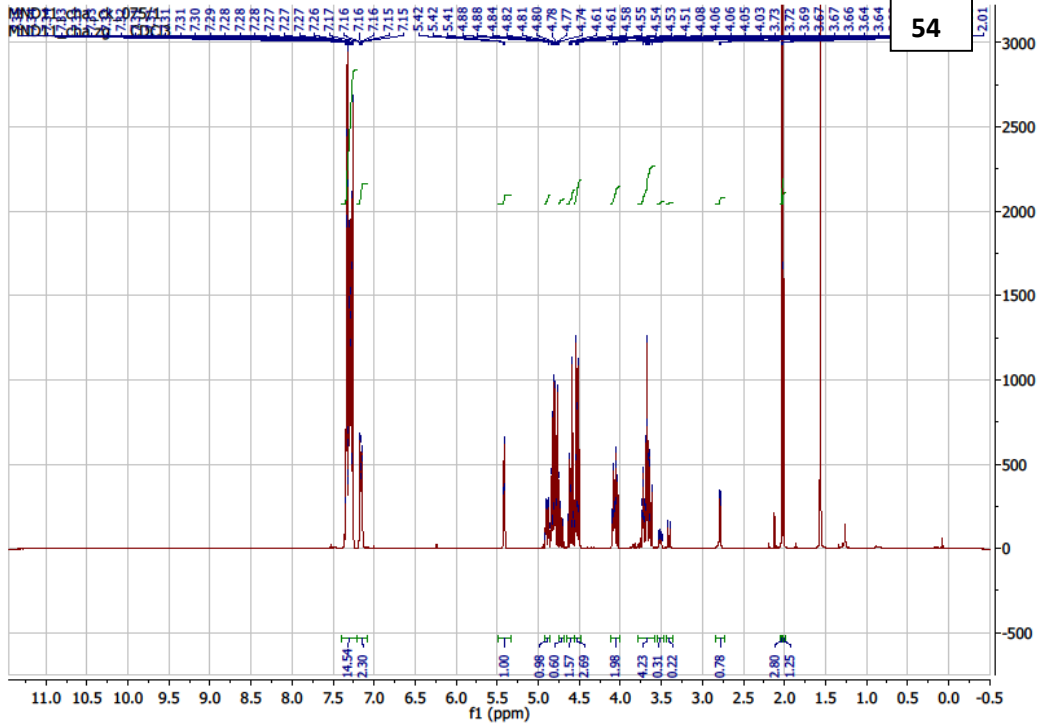
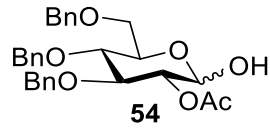


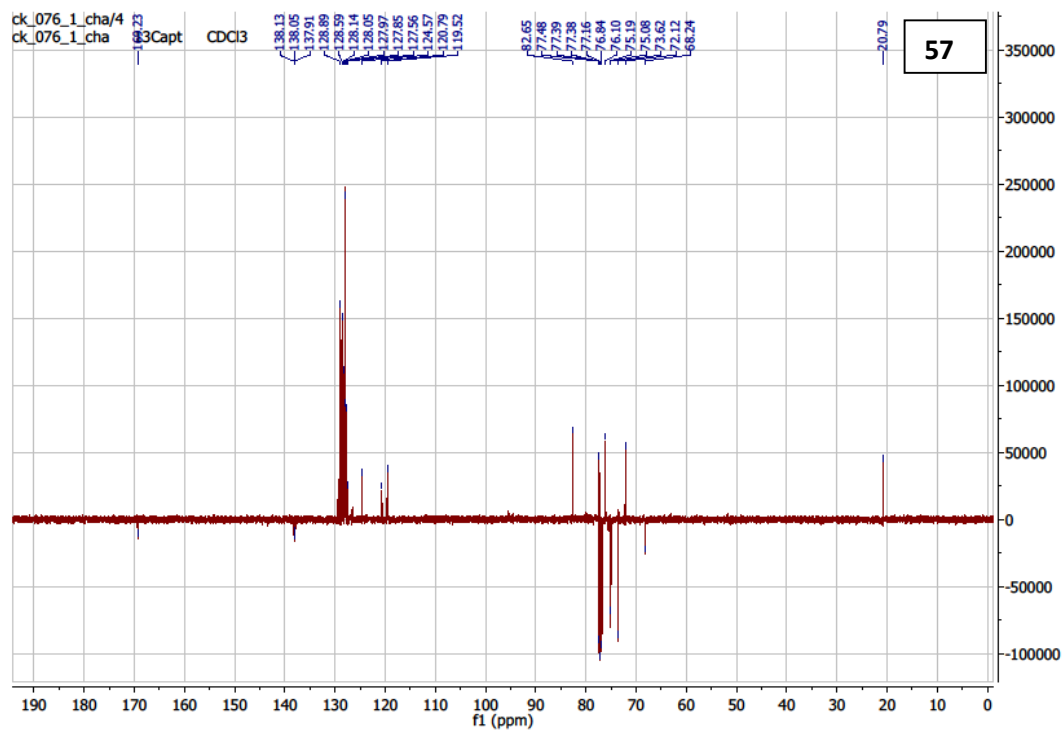
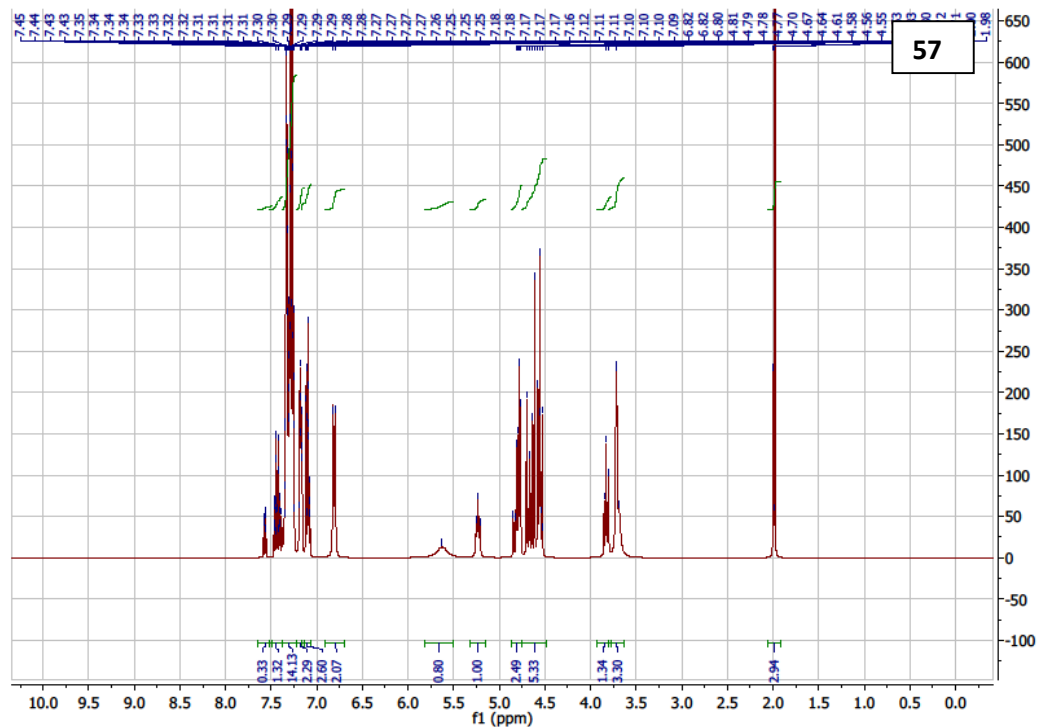
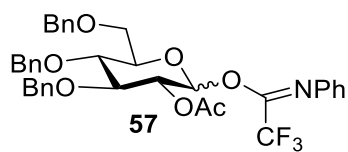


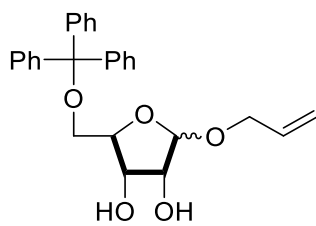




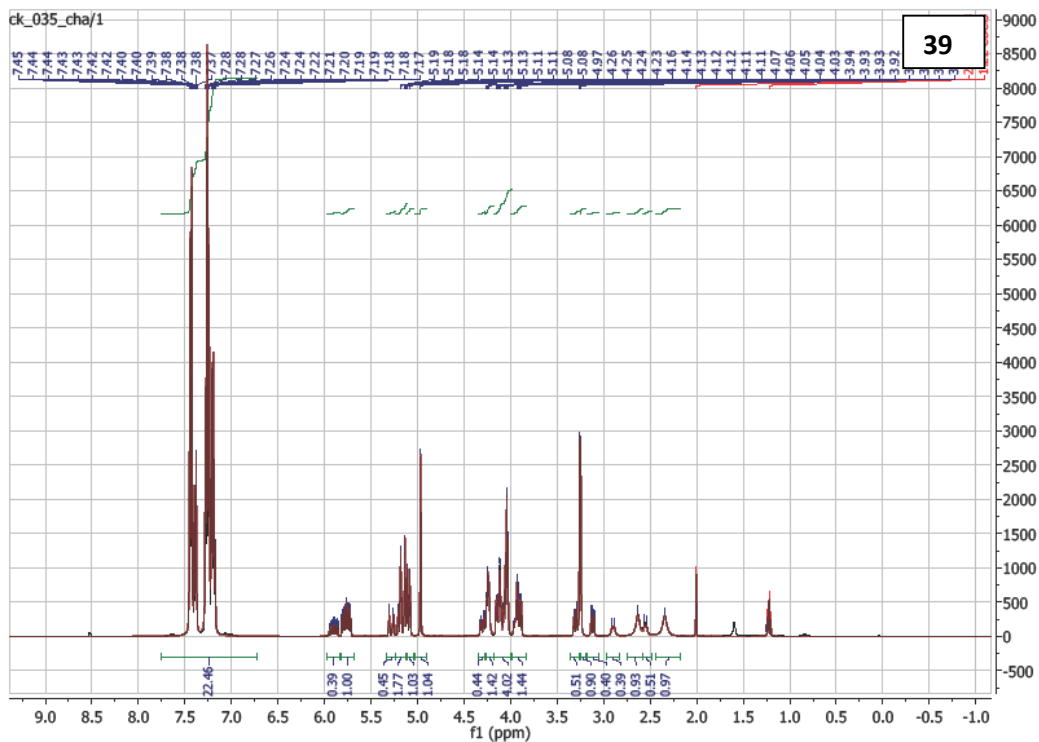




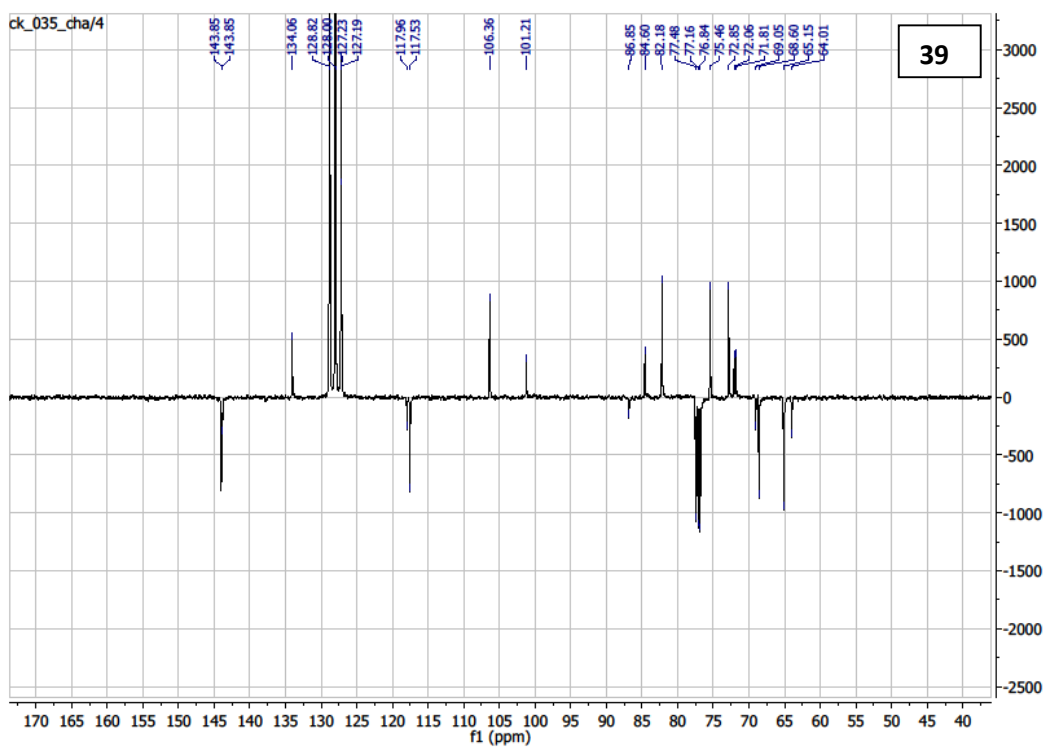




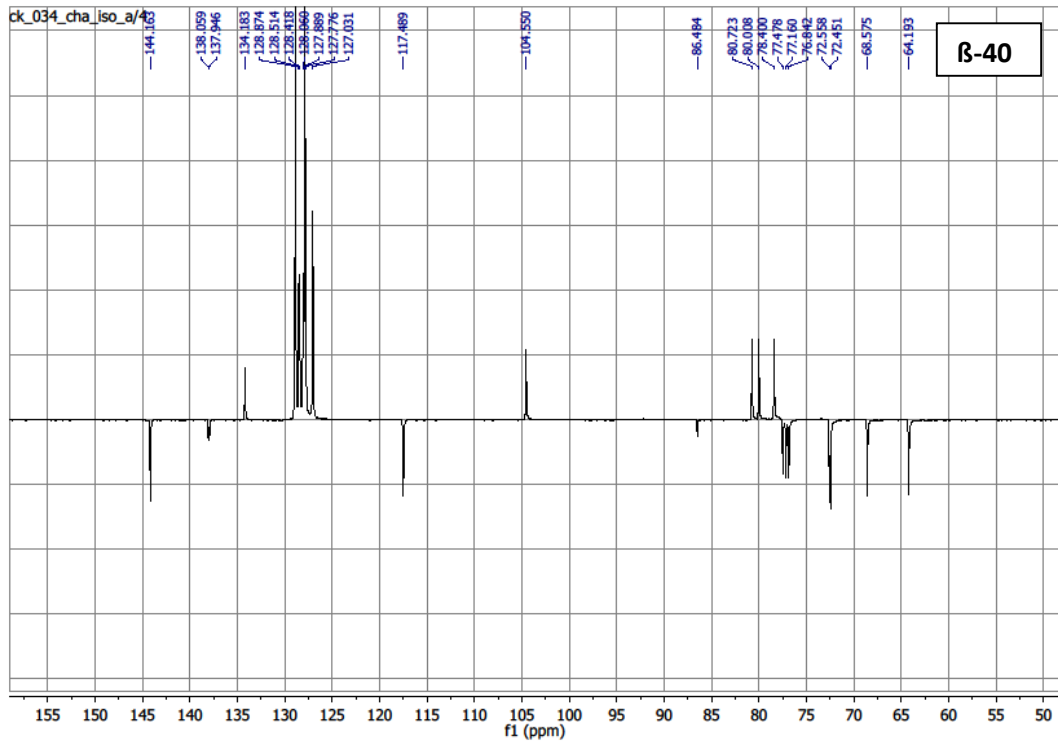
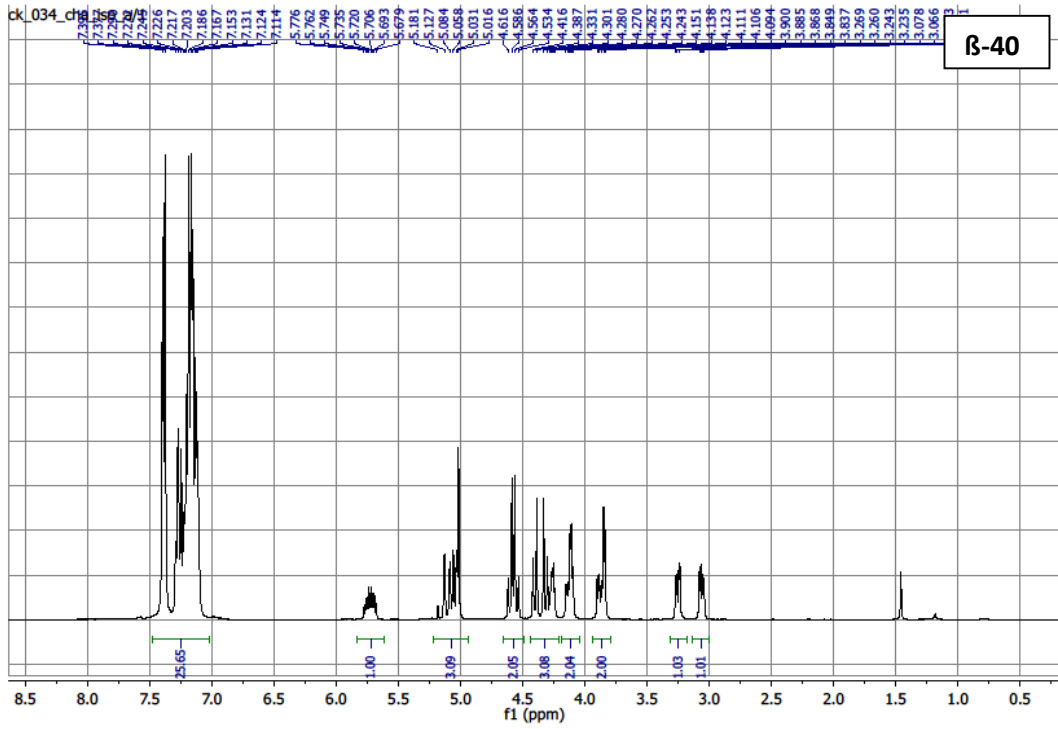
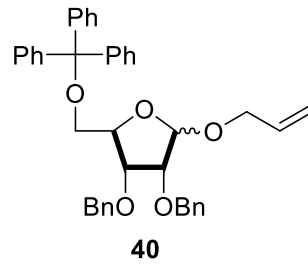
39

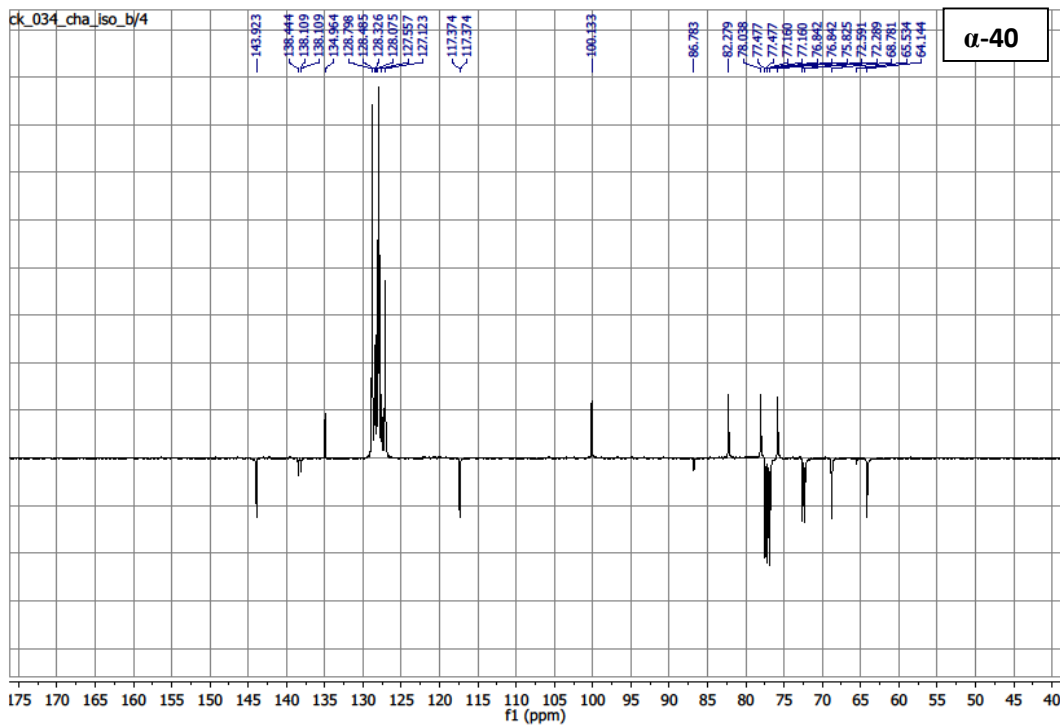
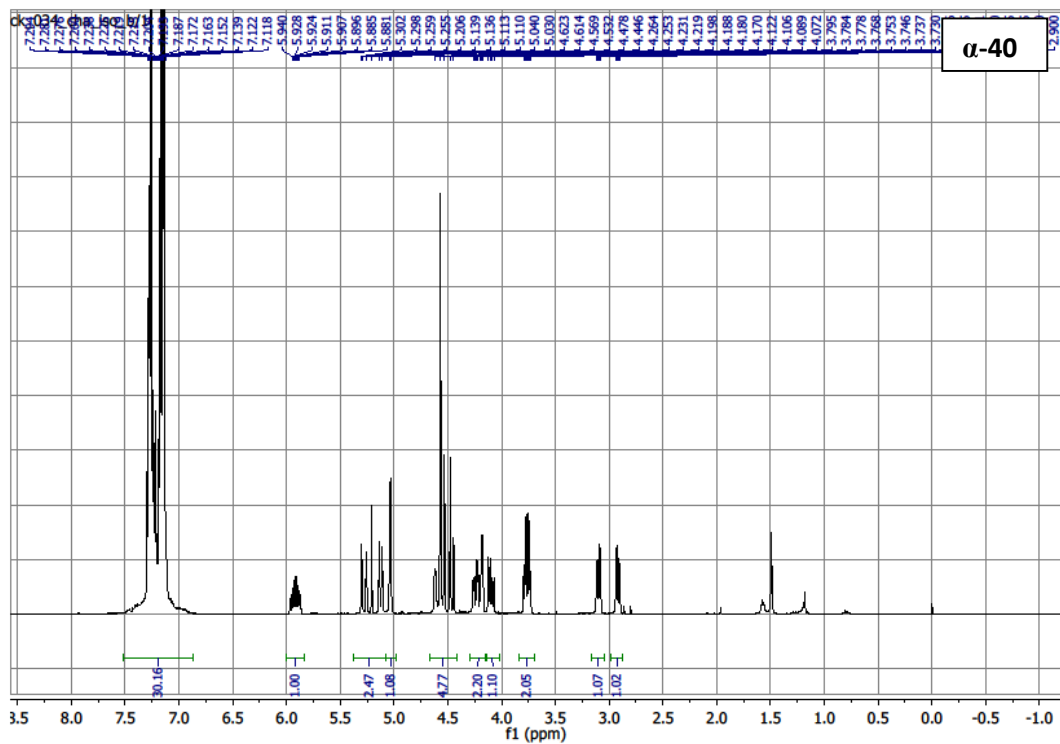


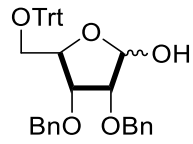
39



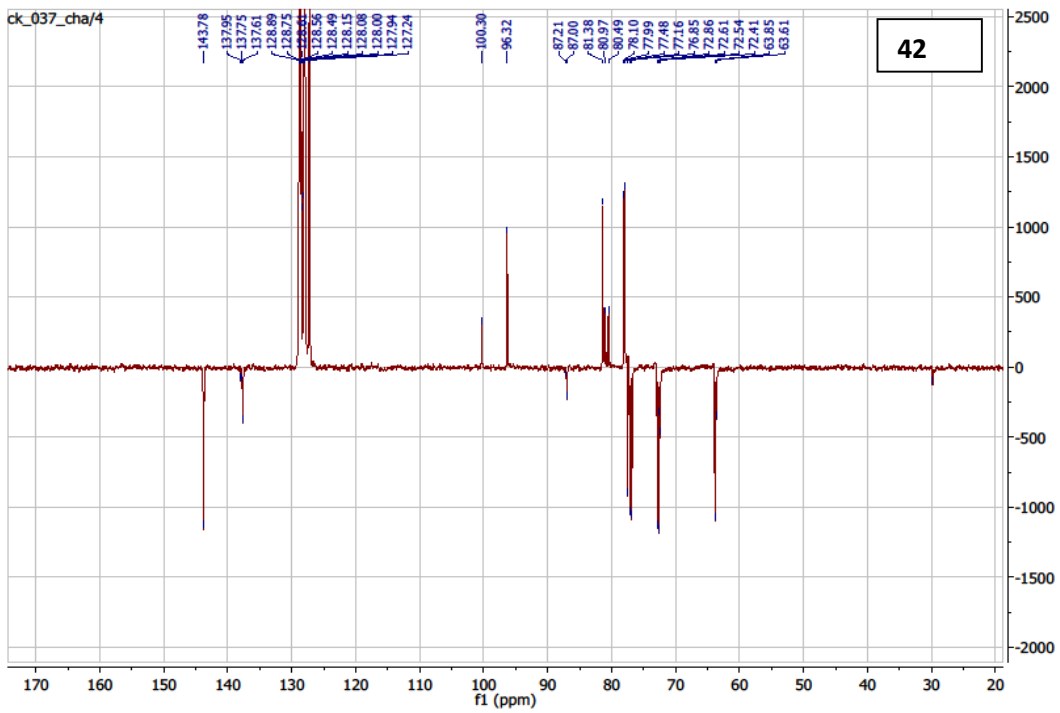
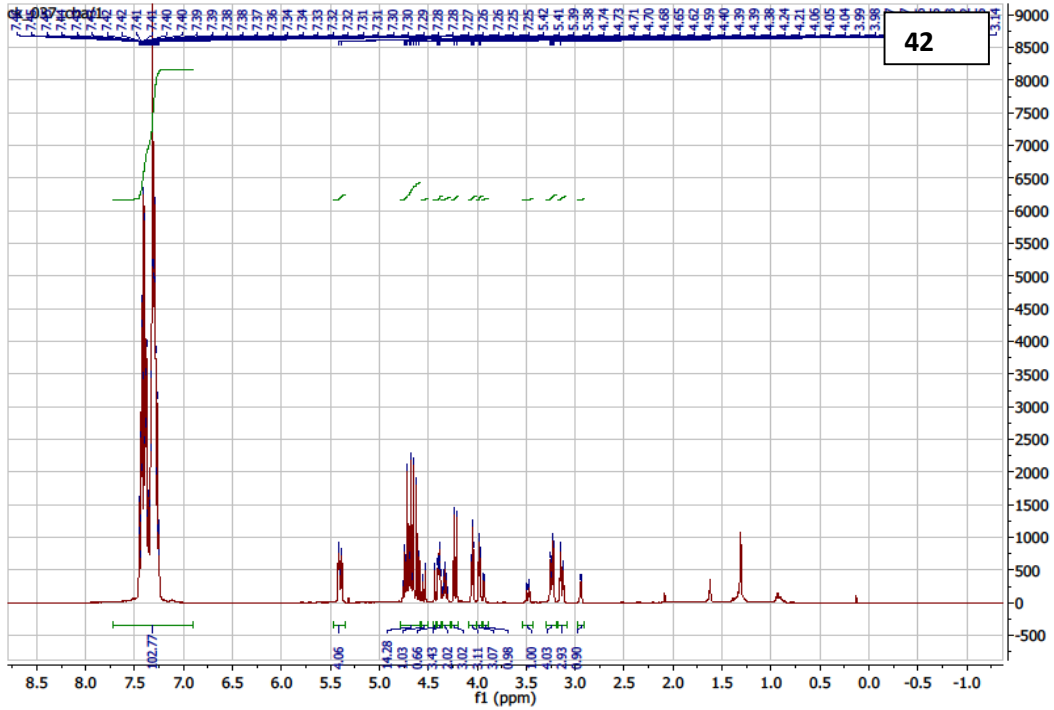
39

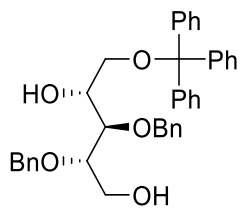




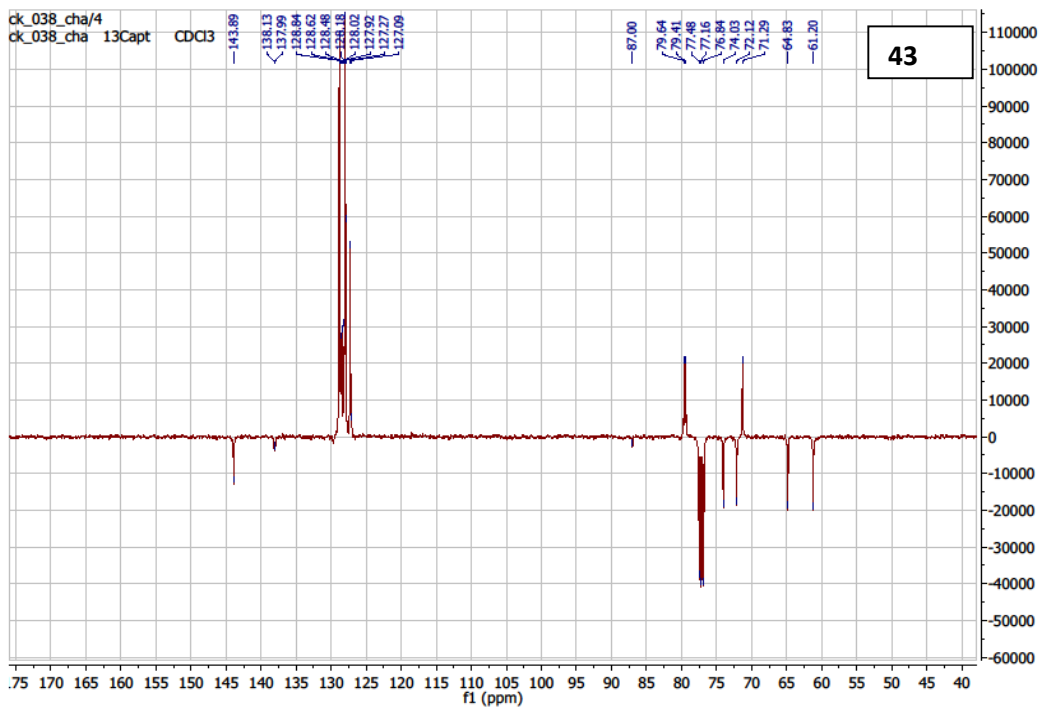
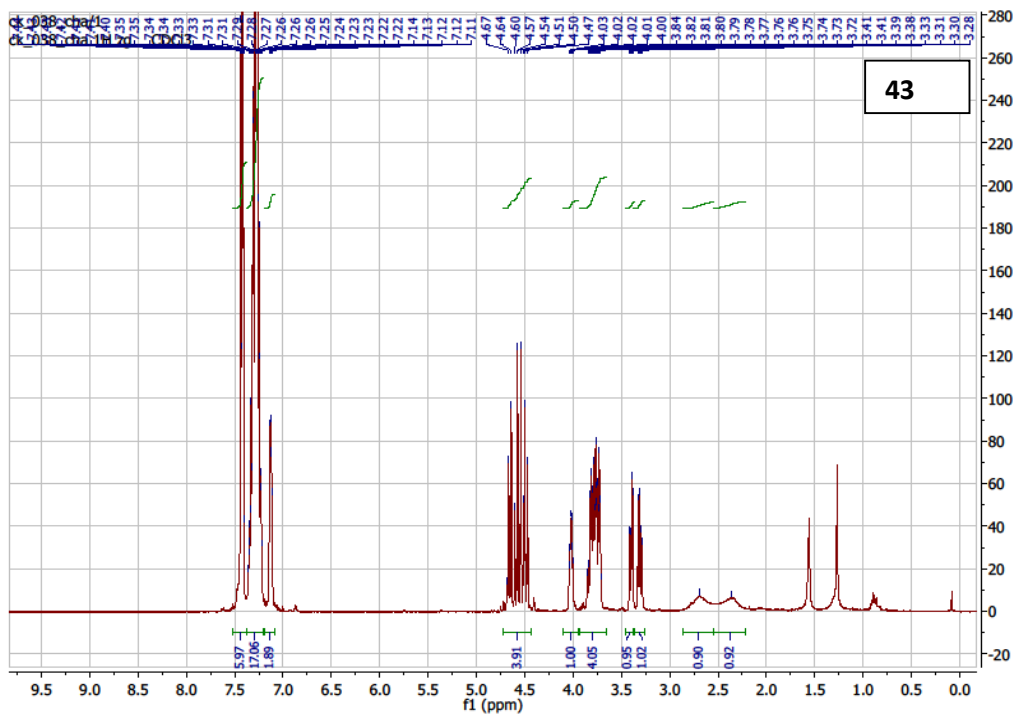


42

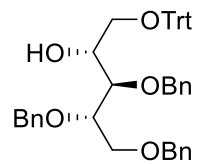




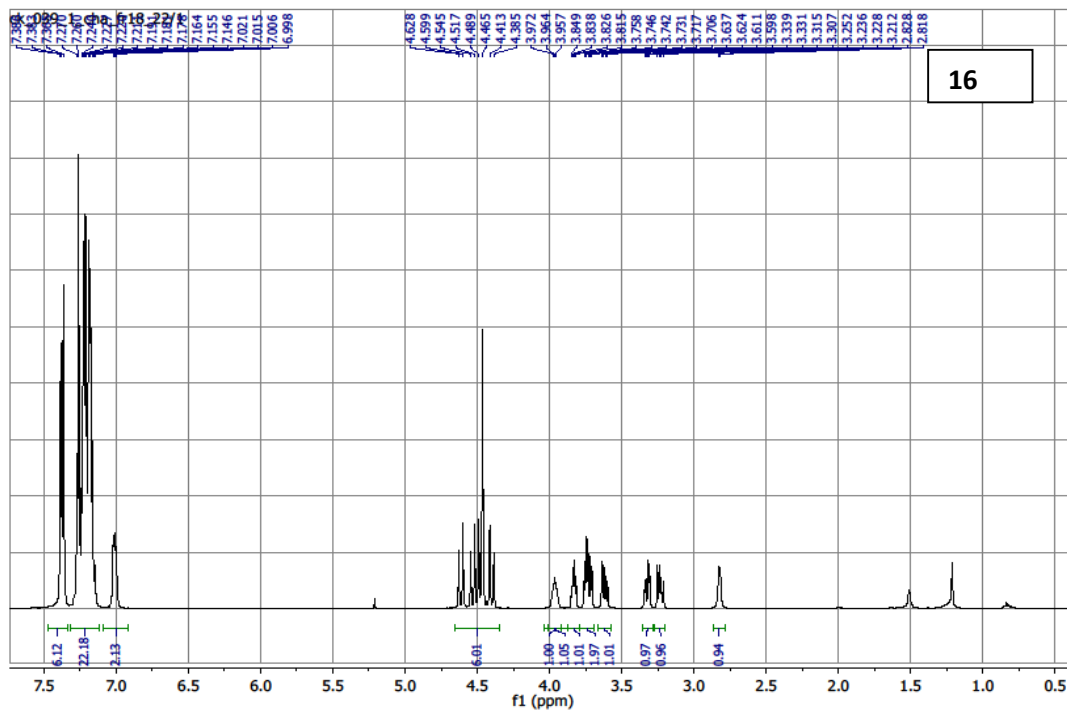
43



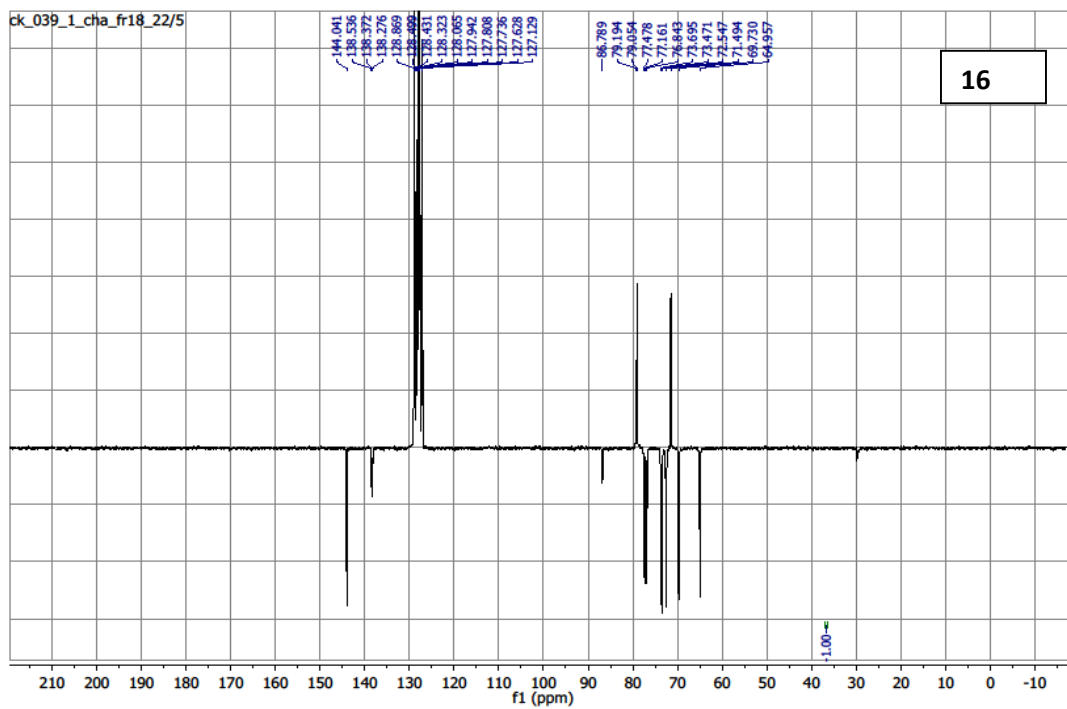




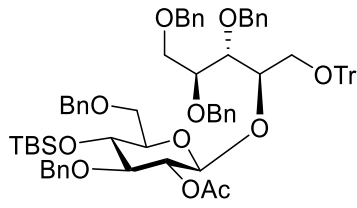
16



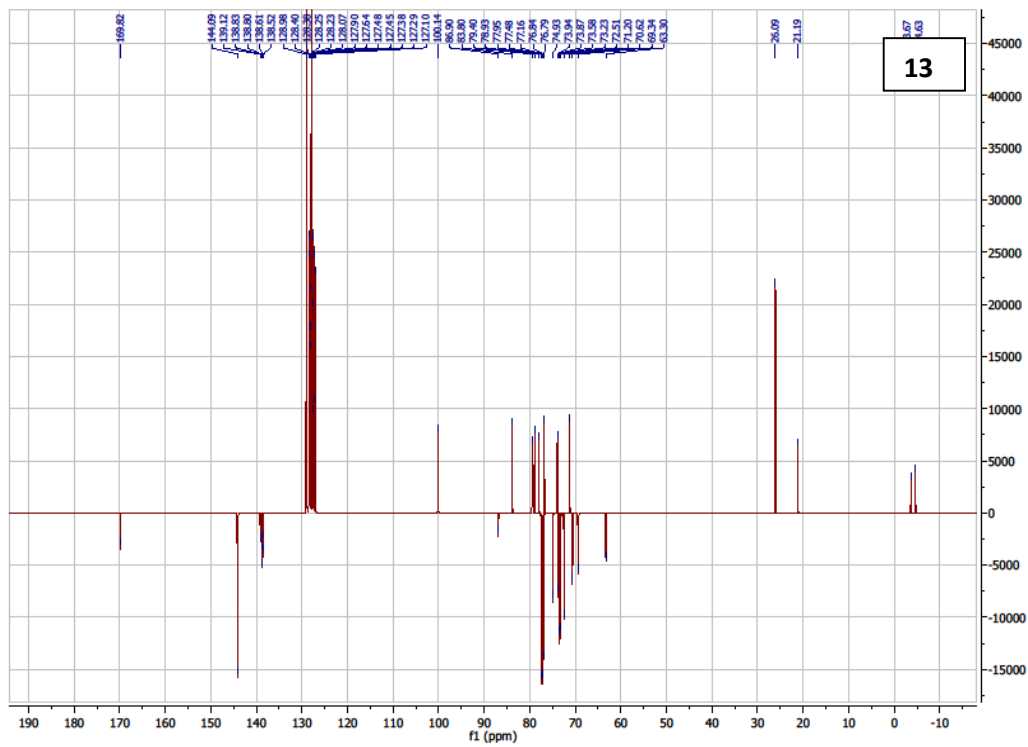
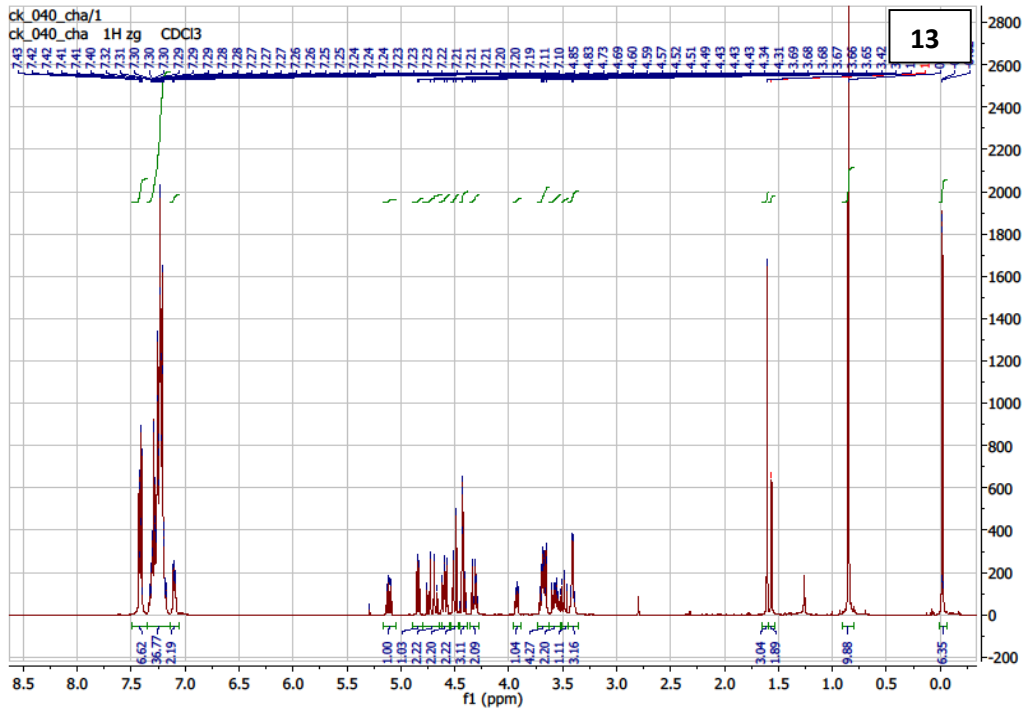
16

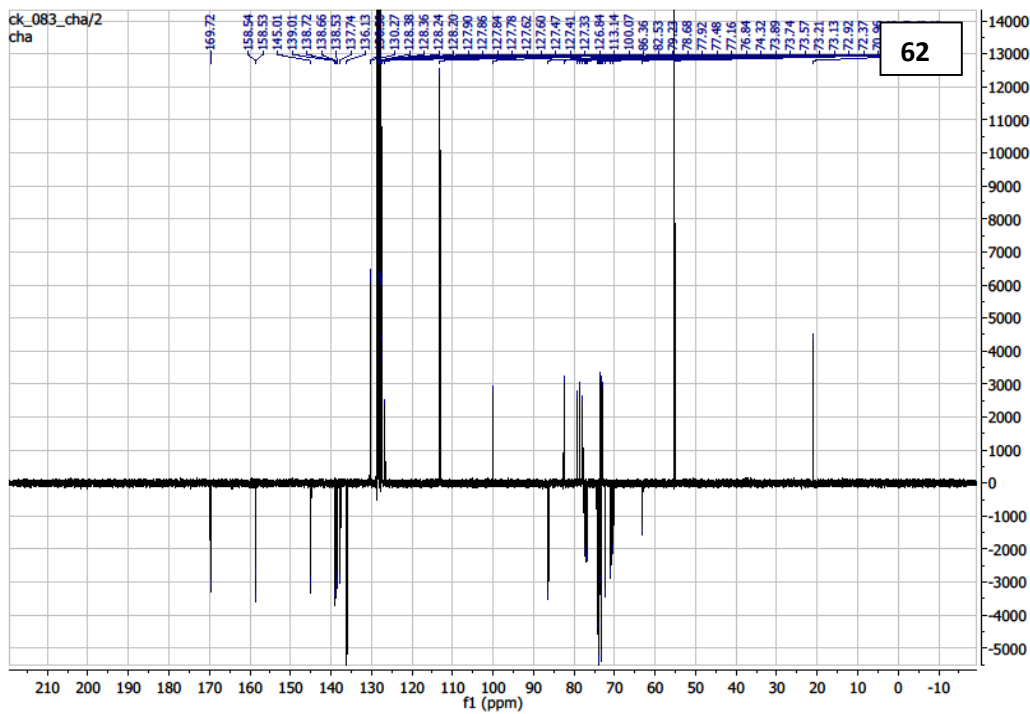
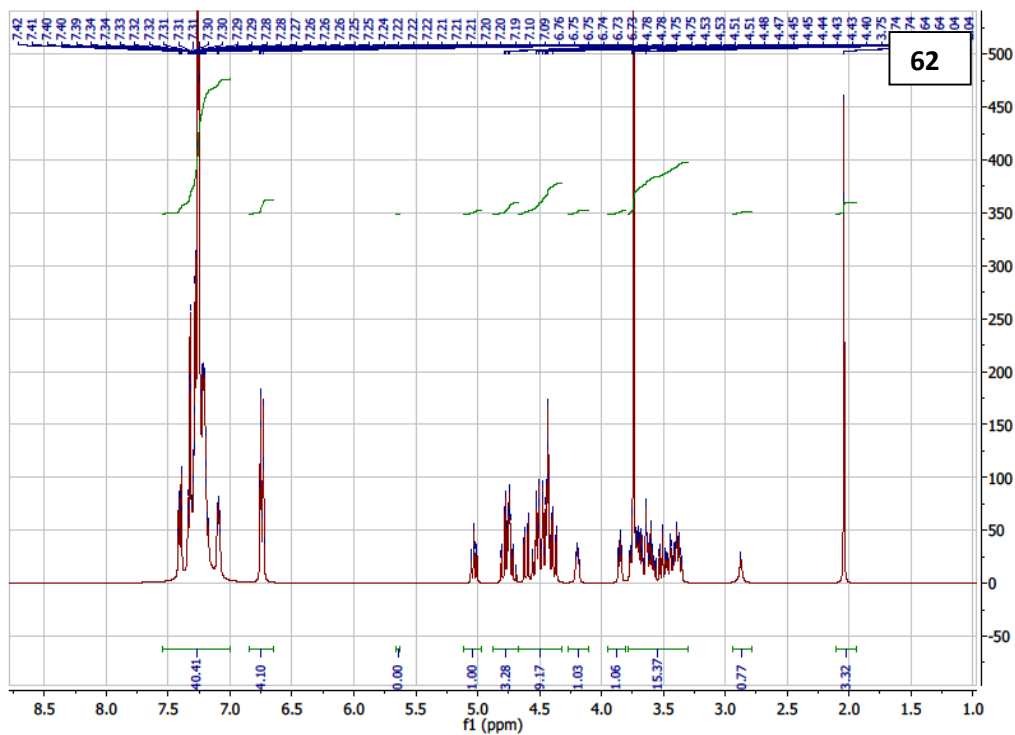
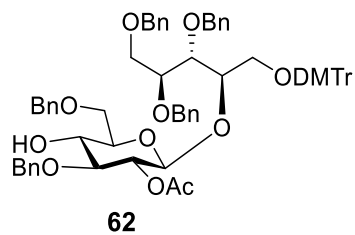


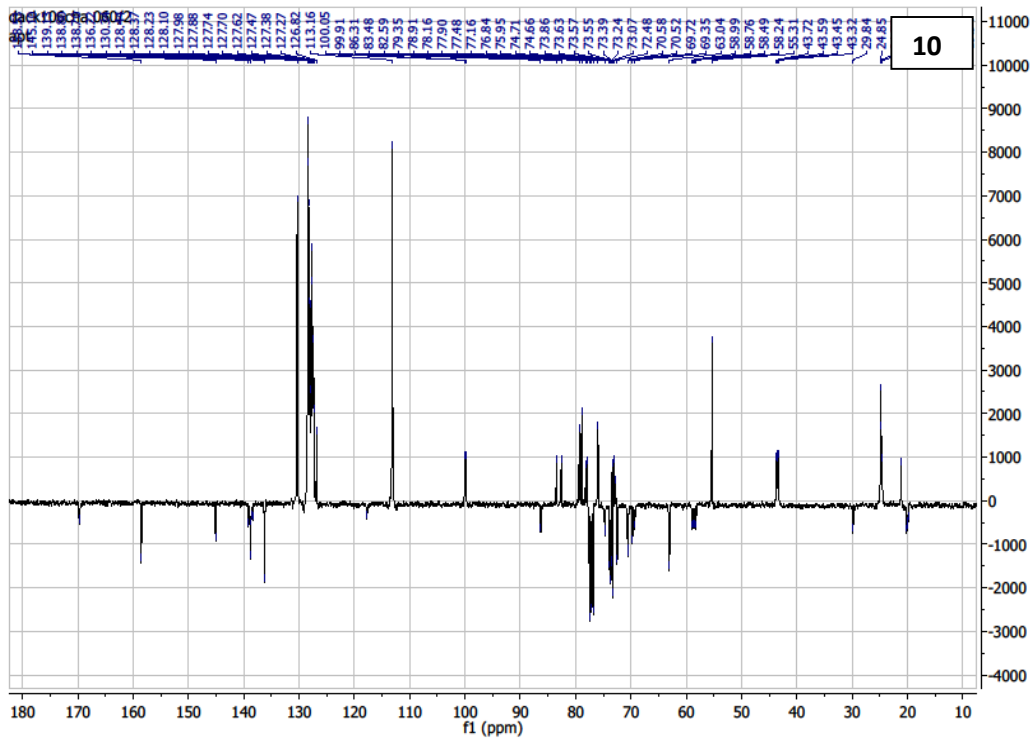
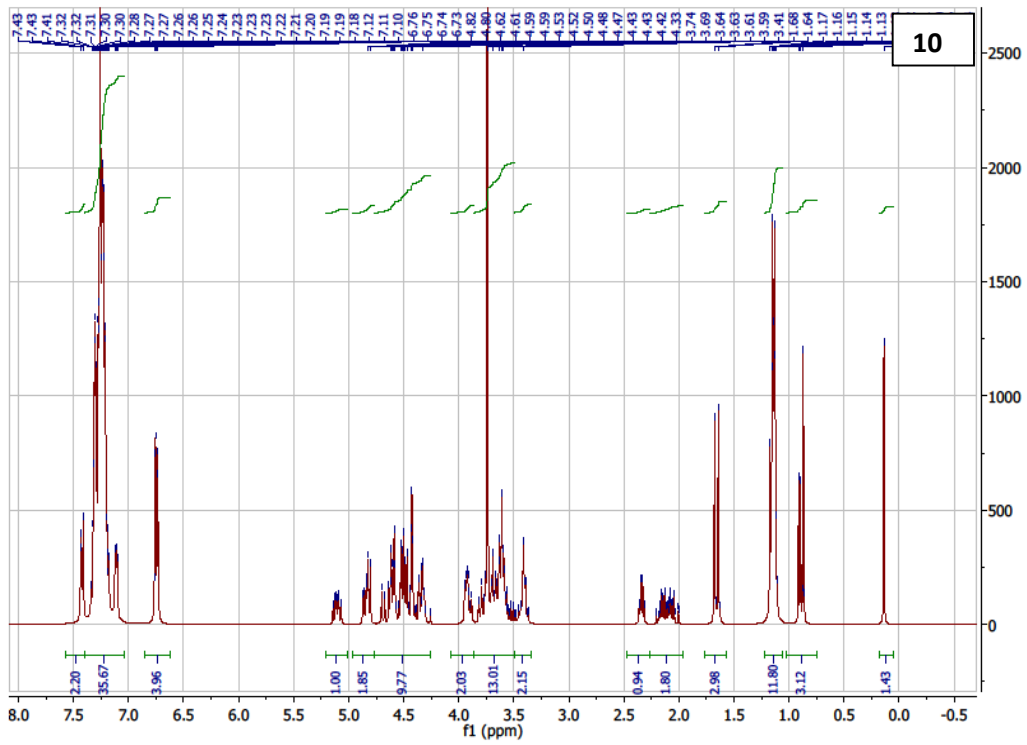
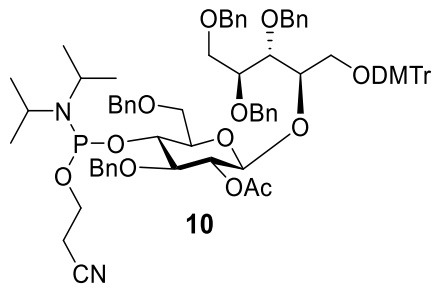
16

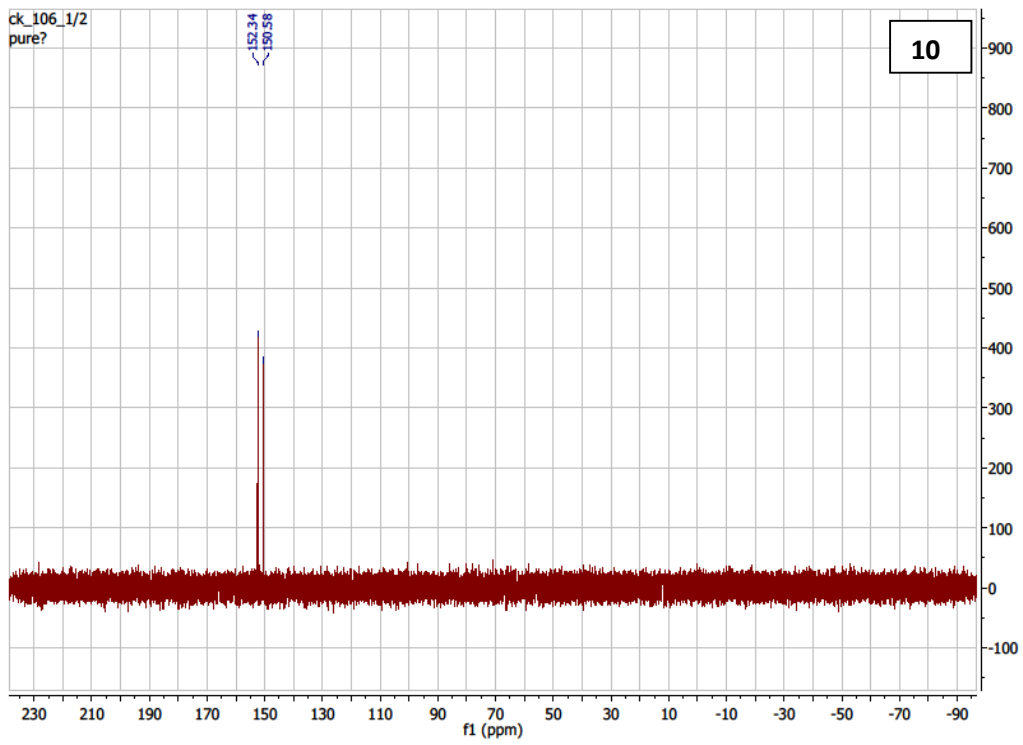


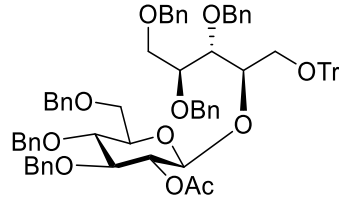
13



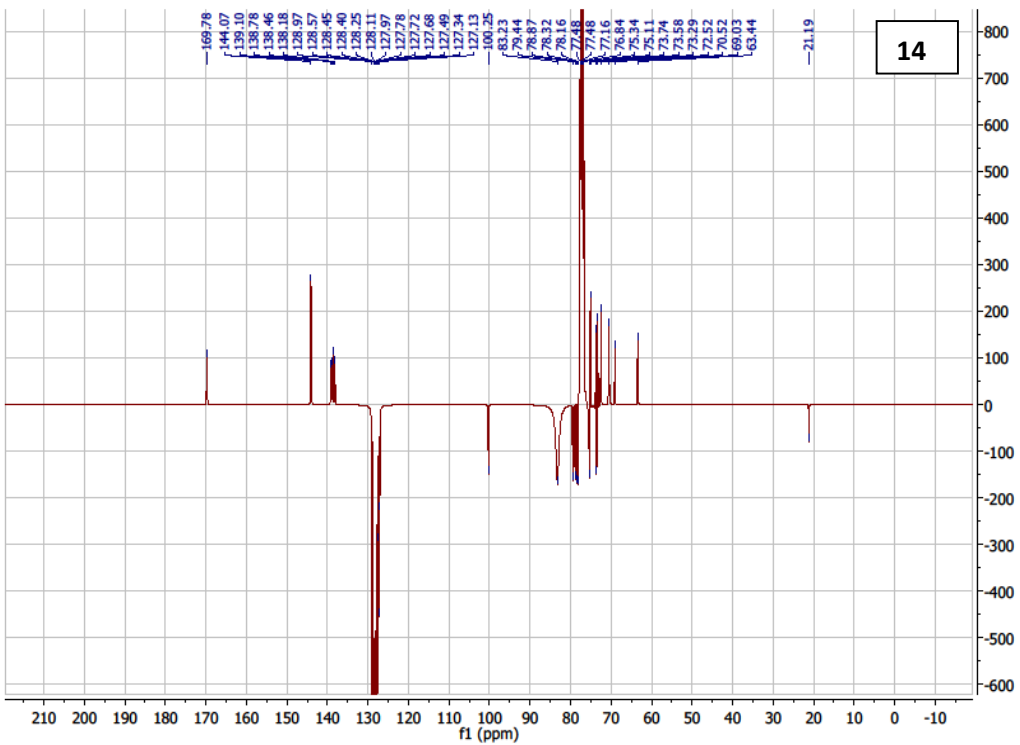
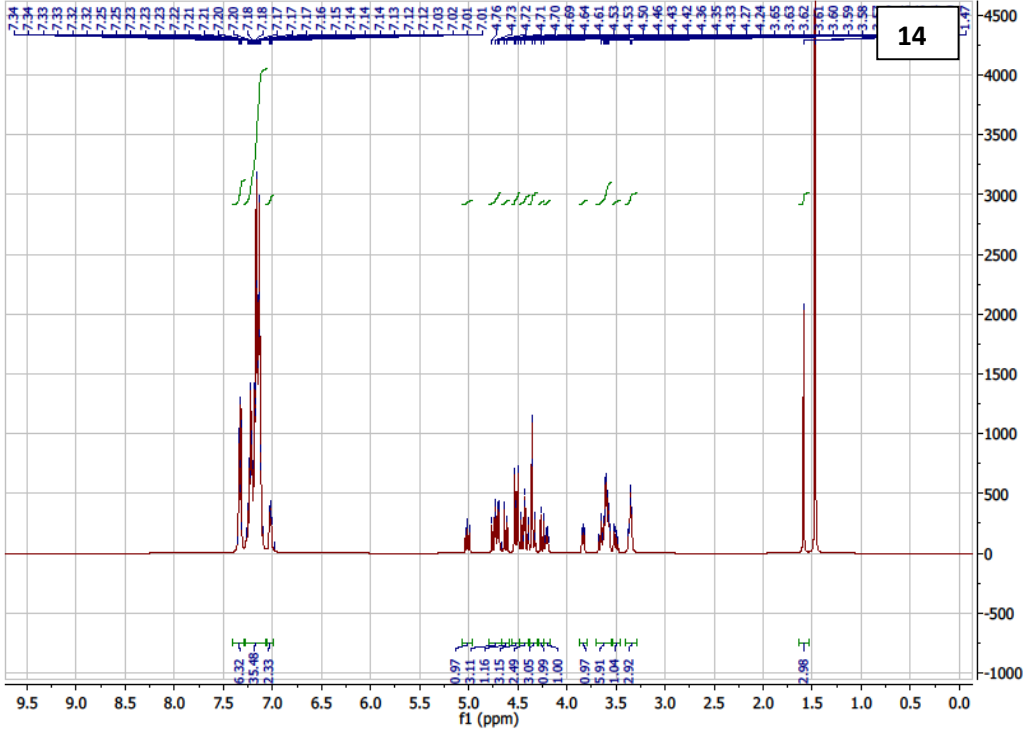


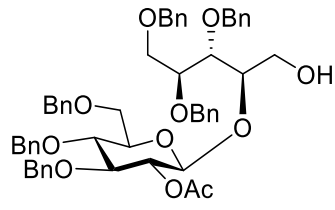




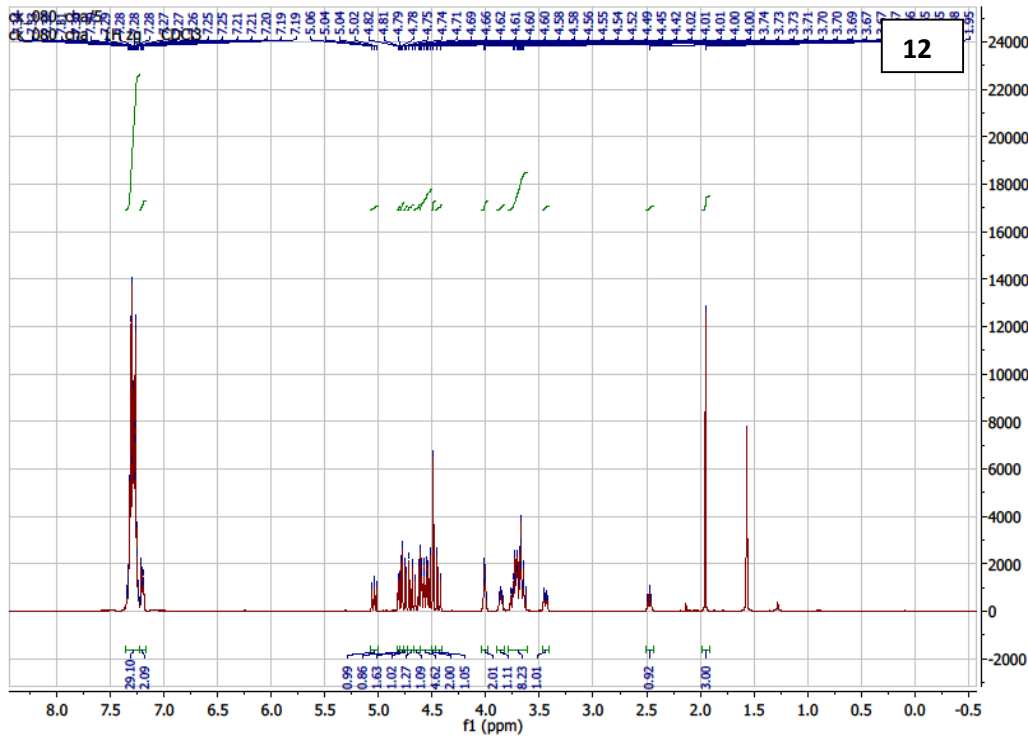


14

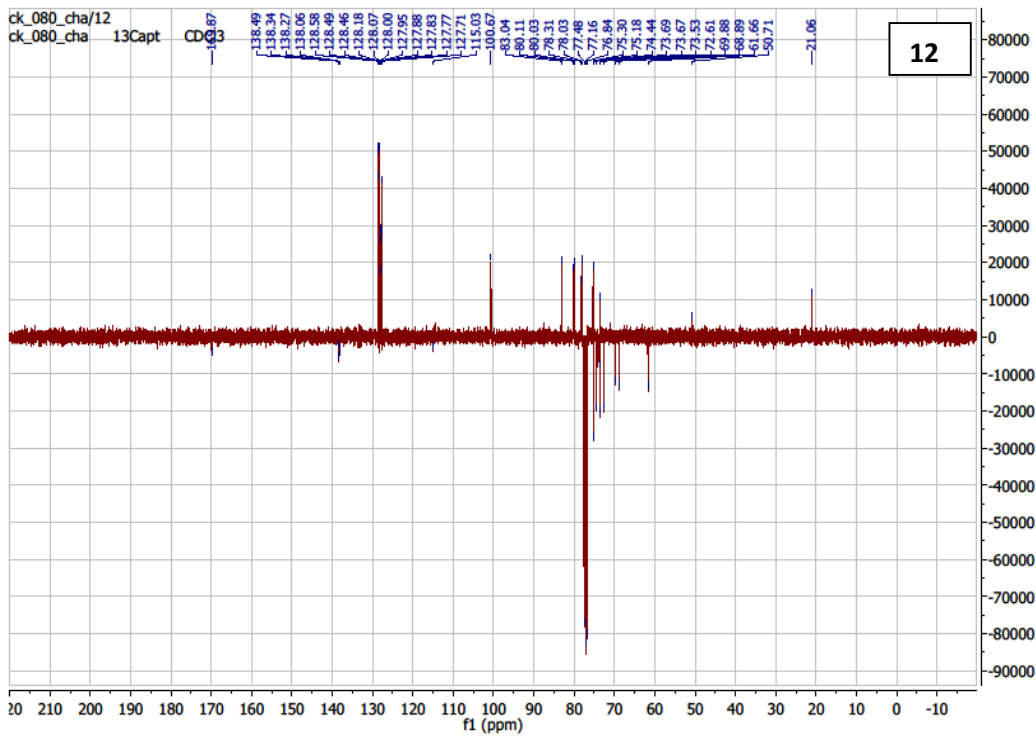




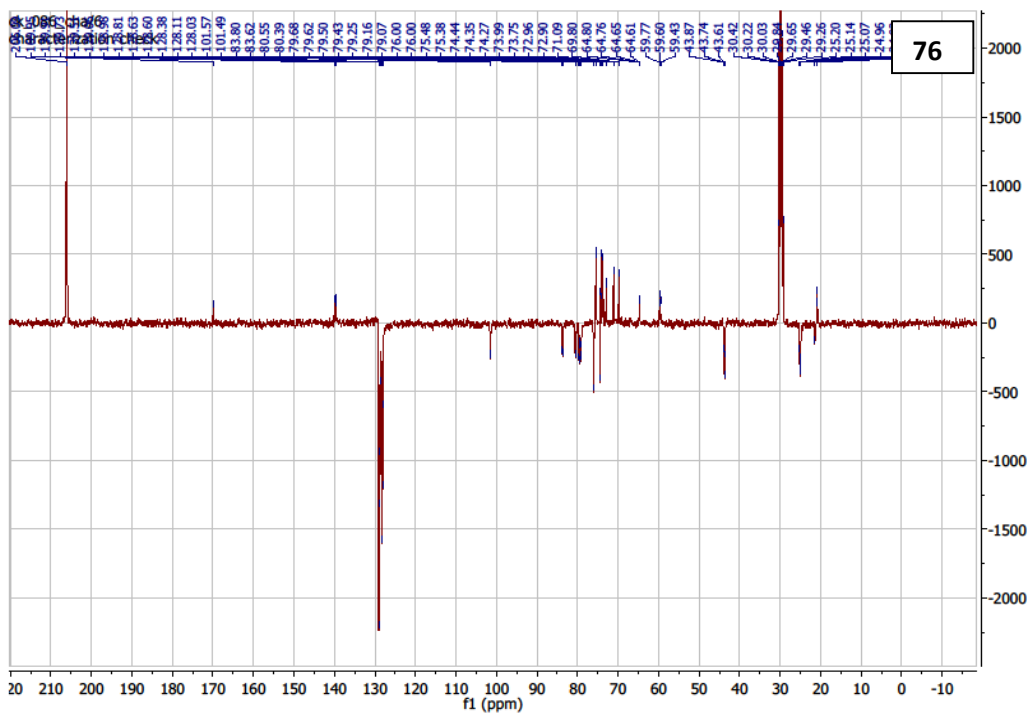
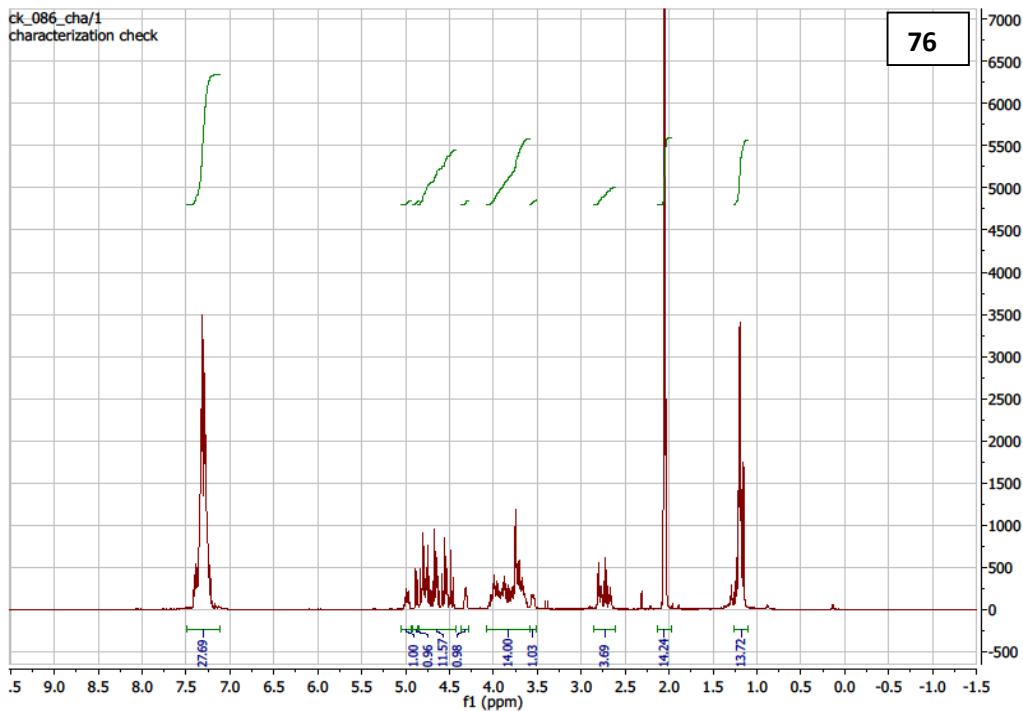
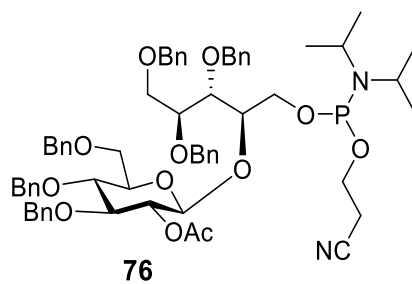
12



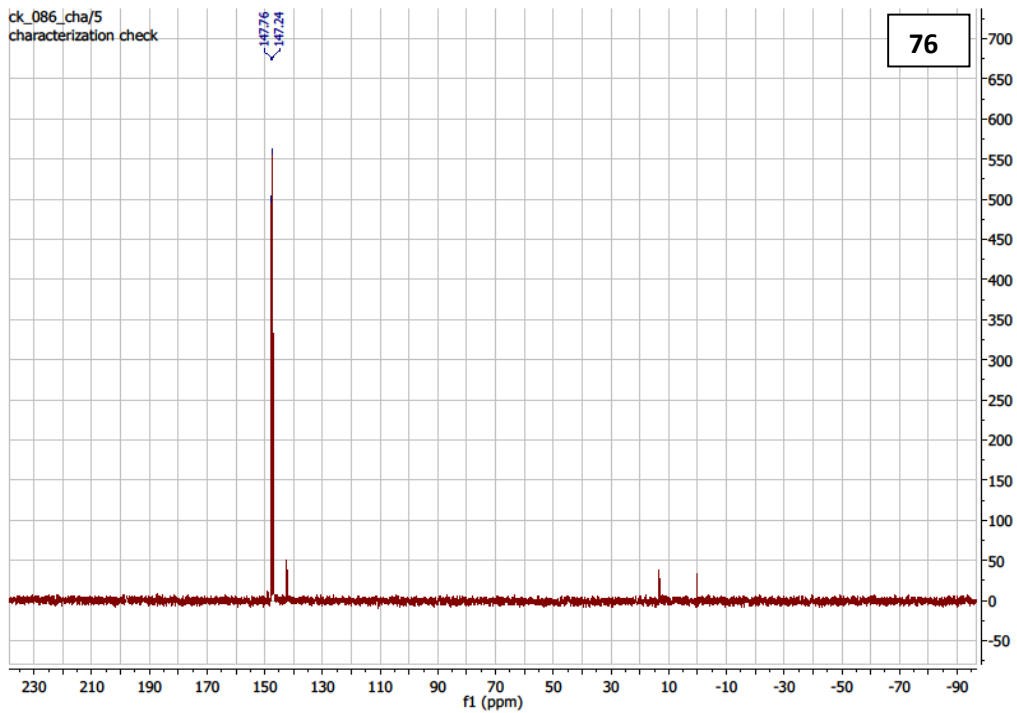
12

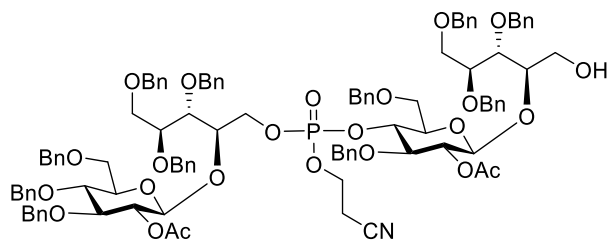


12

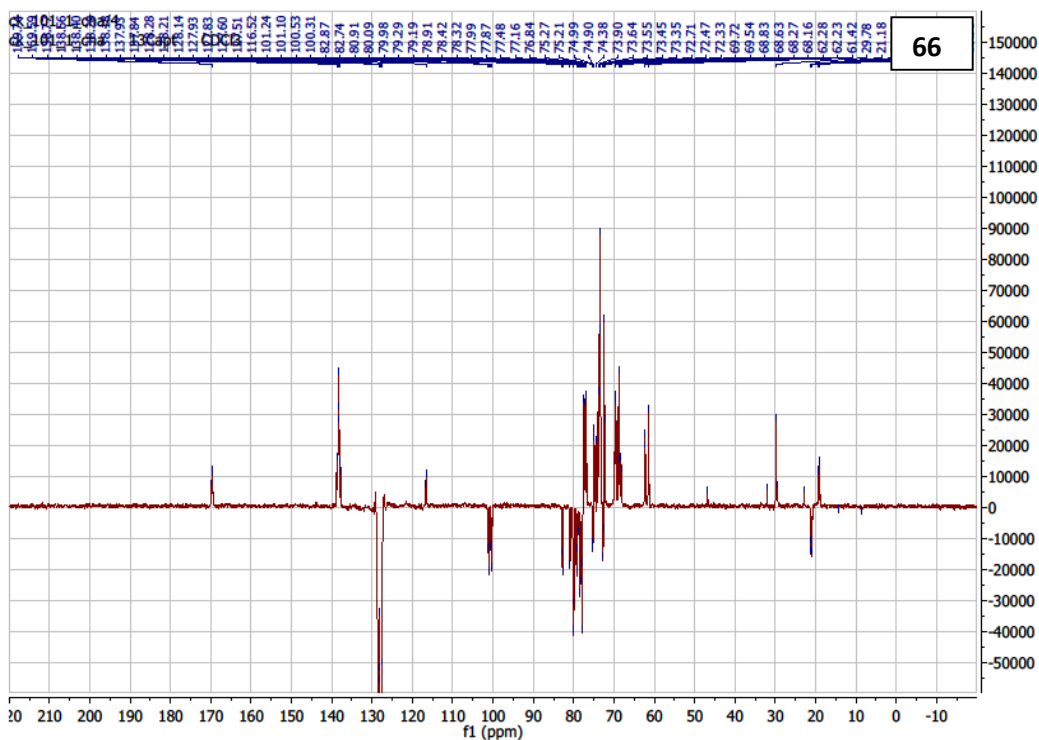
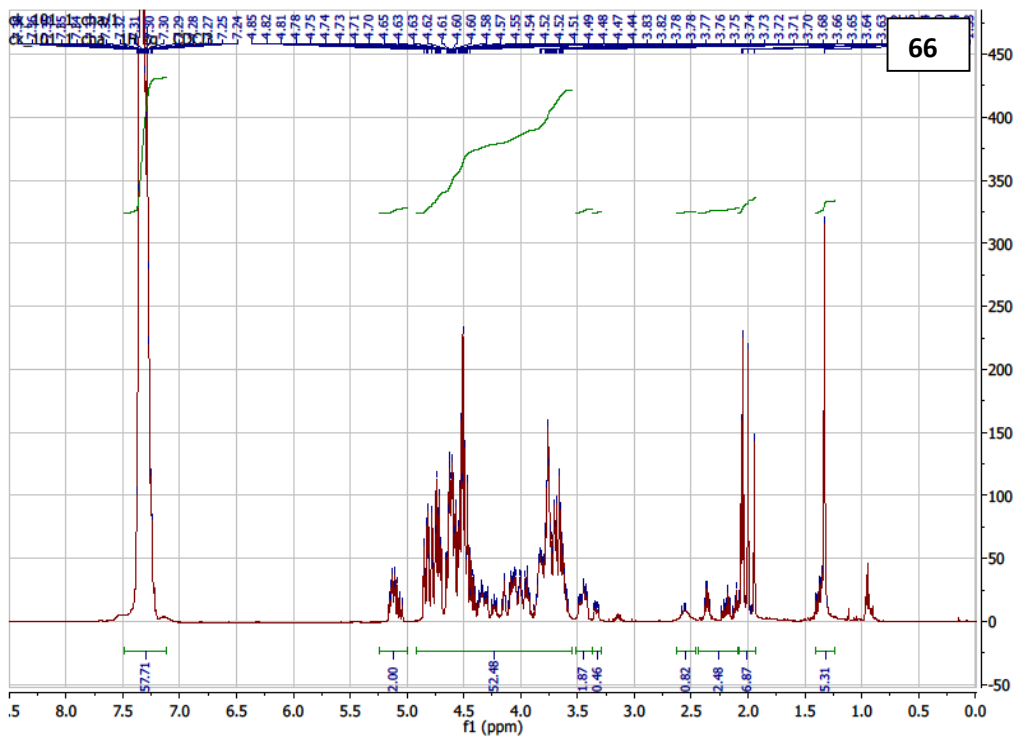


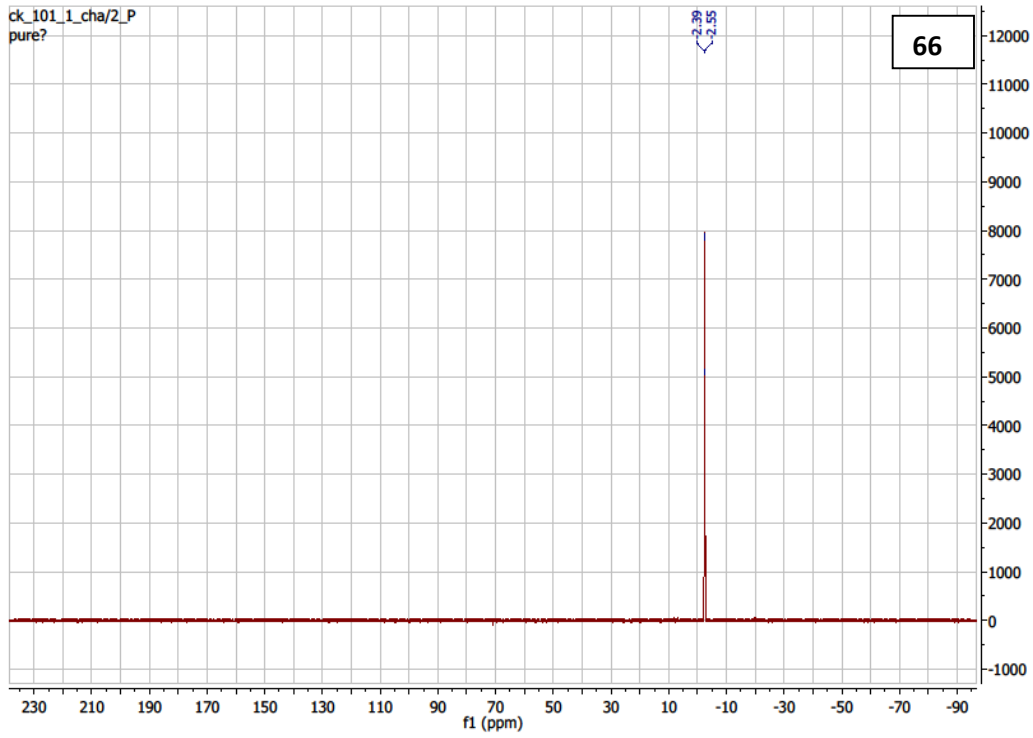


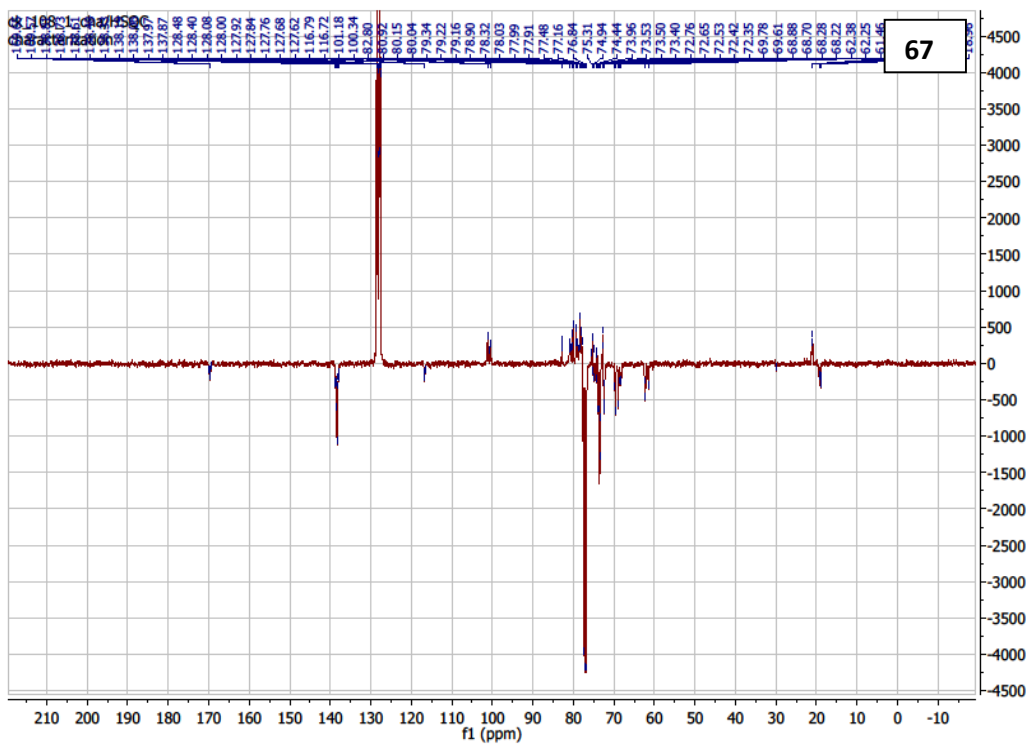
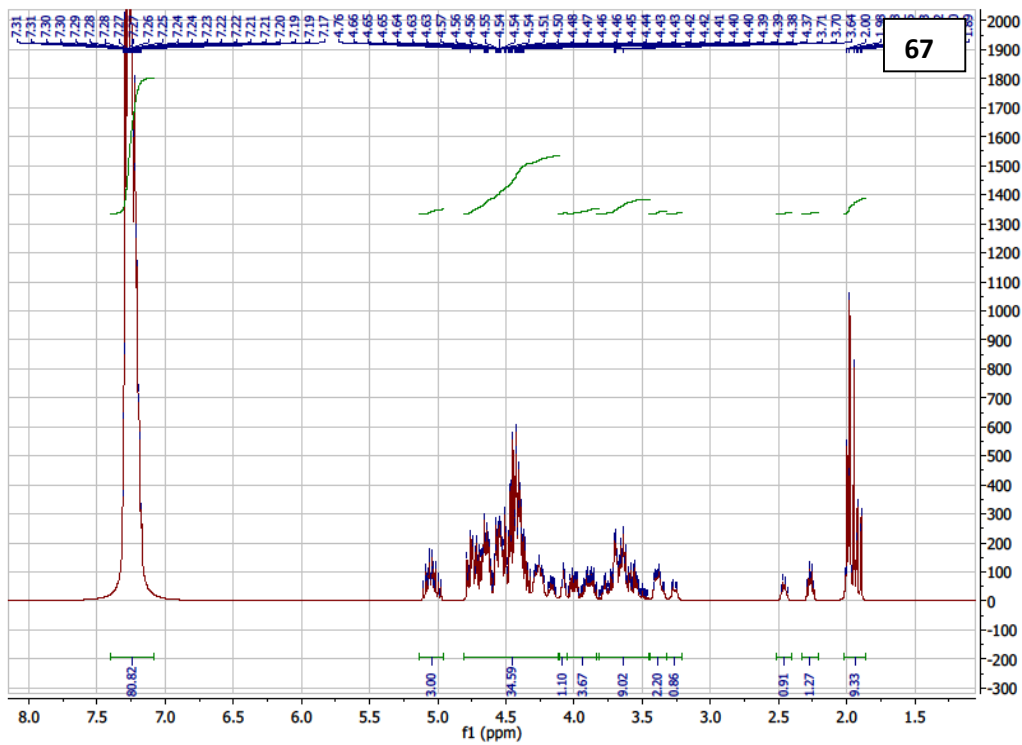
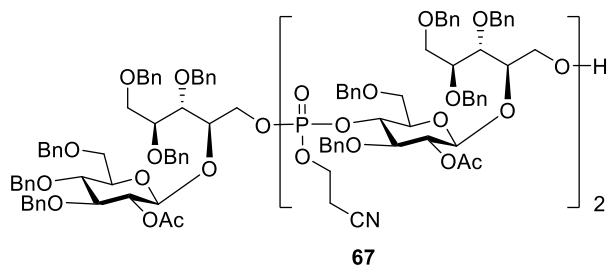


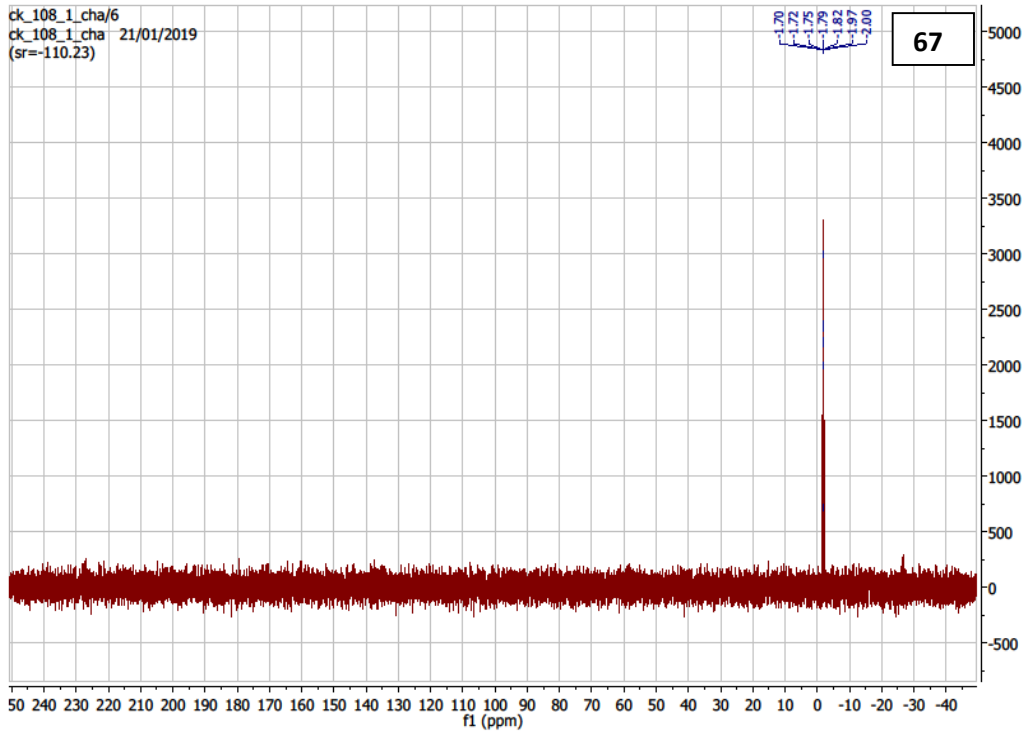


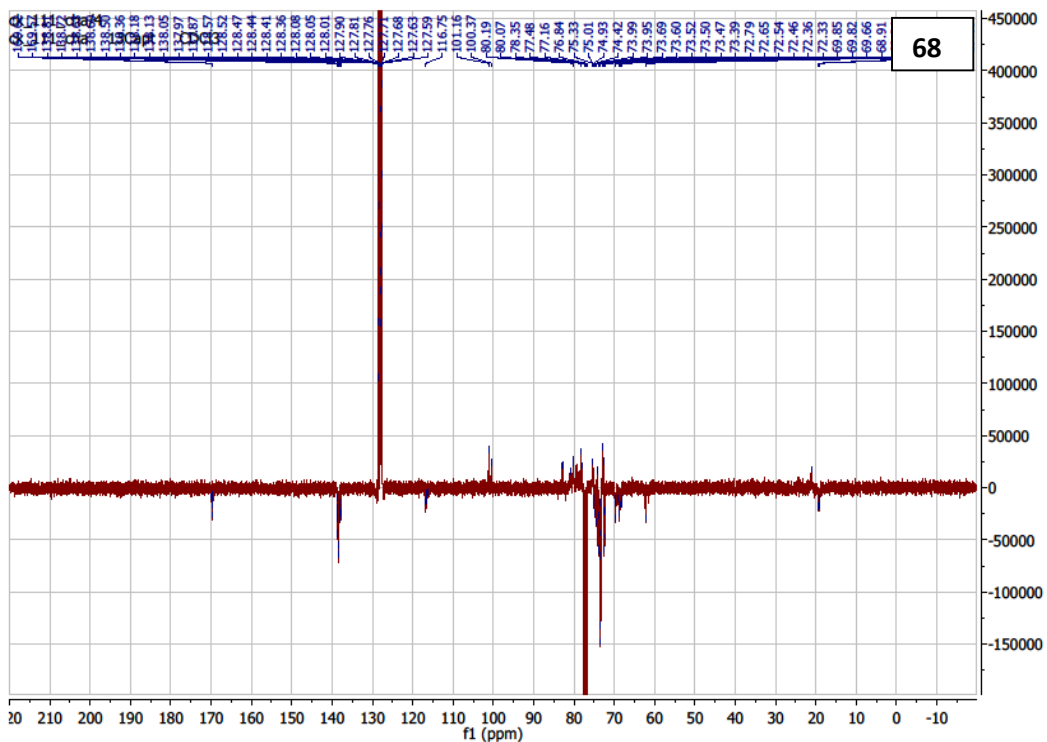
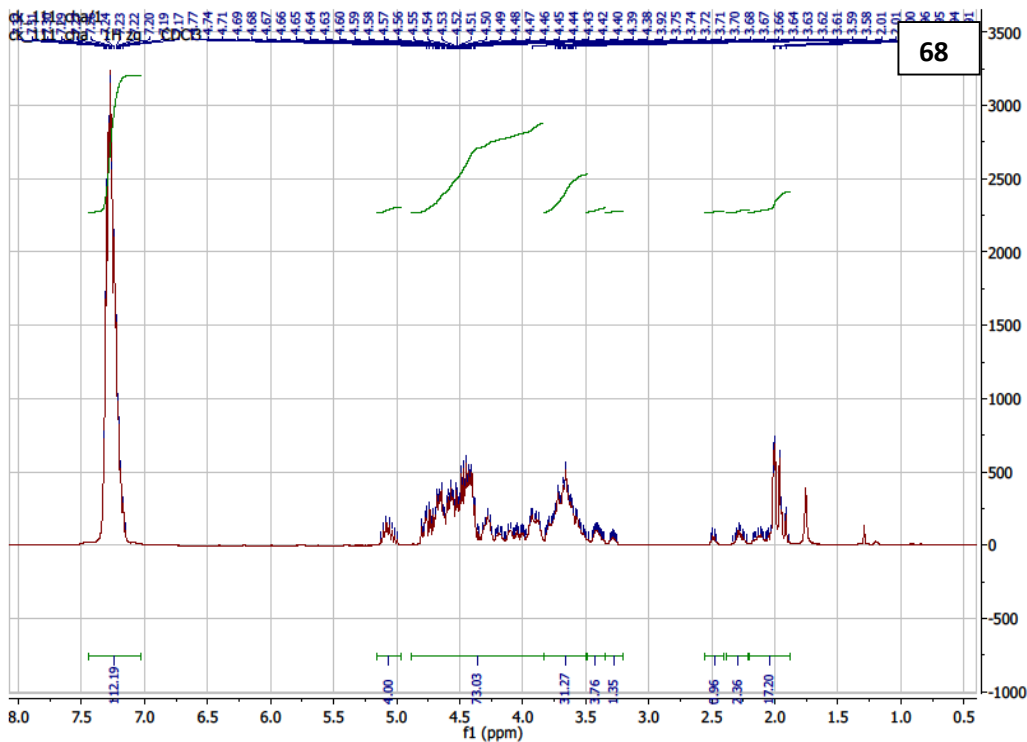
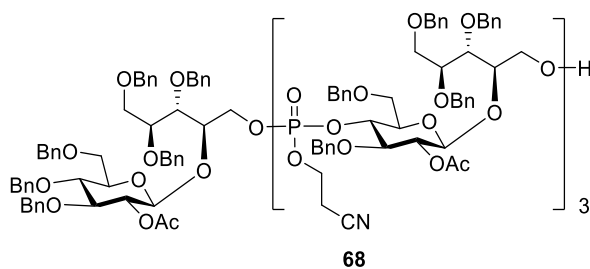
66

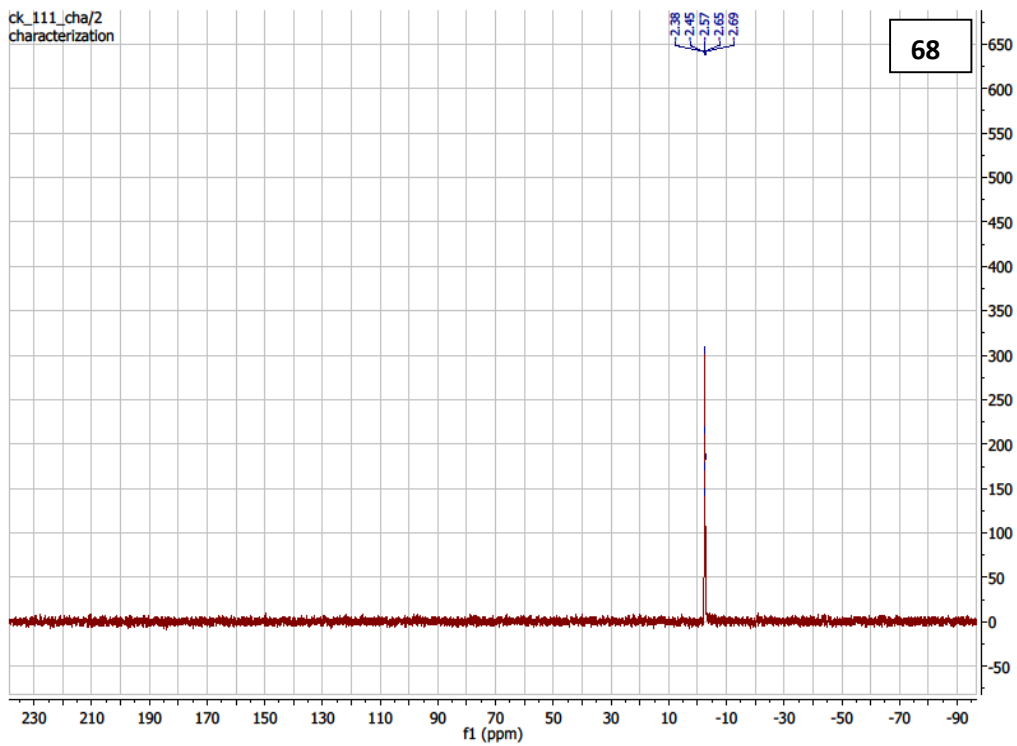


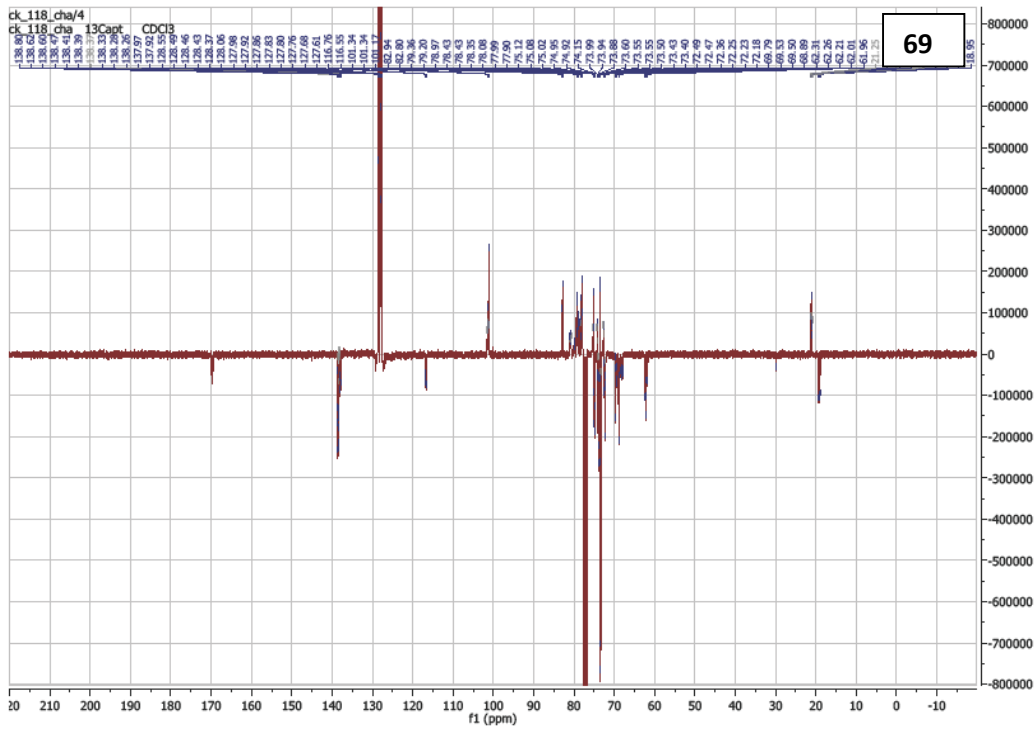
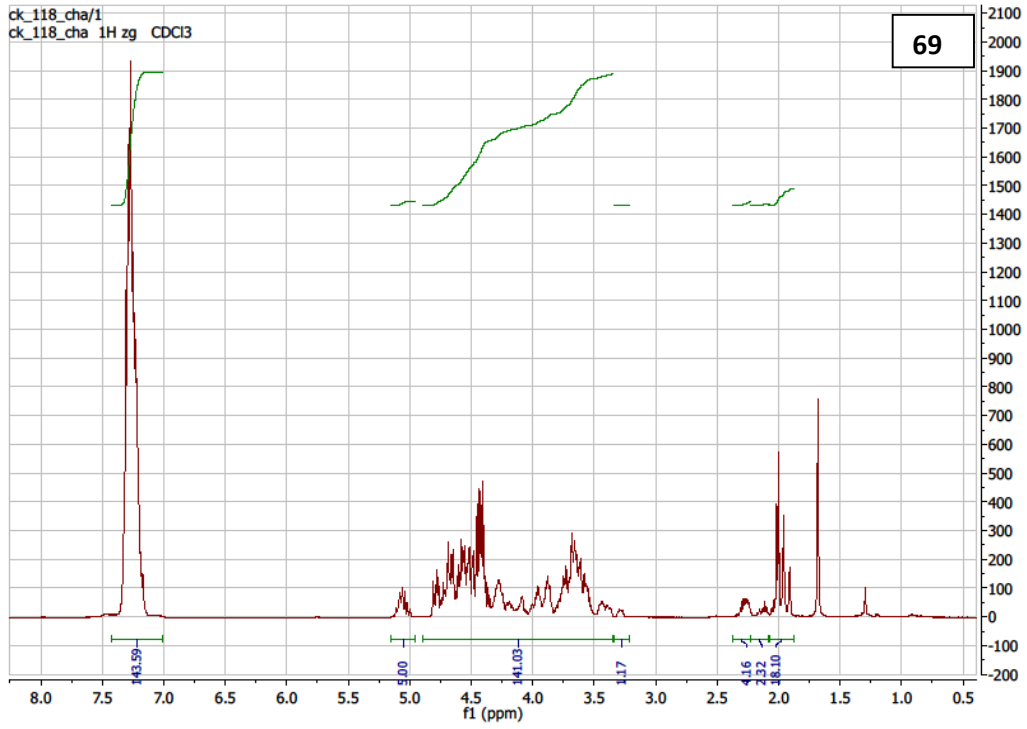
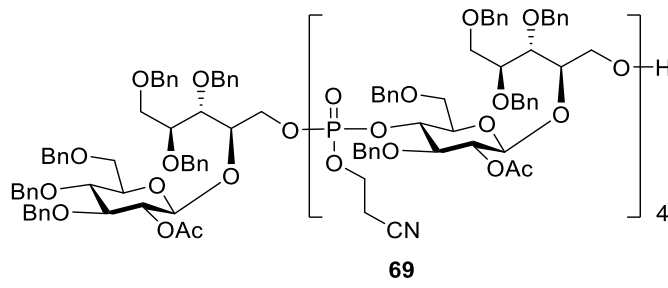




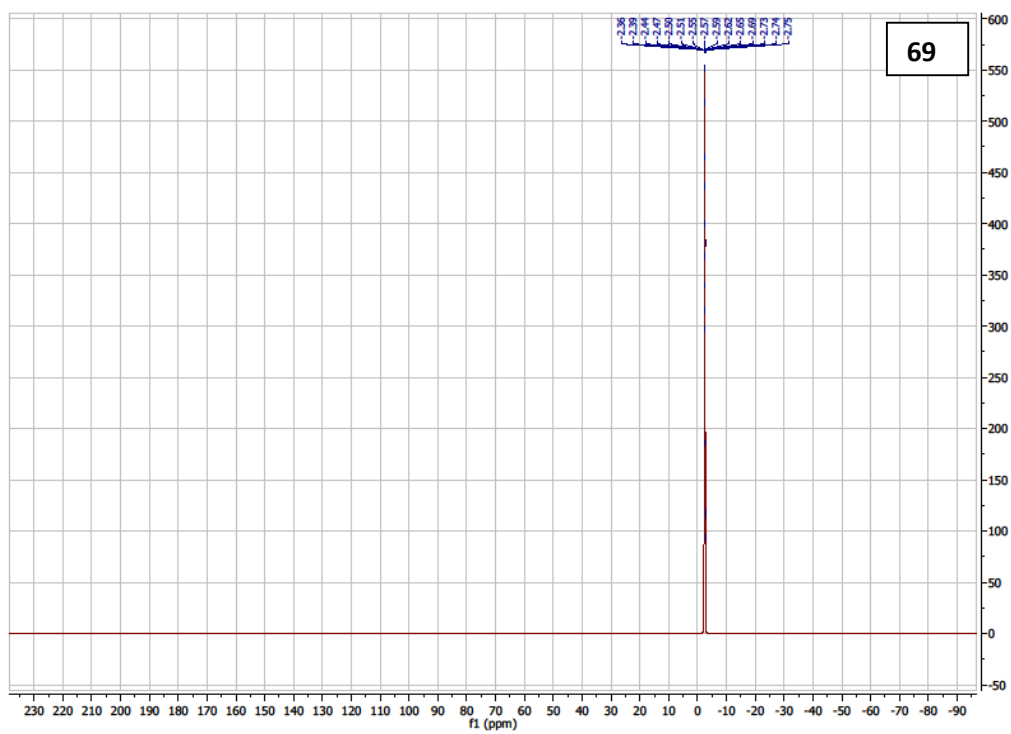


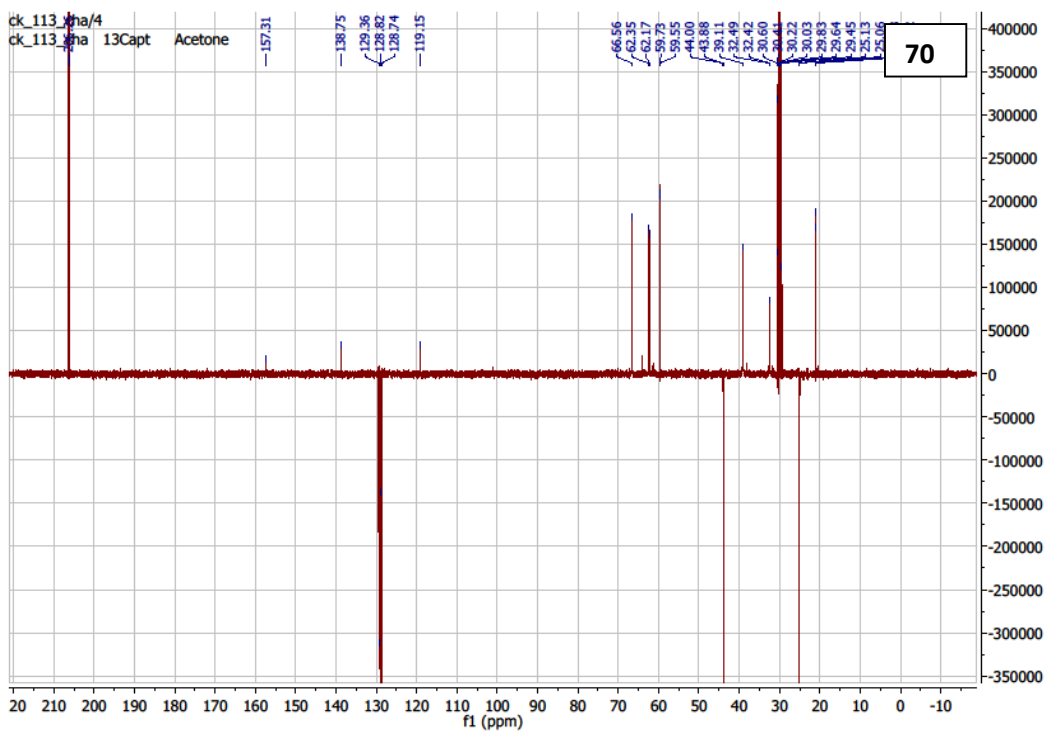
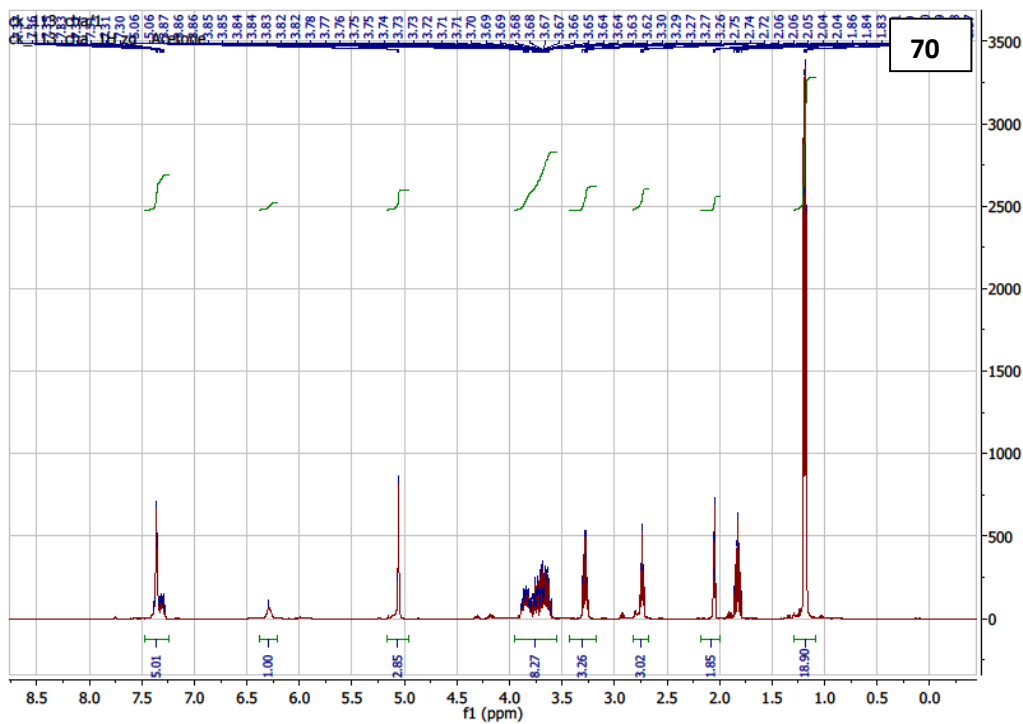
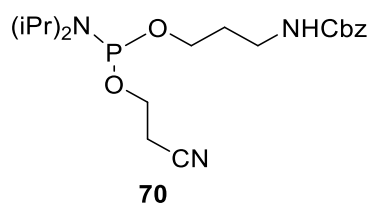


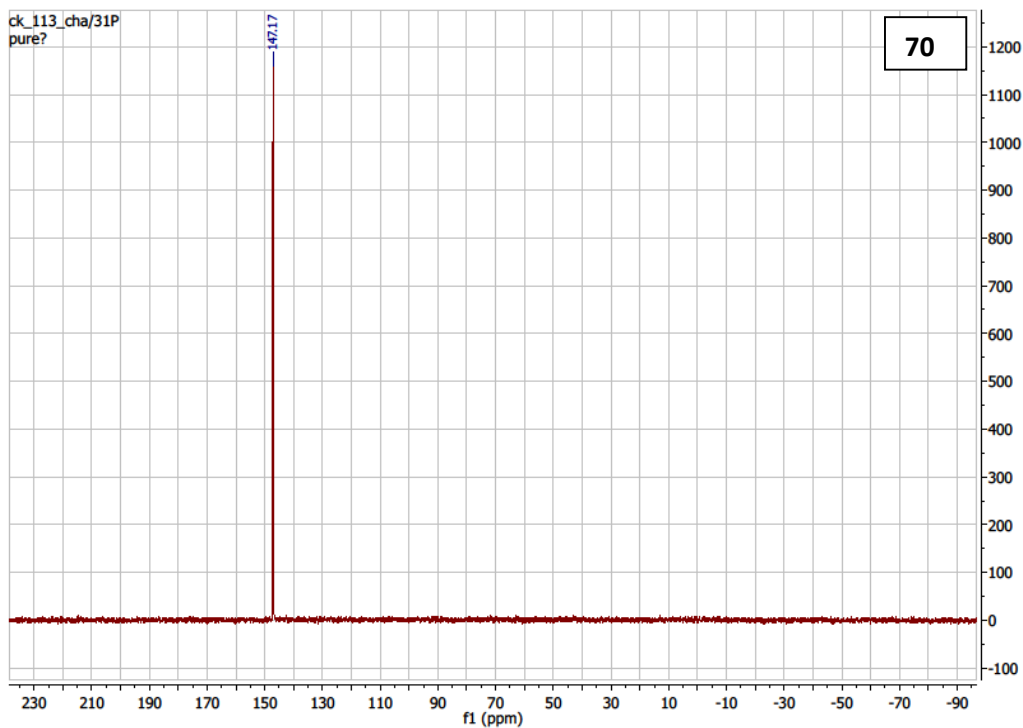


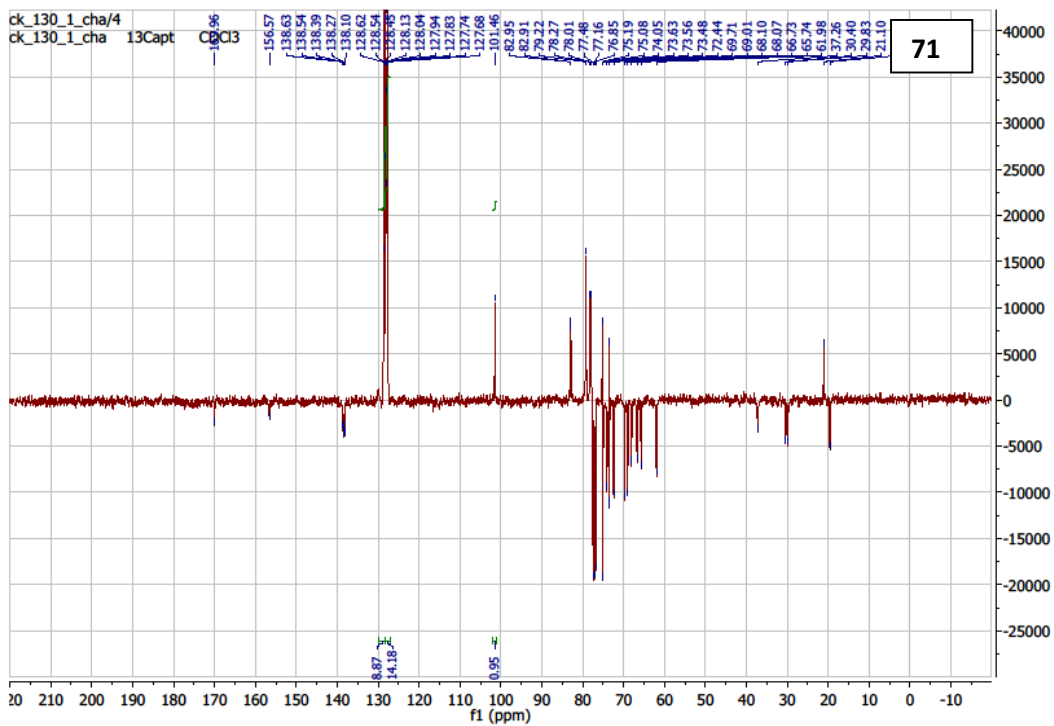
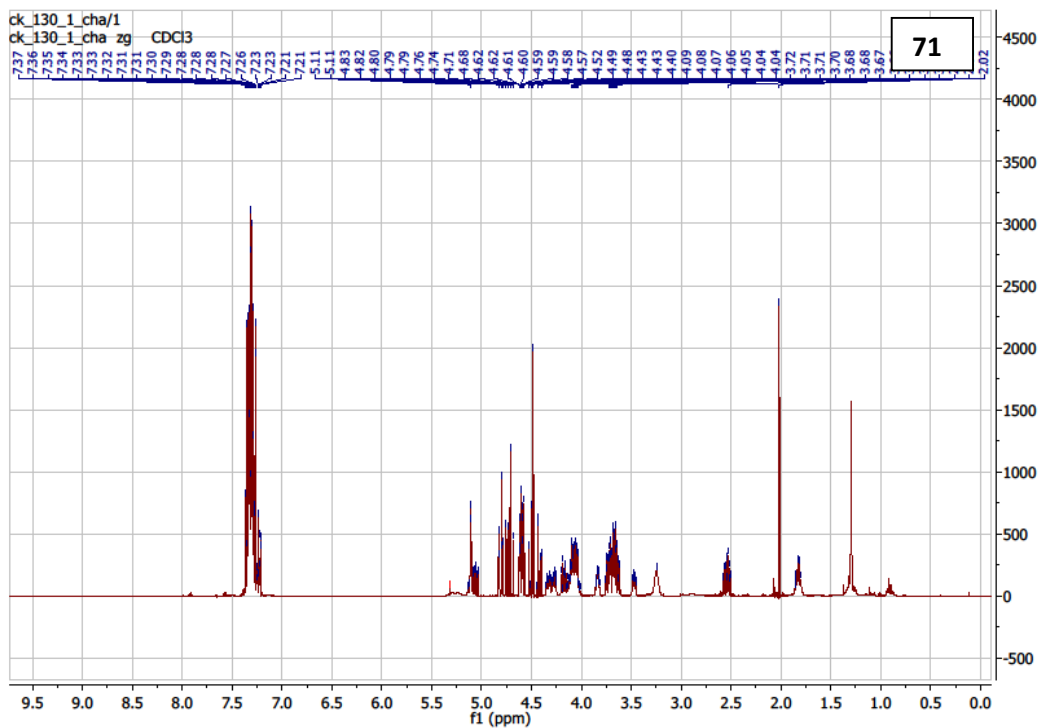
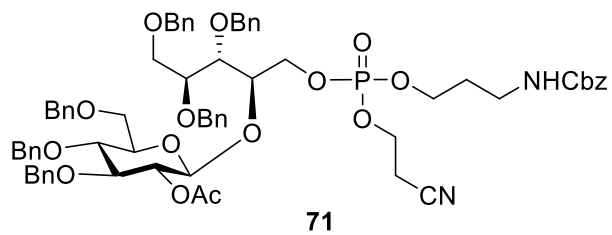


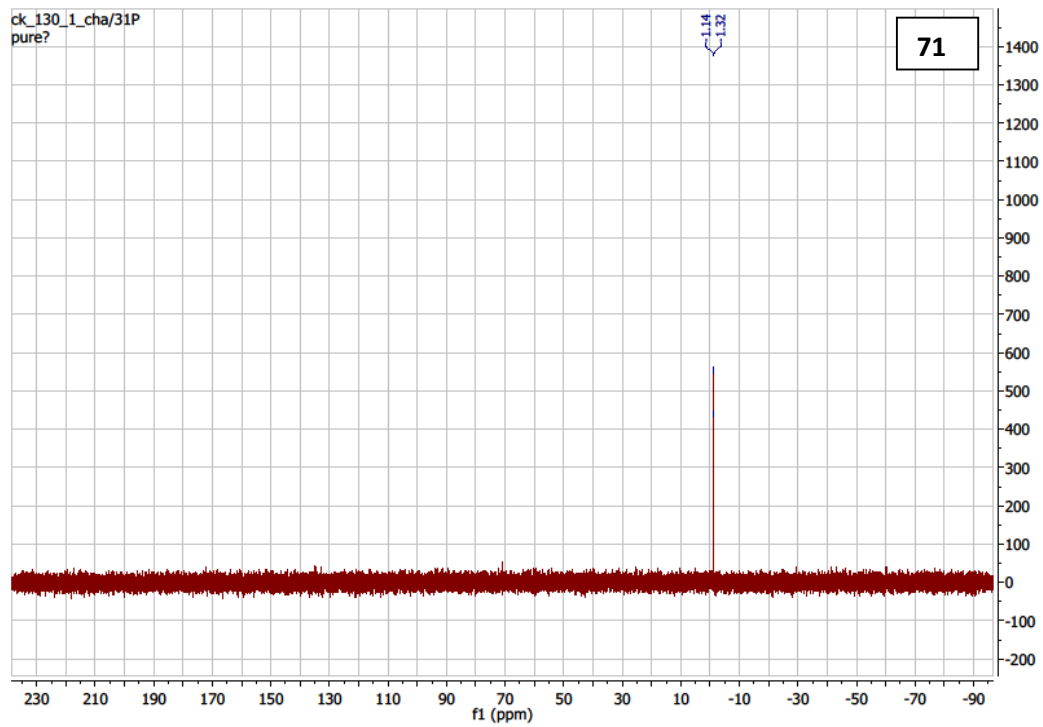


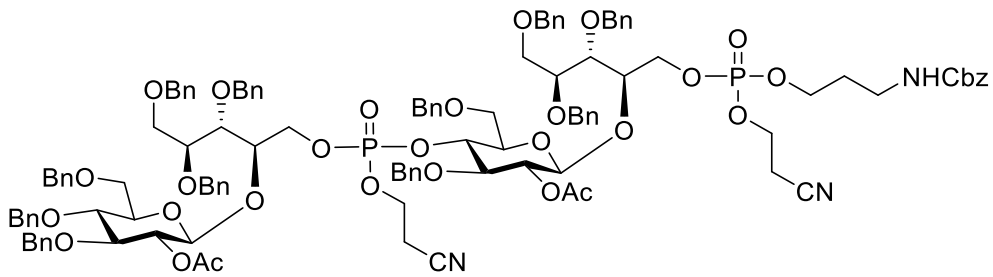




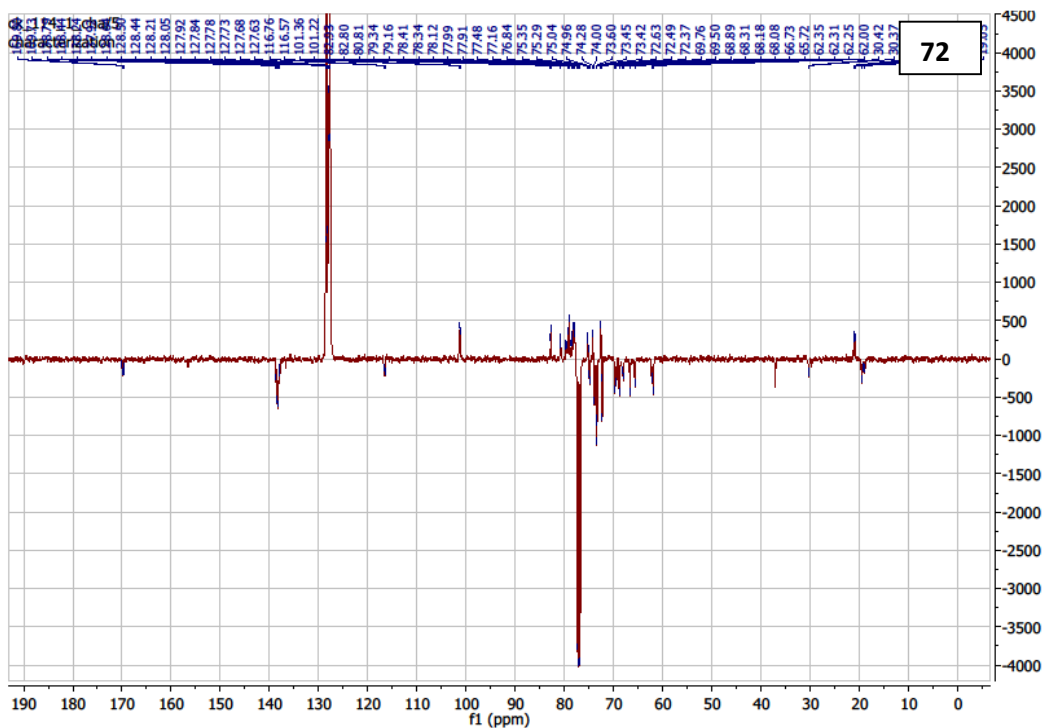
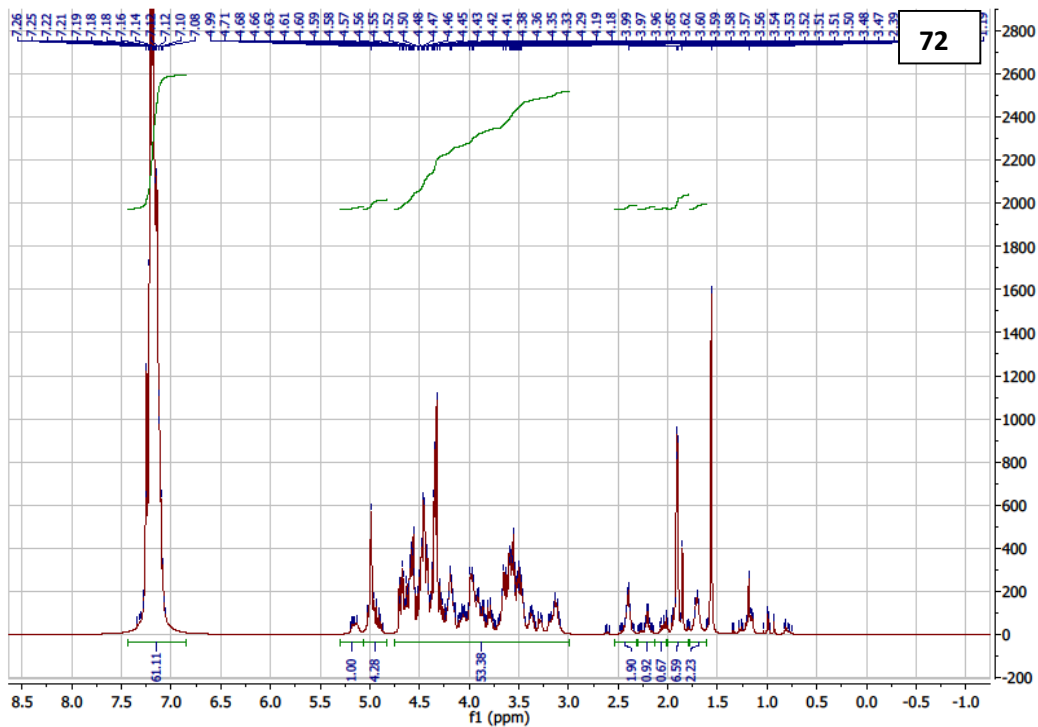


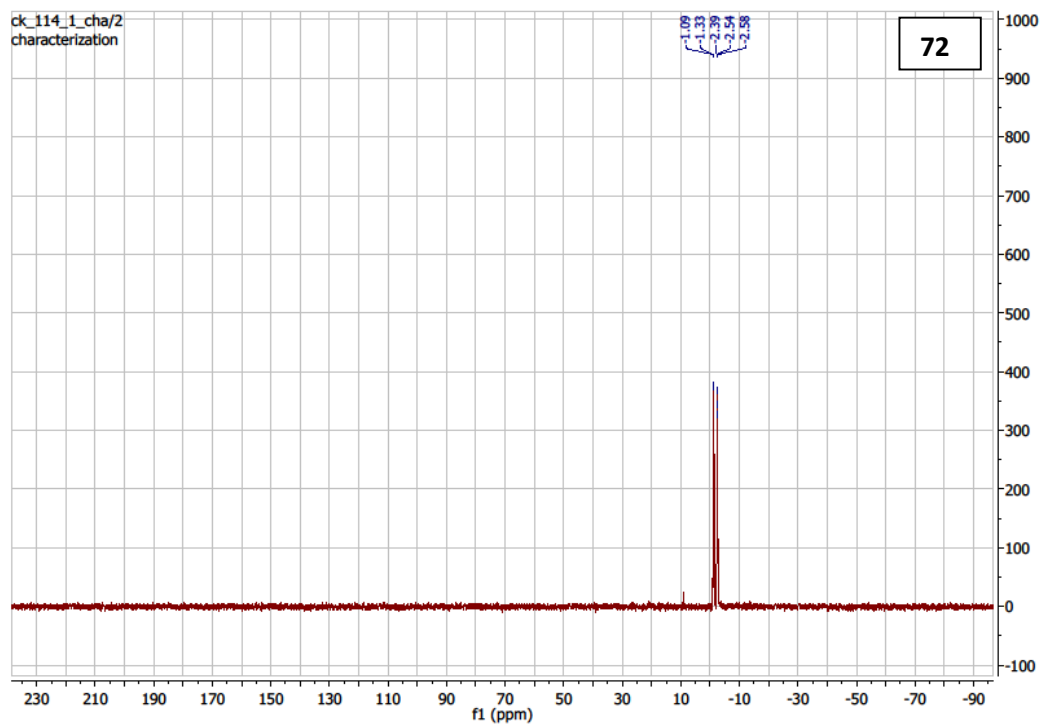


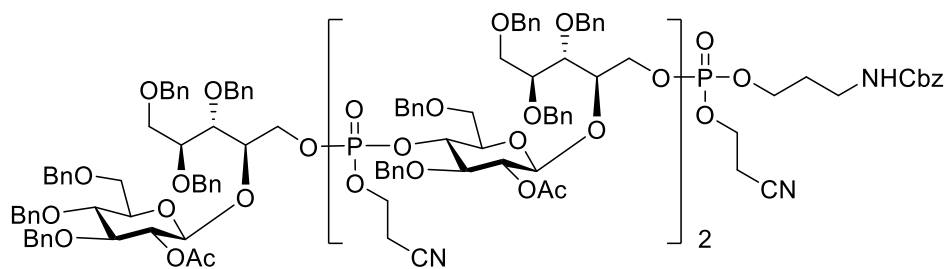




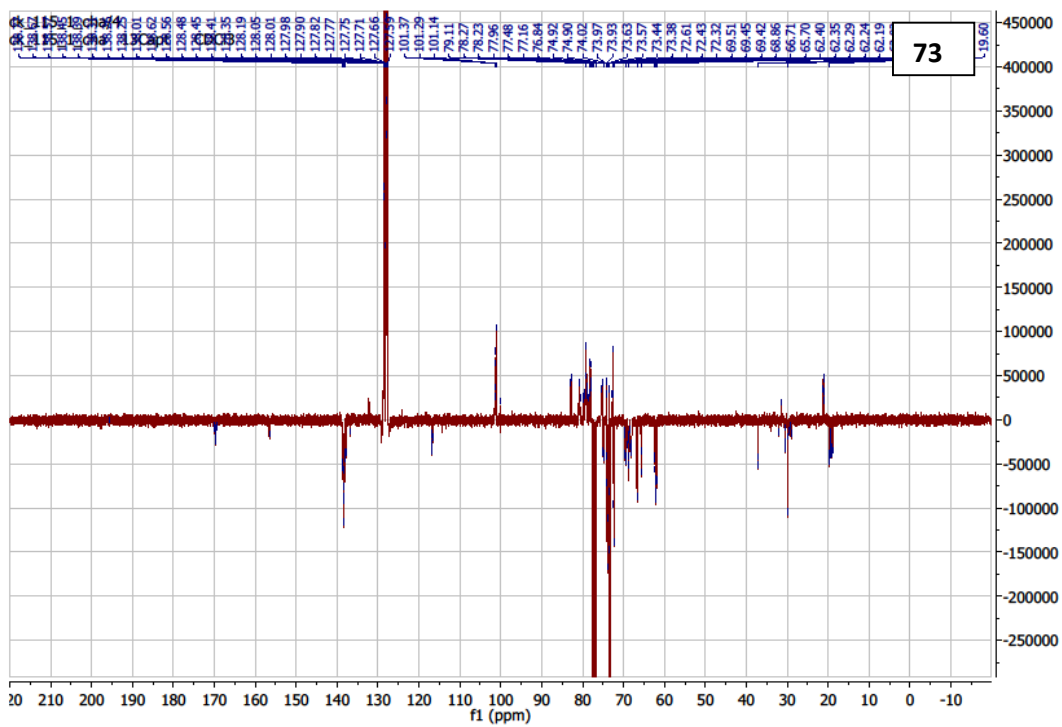
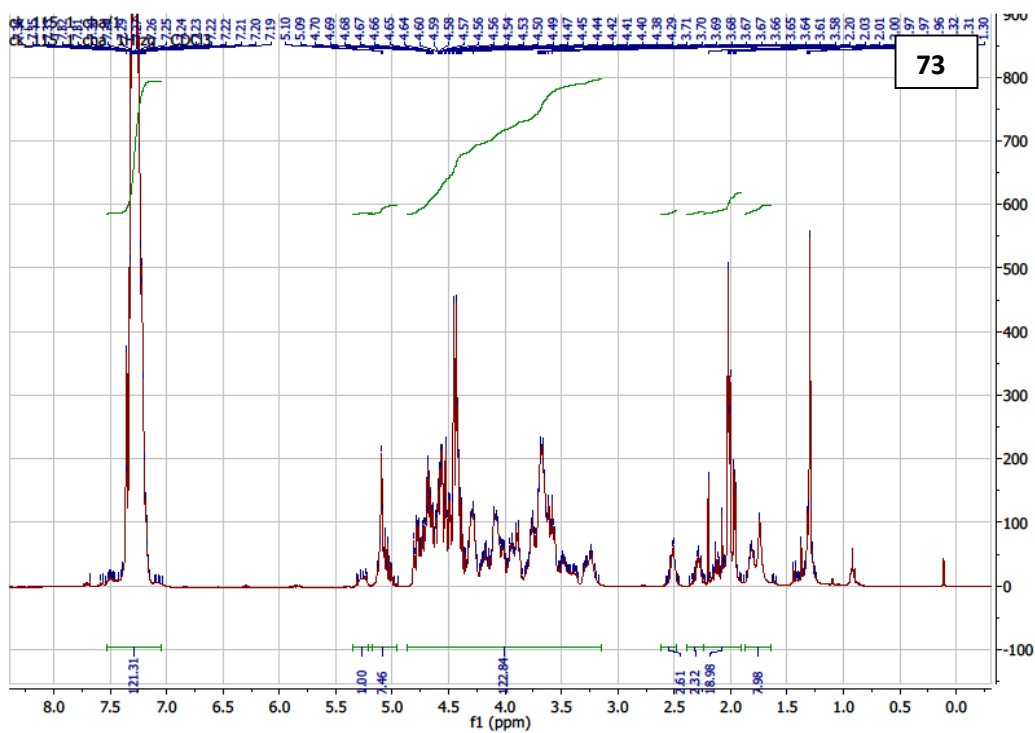
72



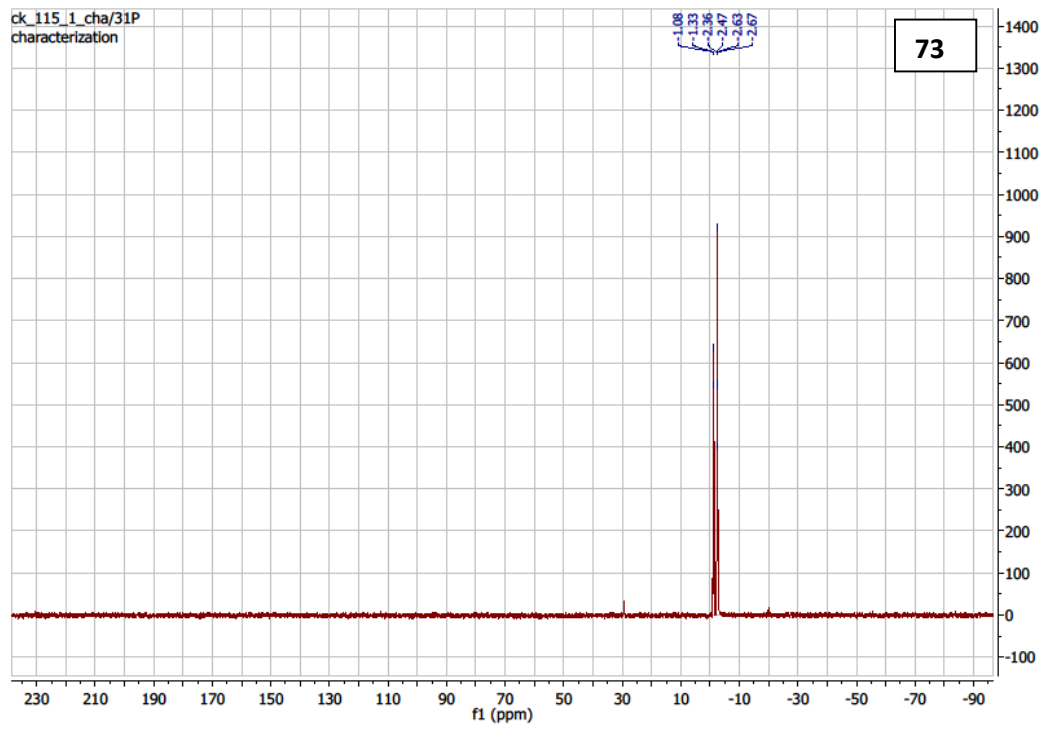


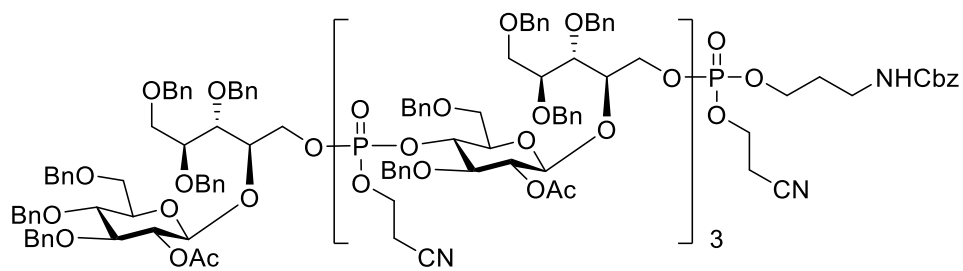


73

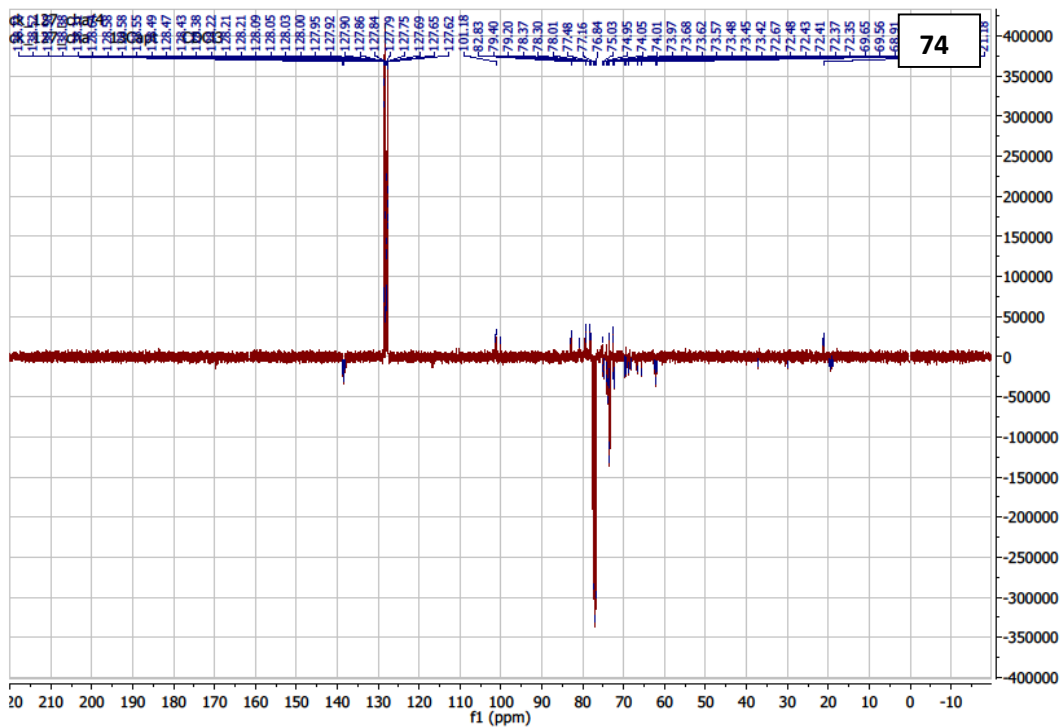
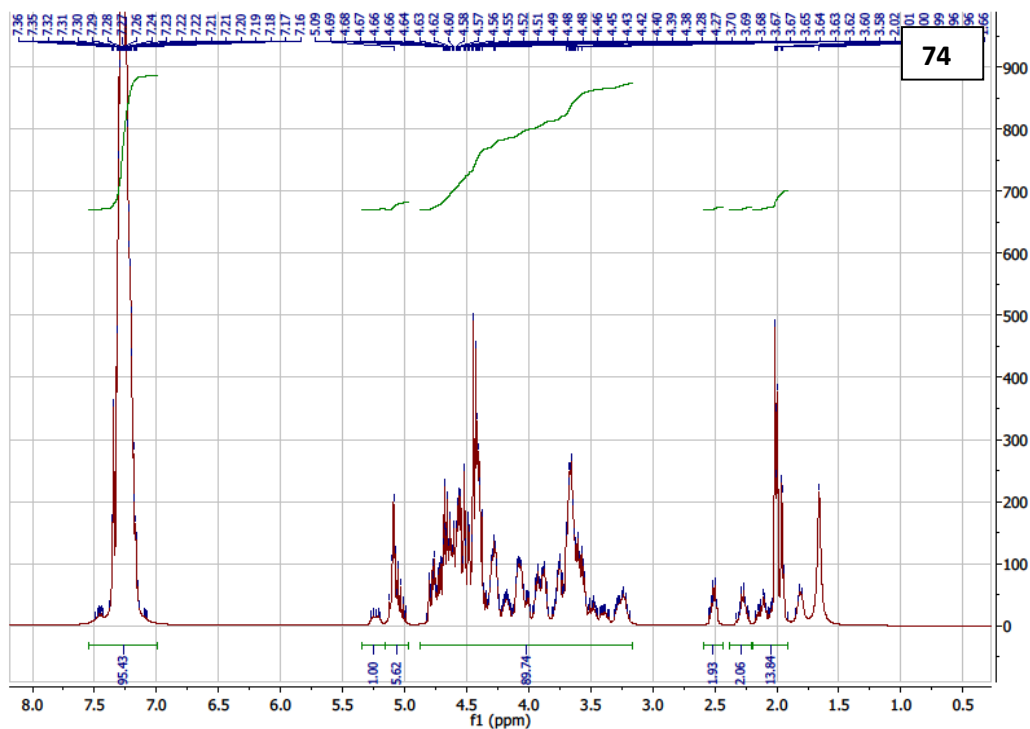


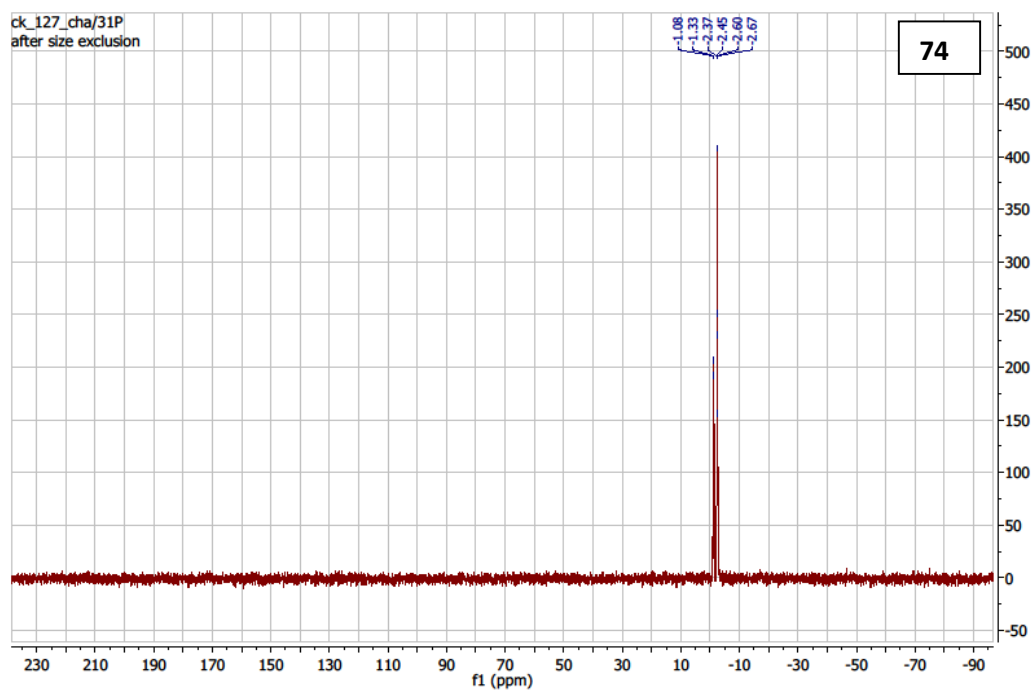


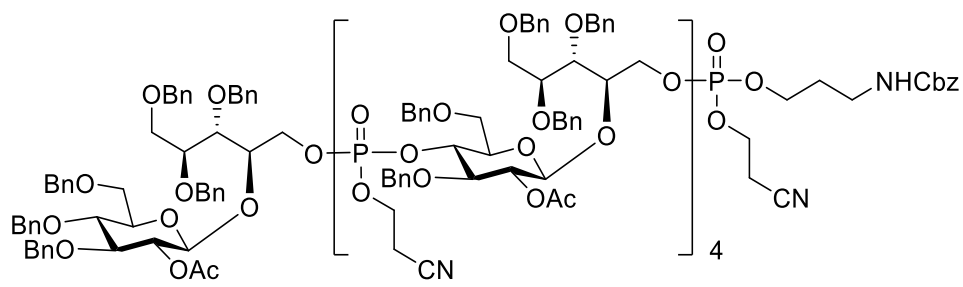




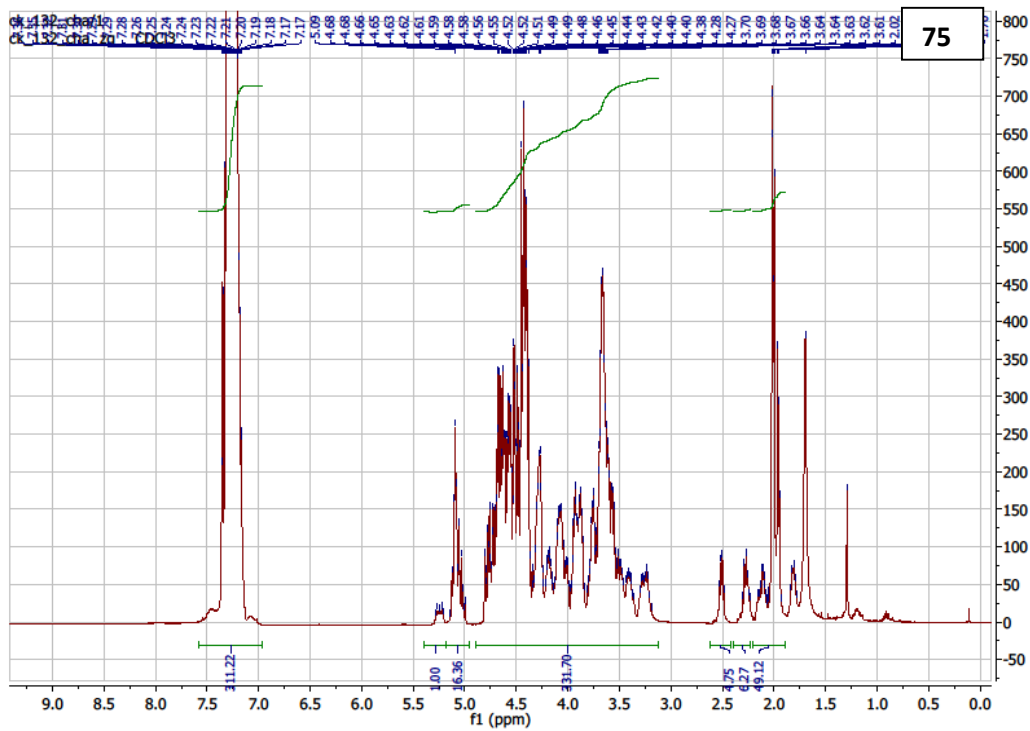
74

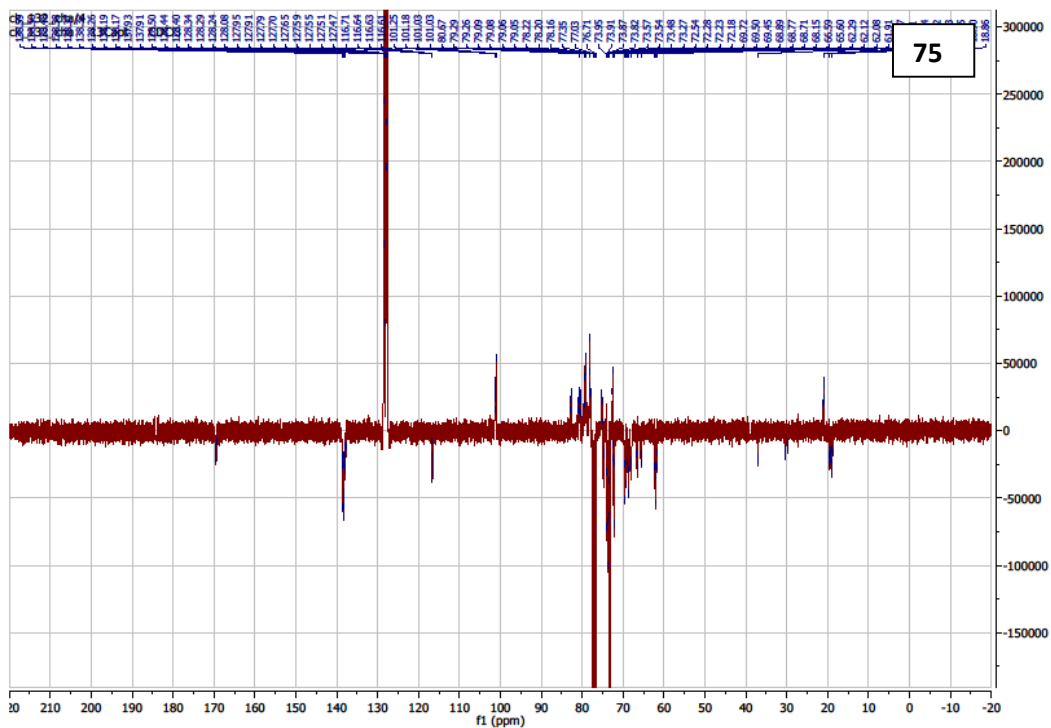


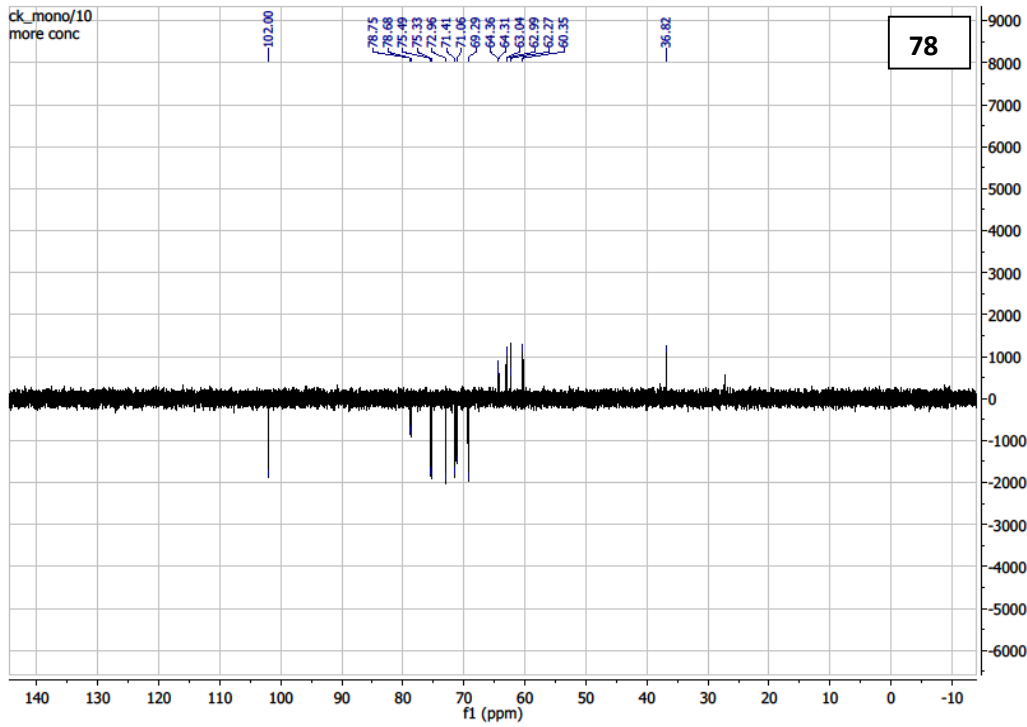
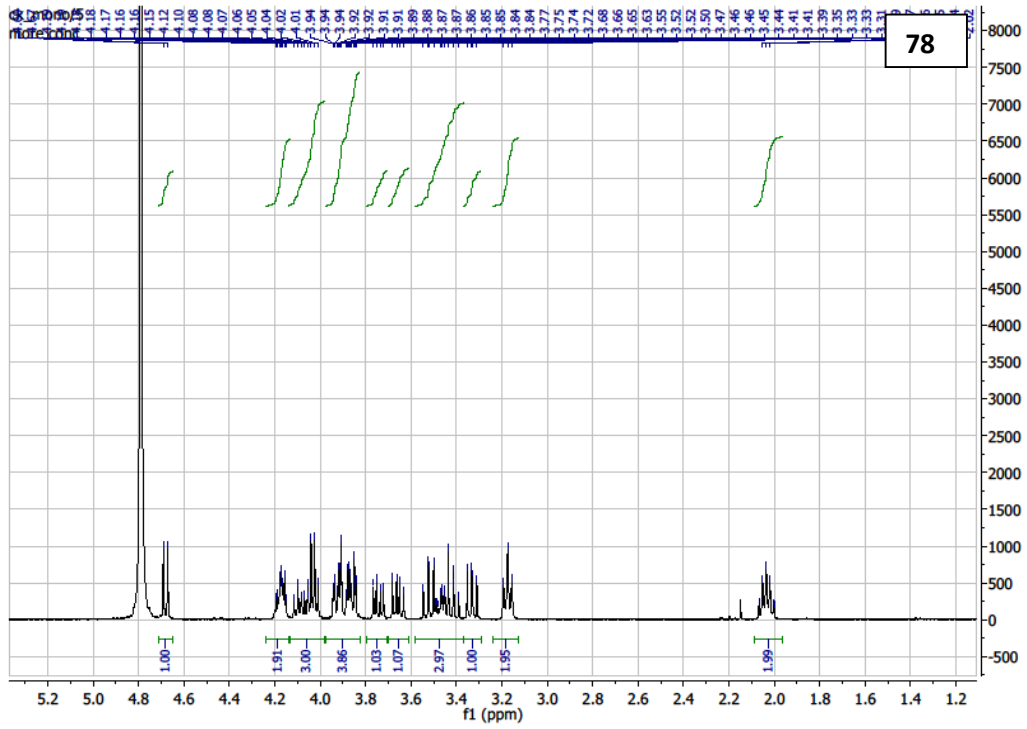
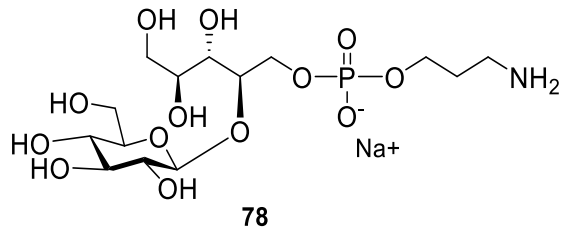


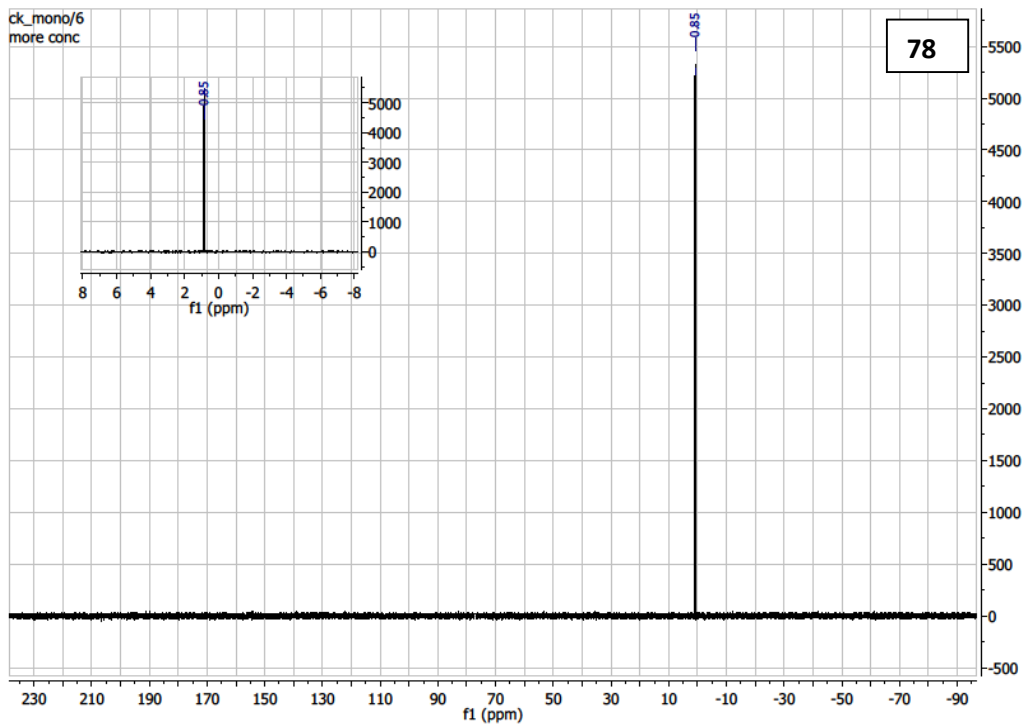


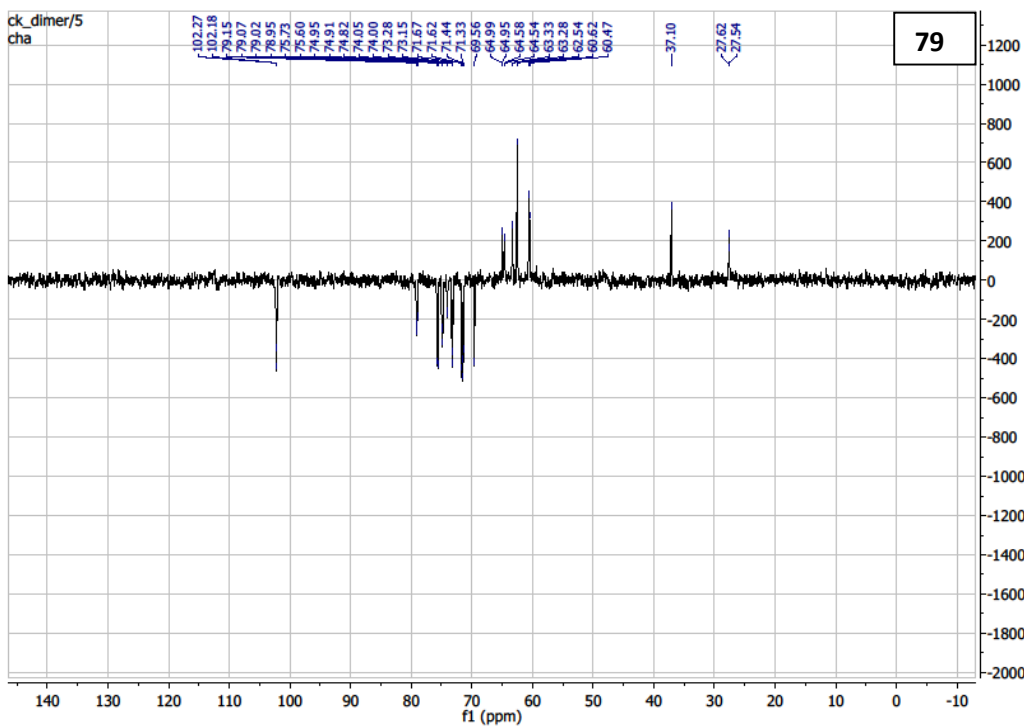
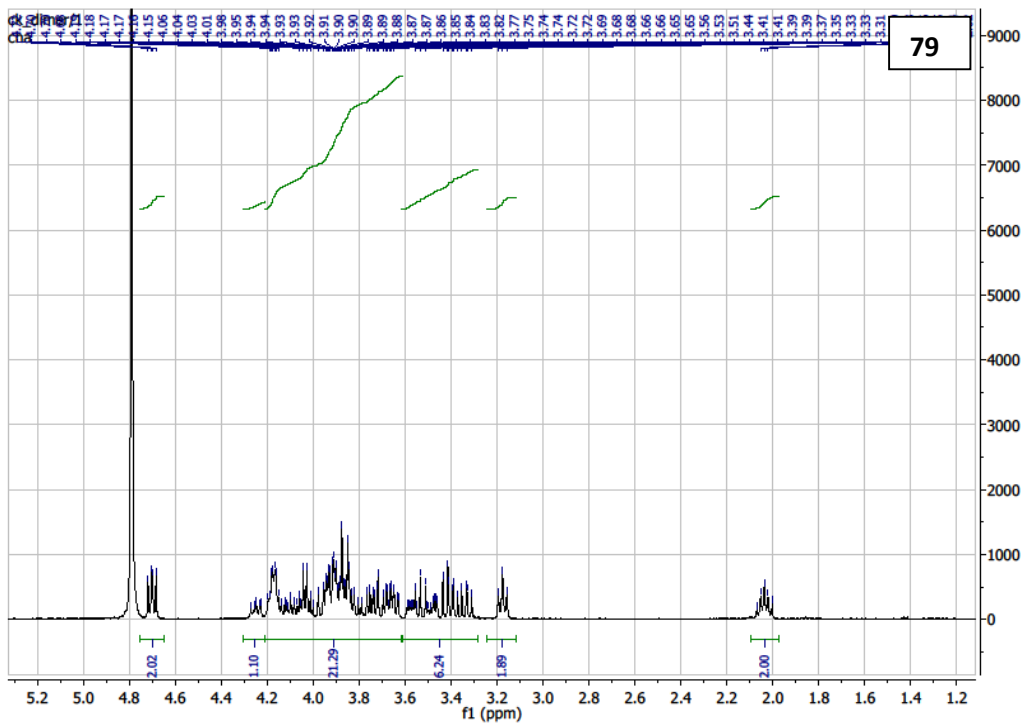
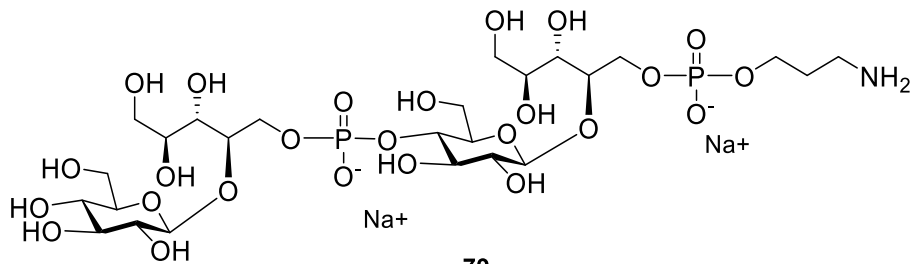
75



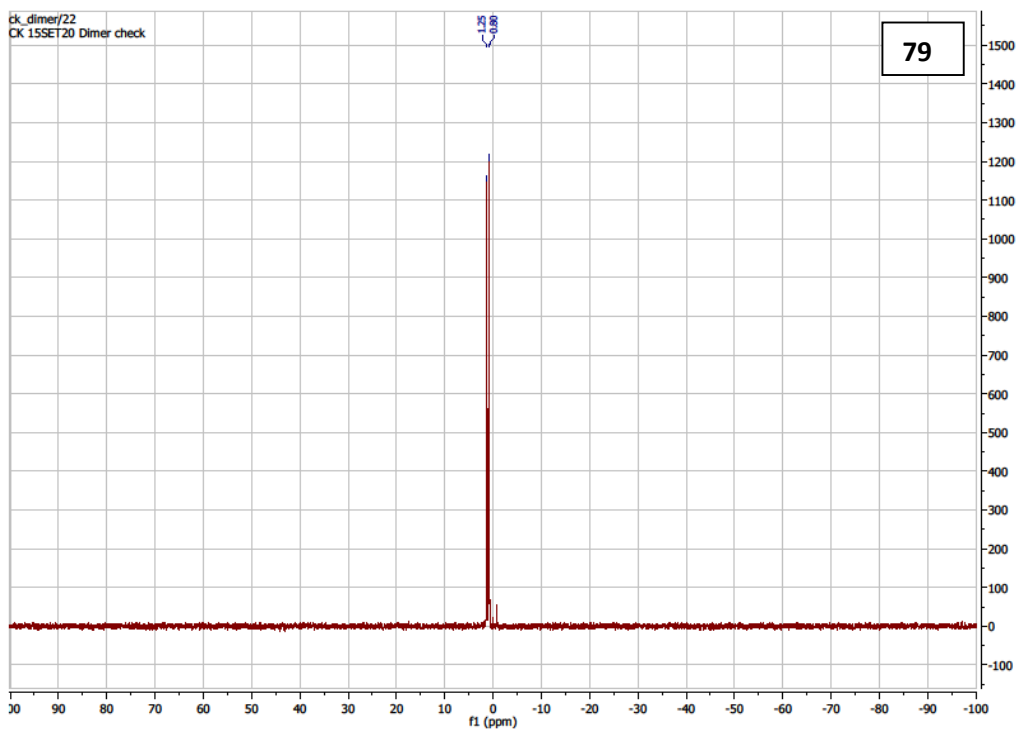


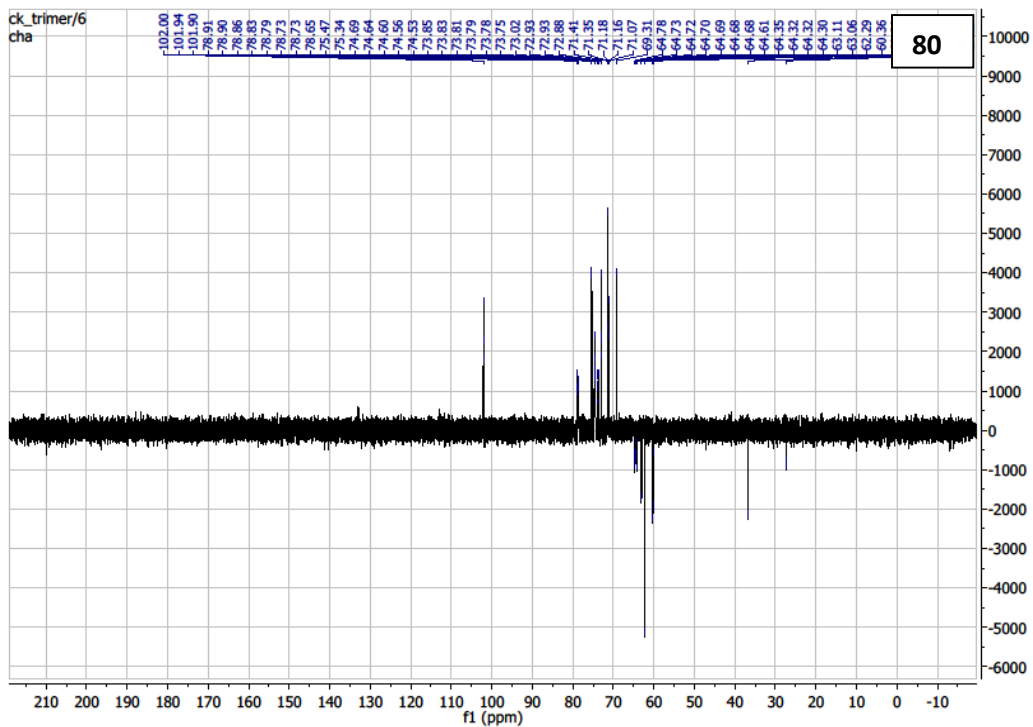
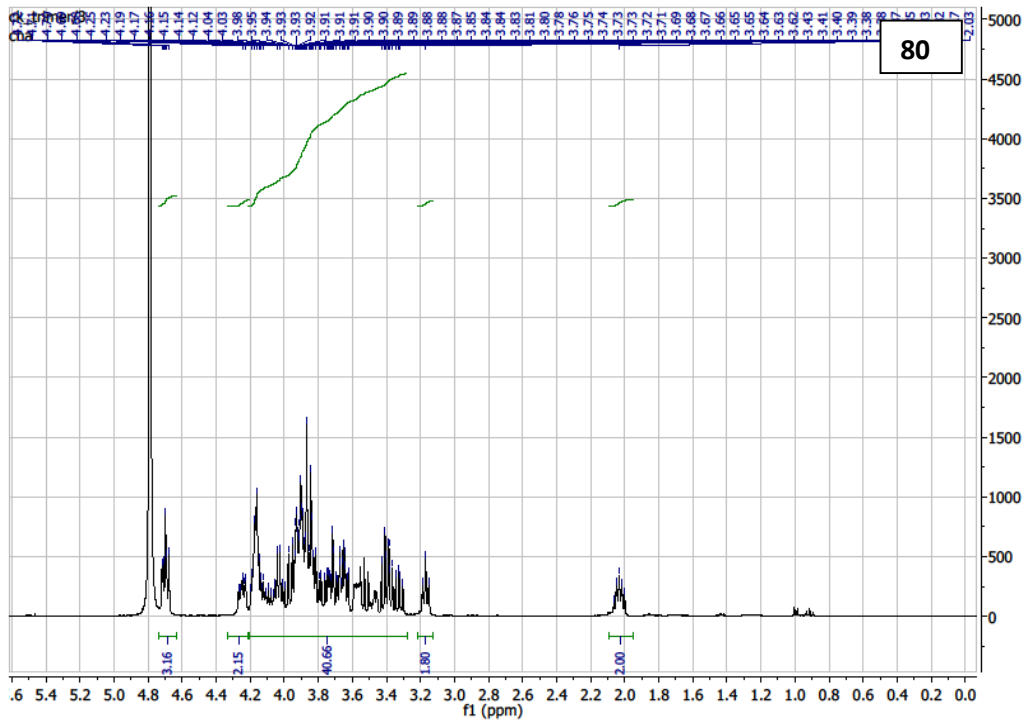
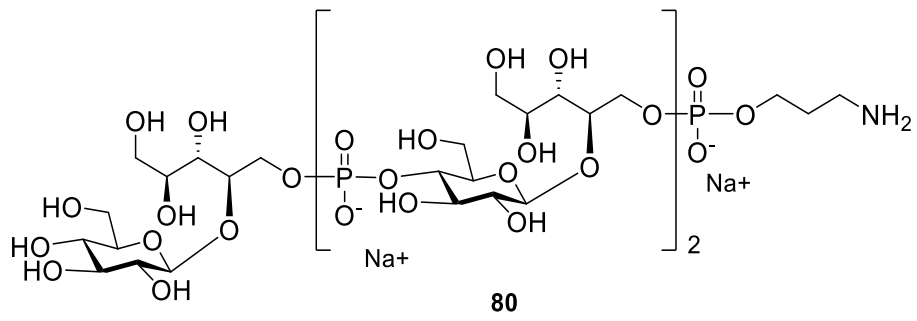


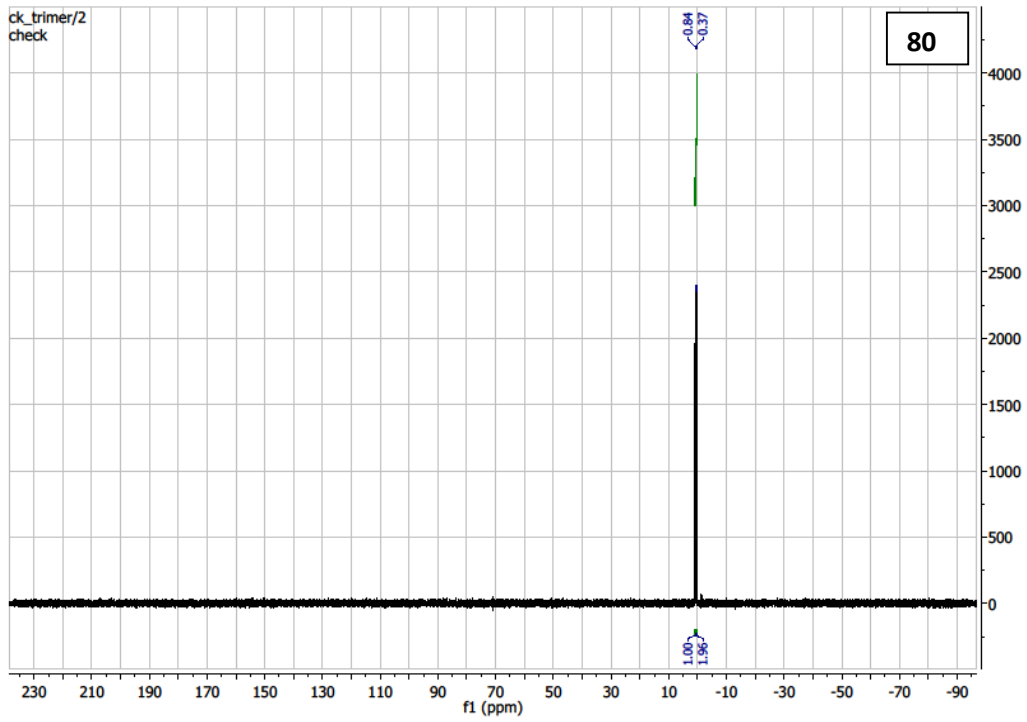


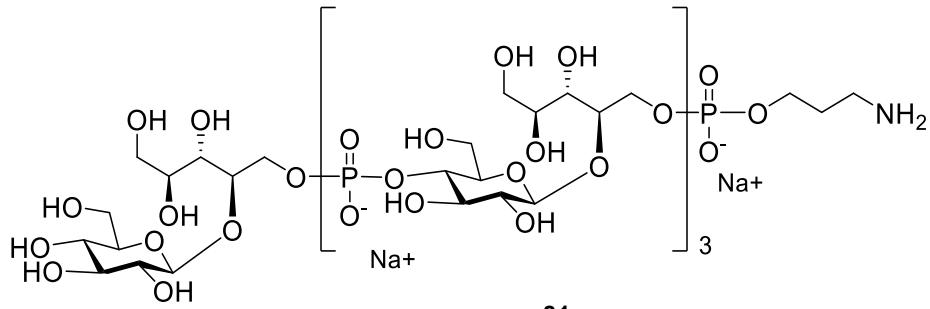




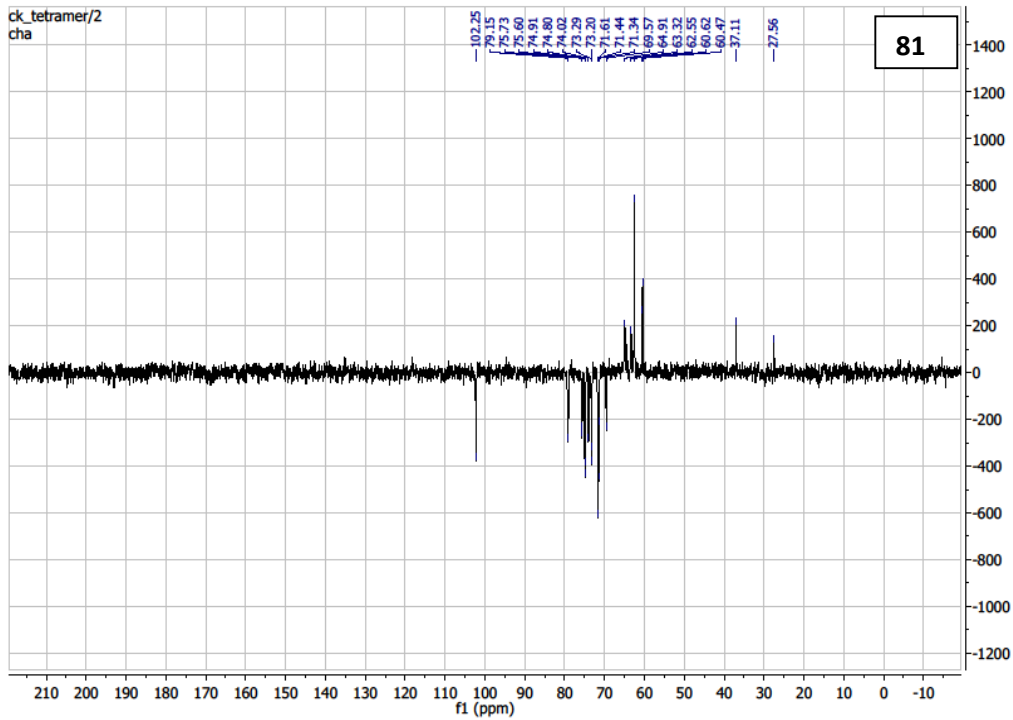
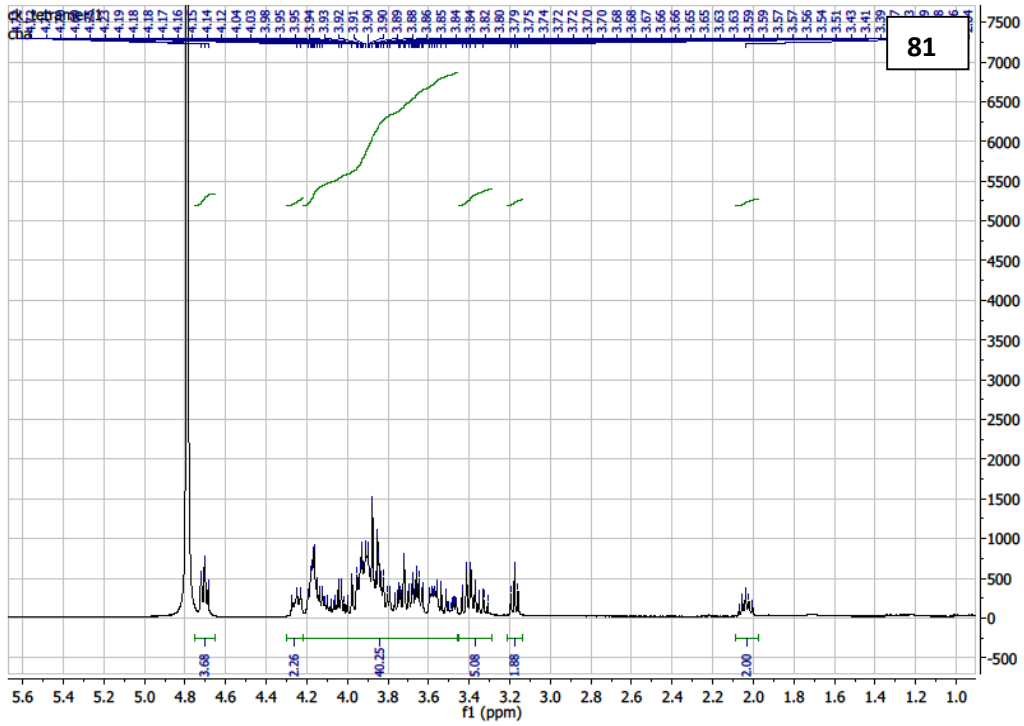


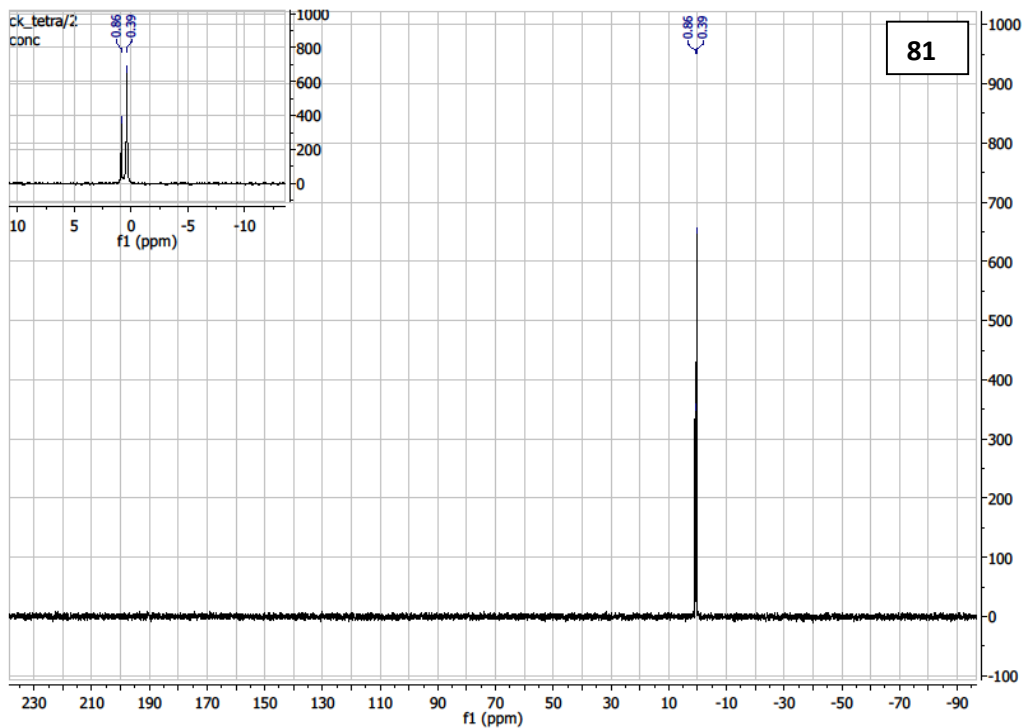


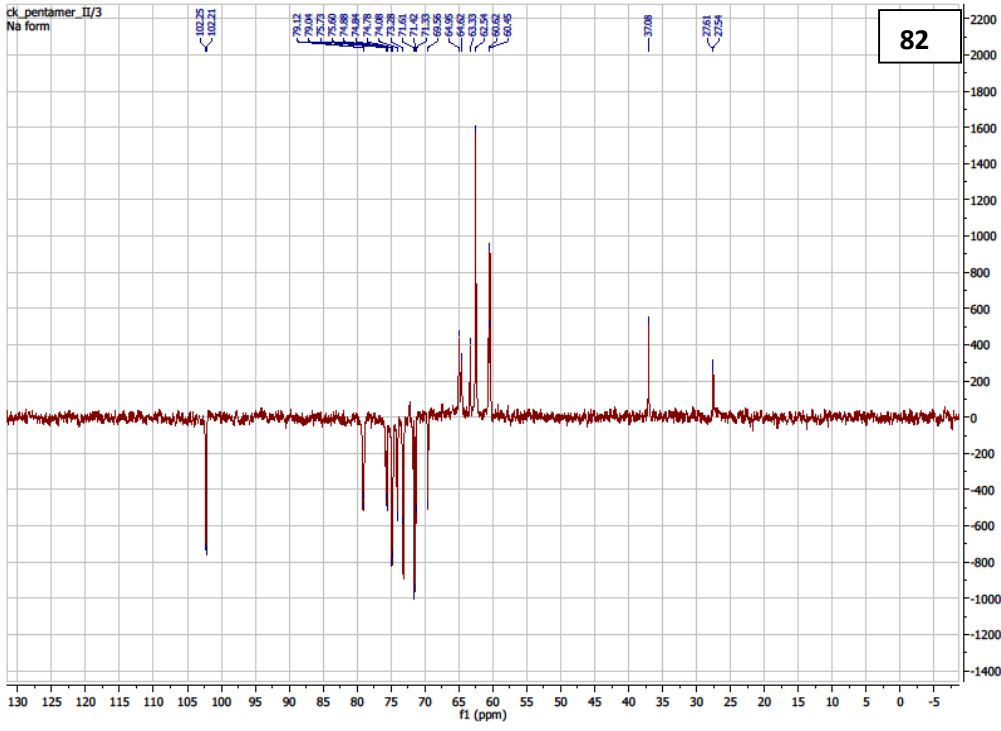
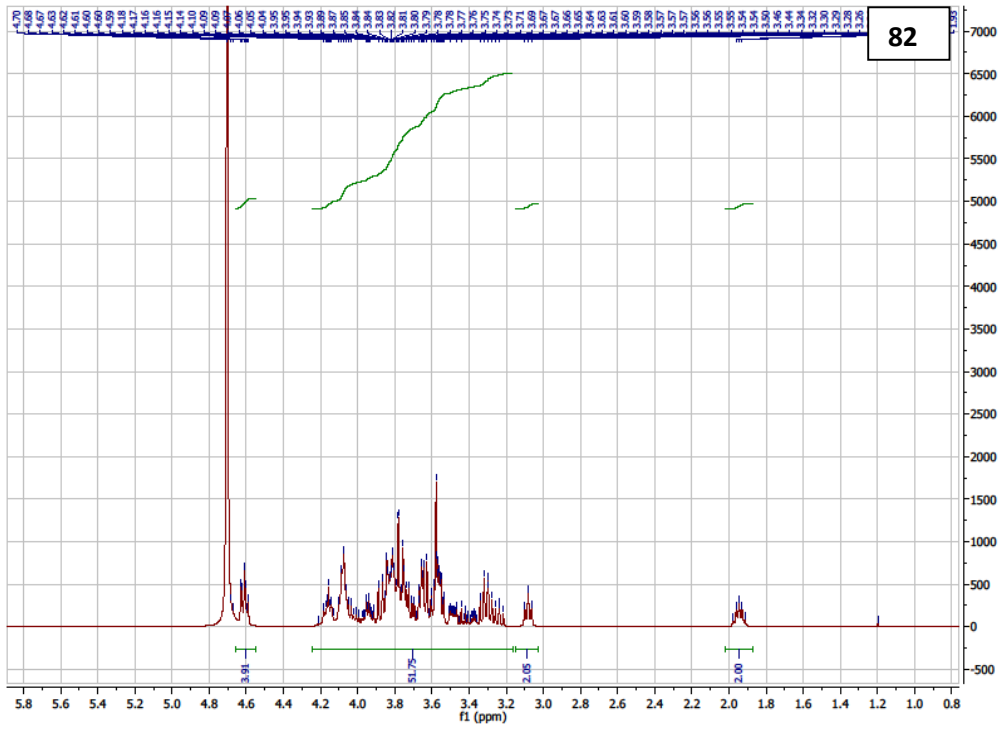
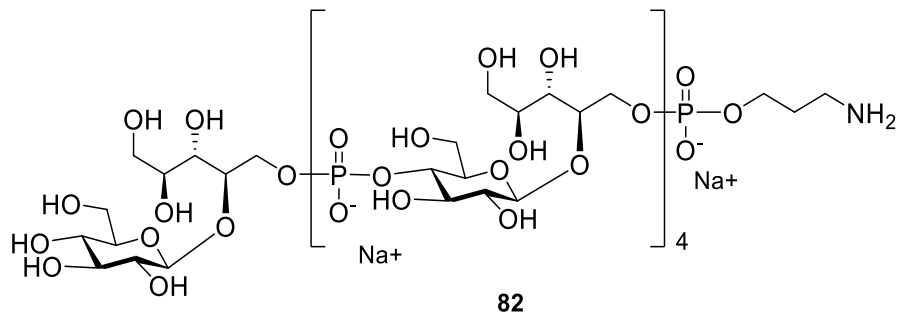


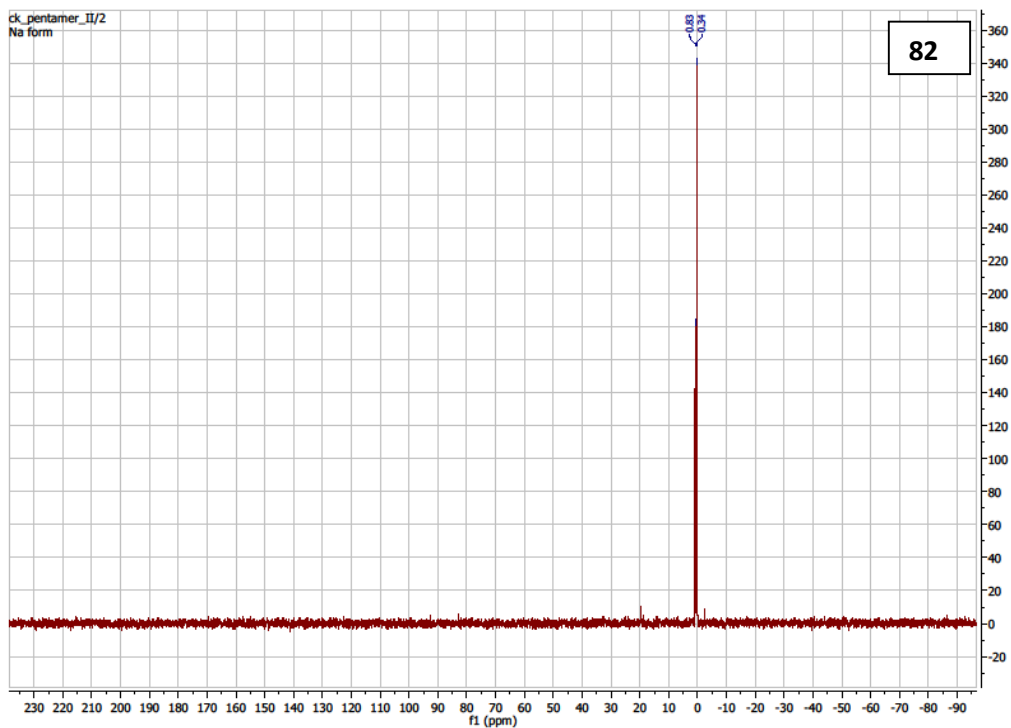


81

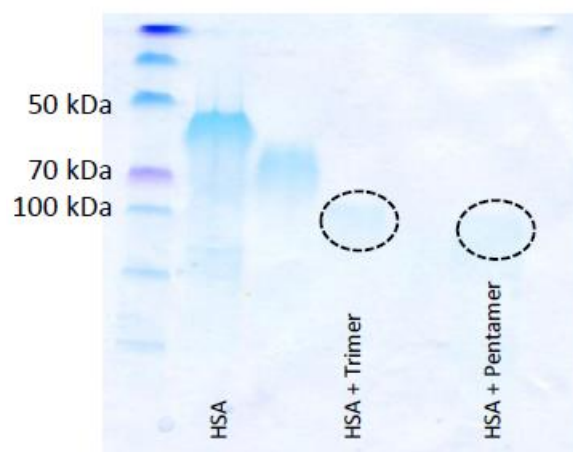








## SDS-PAGE HSA-Conjugates



## Analysis of HSA- Conjugates

Glycoconjugate	Protein concentration (mg/ml)*	Saccharide/Protein ratio**
HSA + Trimer	0.902	~ 18:1
HSA + Pentamer	0.685	~ 16:1

\* protein concentration determined by BCA analysis \*\* Ratio was determined by SDS-PAGE and BCA analysis